



This is to certify that the

## thesis entitled

PRE- AND POST-BUCKLING BEHAVIOR
OF PLATES OF VARIABLE STIFFNESS
USING FINITE DIFFERENCES

presented by

Mohammad Ali Barkhordari

has been accepted towards fulfillment of the requirements for

Ph.D. degree in Civil Engineering

Major professor

Date December 24, 1980

**O**-7639



#### OVERDUE FINES: 25¢ per day per item

RETURNING LIBRARY MATERIALS:
Place in book return to remove charge from circulation records

PRE-AND POST-BUCKLING BEHAVIOR OF PLATES OF VARIABLE STIFFNESS USING FINITE DIFFERENCES

By Mohammad Ali Barkhordari

## A DISSERTATION

Submitted to
Michigan State University
in partial fulfillment of the requirements
for the degree of

DOCTOR OF PHILOSOPHY

Department of Civil and Sanitary Engineering

1980

#### ABSTRACT

### PRE-AND POST-BUCKLING BEHAVIOR OF PLATES OF VARIABLE STIFFNESS USING FINITE DIFFERENCES

By

#### M. Ali Barkhordari

The Von Karman large deflection equation is applied to plates of variable stiffness. Equilibrium equations and the in-plane compatibility equation are derived. The ordinary finite difference technique is employed to solve the nonlinear coupled partial differental equations. Two different methods of formulation are considered:

- a) In terms of lateral displacement w and a stress function,
- b) In terms of displacement components u, v and w. Stiffness variation can be implemented in two different ways, either by varying the thickness of the plate with constant E, or by taking a uniform thickness plate of variable E. Both types of stiffness variation are considered. The nature of in-plane displacements on the boundary is a significant factor in postbuckling. This effect is examined by considering plates with different in-plane displacement boundary conditions.

Several problems with different stiffness variation and boundary conditions are solved. The applicable computer program is utilized to carry out the numerical solutions. In each case the problem is investigated for different stages of loading as follows:

٤

;

:

ganta ganta

Titl 7

38 (65.)

indites.

)že

The street

Str Met

- a) Membrane solution analyzes the behavior of in-plane forces and displacements for undeflected plates.
- b) Stability analysis investigates the buckling and effect of stiffness variation on critical loads and buckling modes.
- c) Postbuckling discusses the behavior of various aspects of the problem due to edge loads or displacements higher than critical values.

For clarity, the results are always accompanied by graphical illustrations of membrane and bending stress as well as displacement components.

The accuracy of the solution is evaluated by comparison of the results obtained with results from past studies and exact results, where these results are available. The influence of the grid-spacing on the accuracy of the results is investigated by taking successively finer grid-spacings. The numerical results are analyzed and the effect of stiffness variation on different aspects of the problem discussed.

One objective is to design a plate with stiffness variation such that it be optimum in some respect. Some possible cases of optimization are discussed and, as examples, some problems related to buckling are solved. The results indicate that a considerable weight and/or material savings can be achieved by using an efficient stiffness variation pattern.

### ACKNOWLEDGMENTS

The author wishes to express his most sincere gratitude to his major Professor, Dr. W. A. Bradley, Professor of civil engineering for his encouragement and constant help and guidance in the author's academic development and preparation of this dissertation.

Thanks are also expressed to the other members of the guidance committee - Dr. N. Altiero, Dr. J. L. Lubkin and Dr. R. K. Wen - for their guidance and encouragement. The author also owes his appreciation to Mrs. Clara Hanna for typing of this dissertation.

Special appreciation is also due his wife and son for their patience and understanding.

# TABLES OF CONTENTS

		Page
	LIST OF TABLES	v
	LIST OF FIGURES	vi
Chapter		
I	INTRODUCTION	1
	1.1 General Remarks	1 3 8 10
II	THEORETICAL DERIVATIONS	13
	2.1 General	13 14
	and Displacements	18
	and w	19
	u, v and w	21 22 22
	(2.2)	26 37
	2.5 Boundary Conditions	45 48
	2.6 Summary	48 49 49 50
III	APPLICATION	52
	3.1 Force Boundary Conditions	56 58
	Membrane Solution	70 77

Chapter			Page
		3.1.2.1 General Buckling	81
		3.1.2.2 Analysis of the Results	88
		3.1.3 Postbuckling	93
		3.1.3.1 General Procedure	93
		3.1.3.2 Numerical Solution	96
		a) Square Plate with $R = 1/10$ .	96
		b) Square Plate with Uniform	
		Stiffness, R = 1	104
		c,d) Square Plate with $R = 1/2$	110
		and R = 10	110
		3.1.3.3 Analysis of Postbuckling	110
		Results	119 119
		3.1.3.3.1 Simply-Supported Edges	119
		<ul><li>a) Uniform Stiffness Plate</li><li>b) Variable Stiffness, R = 1/10</li></ul>	
		c) Variable Stiffness, R = 1/2	124
		d) Variable Stiffness, R = 1/2	
		3.1.3.3.2 Clamped Edges	
		3.1.4 Optimization	
		3.1.5 Summary	
	3.2	Displacement Boundary Condition	
	3.4	3.2.1 Membrane Solution	156
		3.2.2 Buckling Selution	159
		3.2.2.1 Convergence Check and	164
		Comparison	164
		3.2.2.2 Optimization Analysis	169
		3.2.2.3 Analysis of Buckling Modes	172
		3.2.3 Postbuckling	175
		3.2.3.1 Uniform Thickness Plate,	175
		Simply Supported	175
		3.2.3.2 Simply Supported Square Plate	173
		of Variable Thickness	181
		3.2.3.3 Uniform Thickness Plate,	101
		Clamped Boundary	189
		3.2.3.4 Clamped Plate with Variable	
		Thickness	194
	3.3	Comparison of Two Methods	202
IV	CONC	CLUSION	204
	4.1	The Problem Summary	204
	4.2	Conclusions	206
•	4.3		208
	BIBL	LIOGRAPHY	210
	APPE	ENDICES	214

<u>.</u>.:

# LIST OF TABLES

Table		Page
3.1	Stress Function and Stress Resultant Ratios Square Plate with R = 1/10	65
3.2	Stress Function and Membrane Forces, $R = 1/2$	67
3.3	Stress Function and In-plane Resultant Ratios, R = 1	68
3.4	Stress Function and Membrane Forces, R = 10	68
3.5	Convergence of the Solution, R = 1/10	69
3.6	Eigenvalues of Simply-Supported Square Plate, R = 1/10, with Different Grid Spacings	80
3.7	Comparison of First Eigenvalues of Different Solutions (R=1)	80
3.8	Critical Loads of Simply-Supported Square Plate R = 1	82
3.9	Critical Load of Clamped Square Plate Under Bi-axial Uniform Load, R = 1	91
3.10	Boundary Displacement for Square Plate of Figure 3.62	158
3.11	Critical Displacements for a Simply-Supported Plate using Different Mesh Sizes, Uniform Stiffness Plate	165
3.12	Critical Displacements for a Clamped Square Plate using Different Mesh Sizes, Uniform Stiffness	166
3.13	Convergence of Postbuckling Solution with Mesh Size. Simply-Supported Plate	176
3.14	Convergence of Postbuckling Solution with Mesh Size. Clamped Plate	189

\_\_:

Rect

?la:

Sche Mome Defo

Noda No

Nota

Diff Equi

Die:

Dif: Com

<del>့ာ</del>ေ θþe

Georgia Pla

Ş::

Geo: Sti Voj

Ç<sub>07,1</sub>

: Port Plat

# LIST OF FIGURES

Figure		Page
2.1	Rectangular Flat Plate	15
2.2	Plate Element dxdy in Undeformed Configuration	15
2.3	Schematic Illustration of Internal Forces and Moments on the Element of Middle Surface in Deformed Configuration	17
2.4	Function f(x)	23
2.5	Nodal Pattern	24
2.6	Two Dimensional Operator for f	25
2.7	Nodal Arrangement	27
2.8	Difference Operator for Left Hand Side of Equilibrium Equation (2.14)	28
2.9	Difference Operator for Right Hand Side of Equation (2.14)	30
2.10	Difference Operator for Left Hand Side of Compatibility Equation (2.15)	33
2.11	Operators for x-Equilibrium Equation (2.16)	39
2.12	Operators for y-Equilibrium Equation (2.17)	41
3.1	Geometry and Stiffness Variation of Square Plate	54
3.2	Stiffness Variation	57
3.3	Geometrical Plan and $\phi$ Function	61
3.4	Stiffness Ratio at Nodes and Intermediate Nodes, Square Plate, R = 1/10	64
3.5	Convergence of Membrane Solution	70
3.6	Force Distribution for Undeflected Square	71

---: . .; • .: 

Figure		Page
3.7	Contours of In-plane Displacement, Undeflected Square Plate, R = 1	72
3.8	Distribution of In-plane Force and Displace- ment, Square Plate, R = 1/10	73
3.9	Distribution of In-plane Force and Displacement, Square Plate, R = 1/2	75
3.10	Distribution of In-plane Force and Displacement, Square Plate, R = 10	76
3.11	Convergence of Eigenvalue, R = 1/10	79
3.12	Modes of Buckling of Square Plate, R = 1/10, Simply-Supported	84
3.13	Modes of Buckling of Square Plate, R = 1/10, Clamped	84
3.14	Modes of Buckling of Square Plate, R = 1/2, Simply-Supported	85
3.15	Modes of Buckling of Square Plate, R = 1/2, Clamped	. 85
3.16	Modes of Buckling of Square Plate, R = 1, Simply-Supported	
3.17	Modes of Buckling of Square Plate, R = 1, Clamped	
3.18	Modes of Buckling of Square Plate, R = 10, Simply-Supported	. 87
3.19	Modes of Buckling of Square Plate, R = 10, Clamped	. 87
3.20	Deflected Shape for s-s and Clamped Plate	. 90
3.21	Flow Chart of Iterative Procedure	. 94
3.22	Plots of w,U, $N_x$ and $M_x$ , Square Plate, s-s, $R = 1/10$	. 100
3.23	Plots of Stress Components, Square Plate, s-s, R = 1/10	. 101
3.24	Contours of In-plane Force and Profiles of N, s-s, R = 1/10	. 102

3.25	<pre>In-Plane Displacement, Square Plate, s-s, R = 1/10</pre>	103
3.26	Plots of w, U, $N_x$ and $M_x$ , Square Plate, s-s, $R = 1$	105
3.27	Plots of Stress Components, Square Plate, s-s, R = 1	106
3.28	Contours of In-Plane Force and Profiles of N <sub>x</sub> , s-s, R = 1	107
3.29	<pre>In-Plane Displacement, Square Plate, s-s, R = 1</pre>	108
3.30	Square Plate Under Uniform Load, s-s, R = 1	109
3.31	Plots of w, U, $\frac{N}{x}$ and $\frac{M}{x}$ , Square Plate, s-s, $R = 1/2$	111
3.32	Plots of Stress Components, Square Plate, s-s, R = 1/2	112
3.33	Contours of In-Plane Force and Profiles of $N_{x}$ , s-s, $R = 1/2$	113
3.34	<pre>In-Plane Displacement, Square Plate, s-s, R = 1/2.</pre>	114
3.35	Plots of w, U, N and M x, Square Plate, s-s, R = 10	115
3.36	Plots of Stress Components, Square Plate, s-s, R= 10	116
3.37	Contours of In-Plane Force and Profiles of N <sub>x</sub> , s-s, R = 10	11,7
3.38	<pre>In-Plane Displacement, Square Plate, s-s, R = 10.</pre>	118
3.39	Convergence of the Solution with Mesh Size	120
3.40	Deflected Shape for Various R Values	128
3.41	Plots of w, U, N <sub>x</sub> and M <sub>x</sub> , Square Plate, Clamped, R = 1/10x	131
3.42	Plots of Stress Components, Square Plate, Clamped, R = 1/10	132
3.43	Contours of In-Plane Force and Profiles of N <sub>x</sub> , Clamped, R = 1/10x,	133

3.44	In-Plane Displacement, Square Plate, Clamped, R = 1/10	134
3.45	Plots of w, U, N <sub>x</sub> and M <sub>x</sub> , Square Plate, Clamped, R= 1	135
3.46	Plots of Stress Components, Square Plate, Clamped, R= 1	136
3.47	Contours of In-Plane Force and Profiles of N x, Clamped, R = 1x,	137
3.48	<pre>In-Plane Displacement, Square Plate, Clamped, R = 1</pre>	138
3.49	Plots of w, U, N and M, Square Plate, Clamped, R = 1/2x	139
3.50	Plots of Stress Components, Square Plate, Clamped R = 1/2	l 140
3.51	Contours of In-Plane Force and Profiles of N, Clamped, R= 1/2x,	141
3.52	<pre>In-Plane Displacement, Square Plate, Clamped, R = 1/2</pre>	142
3.53	Plots of w, U, N and M, Square Plate, Clamped, R = 10x	143
3.54	Plots of Stress Components, Square Plate, Clamped, R = 10	144
3.55	Contours of In-Plane Force and Profiles of N <sub>x</sub> , Clamped, R = 10	145
3.56	<pre>In-Plane Displacement, Square Plate, Clamped, R = 10</pre>	146
3.57	Thickness Variation	148
3.58	Critical Load vs. RT, Square Plate, Simply-Supported	152
3.59	Critical Load vs. RT, Square Plate, Clamped	153
3.60	Central Deflection for Different R Values, s-s and Clamped	155
3.61	Plan	156

3.62	Node Arrangement, Square Plate, $h = a/8$	157
3.63	Contours of Membrane Force, Principal Stress and U-displacement, Undeflected Plate, RT = 1	160
3.64	Contours of Membrane Force, Principal Stress and U-displacement, Undeflected Plate, RT=1/4	162
3.65	Contours of Membrane Force, Principal Stress and U-displacement, Undeflected Plate, RT = 2	163
3.66	Convergence of Buckling Solution	165
3.67	Convergence of Buckling Solution	166
3.68	Plan	168
3.69	Variation of Critical Displacement Versus RT	170
3.70	Variation of Critical Displacement Versus RT	171
3.71	Buckling Modes of Simply-Supported Square Plate, RT = 1	174
3.72	Buckling Modes of Clamped, Square Plate, RT = 1	174
3.73	Convergence of Center Deflection, s-s, Square Plate	176
3.74	Plots of Stress Components, Square Plate, s-s, RT = 1	178
3.75	<pre>In-Plane Displacement, Square Plate, s-s, RT = 1</pre>	179
3.76	Square Plate Under Uniform Lateral Load	180
3.77	Central Deflection Versus Edge Displacement for Different RT Values, Simply-Supported Square Plate	182
3.78	Plots of Stress Components, Square Plate, Simply-Supported, RT = 1/4	183
3.79	Plots of Stress Components, Square Plate, Simply-Supported, RT = 2	185
3.80	Principal Stress Versus Edge Displacement for Different RT Values, Simply-Supported Square Plate	187

jî, . . ä ... .... ; **3** : ÷. 1 : ċ •

3.81	Supported, RT = 1/4	188
3.82	<pre>In-Plane Displacement, Square Plate, Simply- Supported, RT = 2</pre>	188
3.83	Convergence of Solution	190
3.84	Central Deflection Versus Edge Displacement for Different RT Values, Clamped Edges	190
3.85	Plots of Stress Components, Square Plate, Clamped, RT = 1	192
3.86	<pre>In-Plane Displacement, Square Plates, Clamped, RT = 1</pre>	193
3.87	Plots of Stress Components, Square Plate, Clamped, RT = 1/4	196
3.88	Plots of Stress Components, Square Plate, Clamped, RT = 2	
3.89	Max. Principal Stress Versus Edge Displacement for Different RT Values, Square Plate, Clamped	199
3.90	<pre>In-Plane Displacement, Square Plate, Clamped, RT = 1/4</pre>	201
3.91	<pre>In-Plane Displacement, Square Plate, Clamped, RT = 2</pre>	201
A1	Difference Operator for Left Hand Side of Equi- librium equation (2.24), $\alpha = 1$	215
A2	Difference Operator for Left Hand Side of Equation (2.14), $\alpha$ = 1, Uniform Stiffness Plate	216
A3	Finite Difference Operator for Left Hand Side of Compatibility Equation (2.15), $\alpha = 1$	217
A4	Finite Difference Approximation of Equation (2.29) $\alpha = 1$	218
B1	Node Arrangement for Force Boundary Condition, SquaPlate, h = a/8	are 220
B2	Node Arrangement for Force Boundary Condition, Squa Plate, h = a/16	



В3	Node Arrangement for Displacement Boundary Condition, h = a/12	222
В4	Node Arrangement for Displacement Boundary Conditon, h = a/16	223
C1	Node Numbers	227
C2	Arrangement of Vector K	228
С3	Arrangement of Nodes in Vector KK	231

### CHAPTER I

### INTRODUCTION

### 1.1 GENERAL REMARKS

The widespread use of plate elements in many engineering structures such as buildings, bridges, pavements, missiles, containers, ship structures and space structures has made plate analysis the subject of scientific investigation for more than 200 years. Because of their two dimensional action, the mechanical behavior of plates under thrust loads is completely different from beam elements. In contrast to beam elements, in which buckling is usually associated with collapse of the structure, the buckling of a plate is not an end point in the serviceability of the structure.

The capability of a plate to carry load after buckling is an interesting subject which has motivated many investigators to study posbuckling behavior of plates, especially in connection with weight-sensitive space applications. Most of the plate analyses involve uniform stiffness plates. However, elastic plates of variable stiffness are used in many engineering structures such as aircraft wings, turbine disks, etc. The need to conserve material and/or minimize weight motivates the designers to make optimum use of the material.

From the structural point of view, knowledge of critical buckling loads is of great importance. To make an optimum design with respect to some variables, an extensive analysis of the variable-stiffness plate is necessary. The failure strength of a thin plate can exceed the buckling strength appreciably. In many cases, the structure is not sensitive to large deflection. Thus, it is of technical importance to consider the postbuckling behavior of plates (especially the variable stiffness plate) in order to optimize the design.

Although a considerable amount of work has been done in the area of variable stiffness plates, most studies have achieved solutions by analytical methods which are restricted to some specific geometry and boundary conditions. (See Section 1.2)

The purpose herein is to investigate the behavior of a variable stiffness plate so that a full history of the stress and strain components of plates with different stiffness variation can be presented. Such a history will help give the designer a better understanding of the behavior of the plate and the effect of stiffness variation on various aspects of the problem so that a morenearly optimum design may be achieved. Two different types of variation in stiffness are possible: one with uniform thickness and varying E, such as reinforced concrete or fiber-reinforced plastic. The other has variable thickness and constant E. Both cases are considered and analyzed.

-:: 5E. **\*.**, <u> Tü</u>i .... .... Ü., ... ..... .: j"j 3 : : . 44 · \$ (;

### 1.2 PREVIOUS DEVELOPMENTS

The study of plate theory began in the 1760's. Euler (17) presented the first mathematical approach to plate studies in 1766.

In 1815, Sophie Germain (22) presented a fairly satisfactory fundamental equation for the flexural vibrations to the French Institut as the result of her investigation during the 1809 to 1815 period. Within the same period (in 1811), Lagrange arrived at his equation, which is known, therefore, as Lagrange's equation for the flexure and the vibration of plates. Kirchhoff (1824-1887) is considered the founder of the extended plate theory which takes into account combined bending and stretching. In 1910, Von Karman introduced a set of differential equations valid for plates subject to large deflection. These equations are referred to in the literature as the large deflection equations.

The development of the modern aircraft industry directed the attention of many scientists and researchers toward the study of plate vibration, plates subject to in-plane loads and postbuckling behavior of plates. The earliest solution of a flat plate stability problem apparently was given by Bryan (10) in 1891.

The ability of a plate to carry additional load after buckling was apparently discovered in the late 1920's through experimental studies made in connection with the design of airplanes. In 1929, Wagner (49) studied a shear web and based on his findings, established a criterion for postbuckling strength of the web. In 1942, Levy (29) presented solutions to the plates with

### 1.2 PREVIOUS DEVELOPMENTS

The study of plate theory began in the 1760's. Euler (17) presented the first mathematical approach to plate studies in 1766.

In 1815, Sophie Germain (22) presented a fairly satisfactory fundamental equation for the flexural vibrations to the French Institut as the result of her investigation during the 1809 to 1815 period. Within the same period (in 1811), Lagrange arrived at his equation, which is known, therefore, as Lagrange's equation for the flexure and the vibration of plates. Kirchhoff (1824-1887) is considered the founder of the extended plate theory which takes into account combined bending and stretching. In 1910, Von Karman introduced a set of differential equations valid for plates subject to large deflection. These equations are referred to in the literature as the large deflection equations.

The development of the modern aircraft industry directed the attention of many scientists and researchers toward the study of plate vibration, plates subject to in-plane loads and postbuckling behavior of plates. The earliest solution of a flat plate stability problem apparently was given by Bryan (10) in 1891.

The ability of a plate to carry additional load after buckling was apparently discovered in the late 1920's through experimental studies made in connection with the design of airplanes. In 1929, Wagner (49) studied a shear web and based on his findings, established a criterion for postbuckling strength of the web. In 1942, Levy (29) presented solutions to the plates with

large deflections under combined edge compression and lateral loading. His investigation was based on analytical solutions using Fourier series. He also considered postbuckling analysis of plates. In 1970, Supple (42) analyzed a rectangular plate with constant in-plane compressive loads on opposite edges using the out-of-plane deflection, w, and the Airy stress function as variables.

A considerable amount of work has been done on plate analysis by different methods; among these are solutions of the equilibrium equations by series expansion, energy methods, and Vlasov's method (46). Until relatively recent times, however, the investigations have centered on analytical solutions, which are in most cases limited to relatively simple geometry, load, and boundary conditions.

In many particular cases where these conditions are more complex, the analysis via the classical route becomes increasingly difficult and is often impossible. In such cases, the use of an approximate approach becomes more practical due to the flexibility and quick results.

Near the end of World War II, the invention of digital computers, with their capability of processing large numerical problems, caused rapid development of various numerical techniques.

Of these, the finite element, finite difference and boundary integral methods are of most general use.

Although previous analysis of variable stiffness plates has been limited, there has been a considerable amount of work done on uniform stiffness plates using finite element techniques, and dealing with stability and postbuckling of plates. The finite

element method was introduced by Turner, Clough, Martin, and Topp

(45) in 1956. Argyris (4) and Zienkiewicz (53) have made numerous
contributions in this field. Gallagher (20) and Hartz (24) also
have made great contributions in improving the method and including
nonlinear terms. A series of studies considering postbuckling
behavior of plates was made in the 1970's (13, 19, 52) using the
finite element technique. Murray and Wilson (31) have conducted
research on postbuckling of plates, considering various aspect
ratios and applying the finite element method. Other significant
contributions include papers by Conner (14) and Yang (52). They
applied the finite element methods to solve postbuckling plate problems.

The finite difference method is also one of the general numerical solution techniques which has been frequently used. The finite difference method was first used by N. J. Neilsen (33) for analysis of plates in 1920.

The first finite difference solution of the large deflection of plates is due to Kaiser (26). More recently, Basu and Chapman (5) contributed to this study. Kaiser also carried out some experimental tests which verified the theoretical results. Both aforementioned investigations were formulated in terms of lateral deflection, w, and a stress function. The finite difference approach to large deflection of plates was also used by Brown and Harvey(9) who have studied large deflection of plates subject to lateral pressure combined with different ranges of edge loadings. More recently a new method of solving finite difference equations—namely, the dynamic relaxation method was described by Otter (35). The

		;
		3
		:
		:
ar.		
!		

basis of the method is to add dynamic terms to the equations. The addition of dynamic terms such as acceleration and viscous damping makes the problem analogous to a vibration problem. The damping coefficients are taken corresponding to critical damping resulting in a motion which dies out quickly. Thus, the solution to the static problem is obtained. Rushton (38,39,40) has published papers applying the dynamic relaxation method to large deflection of plates subject to lateral load and to postbuckling of plates under in-plane loads. Since the method is an alternative technique to solution of the finite difference equations, it has the advantage that variations in stiffness can be included. Rushton has stated that, with appropriate time increment and damping coefficient, a solution can be obtained with no difficulties.

The Boundary integral equation (BIE) method has also proved to be successful in solving plate bending problems. Jaswon (25) and Maiti (30) introduced the direct method of solution and recently Altiero and Sikarskie (3) presented the indirect method of solution which proved to be more efficient. In 1980, Wu (50) modified the method by moving the integration contours outside the real boundaries. The plate of interest is embedded in a fictitious plate for which the Green's function is readily known. Fictitious forces and moments are then applied outside the real boundary and the solution can be be tained by finding the magnitude of these fictitious loads such that the original boundary conditions are satisfied. The method was proved to be very efficient in general plate bending problems.

Particularly pertinent to this study is a paper by Prabhakara

). In his paper, he considered postbuckling of orthotropic

ites. Recently (in 1980), Kennedy and Prabhakara (27) have

idied the postbuckling behavior of orthotropic skew plates and

:ained solutions to some problems using a series expansion method.

	-
	•

## .3 PRESENT INVESTIGATION

In the study of thin plates subject to lateral and edge loading, especially in the postbuckling range where the deflections are not small, the Kirchhoff theory (which neglects stretching and shearing in the middle surface) can not yield satisfactory results. In this case the Von Karman large deflection equation can be employed to obtain more accurate results.

In Chapter II, a brief review of the theoretical background is given and the derivation of the compatibility and equilibrium equations is first presented. Next, by applying the ordinary finite difference method, the required operators are derived and the procedures for solution of different problems are briefly discussed.

Two different alternative methods of formulation are considered:

- a) in terms of lateral displacement, w, and a stress function,
- b) in terms of the displacement components, u, v, and w. The solution procedures for both methods are also discussed. A few many conditions are listed and theoretical elations for each boundary condition are mentioned.

Chapter III includes numerical solutions and analysis

f the results. A computer program and the required subroutines

see computer program in Appendix C) have been developed to facilitate

Polication of procedures discussed in Chapter II.

In order to provide a more complete view of the variable

Liffness plate and it's behavior relative to the uniform stiff
Ss plate, several different types of variation in stiffness are

Disidered. Uniform stiffness plate results are given for comparison.

For clarity, in the procedure presented, the results are always accompanied by graphical illustrations of membrane and bending stress as well as displacement components. The behavior of those graphs and their relations with applied load is discussed.

The accuracy of the solutions is evaluated by comparison of the results obtained with results from past studies and exact results, where these results are available.

Convergence of the solutions is examined by using different mesh sizes with extrapolation.

Results obtained for the effect of stiffness variation on in-plane forces, bending moments, in-plane displacements and lateral deflection, provide a good source of information for optimization in each case. Although the optimization procedure is straight-forward, the stability optimization with respect to amount of material used is presented as an example. Two computer programs are provided, One for force boundary conditions and the other for displacement boundary conditions. Both programs are listed in appendix (C). It was found that convergence was easily obtained for the range of loading less than the second critical load because the assumed Single-wave buckled shape is the only possible pattern of stable equilibrium other than the flat plate. For loading beyond the second critical load, due to different possible equilibrium states, the problem does not converge easily. For solution beyond that Fange a proper deflection shape must be enforced, as appropriate for the physical conditions of the problem.

#### NOTATIONS

The symbols are properly identified when first introduced; for the reader's convenience, symbols are tabulated here.

a Side length of square plate

c<sub>1</sub>,c<sub>2</sub>,... Constants

 $D = \frac{Et^3}{12(1-v^2)}$  Flexural rigidity of the plate

D Stiffness of a uniform stiffness, unit thickness

plate

D Reference stiffness = stiffness at center of the plate

E Young's modulus

F Force function

h,k Mesh intervals in x and y

K = Et Membrane rigidity

 $R_{r}$  Reference membrane stiffness = Et at center of the

plate

K Membrane rigidity of a uniform stiffness, unit

thickness plate

 $M_{x}, M_{v}, M_{xv}$  Bending and twisting moments per unit width

of plate

 $(\overline{M}_{x}; \overline{M}_{y}; \overline{M}_{xy}) = (\frac{a^{2}}{D_{o}t_{i}})(M_{x}; M_{y}; M_{xy})$  Dimensionless moments per unit width

N Applied edge force per unit width of plate

 $N_{\chi}$ ,  $N_{v}$ ,  $N_{xv}$  In-plane stress resultants per unit width of plate

 $(N_x^*; N_y^*; N_{xy}^*) = (\frac{a}{D_0})(N_x; N_y; N_{xy})$  Dimensionless membrane forces per unit width of plate

 $(\overline{N}_x; \overline{N}_y; \overline{N}_{xy}) = (N_x; N_y; N_{xy})/N$  Membrane force ratios

```
(N'_{x}; N'_{y}; N'_{xy}) = (N_{x}; N_{y}; N_{xy})/N_{cr} Membrane force ratios
                          Lateral distributed load per unit area of plate
\overline{Q} = qa^4/D_ot_i
                          Dimensionless lateral load per unit width of plate
                          Transverse shear per unit width of plate
 R = \frac{\text{edge stiffness}}{\text{central stiffness}}
                                      Stiffness ratio
 RT = \frac{\text{edge thickness}}{\text{central thickness}}
                                      Thickness ratio
                          Plate thickness
 t
                          Unit
                                   thickness
 t,
 T
                          Temperature
 u,v,w
                          Displacement components in x,y, and z directions
                          Volume 

                          Edge displacement
(U; V) = (u; v) a/t_1^2 Dimensionless displacement
\overline{U} = U/U_{cr}
```

 $W = \frac{w}{t_i}$  Dimensionless lateral deflection

x,y,z Cartesian coordinates (X; Y) = (x; y)/a Dimensionless coordinates

 $\alpha = \frac{h}{k}$  Grid size ratio

 $\beta_{1} = \frac{K_{1}}{K_{r}}$  Membrane stiffness ratio

Coefficient of thermal expansion

 $\delta_{\underline{i}} = \frac{D_{\underline{i}}}{D_{\underline{r}}}$  Flexural stiffness ratio

Eigenvalues

Eigenvectors

Strain components

Components of normal stress

Eigenvectors

Strain components

Components of normal stress

Shear stress components

= tφ' Stress function

Airy's stress function

=  $\phi/\text{Na}^2$  Dimensionless stress function

Coefficient matrix for φ

w], [bw] Coefficient matrices for w

Aw]; [Bw]) = ([aw]; [bw])×h<sup>4</sup> Coefficient matrices for w

u], [Bu] Coefficient matrices for u

v], [Bv] Coefficient matrices for v

ul], [Au2] Coefficient matrices for u

Vl], [Av2] Coefficient matrices for v

#### CHAPTER II

#### THEORETICAL DERIVATIONS

#### 2.1 General

In this chapter, the equilibrium and compatibility equations of the plate based on the theory of elasticity are first derived. Then, the finite difference approximations to these equations are developed. These will be used to facilitate numerical solutions of those equations, for which, in most of the cases, closed form solutions, if not impossible, are very tedious.

Thin plate theory is applied and homogeneous, isotropic material is assumed.

Depending on the boundary conditions, two different approaches are possible. Here, both approaches will be discussed.

Geometrical and material nonlinearity can arise in plate Problems. In this study only geometrical nonlinearity will be considered.

Figure (2.1) shows the geometry and orientation of a plate

in the cartesian coordinate system. The x-y plane lies in the middle

Plane of the plate and z is normal to the middle plane.

Internal forces and moments acting on the edges of a dx by dy

Plate element, as shown in Figure (2.2), are related to the internal

stresses by the equations:

$$N_{x} = \int_{-t/2}^{t/2} \sigma_{x} dz \qquad N_{y} = \int_{-t/2}^{t/2} \sigma_{y} dz 
N_{xy} = \int_{-t/2}^{t/2} \tau_{xy} dz \qquad N_{yx} = \int_{-t/2}^{t/2} \tau_{yx} dz \qquad (2.1)$$

$$Q_{x} = \int_{-t/2}^{t/2} \tau_{xz} dz \qquad Q_{y} = \int_{-t/2}^{t/2} \tau_{yz} dz 
M_{x} = \int_{-t/2}^{t/2} \sigma_{x} z dz \qquad M_{y} = \int_{-t/2}^{t/2} \sigma_{y} z dz$$

$$M_{xy} = \int_{-t/2}^{t/2} \tau_{xy} z dz \qquad M_{yx} = \int_{-t/2}^{t/2} \tau_{yx} z dz$$

where  $N_x$ ,  $N_y$ ,  $N_{xy}$ ,  $N_{yx}$  = in-plane normal and shearing stress resultants.

 $Q_{x}$ ,  $Q_{v}$  = transverse shearing stress resultants.

 $M_x$ ,  $M_v$  = bending moments.

 $M_{xy}$ ,  $M_{yx}$  = twisting moments.

#### 2.1.1 NONLINEAR EQUILIBRIUM EQUATIONS

In the literature, nonlinear behavior is commonly classified as either

- 1) Material nonlinearity
- 2) Geometric nonlinearity

Material nonlinearity may arise in case of time-dependent

Paterial or materials with nonlinear stress-strain relations (plastic,

Lastoplastic, viscoelastic, etc.).

Geometric nonlinearity is usually associated with large isplacements. It may also occur for small displacement if the

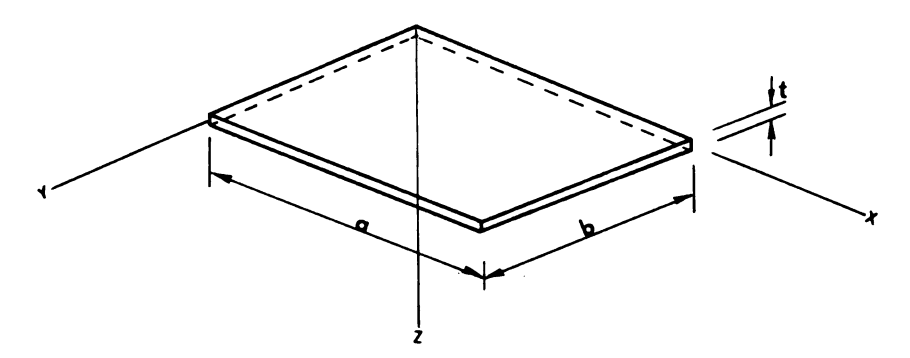


Figure 2.1 Rectangular flat plate

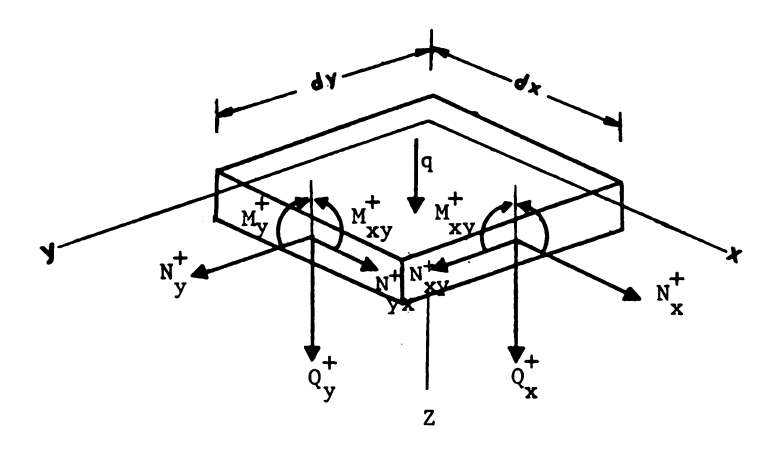


Figure 2.2 Plate element dxdy in undeformed configuration

behavior is such that variation in the applied load alters the distributions of displacement.

In this report only geometric nonlinearity is considered and the material is assumed linear elastic, isotropic, and homogeneous.

To determine equilibrium equations applicable to moderately large deformations, they must be derived using slightly deformed configurations. Figure (2.3) represents stress resultants and internal moments for an element dx by dy in the deformed configuration.  $\beta_x$  and  $\beta_y$  are rotations in the xz and yz planes respectively, and  $N_x^+$  denotes  $N_x + \frac{\partial N_x}{\partial x} dx$  etc.

Summation of forces in the x-direction gives:

$$-N_{x}dy + (N_{x} + \frac{\partial N_{x}}{\partial x} dx)dy - N_{yx}dx + (N_{yx} + \frac{\partial N_{yx}}{\partial y} dy)dx = 0$$

which simplifies to

$$\frac{\partial N}{\partial x} + \frac{\partial N}{\partial y} = 0 \tag{2.2}$$

similarly, summation of forces in the y-direction leads to:

$$\frac{\partial N_{xy}}{\partial x} + \frac{\partial N_{y}}{\partial y} = 0. {(2.3)}$$

From summation of forces in the z-direction, we obtain

$$-\frac{\partial Q_{x}}{\partial x} - \frac{\partial Q_{y}}{\partial y} = q + N_{x} \frac{\partial^{2} w}{\partial x^{2}} + N_{x} \frac{\partial^{2} w}{\partial y^{2}} + 2N_{xy} \frac{\partial^{2} w}{\partial x \partial y}$$
 (2.4)

Summation of moments about x and y axes will result in:

$$Q_{y} = \frac{\partial M}{\partial y} + \frac{\partial M}{\partial x}$$

$$Q_{x} = \frac{\partial M_{x}}{\partial x} + \frac{\partial M_{yx}}{\partial y}$$
(2.5)

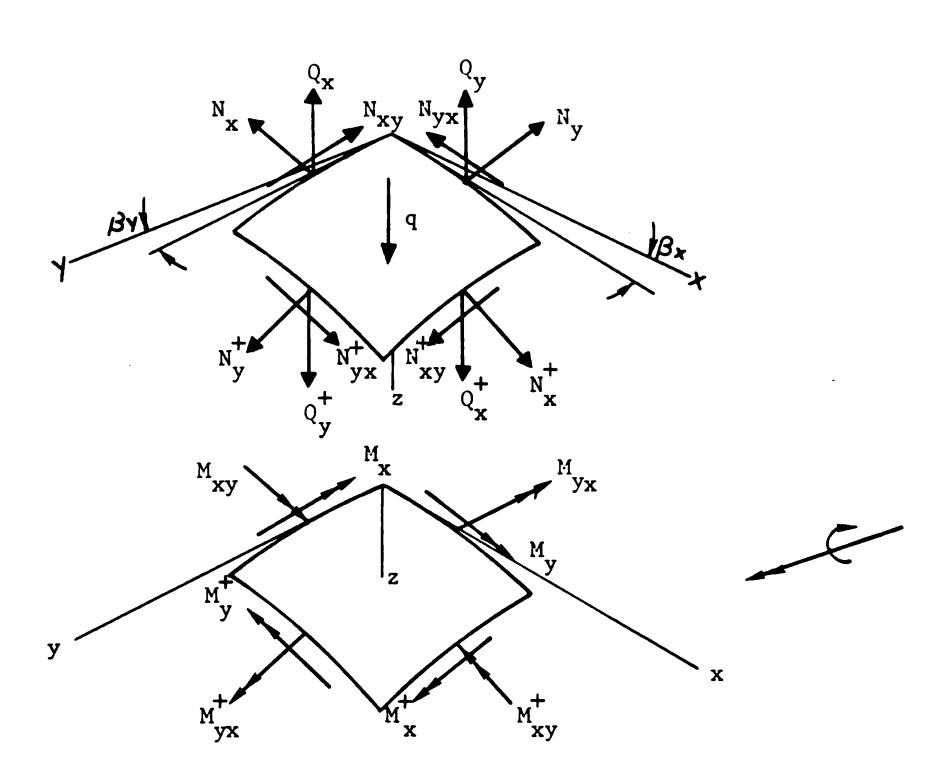


Figure 2.3. Schematic illustration of internal forces and moments on the element of middle surface in deformed configuration.

#### 2.1.2 Relation between stress resultants and displacements.

From Hooke's law, we have

$$N_{x} = \frac{Et}{1-v^{2}} (\varepsilon_{x} + v \varepsilon_{y})$$

$$N_{y} = \frac{Et}{1-v^{2}} (\varepsilon_{y} + v \varepsilon_{x})$$

$$N_{xy} = N_{yx} = \frac{Et}{2(1+v)} \gamma_{xy}$$
(2.6)

where:

$$\varepsilon_{\mathbf{x}} = \frac{\partial \mathbf{u}}{\partial \mathbf{x}} + 1/2 \left(\frac{\partial \mathbf{w}}{\partial \mathbf{x}}\right)^{2}$$

$$\varepsilon_{\mathbf{y}} = \frac{\partial \mathbf{v}}{\partial \mathbf{y}} + 1/2 \left(\frac{\partial \mathbf{w}}{\partial \mathbf{y}}\right)^{2}$$

$$\gamma_{\mathbf{xy}} = \frac{\partial \mathbf{u}}{\partial \mathbf{y}} + \frac{\partial \mathbf{v}}{\partial \mathbf{x}} + \frac{\partial \mathbf{w}}{\partial \mathbf{x}} - \frac{\partial \mathbf{w}}{\partial \mathbf{y}}$$
(2.7)

For moderately large displacements, the relations between moments and lateral displacement are:

$$M_{x} = -D(\frac{\partial^{2}w}{\partial x^{2}} + v \frac{\partial^{2}w}{\partial y^{2}})$$

$$M_{y} = -D(\frac{\partial^{2}w}{\partial y^{2}} + v \frac{\partial^{2}w}{\partial x^{2}})$$

$$M_{xy} = M_{yx} = -D(1-v)\frac{\partial^{2}w}{\partial x \partial y}$$
(2.8)

Where D =  $\frac{Et^3}{12(1-v^2)}$  is the flexural rigidity of the plate.

#### 2.2 Formulation in terms of stress function and w

By substitution of Equation (2.8) into (2.5) and (2.4), we obtain the equilibrium equations in the z-direction in terms of membrane resultants and lateral displacement w:

$$\nabla^{2}(D\nabla^{2}w) - (1-v) \left[ \frac{\partial^{2}D}{\partial x^{2}} \frac{\partial^{2}w}{\partial y^{2}} - 2 \frac{\partial^{2}D}{\partial x\partial y} \frac{\partial^{2}w}{\partial x\partial y} + \frac{\partial^{2}D}{\partial y^{2}} \frac{\partial^{2}w}{\partial x^{2}} \right]$$

$$= q + N_{x} \frac{\partial^{2}w}{\partial x^{2}} + N_{y} \frac{\partial^{2}w}{\partial y^{2}} + 2N_{xy} \frac{\partial^{2}w}{\partial x\partial y}. \qquad (2.9)$$

The compatibility equation for mid-plane strains is:

$$\frac{\partial^{2} \varepsilon_{x}}{\partial y^{2}} + \frac{\partial^{2} \varepsilon_{y}}{\partial x^{2}} - \frac{\partial^{2} \gamma_{xy}}{\partial x \partial y} = \left(\frac{\partial^{2} w}{\partial x \partial y}\right)^{2} - \frac{\partial^{2} w}{\partial x^{2}} \frac{\partial^{2} w}{\partial y^{2}}$$
(2.10)

and from (2.6), the strains in terms of membrane forces are

$$\varepsilon_{x} = \frac{1}{Et} (N_{x} - \nu N_{y})$$

$$\varepsilon_{y} = \frac{1}{Et} (N_{y} - \nu N_{x})$$

$$\gamma_{xy} = \frac{2(1+\nu)}{Et} N_{xy}$$
(2.11)

Now, we define a stress function,  $\phi,$  similar to Airy's stress function, so that:

$$N_{x} = \frac{\partial^{2} \varphi}{\partial y^{2}}$$

$$N_{y} = \frac{\partial^{2} \varphi}{\partial x^{2}}$$

$$N_{xy} = -\frac{\partial^{2} \varphi}{\partial x \partial y}.$$
(2.12)

The Airy's stress functions is defined as

$$\sigma_{\mathbf{x}} = \frac{\partial^{2} \varphi'}{\partial \mathbf{y}^{2}}$$

$$\sigma_{\mathbf{y}} = \frac{\partial^{2} \varphi'}{\partial \mathbf{x}^{2}}$$

$$\tau_{\mathbf{x}\mathbf{y}} = -\frac{\partial^{2} \varphi'}{\partial \mathbf{x} \partial \mathbf{y}}$$
(2.13)

ter ber in the interest of the in-

ere  $N_x = t \sigma_x = t \frac{\partial^2 \varphi'}{\partial y^2}$  etc.

is is suitable for a uniform thickness plate. However, in the case of riable thickness, if we define  $\phi'$ , as (2.13), it will complicate formulation. For example, substitution in equilibrium equations .2), would result in

$$\frac{\partial t}{\partial x} \frac{\partial^2 \varphi'}{\partial y^2} + t \frac{\partial^3 \varphi'}{\partial x \partial y^2} - \frac{\partial t}{\partial y} \frac{\partial^2 \varphi'}{\partial x \partial y} - t \frac{\partial^3 \varphi'}{\partial x \partial y^2} = 0$$

ich in the case of uniform thickness, leads to 0 = 0.

For our purpose the definitions of (2.12) will be used. estitution of (2.12) into (2.9), will result in the equilibrium

lation in terms of φ and w, as

$$\nabla^{2}(D\nabla^{2}w) - (1-v) \left[ \frac{\partial^{2}D}{\partial x^{2}} \frac{\partial^{2}w}{\partial y^{2}} - 2 \frac{\partial^{2}D}{\partial x \partial y} \frac{\partial^{2}w}{\partial x \partial y} + \frac{\partial^{2}D}{\partial y^{2}} \frac{\partial^{2}w}{\partial x^{2}} \right]$$

$$= q + \frac{\partial^{2}\phi}{\partial y^{2}} \frac{\partial^{2}w}{\partial x^{2}} + \frac{\partial^{2}\phi}{\partial x^{2}} \frac{\partial^{2}w}{\partial y^{2}} - 2 \frac{\partial^{2}\phi}{\partial x \partial y} \frac{\partial^{2}w}{\partial x \partial y} . \qquad (2.14)$$

substitution of (2.12) into (2.11) and then into (2.10), we tain the compatibility equation in terms of  $\phi$  and w:

$$\frac{\partial^{2}}{\partial y^{2}} \left[ \frac{1}{Et} (\varphi_{yy} - v\varphi_{xx}) \right] + \frac{\partial^{2}}{\partial x^{2}} \left[ \frac{1}{Et} (\varphi_{xx} - v\varphi_{yy}) \right] + \frac{\partial^{2}}{\partial x \partial y} \left[ \frac{2(1+v)}{Et} \varphi_{xy} \right] =$$

$$(\frac{\partial w}{\partial x \partial y})^{2} - \frac{\partial w}{\partial x^{2}} \frac{\partial w}{\partial y^{2}}$$

$$(2.15)$$

where  $\varphi_{xx} = \frac{\partial^2 \varphi}{\partial x^2}$ , etc.

### 2.3 Formulation in terms of 3 displacements u,v, and w

Substituting equation (2.7) into (2.6) and then into (2.2) and (2.3), along with substitution of (2.8) into (2.5) and then into (2.4), results in 3 equilibrium equations in terms of u,v, and w.

The equation of equilibrium in the  $\,\mathbf{x}\,$  direction (2.2) becomes

$$\frac{Et}{1-v^{2}} \left[ \frac{\partial^{2} u}{\partial x^{2}} + \frac{\partial^{2} w}{\partial x^{2}} \frac{\partial w}{\partial x} + v(\frac{\partial^{2} v}{\partial x \partial y} + \frac{\partial^{2} w}{\partial x \partial y} \frac{\partial w}{\partial y}) \right] + \frac{1-v}{2} \frac{Et}{1-v^{2}} \left[ \frac{\partial^{2} u}{\partial y^{2}} + \frac{\partial^{2} v}{\partial x \partial y} + \frac{\partial^{2} v}{\partial x \partial y} \right] + \frac{1}{1-v^{2}} \frac{\partial(Et)}{\partial x} \left[ \frac{\partial u}{\partial x} + \frac{1}{2}(\frac{\partial w}{\partial x})^{2} + v(\frac{\partial v}{\partial y}) + \frac{v}{2}(\frac{\partial w}{\partial y})^{2} \right] + \frac{1-v}{2(1-v^{2})} \frac{\partial(Et)}{\partial y} \left[ \frac{\partial u}{\partial x} + \frac{\partial w}{\partial x} \frac{\partial w}{\partial y} \right] = 0.$$
(2.16)

Similarly, the equation of equilibrium in the y-direction (2.3),

becomes

$$\frac{\operatorname{Et}}{1-v^{2}} \left[ \frac{\partial^{2} \mathbf{v}}{\partial \mathbf{y}^{2}} + \frac{\partial^{2} \mathbf{w}}{\partial \mathbf{y}^{2}} \frac{\partial \mathbf{w}}{\partial \mathbf{y}} + v(\frac{\partial^{2} \mathbf{u}}{\partial \mathbf{x} \partial \mathbf{y}} + \frac{\partial^{2} \mathbf{w}}{\partial \mathbf{x} \partial \mathbf{y}} \frac{\partial \mathbf{w}}{\partial \mathbf{x}}) \right] + \frac{1-v}{2} \frac{\operatorname{Et}}{1-v^{2}} \left[ \frac{\partial^{2} \mathbf{v}}{\partial \mathbf{x}^{2}} + \frac{\partial^{2} \mathbf{u}}{\partial \mathbf{x} \partial \mathbf{y}} + \frac{\partial^{2} \mathbf{u}}{\partial \mathbf{x} \partial \mathbf{y}} + \frac{\partial^{2} \mathbf{w}}{\partial \mathbf{x}^{2}} + \frac{\partial^{2} \mathbf{u}}{\partial \mathbf{x}^{2}} \right] + \frac{1}{1-v^{2}} \frac{\partial(\operatorname{Et})}{\partial \mathbf{y}} \left[ \frac{\partial \mathbf{v}}{\partial \mathbf{y}} + \frac{1}{2} (\frac{\partial \mathbf{w}}{\partial \mathbf{y}})^{2} + \frac{1-v}{2} \frac{\partial(\operatorname{Et})}{\partial \mathbf{x}} \left[ \frac{\partial \mathbf{v}}{\partial \mathbf{x}} + \frac{\partial \mathbf{u}}{\partial \mathbf{y}} + \frac{\partial \mathbf{w}}{\partial \mathbf{x}} \frac{\partial \mathbf{w}}{\partial \mathbf{y}} \right] = 0 \tag{2.17}$$

Interchanging u and x with v and y respectively in equation (2.17) results in equation (2.16).

The equilibrium equation in the z-direction (out of plane) can be expressed in terms of 3 displacements by substituting (2.7) into (2.6) and then the results into (2.9). We obtain:

$$\nabla^{2}(D\nabla^{2}w) - (1-\nu)\left[\frac{\partial^{2}D}{\partial x^{2}}\frac{\partial^{2}w}{\partial y^{2}} - 2\frac{\partial^{2}D}{\partial x\partial y}\frac{\partial^{2}w}{\partial x\partial y} + \frac{\partial^{2}D}{\partial y^{2}}\frac{\partial^{2}w}{\partial x^{2}}\right]$$

$$= q + \frac{Et}{1-\nu^{2}}\left[\frac{\partial u}{\partial x} + \frac{1}{2}(\frac{\partial w}{\partial x})^{2} + \nu\frac{\partial v}{\partial y} + \frac{\nu}{2}(\frac{\partial w}{\partial y})^{2}\right]\frac{\partial^{2}w}{\partial x^{2}} + \frac{Et}{1-\nu^{2}}\left[\frac{\partial v}{\partial y} + \frac{1}{2}(\frac{\partial w}{\partial y})^{2} + \nu\frac{\partial u}{\partial y} + \frac{\partial v}{\partial x} + \frac{\partial w}{\partial x}\frac{\partial w}{\partial y}\right]\frac{\partial^{2}w}{\partial x\partial y}$$

$$+ \nu\frac{\partial u}{\partial x} + \frac{\nu}{2}(\frac{\partial w}{\partial x})^{2}\right]\frac{\partial^{2}w}{\partial y^{2}} + \frac{Et(1-\nu)}{1-\nu^{2}}\left[\frac{\partial u}{\partial y} + \frac{\partial v}{\partial x} + \frac{\partial w}{\partial x}\frac{\partial w}{\partial y}\right]\frac{\partial^{2}w}{\partial x\partial y}$$
(2.18)

Note: Since in this approach we are working with displacements, compatibility need not be checked.

# 2.4 FINITE DIFFERENCE APPROXIMATION

So far we have derived the necessary equations for analysis of the plate, but solving these coupled nonlinear partial differential equations analytically may be difficult.

Here we employ finite difference techniques to transform

the differential equations into ordinary algebraic equations in terms

of values of the functions themselves at certain specified points.

# 2.4.1 Principle of finite differences

The derivation of finite difference expressions is based on a Taylor series expansion. We expand the function at some successive grid points, truncate higher order terms, and solve for desired derivatives, we can obtain approximate expressions

for first, second, or higher order derivatives in terms of values of function at the discrete points.

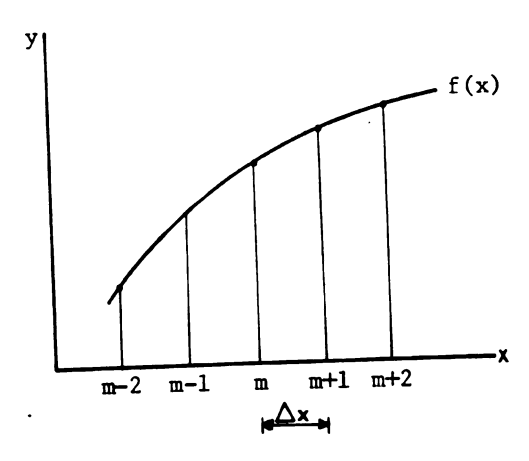


Figure 2.4. Function f(x).

In one dimensional cases we obtain the following approximation of the derivatives of the function:

$$f'(x)_{m} = \frac{1}{2(\Delta x)} (f_{m+1} - f_{m-1}) - \frac{1}{6} (\Delta x)^{2} f_{m}''' + \dots$$

$$f''(x)_{m} = \frac{1}{(\Delta x)^{2}} (f_{m+1} - 2f_{m} + f_{m-1}) - \frac{1}{12} (\Delta x)^{2} f_{m}^{iv} + \dots (2.19)$$

$$f''(x)_{m} = \frac{1}{2(\Delta x)^{3}} (f_{m+2} - 2f_{m+1} + 2f_{m-1} - f_{m-2}) - \frac{1}{4} (\Delta x)^{2} f_{m}^{v} + \dots$$

$$f(x)_{m} = \frac{1}{(\Delta x)^{4}} (f_{m+2} - 4f_{m+1} + 6f_{m} - 4f_{m-1} + f_{m-2})$$

$$- \frac{1}{6} (\Delta x)^{2} f_{m}^{vi} + \dots$$

In practice, we truncate the terms following the parentheses.

These represent the error in the approximation. We will refer to these error terms later in the discussion of accuracy.

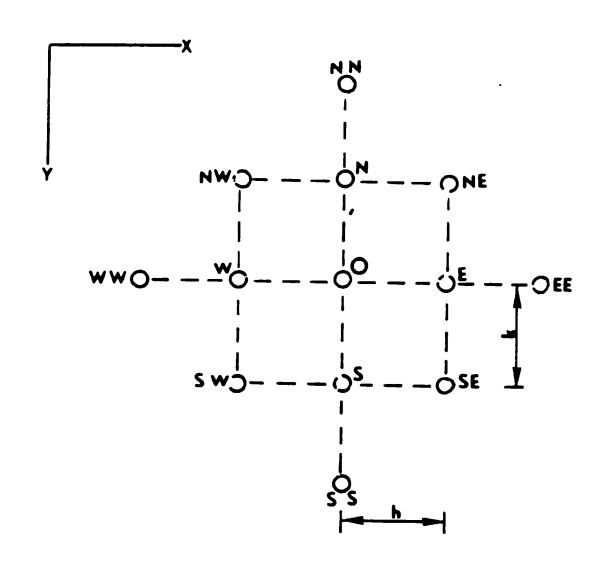


Figure 2.5

To determine the finite difference approximation for two dimensional problems, we consider Figure (2.5), and the fact that similar relations for the approximations to the derivatives in the x-direction hold also in y-direction.

Thus, we will be able to derive expressions for any order  ${}^{\circ}$ f derivatives in x and y and combinations of x and y derivatives.

For example, if we consider grid points of Figure (2.5), the derivatives with respect to x and y at point 0 are

$$f_x = \frac{1}{2h} (f_E - f_W)$$

$$f_{y} = \frac{1}{2k} (f_{S} - f_{N})$$

$$f_{xx} = \frac{1}{h^{2}} (f_{E}^{-2}f_{0} + f_{W})$$

$$f_{yy} = \frac{1}{h^{2}} (f_{S}^{-2}f_{0} + f_{N})$$

$$f_{xy} = \frac{1}{4hk} (f_{SE}^{-1}f_{SW} + f_{NW})$$
or if  $\frac{h}{k} = \alpha$  then
$$f_{xy} = \frac{\alpha}{4h^{2}} (f_{SE}^{-1}f_{SW} + f_{NW}) \quad \text{etc.}$$

Often, these formulas for derivatives are represented geometrically by stencil patterns, such as in Figure 2.6.

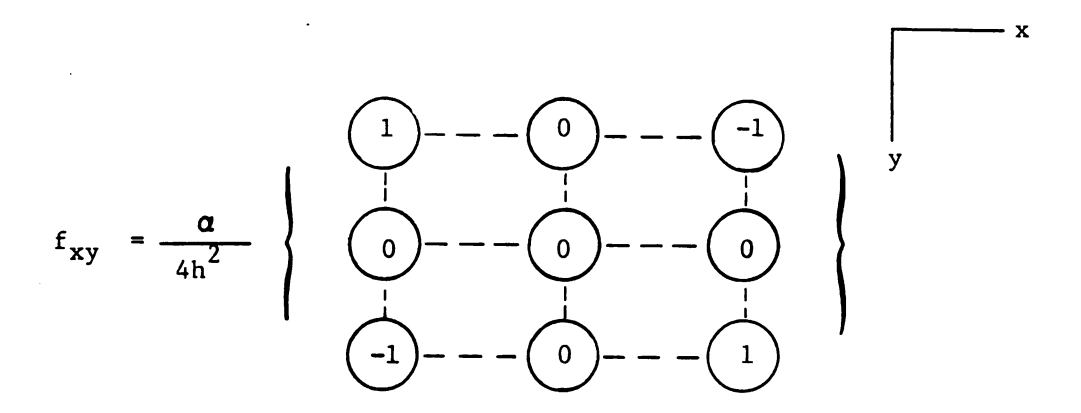


Figure 2.6. Two dimensional operator for  $f_{xy}$ .

#### 2.4.2 FINITE DIFFERENCE APPROXIMATION OF METHOD DISCUSSED IN SECTION (2.2)

In section (2.2), we derived equations of equilibrium and compatibility as well as the components of internal forces and displacements, in terms of lateral displacement, w, and stress function,  $\varphi$ . In this section, we will discuss numerical solution of those equations using finite difference techniques.

To find a solution to a plate problem, we must satisfy both equilibrium in the z direction, and compatibility.

#### a) Equilibrium Equation

For this purpose, we will apply relations (2.20) to equilibrium equation (2.14), and the results will be represented in two dimensional operator form. Introducing

 $D_r$  = flexural stiffness of the plate at some reference point (center of the plate in this case),

$$\delta_{\mathbf{i}} = \frac{D_{\mathbf{i}}}{D_{\mathbf{r}}}$$

A finite difference operator for the left hand side of the equilibrium equation (2.14) is given in Figure 2.8 where  $\delta_a$ ,  $\delta_b$ ,  $\delta_c$  and  $\delta_d$  refer to midpoints a, b, c and d of Figure (2.7) as explained in reference (8).

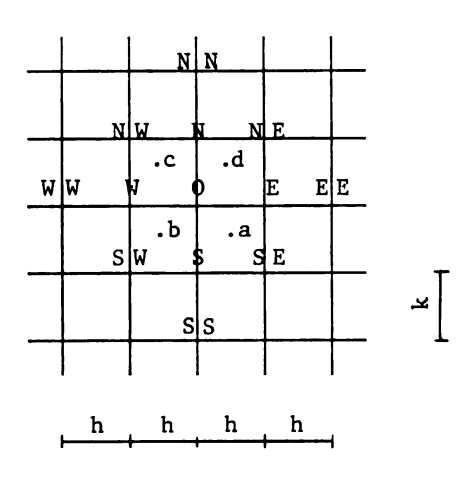


Figure 2.7

Note: All terms in the operator of Figure (2.8) are coefficients of w.

If the grid spacing is the same in the x and y directions ( $\alpha = 1$ ), OPerator (2.8) will be simplified to the operator given in appendix (A.1).

In case of a uniform stiffness plate, where  $\delta_1 = \frac{D_1}{D_r} = 1$ for all points, the operator reduces to the usual finite difference operator for  $\nabla^4 w$ , as given in appendix (A.2).

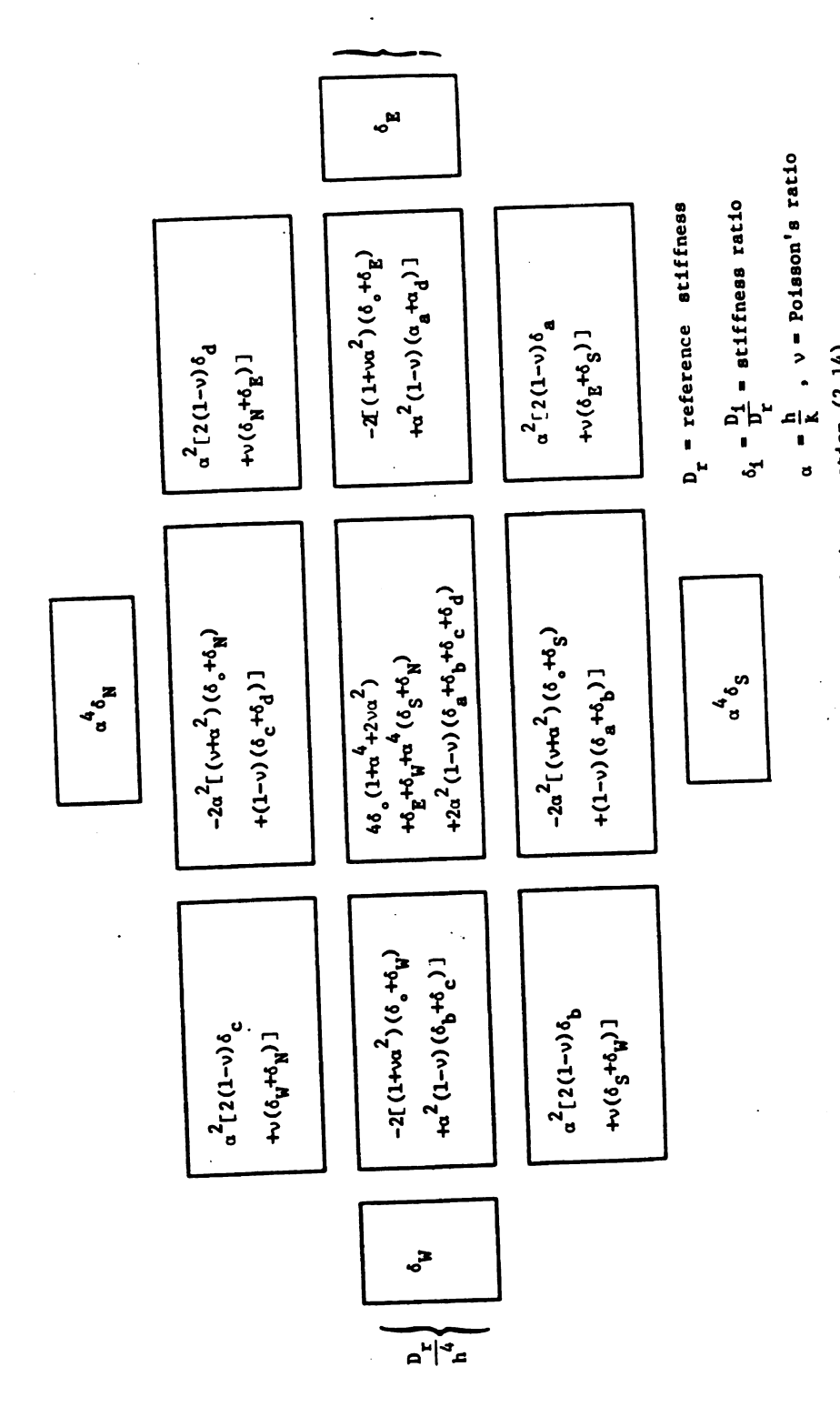


Figure 2.8. Difference operator for left hand side of equilibrium equation (2.14).

.: : . ••• ₹: 3 For the right hand side, if  $\phi$  values are known, we can derive the finite difference operator as coefficients of w, as shown in Figure (2.9.a), where

$$\begin{split} \phi_{\mathbf{x}\mathbf{x}} &= \frac{\partial^2 \phi}{\partial \mathbf{x}^2} = \frac{\phi_{\mathrm{E}} - 2\phi_{\mathrm{0}} + \phi_{\mathrm{W}}}{h^2} \\ \phi_{\mathbf{y}\mathbf{y}} &= \frac{\partial^2 \phi}{\partial \mathbf{y}^2} = \frac{\phi_{\mathrm{N}} - 2\phi_{\mathrm{0}} + \phi_{\mathrm{S}}}{k^2} = \frac{\alpha^2 (\phi_{\mathrm{N}} - 2\phi_{\mathrm{0}} + \phi_{\mathrm{S}})}{h^2} \\ \phi_{\mathbf{x}\mathbf{y}} &= \frac{\partial^2 \phi}{\partial \mathbf{x} \partial \mathbf{y}} = \frac{\phi_{\mathrm{SE}} + \phi_{\mathrm{NW}} - \phi_{\mathrm{SW}} - \phi_{\mathrm{NE}}}{4hk} = \frac{\alpha (\phi_{\mathrm{SE}} + \phi_{\mathrm{NW}} - \phi_{\mathrm{SW}} - \phi_{\mathrm{NE}})}{4h^2} \end{split}$$

For  $\alpha = 1$ , we get the expression shown in Figure 2.9(b).

## SOLUTION OF THE EQUILIBRIUM EQUATION

To solve the equilibrium equation for w, we must have either the  $\phi$  values, or the in-plane forces  $(\phi_{xx},\,\phi_{yy}$  and  $\phi_{xy}).$ 

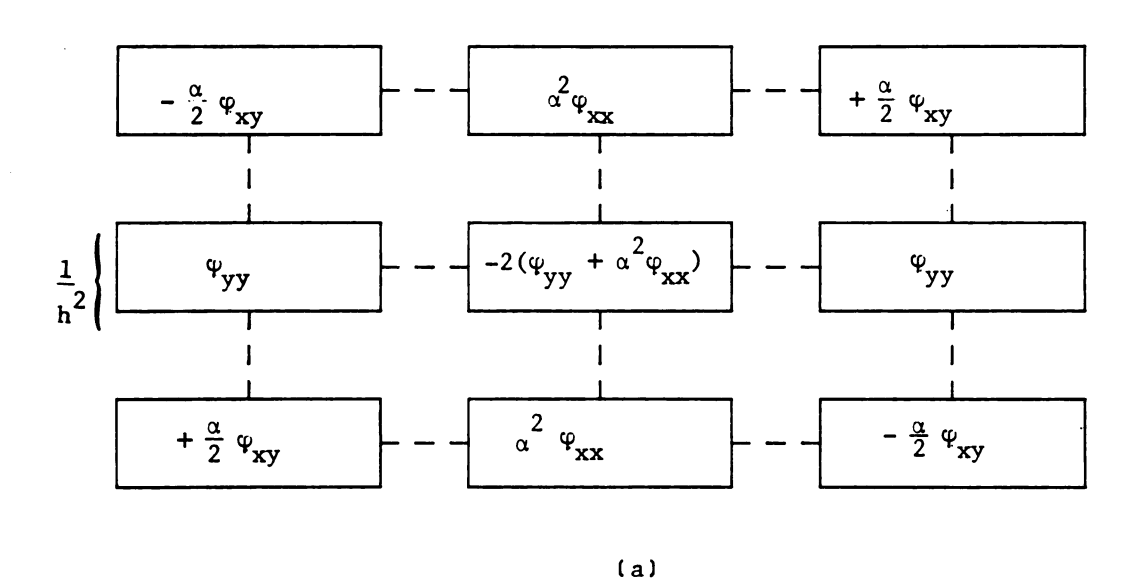
Substitution of these values into the operator of Figure 2.9 (a) or (b) will result in a known operator at each node.

By applying the operator at each node, we will be able to form a matrix of coefficients of w, which along with the  $q_i$  vector will form the right hand side of equation (2.14) as

$$\{q\} + [bw] \{w\}$$

where {q} is the lateral load vector and [bw] is the coefficient matrix containing constants. Similarly, application of the operator of Figure (2.8) will result in the formation of matrix  $D_r[aw]\{w\}$  in the left hand side of equation (2.14). [aw] is a constant coefficient matrix.

Therefore, we can represent the equilibrium equation in  $\mathbf{n}_{\mathbf{u}}$ 



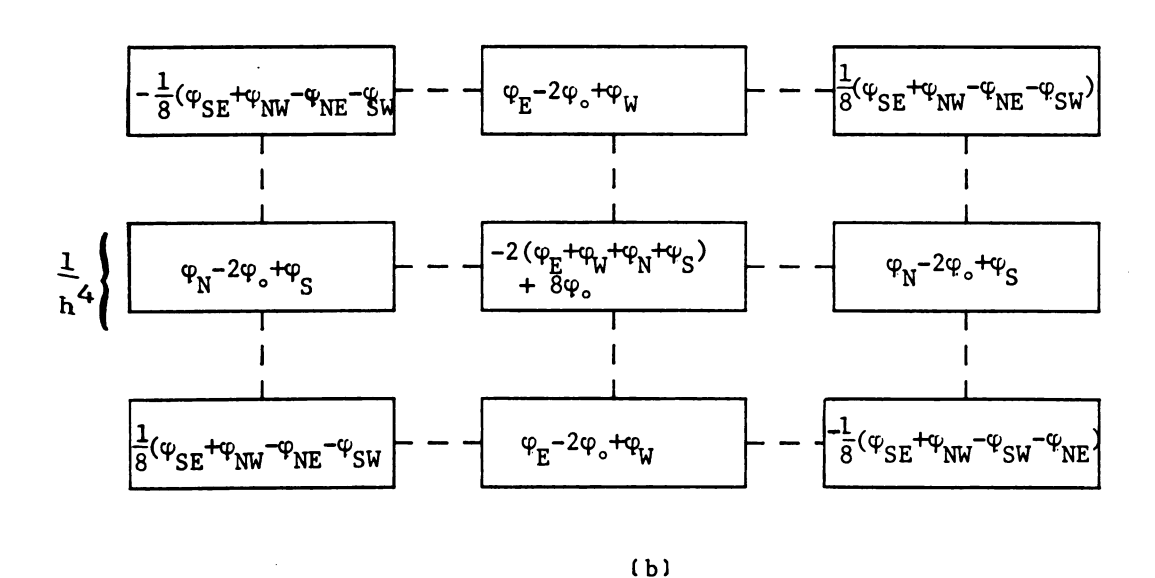


FIG 2.9 DIFFERENCE OPERATOR FOR RIGHT HAND SIDE OF EQUILIBRIUM EQUATION 2.14

$$D_r[aw]\{w\} = \{q\} + [bw]\{w\}.$$
 (2.22)

In complete matrix form we can write

$$D_r[aw]\{w\} = [I]\{q\} + [bw]\{w\}.$$
 (2.23)

Both [aw] and [bw] have a factor of  $\frac{1}{4}$ ; so, we can rewrite

$$D_r[Aw]\{w\} = [I]\{qh^4\} + [Bw]\{w\}$$
 (2.24)

where  $[Aw] = [aw]h^4$ ,  $[Bw] = h^4[bw]$ 

We will discuss solution of this equation later.

#### b) Compatibility Equations.

To approximate the right hand side of the compatibility equation (2.15), we apply relations (2.20) to get

$$\frac{\partial^2 w}{\partial x \partial y} = \frac{w_S E + w_{NW} - w_{SW} - w_{NE}}{4hk}$$

$$\frac{\partial^2 w}{\partial x^2} = \frac{w_E - 2w_0 + w_W}{h^2}$$

$$\frac{\partial^2 w}{\partial y^2} = \frac{w_N - 2w_0 + w_S}{k^2}$$
(2.26)

In order to obtain a finite difference operator representing the left hand side of equation (2.15), we will differentiate and regroup terms, resulting in

$$\frac{1}{\text{Et}} \left\{ \nabla^{4} \varphi - \frac{2}{\text{Et}} \left[ \frac{\partial (\text{Et})}{\partial \mathbf{x}} \frac{\partial}{\partial \mathbf{x}} (\nabla^{2} \varphi) + \frac{\partial (\text{Et})}{\partial \mathbf{y}} \frac{\partial}{\partial \mathbf{y}} (\nabla^{2} \varphi) \right] - \left[ \left( \frac{1}{\text{Et}} \frac{\partial^{2} (\text{Et})}{\partial \mathbf{x}^{2}} - \frac{2}{(\text{Et})^{2}} (\frac{\partial (\text{Et})}{\partial \mathbf{x}})^{2} \right) \right] \\
\left( \frac{\partial^{2} \varphi}{\partial \mathbf{x}^{2}} - \nu \frac{\partial^{2} \varphi}{\partial \mathbf{y}^{2}} \right) \left[ - \left( \frac{1}{\text{Et}} \frac{\partial^{2} (\text{Et})}{\partial \mathbf{y}^{2}} - \frac{2}{(\text{Et})^{2}} (\frac{\partial (\text{Et})}{\partial \mathbf{y}})^{2} \right) \left( \frac{\partial^{2} \varphi}{\partial \mathbf{y}^{2}} - \nu \frac{\partial^{2} \varphi}{\partial \mathbf{x}^{2}} \right) \right] \\
+ 2(1 + \nu) \left[ \frac{\partial (\text{Et})}{\partial \mathbf{x}} \frac{\partial (\text{Et})}{\partial \mathbf{y}} - \frac{2}{(\text{Et})^{2}} - \frac{1}{\text{Et}} \frac{\partial^{2} (\text{Et})}{\partial \mathbf{x} \partial \mathbf{y}} \right] \frac{\partial^{2} \varphi}{\partial \mathbf{x} \partial \mathbf{y}} \right\}.$$

Now by applying relations (2.20) and adding all contributions at each node, we will obtain the finite difference operator of Figure (2.10),

where

$$\beta_{\mathbf{i}} = \frac{K_{\mathbf{i}}}{K_{\mathbf{r}}}$$

 $K_r$ = Et = in-plane rigidity of the plate at center.

 $K_i = in-plane rigidity at point i.$ 

If  $\alpha = \frac{h}{k} = 1$ , this operator will be simplified to the one given in Appendix (A.03)

An alternate approximation to the compatibility equation (2.15) in finite difference form can be developed.

# Denoting

$$F_{1} = \frac{1}{K} (\varphi_{yy} - \vee \varphi_{xx})$$

$$F_{2} = \frac{1}{K} (\varphi_{xx} - \vee \varphi_{yy})$$

$$F_{3} = \frac{1}{K} \varphi_{xy}$$
(2.28)

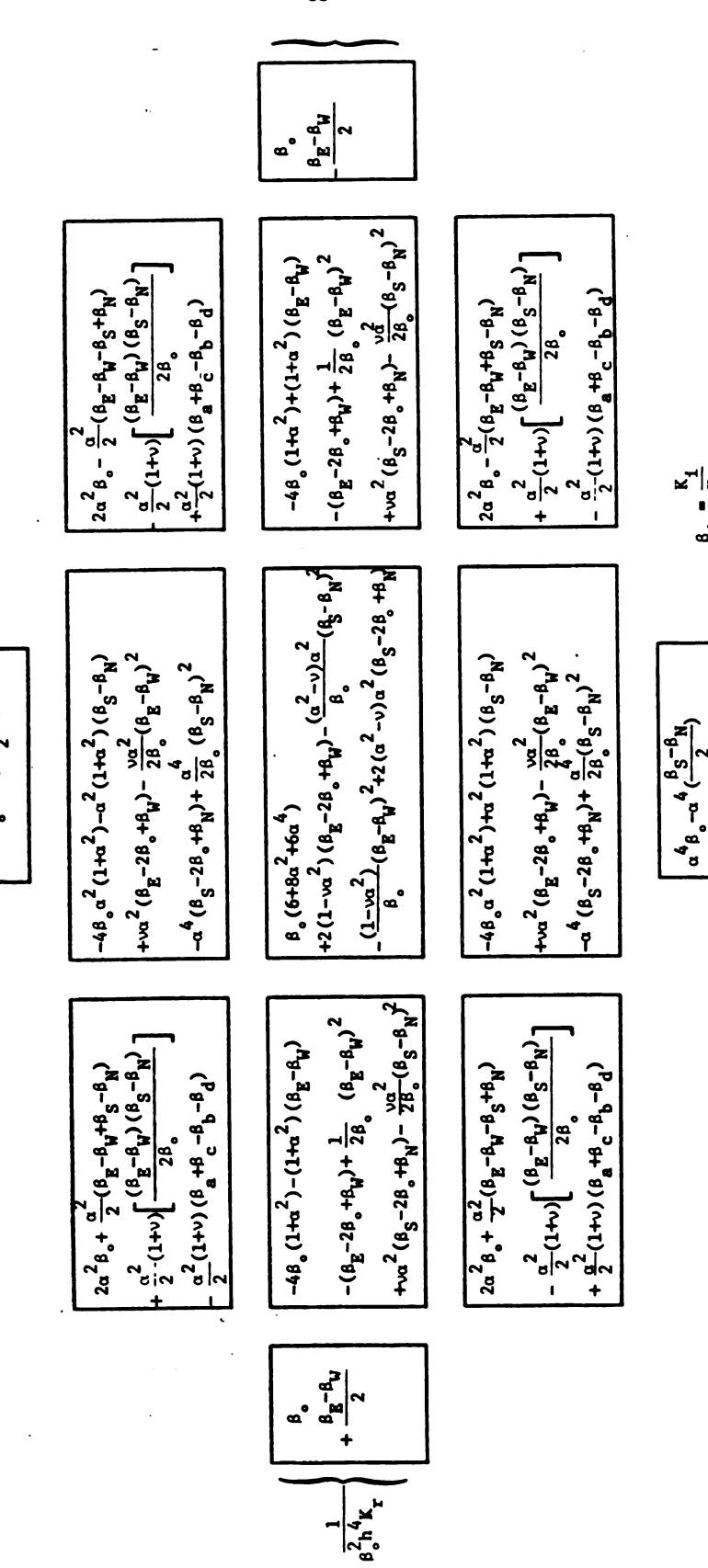


Figure 2.10. Difference operator for left hand side of compatibility equation (2.15).

Equation (2.15) can be written as

$$\frac{\partial^2 F_1}{\partial y^2} + \frac{\partial^2 F_2}{\partial x^2} + 2(1+v) \frac{\partial^2 F_3}{\partial x \partial y} = \left(\frac{\partial^2 w}{\partial x \partial y}\right)^2 - \frac{\partial^2 w}{\partial x^2} \frac{\partial^2 w}{\partial y^2} . \tag{2.29}$$

Now we can approximate derivatives of  $F_1$ ,  $F_2$ ,  $F_3$  as

$$\frac{\partial^2 F_1}{\partial y^2} = \frac{F_1 - 2F_1}{S} \frac{+ F_1}{0} + F_1$$
, etc., where  $F_1$ , according to (2.27), can be

approximated as

$$F_{1_{S}} = \frac{1}{K_{S}} \left[ \frac{\varphi_{SS}^{-2\varphi} + \varphi_{0}}{k^{2}} - v \frac{(\varphi_{SE}^{-2\varphi} + \varphi_{SW})}{h^{2}} \right], \text{ etc.}$$

For  $\alpha = \frac{h}{k} = 1$ , this approximation results in the operator given in Appendix (A.4)

# SOLUTION TO THE COMPATIBILITY EQUATION

To be able to solve the compatibility equation, we must have values of w at nodal points. Then, we are able to compute the right hand side at each node using expressions (2.26).

To determine the left hand side, we apply the operator of Figure (2.10) or the one in Appendix (A.3) or (A.4) at each node.

By adding all contributions, a coefficient matrix will be formed. Thus, we have:

$$[A]\{\varphi\} = \{w\} \tag{2.30}$$

where the  $\,\,w\,\,$  vector is known, and solutions of this system of equations results in the  $\,\phi\,\,$  values at prescribed nodes.

# c) Approximation to other equations

After solving equilibrium and compatibility equations, we may be interested in calculating in-plane forces and displacements as well as bending stresses. Finite difference approximation to some of these equations will be discussed below.

#### In-plane forces

By definition (2.12) we have:

$$N_{x} = \frac{\partial^{2} \varphi}{\partial y^{2}} = \frac{\varphi_{S}^{-2} \varphi_{0} + \varphi_{N}}{k^{2}}$$

$$N_{y} = \frac{\partial^{2} \varphi}{\partial x^{2}} = \frac{\varphi_{E}^{-2} \varphi_{0} + \varphi_{W}}{k^{2}}$$

$$N_{xy} = -\frac{\partial^{2} \varphi}{\partial x^{2}} = -\frac{\varphi_{SE}^{-2} \varphi_{NW}^{-2} \varphi_{SW}^{-2}}{4kk}$$
(2.31)

## In-plane Displacements

Comparing equations (2.7) and (2.11)

$$\varepsilon_{x} = \frac{\partial u}{\partial x} + \frac{1}{2} (\frac{\partial w}{\partial x})^{2} = \frac{1}{Et} (N_{x} - vN_{y})$$

or

$$\frac{\partial u}{\partial x} = \frac{1}{Et} (N_x - vNy) - \frac{1}{2} (\frac{\partial w}{\partial x})^2$$

The right hand side of this equation is known. By approximating the left hand side in finite difference form we have

$$\frac{u_E^{-u}W}{2h} = \frac{1}{Et}(N_x - vN_y) - \frac{1}{2}(\frac{\partial w}{\partial x})^2$$

or

$$\mathbf{u}_{\mathbf{E}} - \mathbf{u}_{\mathbf{W}} = 2h \left[ \frac{1}{Et} (\mathbf{N}_{\mathbf{x}} - \mathbf{v} \mathbf{N}_{\mathbf{y}}) - \frac{1}{2} \left( \frac{\partial \mathbf{w}}{\partial \mathbf{x}} \right)^{2} \right]$$
 (1)

similarly, for v displacement, we obtain

(2.32)

$$\mathbf{v}_{S}^{-}\mathbf{v}_{N} = 2k\left[\frac{1}{Et}(\mathbf{N}_{y}^{-}\vee\mathbf{N}_{x}) - \frac{1}{2}(\frac{\partial\mathbf{w}}{\partial y})^{2}\right]$$
 (ii)

If we apply the operator of the left hand side of equations (2.32) (i) and (ii) at each node and add all contributions, we can form two coefficient matrices for u and v as

$$[Au]{u} = {Bu}$$
 (2.33)

$$[Av]{v} = {Bv}.$$
 (2.34)

where [Au], [Bu], [Av] and [Bv] consist of constants only.

Solving these systems of equations, we obtain  $\, u \,$  and  $\, v \,$ , the displacements at each node.

#### Note:

In order to get compatible displacements, we need to have some points at which u, v or both are known. Points of this nature can be found on boundaries or lines of symmetry.

#### BENDING MOMENTS

Having the solution for w displacement, we use approximations (2.20) to compute bending moments according to equations (2.8).

787 Uni

> Sir Sir

.../

7.

ì

$$M_{x} = -D(\frac{\partial^{2}w}{\partial x^{2}} + v\frac{\partial^{2}w}{\partial y^{2}}) = -D[\frac{w_{E}^{-2w_{O}^{+}w_{W}}}{h^{2}} + v\frac{w_{S}^{-2w_{O}^{+}w_{N}}}{k^{2}}]$$

$$M_{y} = -D(\frac{\partial^{2}w}{\partial y^{2}} + v\frac{\partial^{2}w}{\partial x^{2}}) = -D[\frac{w_{S}^{-2w_{O}^{+}w_{W}}}{k^{2}} + v\frac{w_{E}^{-2w_{O}^{+}w_{W}}}{h^{2}}]$$

$$M_{xy} = -D(1-v)\frac{\partial^{2}w}{\partial x\partial y} = D(1-v)(\frac{w_{SE}^{+w_{NW}^{-w_{SW}^{-}w_{NE}}}}{4hk})$$
(2.35)

where D is already defined.

# 2.4.3 FINITE DIFFERENCE APPROXIMATION OF METHOD DISCUSSED IN SECTION (2.3)

In this method, 3 equilibrium equations in the x, y and z directions, as derived in (2.16), (2.17) and (2.18) respectively, must be solved. In this section, the finite difference approximation of each equation will be derived.

#### a) Equilibrium in x-direction

Considering the equilibrium equation (2.16) and regrouping variables results in

$$\begin{bmatrix} K \frac{\partial^{2} u}{\partial x^{2}} + \frac{K(1-v)}{2} \frac{\partial^{2} u}{\partial y^{2}} + \frac{\partial K}{\partial x} \frac{\partial u}{\partial x} + \frac{1-v}{2} \frac{\partial K}{\partial y} \frac{\partial u}{\partial y} \end{bmatrix} + \\
\begin{bmatrix} \frac{K(1+v)}{2} \frac{\partial^{2} v}{\partial x \partial y} + v \frac{\partial K}{\partial x} \frac{\partial v}{\partial y} + \frac{1-v}{2} \frac{\partial K}{\partial y} \frac{\partial v}{\partial x} \end{bmatrix} + \\
\{ K \frac{\partial^{2} w}{\partial x^{2}} \frac{\partial w}{\partial x} + \frac{K(1+v)}{2} \frac{\partial^{2} w}{\partial x \partial y} \frac{\partial w}{\partial y} + \frac{K(1-v)}{2} \frac{\partial^{2} w}{\partial y^{2}} \frac{\partial w}{\partial x} + \\
\frac{1}{2} \frac{\partial K}{\partial x} \left[ (\frac{\partial w}{\partial x})^{2} + v(\frac{\partial w}{\partial y})^{2} \right] + \frac{1-v}{2} \frac{\partial K}{\partial y} \frac{\partial w}{\partial x} \frac{\partial w}{\partial y} \frac{\partial w}{\partial y} = 0$$

where K = Et and both sides of equation (2.16) have been multiplied by  $(1-v^2)$ 

Now, the difference approximations, (2.20), will be applied and the results will be represented as finite difference operators.

2 3 I .... i, `÷. ... The operator representing the u contribution to this equation is given in Figure (2.11-a). Similarly, difference approximation to v results in operator Figure (2.11-b).

The contribution of w to this equation can be approximated as

Therefore, the equilibrium in the x-direction can be schematically shown as.

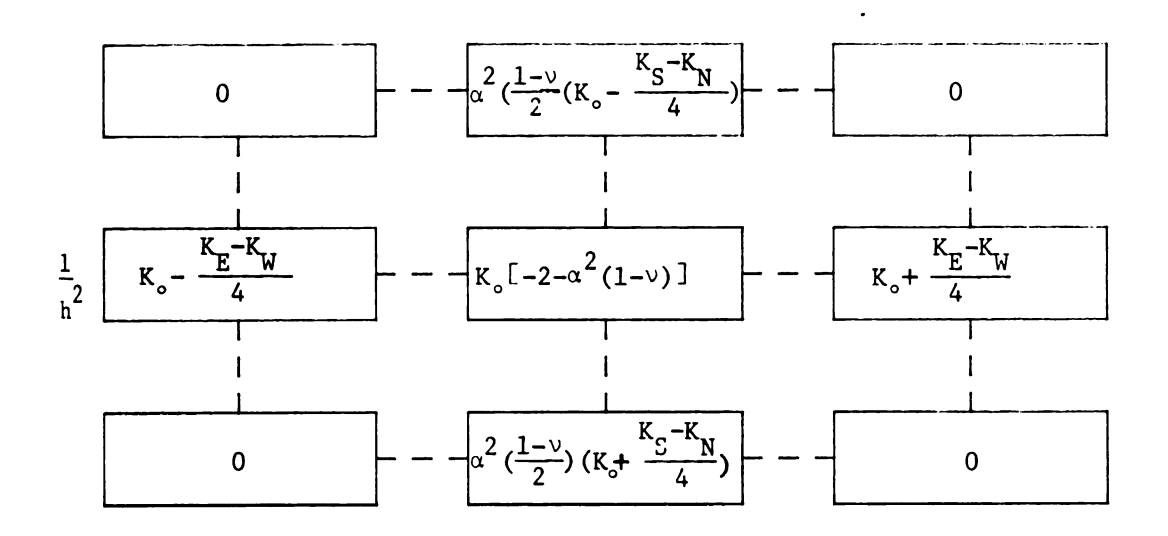
(u-operator) 
$$u + (v-operator) v + xw$$
 function = 0 (2.36)

Note: In this case, because of the absence of body force in the x-direction, the right hand side of the equation is always zero; thus the equation is first divided by  $(\frac{1}{1-\nu^2})$ .

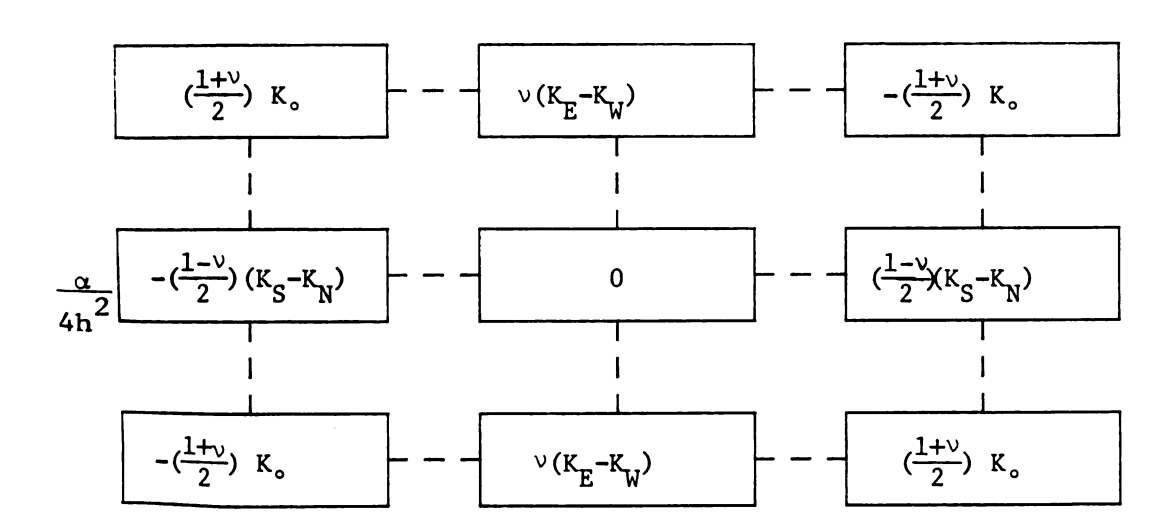
#### b) Equilibrium in y-direction

The same procedure will be followed to derive operators representing finite difference approximations to equilibrium in the y-direction.

Equilibrium equation (2.17) can be rewritten (after regrouping variables u, v and w, and dividing by  $(\frac{1}{1-v^2})$ ) as



a) U-OPERATOR



ы V-OPERATOR

FIG 2.11 OPERATORS FOR X-EQUILIBRIUM EQ.(2.16)

$$\left[K\frac{(1+\nu)}{2} \frac{\partial^{2} u}{\partial x \partial y} + \frac{1-\nu}{2} \frac{\partial K}{\partial x} \frac{\partial u}{\partial y} + \nu \frac{\partial K}{\partial y} \frac{\partial u}{\partial x}\right] + \left[\frac{K(1-\nu)}{2} \frac{\partial^{2} v}{\partial x^{2}} + K \frac{\partial^{2} v}{\partial y^{2}} + \frac{1-\nu}{2} \frac{\partial K}{\partial x} \frac{\partial v}{\partial x} + \frac{\partial K}{\partial y} \frac{\partial v}{\partial y}\right] + \left[K \frac{\partial^{2} w}{\partial y^{2}} \frac{\partial w}{\partial y} + \frac{K(1+\nu)}{2} \frac{\partial^{2} w}{\partial x \partial y} \frac{\partial w}{\partial x} + \frac{K(1-\nu)}{2} \frac{\partial^{2} w}{\partial x^{2}} \frac{\partial w}{\partial y} + \dots \right] + \left[\frac{1}{2} \frac{\partial K}{\partial y} \left(\frac{\partial w}{\partial y}\right)^{2} + \nu \left(\frac{\partial w}{\partial x}\right)^{2}\right] + \frac{1-\nu}{2} \frac{\partial K}{\partial x} \frac{\partial w}{\partial x} \frac{\partial w}{\partial x} \frac{\partial w}{\partial y}\right] = 0$$

By finite difference approximation, we obtain the operator of Figure (2.12-a) to represent the u-contribution and (2.12-b) as the v-operator.

Terms including w can be approximated as:

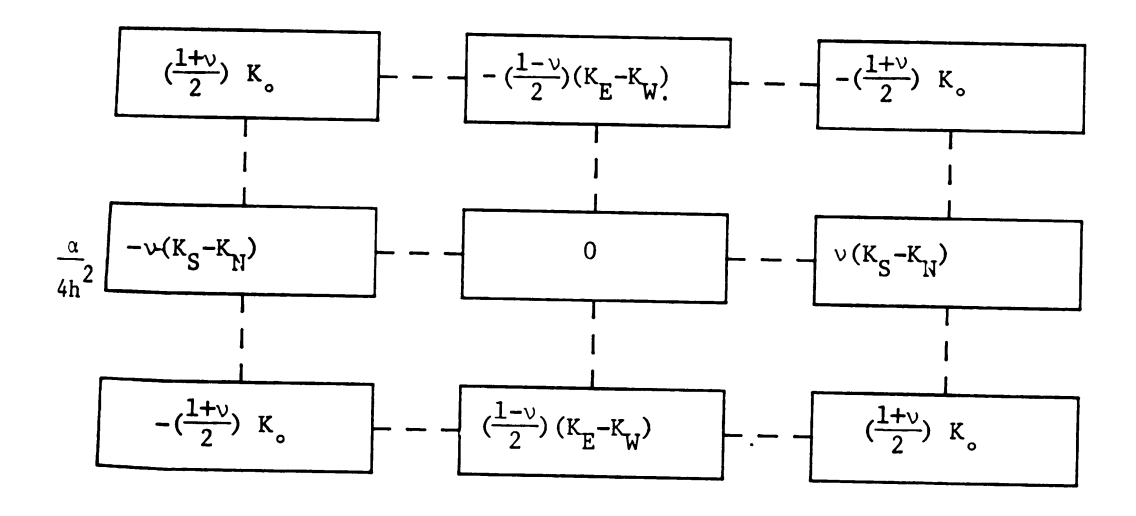
$$\begin{array}{l} \text{yw function} \, = \, \frac{\alpha^2 K_0^{\left(1+\nu\right)}}{2} [\, (\frac{w_{SE}^{+w}_{NW}^{-w}_{SW}^{-w}_{NE}}{4h^2}) \, (\frac{w_{E}^{-w}_{W}}{2h})] + \frac{K_0^{\left(1-\nu\right)}}{2} [\, (\frac{w_{E}^{-2w}_0^{+w}_{W}}{h^2}) \, (\frac{w_{S}^{-w}_{N}}{2h}) \, ] + \\ K_0^{\alpha^3} [\, (\frac{w_{S}^{-2w}_0^{+w}_N}{h^2}) \, (\frac{w_{S}^{-w}_N}{2h}) \, ] + (\frac{1-\nu}{2}) \frac{K_E^{-K}_W}{2h} \alpha \, (\frac{w_{E}^{-w}_W}{2h}) \, (\frac{w_{S}^{-w}_N}{2h}) \, + \\ \alpha \, (\frac{K_S^{-K}_N}{2h}) \, [\frac{\alpha^2}{2} (\frac{w_{S}^{-w}_N}{2h})^2 \, + \frac{\nu}{2} (\frac{w_{E}^{-w}_W}{2h})^2] \end{array}$$

Finally, the equilibrium equation in the y-direction can be represented in the following operator scheme:

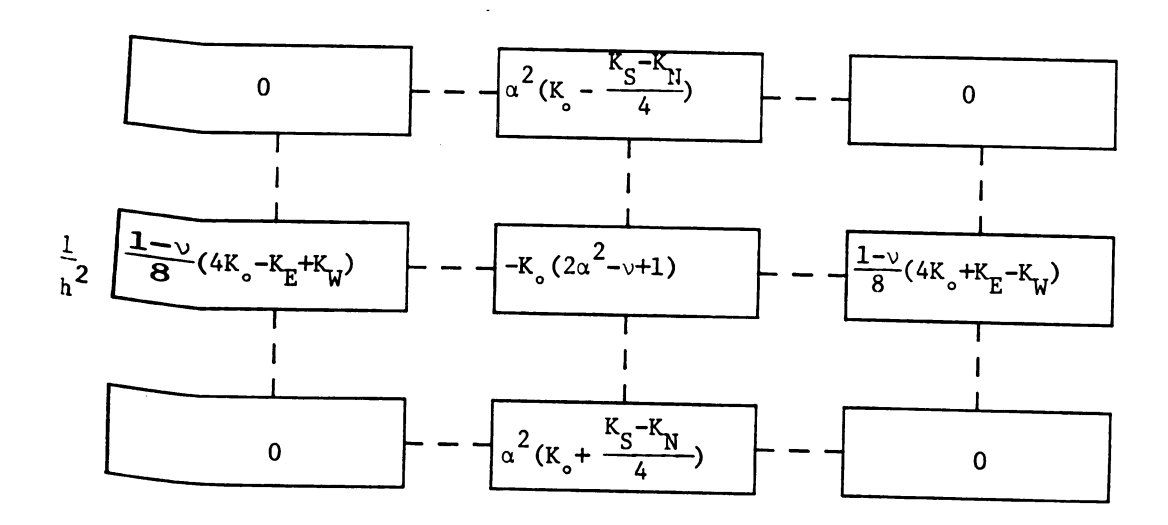
$$(u-operator) u + (v-operator) v + yw function = 0$$
 (2.38)

# c) Equilibrium in z-direction

The equation of equilibrium in the out-of-plane direction is introduced in Equation (2.18).



### a) U-OPERATOR



# b) V-OPERATOR

FIG 2.12 OPERATORS FOR Y-EQUILIBRIUM EQ.(2.17)

Approximation to the left hand side of this equation has already been explained in Section (2.3.2-a).

As for the right hand side, we approximate the derivatives of displacements to get .

$$(RHS) = q + \frac{K}{1-v^2} \left\{ \left[ \left( \frac{u_E^{-u}W}{2h} \right) + \frac{1}{2} \left( \frac{w_E^{-w}W}{2h} \right)^2 + v\alpha \left( \frac{v_S^{-v}N}{2h} \right) + \frac{v\alpha^2}{2} \left( \frac{w_S^{-w}N}{2h} \right)^2 \right]$$

$$\left( \frac{w_E^{-2w}O^{+w}W}{h^2} \right) + \left[ \alpha \left( \frac{v_S^{-v}N}{2h} \right) + \frac{\alpha^2}{2} \left( \frac{w_S^{-w}N}{2h} \right)^2 + v \left( \frac{u_E^{-u}W}{2h} \right) + \frac{v}{2} \left( \frac{w_E^{-w}W}{2h} \right)^2 \right]$$

$$\alpha^2 \left( \frac{w_S^{-2w}O^{+w}N}{h^2} \right) + (1-v) \left[ \alpha \left( \frac{u_S^{-u}N}{2h} \right) + \left( \frac{v_E^{-v}W}{2h} \right) + \alpha \left( \frac{w_E^{-w}W}{2h} \right) \left( \frac{w_S^{-w}N}{2h} \right) \right]$$

$$\alpha \left( \frac{w_SE^{+w}Nw^{-w}Sw^{-w}NE}{4h^2} \right)$$

$$(2.39)$$

Finally, equilibrium in the z-direction can be represented

$$[Aw]{w} = RHS \tag{2.40}$$

where matrix [Aw] consists of contants.

# d) Solution procedure using this method

In order to perform numerical analysis in computer programs, we arrange the equations in such a way that the equations can be represented in matrix form.

To find a solution by this method, we must satisfy all three equilibrium equations. These contain three unknowns, u, v, and w.

There is no simple technique providing a direct solution to these coupled nonlinear equations; thus, we employ an iterative technique solve them.

If w is known (or assumed), the first two equations of equilibrium will become two uncoupled equations in u and v

and can be solved as follows.

Applying the u-operator corresponding to equilibrium in x at each node and adding the contributions, and doing the same to the v-operator, we get a matrix representation of equation (2.16) as

$$[Au1]_{N\times N} \{u\}_{N\times 1} + [Av1]_{N\times N} \{v\}_{N\times 1} = -\{xw \text{ Function}\}_{N\times 1}$$
 (2.41)

Repeating the same procedure for y-equilibrium equation (2.17) we obtain

$$[Au2]_{N\times N}^{\{u\}}_{N\times 1} + [Av2]_{N\times N}^{\{v\}}_{N\times 1} = -\{yw Function\}_{N\times 1}$$
 (2.42)

where [Aul], [Avl], [Au2] and [Av2] are constant coefficient matrices.

Both equations are coupled in u and v, and each contains N equations in 2N unknowns.

One way of approaching this problem is to try to solve the equations by iteration until reaching a solution that satisfies both equations.

An easier approach can be employed if we realize that, although the equations are coupled in u and v, there are no mixed terms containing both u and v.

Therefore, we can combine the two, to get

$$\begin{bmatrix} Aul & Av1 \\ ----- \\ Au2 & Av2 \end{bmatrix} \begin{cases} u \\ v \end{cases} = - \begin{cases} xw \text{ Function} \\ ----- \\ yw \text{ Function} \end{cases}$$
 (2.43)

which is not only more efficient in computer programming but leads
to a unique solution for the u and v displacements at specified
node points, based on an assumed (or known) w.

of u, v and w, in the right hand side (2.39), and solve equation (2.40) for new values of w. The iteration will continue until the new values of u, v and w, are equal to or very close to old ones. A practical use of this method, including the details, will be demonstrated in chapter 3.

## POST SOLUTION DETAILS

After a solution is found for the three displacements  ${\bf u}$ ,  ${\bf v}$  and  ${\bf w}$ , any components of stress and strain can be computed.

# Average strain

Average strain at each node can be found by the finite difference approximation of equations (2.7).

$$\varepsilon_{\mathbf{x}} = \frac{\mathbf{u}_{\mathbf{E}}^{-\mathbf{u}_{\mathbf{W}}}}{2h} + \frac{1}{2} \left( \frac{\mathbf{w}_{\mathbf{E}}^{-\mathbf{w}_{\mathbf{W}}}}{2h} \right)^{2}$$

$$\varepsilon_{\mathbf{y}} = \frac{\mathbf{v}_{\mathbf{S}}^{-\mathbf{v}_{\mathbf{N}}}}{2h} + \frac{\alpha^{2}}{2} \left( \frac{\mathbf{w}_{\mathbf{S}}^{-\mathbf{w}_{\mathbf{N}}}}{2h} \right)^{2}$$

$$\gamma_{\mathbf{x}\mathbf{y}} = \alpha \left( \frac{\mathbf{u}_{\mathbf{S}}^{-\mathbf{u}_{\mathbf{N}}}}{2h} \right) + \frac{\mathbf{v}_{\mathbf{E}}^{-\mathbf{v}_{\mathbf{W}}}}{2h} + \alpha \left( \frac{\mathbf{w}_{\mathbf{E}}^{-\mathbf{w}_{\mathbf{W}}}}{2h} \right) \left( \frac{\mathbf{w}_{\mathbf{S}}^{-\mathbf{w}_{\mathbf{N}}}}{2h} \right)$$
(2.44)

# Membrane Forces

Substitution of equations (2.7) into (2.6) and approximating the derivatives by finite differences, will result in

$$\mathbf{N}_{\mathbf{x}} = \frac{K}{1-\nu^{2}} \left[ \frac{\mathbf{u}_{E}^{-\mathbf{u}_{W}}}{2h} + \frac{1}{2} \left( \frac{\mathbf{w}_{E}^{-\mathbf{w}_{W}}}{2h} \right)^{2} + \nu\alpha \left( \frac{\mathbf{v}_{S}^{-\mathbf{v}_{N}}}{2h} \right) + \frac{\nu\alpha^{2}}{2} \left( \frac{\mathbf{w}_{S}^{-\mathbf{w}_{N}}}{2h} \right)^{2} \right]$$

$$\mathbf{N}_{\mathbf{y}} = \frac{K}{1-\nu^{2}} \left[ \alpha \left( \frac{\mathbf{v}_{S}^{-\mathbf{v}_{N}}}{2h} \right) + \frac{\alpha^{2}}{2} \left( \frac{\mathbf{w}_{S}^{-\mathbf{w}_{N}}}{2h} \right)^{2} + \nu \left( \frac{\mathbf{u}_{E}^{-\mathbf{u}_{W}}}{2h} \right) + \frac{\nu}{2} \left( \frac{\mathbf{w}_{E}^{-\mathbf{w}_{W}}}{2h} \right)^{2} \right]$$

$$\mathbf{N}_{\mathbf{x}, \mathbf{y}} = \frac{K(1-\nu)}{2(1-\nu^{2})} \left[ \alpha \left( \frac{\mathbf{u}_{S}^{-\mathbf{u}_{N}}}{2h} \right) + \left( \frac{\mathbf{v}_{E}^{-\mathbf{v}_{W}}}{2h} \right) + \alpha \left( \frac{\mathbf{w}_{E}^{-\mathbf{w}_{W}}}{2h} \right) \left( \frac{\mathbf{w}_{S}^{-\mathbf{w}_{N}}}{2h} \right) \right]$$
(2.45)

#### BENDING MOMENTS

The bending moment approximation is given in equations (2.35).

#### 2.5 BOUNDARY CONDITIONS

In the small deflection theory of plates, we consider only

out of plane (or flexural) boundary conditions because the effect

of in-plane displacements on the boundary is negligible. However,

they become the chief factor in large deflections behavior and in

the postbuckling range. Thus, we discuss in-plane boundary conditions

as well as out of plane conditions.

The flexural boundary conditions, as commonly discussed in elementary plate theory, are:

a) Simply-supported boundary

$$w = 0$$

$$M_{x} = -D \left( \frac{\partial^{2} w}{\partial x^{2}} + v \frac{\partial^{2} w}{\partial y^{2}} \right) = 0$$
 (on boundaries parallel to y)

b) Fixed boundary:

$$\frac{\partial \mathbf{w}}{\partial \mathbf{n}} = 0$$
 (n, normal to the boundary)

Free boundary:

$$M_{\mathbf{x}} = 0$$

$$V_{x} = Q_{x} + \frac{\partial M}{\partial y} = 0$$

Others, such as elastic support, or partially fixed support, etc.

For the in-plane boundary conditions, there is a variety of possible combinations that may occur in the postbuckling range.

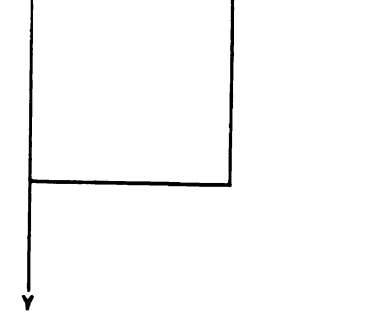
On each edge, either u or v displacements can either be unrestrained or have some specified values; also, there could be restrictions on derivatives of either u or v, or both.

In terms of in-plane boundary conditions, we can classify the problem in three major types.

1) - Force boundary conditions (i.e. in-plane forces are specified on the boundary).

If applied forces  $N_x$ ,  $N_y$  and  $N_{xy}$  are known, we can use relations (2.12) to choose values of the  $\varphi$  functions on the boundary points so that they satisfy boundary conditions. A practical example of this nature is discussed in chaper 3.

- 2) Displacement boundary condition Some possible cases are:
- a) u and/or v are specified on the boundary, in which case the values of displacements would be
- assigned to boundary points.



- Edge remains straight and parallel to y. (u-displacement is constant all along the x = 0 edge).
- Edge remains straight with no shear force along the edge; in this case, from equations (2.7) and (2.6), we have along edge x = 0,

$$N_{xy} = \frac{Et}{2(1+v)} \left[ \frac{\partial u}{\partial y} + \frac{\partial v}{\partial x} + \frac{\partial w}{\partial x} \frac{\partial w}{\partial y} \right] = 0$$
 (2.46)

On supported edges (fixed or hinged),  $\frac{\partial w}{\partial y} = 0$ , thus

$$-\frac{\partial \mathbf{v}}{\partial \mathbf{x}} = \frac{\partial \mathbf{u}}{\partial \mathbf{v}} \quad . \tag{1}$$

If the x-edge (x = constant) is straight with u constant, then  $\frac{\partial \mathbf{u}}{\partial \mathbf{y}} = 0$ ; therefore, equation (i) results in  $\frac{\partial \mathbf{v}}{\partial \mathbf{x}} = 0$  along the edge.

- d) Other conditions include possible restrictions on u, v or their derivatives which lead to particular relations between displacements or their difference approximations. For example, the edge can be subjected to thermal expansion (see section 3.2) such that  $\frac{\partial u}{\partial x} = \varepsilon_x = \text{constant along edge } y = 0$ .
- 3) Mixed boundary conditions. i.e., case 1 applies to part of the boundary, while the rest of the boundary is defined by case 2.

The computer program developed can solve either case 1 or 2.

Therefore, to handle a problem with mixed boundary conditions, we can solve the problem by trial and error, as follows.

- i) Assign some fictitious displacement values to the points at which forces are specified, and solve the problem as one with displacement boundary conditions.
- ii) Compute forces at the boundary points.
- iii) Compare with actual forces at the points.
- iv) Correct previous fictitious displacements in such a way that the solution is improved.
- v) Repeat steps (ii) to (iv) until the computed forces are equal to or close enough to the actual ones.

## 2.5.1 SOME EXAMPLES OF PRACTICAL B.C.

Following is a list of some practical examples of plates subject to various loading and boundary conditions.

- Window glass can undergo large deflection under lateral wind pressure; the out-of-plane boundary condition is in most cases simply-supported or sometimes built-in. Either case may be accompanied by:
  - a) in-plane displacement possible.
  - b) in-plane displacement restricted.
- Plates on stringers forcing the plate edges to remain straight,
   as in many ship and aircraft sections surrounded by stringers.
- 3. Mechanical and instrumental plate elements subject to temperature change will be subjected to tension or compression on some or all edges due to temperature change in surrounding elements. Various combinations of boundary conditions are possible.
- 4. The webs of structural steel profiles used in construction can be categorized as plates subject to in-plane shear and normal forces along the edges.

# 2.6 SUMMARY

We will summarize the theoretical formulations discussed in Chapter 2, and mention procedures of solving some problems.

Among several types of problems which can be solved numerically based on the finite difference approximations shown, and using the computer program which has been written, are:

#### 2.6.1 MEMBRANE SOLUTION

For flat plate with w = 0 everywhere, the equilibrium in the z-direction (normal to the plane of the plate) is trivial; to find a solution for in-plane resultants and displacements,

a) In the case of force boundary condition, we solve compatibility equation (2.30) with the w vector equal to zero.

$$[A]\{\varphi\} = 0 \tag{2.47}$$

The solution results in  $\phi$  values at discrete nodes, which can be used in equations (2.31), (2.32), and (2.33) to find in-plane forces and displacements.

b) If the displacements are specified on the boundaries, we solve equation (2.43). Considering w = 0 everywhere, we have

$$\begin{bmatrix}
Au1 & Av1 \\
----- \\
Au2 & Av2
\end{bmatrix}
\begin{cases}
u \\
v
\end{bmatrix}
=
\begin{bmatrix}
0 \\
0
\end{bmatrix}$$
(2.48)

For which the solution results in displacement values at the nodes.

Application of equation (2.45) then leads to the membrane resultants.

2.6.2 LATERAL LOADING

## a) Force boundary conditions.

i) Small displacement. In this case, the  $\phi$  values and in-plane resultants are known from (2.5.1), so we can solve the equilibrium equation (2.25) to obtain w. Then (2.33), (2.34) and (2.35), can be applied to

compute in-plane resultants, displacements and bending moments.

ii) Large deflection.

Compatibility equation (2.30) and equilibrium equation (2.24) could be solved iteratively, and the force resultants and displacements can be calculated as discussed in (i).

- b) Displacement boundary conditions
  - i) For small deflections, we can solve equation (2.48), neglecting the effect of w on in-plane solutions; then, solve the z-equilibrium equation (2.40) for w, by ignoring w-terms in the RHS.
  - ii) Large displacement problem this requires an iterative solution of equations (2.40) and (2.43) as discussed in 2.3.3 (d).

# 2.6.3 STABILITY ANALYSIS

a) Force boundary conditions.

The in-plane forces and  $\phi$  values are known from part 2.5.1 -a; then, we can use the equilibrium equation (2.25). If q=0, this will result in a characteristic matrix, the eigenvalues of which lead to the critical forces and the eigenvectors represent the buckling modes.

b) Displacement boundary condition.

Using in-plane resultants and displacements obtained from (2.5.1.b) and forming the R.H.S. as a coefficient matrix for w, with q=0, results in the characteristic matrix equation

$$\{[Aw] - [Bw]\} \{w\} = 0,$$
 (2.49)

for which the eigenvalues and eigenvectors lead to critical boundary displacements and the mode shapes, respectively.

## 2.6.4 POSTBUCKLING

Since after buckling the plate takes on a state of stable equilibrium, we can analyze the plate as a regular large deflection case.

- a) Force boundary condition.
  We solve the equilibrium equation (2.24) and the compatibility equation (2.30) iteratively.
- b) Displacement boundary condtions.

  In this case we employ the iteration technique to solve the z-equilibrium equation (2.40) and the in-plane equilibrium equation (2.48).

#### CHAPTER III

#### APPLICATION AND RESULTS

In this chapter, the theory and the methods developed in the preceding chapters are applied to a variety of problems. A computer program has been developed which is applicable to rectangular plates with different boundary conditions and variation in stiffness. The objective is to illustrate the application of the method to plates with several types of variations in stiffness, as well as to the uniform stiffness plates. Since solutions to the uniform stiffness plate are known, it provides a good measure for verifying the accuracy of the solution procedure. For the plates considered, the solution is obtained for a few problems for all successive steps of loading from zero load up to secondary buckling and the results are analyzed.

Convergence of the solution is checked and accuracy of the results is examined via comparison with known results when possible. Some optimization problems are presented at the end of each section.

Chapter III is divided into two sections. Section 3.1

deals with force boundary conditions. In section 3.2, plates with

displacement boundary conditions are considered.

A square plate with a symmetrical variation in stiffness is considered. Stiffness is symmetric with respect to both centerlines and diagonals as shown in Figure 3.1; thus only a quadrant of the plate will be considered. The variation in stiffness is such that

in quadrant (I) of the plate (see Figure 3.1) the stiffness is a function of x only. For example, in section 3.1 a parabolic variation in stiffness is considered; the flexural stiffness can be represented by a parabolic equation:

$$D(x) = D_{r}[R + 4(1-R)(\frac{x}{a})^{2}]$$
 (3.1)

where D is stiffness at point x

 $D_{r}$  is stiffness at center of the plate

R is ratio of edge stiffness to center stiffness

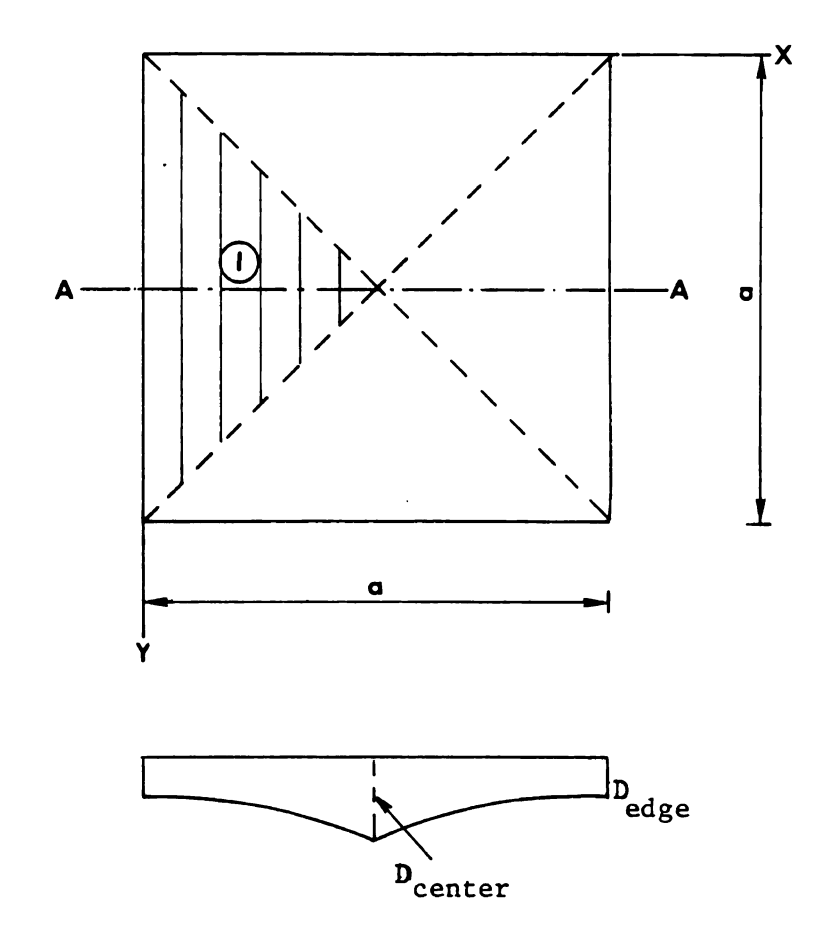
a is length of each edge of square plate

# Note:

Since bending stiffness,  $D=\frac{Et^3}{12(1-v^2)}$ , and membrane stiffness, K=Et, are both present in the plate equations, it will make a difference whether the stiffness variation is due to a variation in E or in t.

a) For the variation in E, with t constant, the D variation and K variation will have the same pattern. Let  $\beta_i = \frac{K_i}{K_r}$ , the ratio of membrane stiffness at point i to membrane stiffenss at reference point, and let  $\delta_i = \frac{D_i}{D_r}$  be the bending stiffness ratio at corresponding points. Then,

$$\frac{\beta_{i}}{\delta_{i}} = \frac{E_{i}t/E_{r}t}{E_{i}t^{3}/E_{r}t^{3}} = 1 \qquad \text{or} \quad \beta_{i} = \delta_{i}$$



Stiffness variation at section A-A

Figure 3.1. Geometry and stiffness variation of square plate.

b) For the variation in t, with E constant,

$$\beta_{i} = \frac{K_{i}}{K_{r}} = \frac{Et_{i}}{Et_{r}} = \frac{t_{i}}{t_{r}}$$

$$\delta_{i} = \frac{D_{i}}{D_{r}} = \frac{\frac{Et_{i}^{3}}{12(1-v^{2})}}{\frac{Et_{r}^{3}}{12(1-v^{2})}} = \frac{t_{i}^{3}}{t_{r}^{3}} = \left(\frac{t_{i}}{t_{r}}\right)^{3} = \beta_{i}^{3}, \text{ or } \beta_{i} = \sqrt[3]{\delta_{i}}.$$

Both cases can be considered without any major difficulties. In section 3.1 (excluding 3.1.4) case (a) is assumed, and in 3.1.4 and the entire section 3.2, the variable thickness case (b) is considered.

In terms of boundary conditions, two separate classes of Problems are considered:

- 1 Force boundary condition
- 2 Displacement boundary conditon

In order to avoid computational difficulties, the following non-dimensional variables are introduced and frequently used in the analysis.

$$t' = t/t_i$$
 where  $t_i = unit thickness.$ 

$$D' = D/t_i^3,$$

 $_{\rm O}^{\rm D}$  = flexural stiffness of a uniform stiffness, unit thickness plate.

K membrane rigidity of a uniform stiffness, unit thickness plate.

$$Y = v/a$$

$$W = w/t_i$$

$$U = ua/t_{1}^{2}$$

$$V = va/t_{1}^{2}$$

$$(N'_{x}; Ny'; N'_{xy}) = (N_{x}; N_{y}; N_{xy})/N_{cr}$$

$$(N'_{x}; N'_{y}; N'_{xy}) = (\frac{a^{2}}{D_{o}})(N_{x}; N_{y}; N_{xy})/N_{cr}$$

$$(N'_{x}; N'_{y}; N'_{xy}) = (\frac{a^{2}}{D_{o}})(N_{x}; N_{y}; N_{xy})/N$$

$$(N'_{x}; N'_{y}; N'_{xy}) = (N_{x}; N_{y}; N_{xy})/N$$

$$(N'_{x}; N'_{y}; N'_{xy}) = (\frac{a^{2}}{D_{o}t_{1}})(M'_{x}; M'_{y}; M'_{xy})$$

$$(N'_{x}; N'_{y}; N'_{xy}) = (N'_{x}; N'_{y}; N'_{xy})/N$$

$$($$

# 3.1 Force Boundary Condition

The previously mentioned plate case (a) is considered subject to a compressive normal in-plane force 'N' on all edges (no restraint on in-plane displacements). The solution is obtained for three successive ranges of loading (membrane, buckling, and postbuckling), for different variations in stiffness, and for both simply supported and fixed edges. The effect of a transverse load is also examined.

The behavior of the plate within each range is observed. For each range the in-plane stress resultants, the in-plane displacements and the out-of-plane displacement are calculated and Plots are given. The results of solution for variable stiffness Plates are compared with those for the uniform stiffness plate. Section 3.1 deals with different phases of the behavior, as follows:

- 3.1.1 Membrane solution
- 3.1.2 Stability analysis
- 3.1.3 Postbuckling behavior

12 32 3

> 11. 28

ä,

in in its

I

. 1e

i at

In order to have a common base in different cases of stiffness variation for comparison of the results, the reference stiffness,  $D_r$ , is taken such that the volume under the stiffness curve be constant for all cases. (i.e., mean stiffness is constant) The stiffness variation in this section is

 $D(x) = D_{r}[R + 4(1-R)(\frac{x}{a})^{2}]$ as introduced in equation
(3.1). The volume under
the curve over a quadrant
of the plate (see Figure
3.2) is vol. =  $2\int_{0}^{a/2} \ln D(x) dx$ where  $\ln \frac{a}{2} - y = \frac{a}{2} - x$ .
Substituting for  $\ln a$  and

D(x) we obtain vol =  $2D_r \int_{a}^{a/2} (\frac{a}{2}x) [R+4(1-R)(\frac{x}{a})^2] dx$ .

Integrating produces

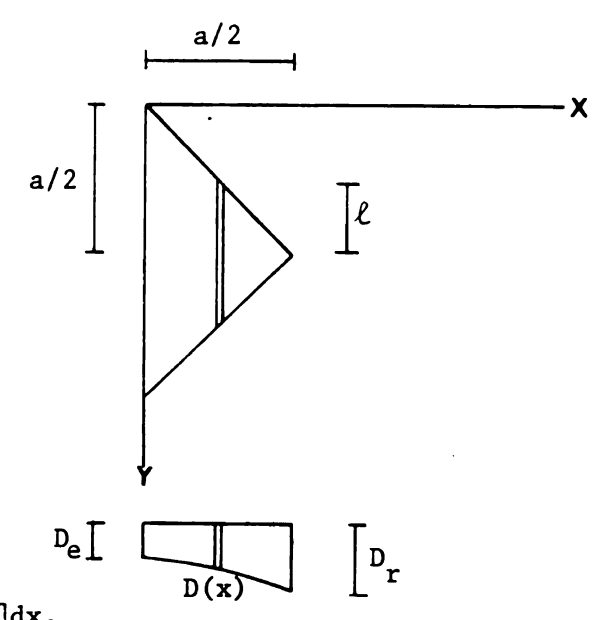


Figure 3.2

$$vol = \frac{a^2D_r}{24} (1 + 5R).$$

This volume is to be constant for all cases; thus, the variation of Dr With R must have the form,

$$D_r = \frac{\text{constant}}{1 + 5R}$$
.

The base stiffness is chosen to be  $\frac{D_r}{D_o} = 1$  for a uniform stiffness plate, and the  $D_r$  for different stiffness ratios are tabulated below:

R D<sub>r</sub>/D<sub>o</sub>

1 1.

1/10 4.

1/2 1.7142857

10 .117647058

## 3.1.1 Membrane Solution

In this part, a flat plate with no initial deflection is considered and the solution obtained. Since w is zero, the solution can be obtained by solving the compatibility equation (2.47) only.

## **Boundary Conditions**

To determine the value of the stress function,  $\varphi$ , along the boundary, recall Equations (2.12); along the x-edges, we have:

$$N_{x} = \frac{\partial^{2} \varphi}{\partial y^{2}} = N \qquad (1)$$

$$N_{xy} = -\frac{\partial^2 \varphi}{\partial x \partial y} = 0 \qquad (ii)$$

From (i) we have

$$\frac{\partial \lambda}{\partial \theta}$$
  $(\frac{\partial \lambda}{\partial \theta}) = -N$ 

integrating

$$\frac{\partial \varphi}{\partial y} = -Ny + c_1 + f_1(x)$$

$$\varphi = \frac{-Ny^2}{2} + c_1 y + y f_1(x) + f_2(x) + c_2$$

but from (ii)

$$\frac{\partial}{\partial y} \left( \frac{\partial \phi}{\partial x} \right) = 0 \to \frac{\partial \phi}{\partial x} = \text{constant along the edge.}$$

$$\therefore \frac{\partial \phi}{\partial x} = y \frac{df_1(x)}{dx} + \frac{df_2(x)}{dx} = \text{constant}$$

From the above we can conclude:

$$\varphi = \frac{-Ny^2}{2} + \overline{c}_1 y + \overline{c}_2$$

similarly, along y-edges, we will get:

$$\varphi = \frac{-Nx^2}{2} + c_3x + c_4$$

The constants must be chosen such that the given boundary conditions are satisfied. Since the second derivatives of  $\phi$  determine the resultants, and, in this case, the plate is symmetrical with respect to its centerlines,  $\phi$  can be chosen such that it will be symmetric about both centerlines. Thus, arbitrarily choosing  $\phi$  = 0 at the corners leads to:

# along edge y = 0

since at corner x = 0,  $\phi = 0$ , and at corner x = a,  $\phi = 0$ 

$$c_4 = 0$$
 ,  $c_3 = \frac{Na}{2}$ 

or

$$\varphi = \frac{N}{2} (ax - x^2) \tag{3.2}$$

$$\frac{\partial \varphi}{\partial \mathbf{x}} = \frac{N}{2} (\mathbf{a} - 2\mathbf{x})$$

$$\frac{\partial \varphi}{\partial \mathbf{x}} = \frac{N\mathbf{a}}{2} \quad \text{at} \quad \mathbf{x} = 0$$

$$\frac{\partial \varphi}{\partial \mathbf{x}} = \frac{-N\mathbf{a}}{2} \quad \text{at} \quad \mathbf{x} = \mathbf{a}$$

similarly, along edge x = 0 we get:

$$\varphi = \frac{N}{2} (ay - y^2) \tag{3.3}$$

Since  $\frac{\partial \phi}{\partial x}$  is constant all along this edge, and from Equation (3.2) above, is equal to  $\frac{Na}{2}$  at the corner,  $\frac{\partial \phi}{\partial x} = \frac{Na}{2}$  all along the x = 0 edge; therefore  $(x = 0, \frac{\partial \phi}{\partial x} = \frac{Na}{2})$  and  $(x = a, \frac{\partial \phi}{\partial x} = -\frac{Na}{2})$ ; similarly from equation (3.3)  $(y = 0, \frac{\partial \phi}{\partial y} = \frac{Na}{2})$  and  $(y = a, \frac{\partial \phi}{\partial y} = -\frac{Na}{2})$ .

Now, we are able to compute  $\phi$  values at each boundary node. Figure 3.3 (a) shows the geometry of the plate and location of node points.

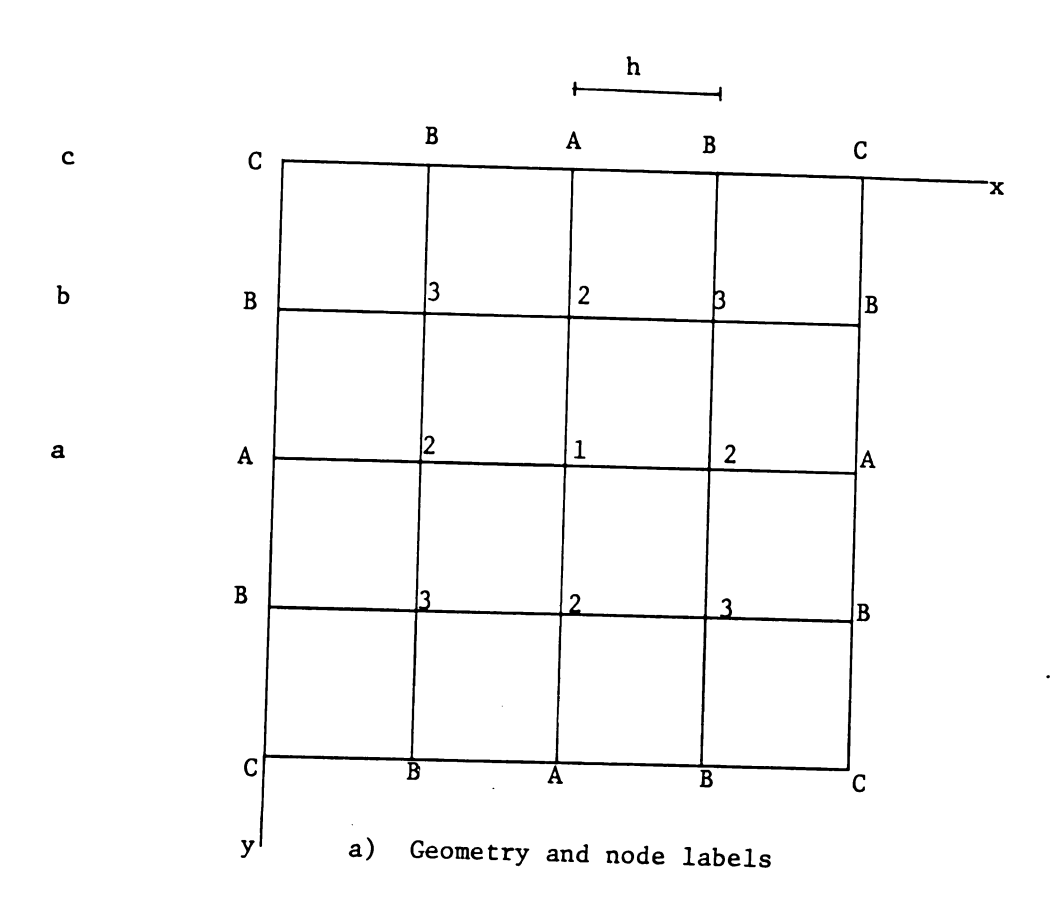
The  $\varphi$  values at nodes A,B, and C according to Equation (3.3) are:

$$\varphi_{A} = \frac{N}{2} \left[ a \left( \frac{a}{2} \right) - \left( \frac{a}{2} \right)^{2} \right] = \frac{Na^{2}}{8}$$

$$\varphi_{B} = \frac{N}{2} \left[ a \left( \frac{a}{4} \right) - \left( \frac{a}{4} \right)^{2} \right] = \frac{3Na^{2}}{32}$$

$$\varphi_{C} = 0$$

The value of  $\,\phi\,$  at some imaginary exterior points such as a and b in Figure (3.3.b) are needed because when the difference operator is applied at the first interior point, such as (2),



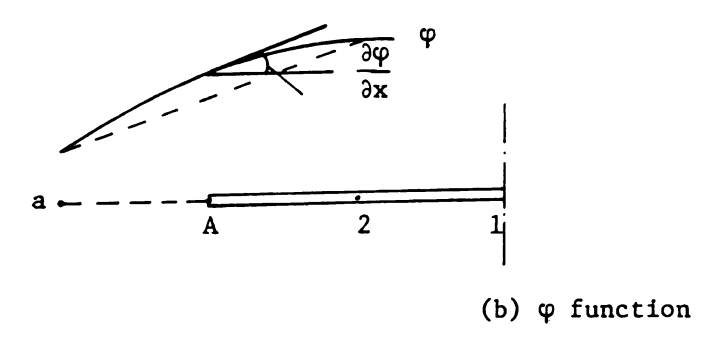
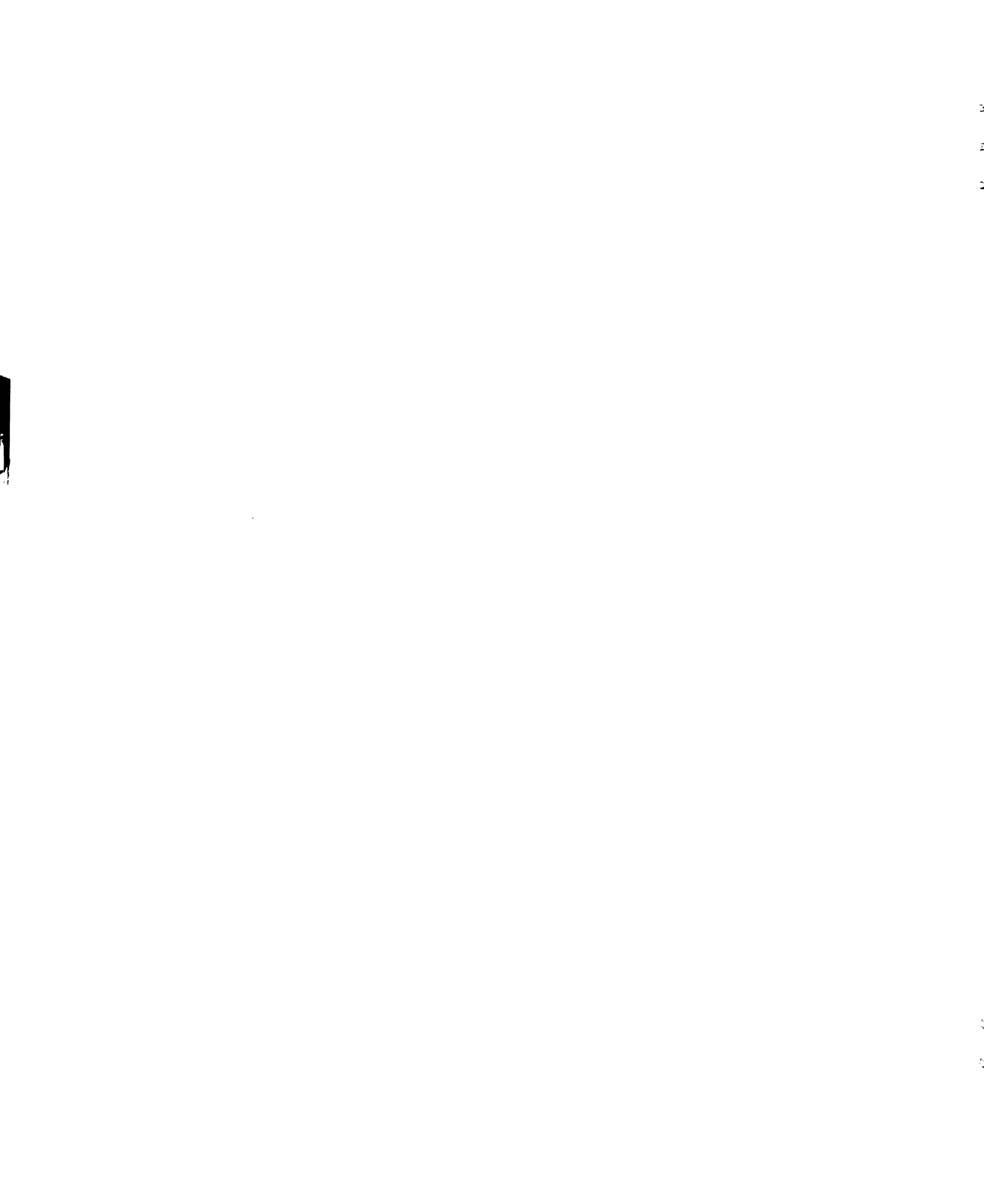


Figure 3.3. Geometrical plan and  $\boldsymbol{\phi}$  function.



the value of  $\varphi$  at the first exterior point, a, is required. This can be determined from the boundary condtions. We already determined that along edge x = 0, the slope  $\frac{\partial \varphi}{\partial x}$  is equal to  $\frac{Na}{2}$ .

Among the  $\frac{\partial \phi}{\partial x}$  approximations which may be used are:

1) Two point difference, using known slope at edge and  $\phi_{\text{A}}\colon$ 

$$\left(\frac{\partial \varphi}{\partial \mathbf{x}}\right)_{\mathbf{A}} = \frac{\varphi_{\mathbf{A}} - \varphi_{\mathbf{a}}}{h}$$

or

$$\varphi_{a} = \varphi_{A} - h \left(\frac{\partial \varphi}{\partial x}\right)_{A} = \varphi_{A} - h \left(\frac{Na}{2}\right)$$

$$\varphi_{a} = \varphi_{A} - h \left(\frac{Na}{2}\right)$$
(3.4)

For  $h = \frac{a}{4}$ ,  $\phi_a = \phi_A - \frac{Na^2}{8}$ , where  $\phi_A$  is already determined.

2) Two point, using known slope at A and the central difference operator:

$$\left(\frac{\partial \varphi}{\partial \mathbf{x}}\right)_{A} = \frac{\varphi_{2} - \varphi_{a}}{2h}$$
,  $\frac{Na}{2} = \frac{\varphi_{2} - \varphi_{a}}{2h}$ 

or

$$\varphi_{a} = \varphi_{2} - h(Na) \tag{3.5}$$

$$Na^{2}$$

For case  $h = \frac{a}{4}$ ,  $\varphi_a = \varphi_2 - \frac{Na^2}{4}$ 

Both of these approximations were tested for the plate of constant stiffness. Approximation (2) led to values of  $N_x = N_y = N$  at all points in the plate but approximations (1) did not.

Approximation (2) was used for the first derivative in this case. In this example the values at exterior points are:

$$\varphi_a = \varphi_2 - \frac{Na^2}{4}$$

$$\varphi_b = \varphi_3 - \frac{Na^2}{4}$$

Next, the finite difference operator Figure (A.4) which represents the compatibility equation (2.15) was applied at each interior node. The right hand side of equation is zero, since w = 0.

# 3.1.1.a The Square Plate With $h = \frac{a}{4}$ , R = 1/10

Stiffness of the plate at each node and intermediate nodes is shown in Figure (3.4).

Application of operator to all nodes results in the following system of linear equations

$$\begin{bmatrix} 34.802542 & -57.451238 & 10.341004 \\ -14.3628095 & 93.0717725 & -58.708963 \\ 2.5852510 & -58.708963 & 122.8929425 \end{bmatrix} \begin{pmatrix} \varphi_1 \\ \varphi_2 \\ \varphi_3 \end{pmatrix} = \begin{pmatrix} -1.5384615 \\ 5.9879807 \\ 11.4951922 \end{pmatrix}$$
 Na<sup>2</sup>

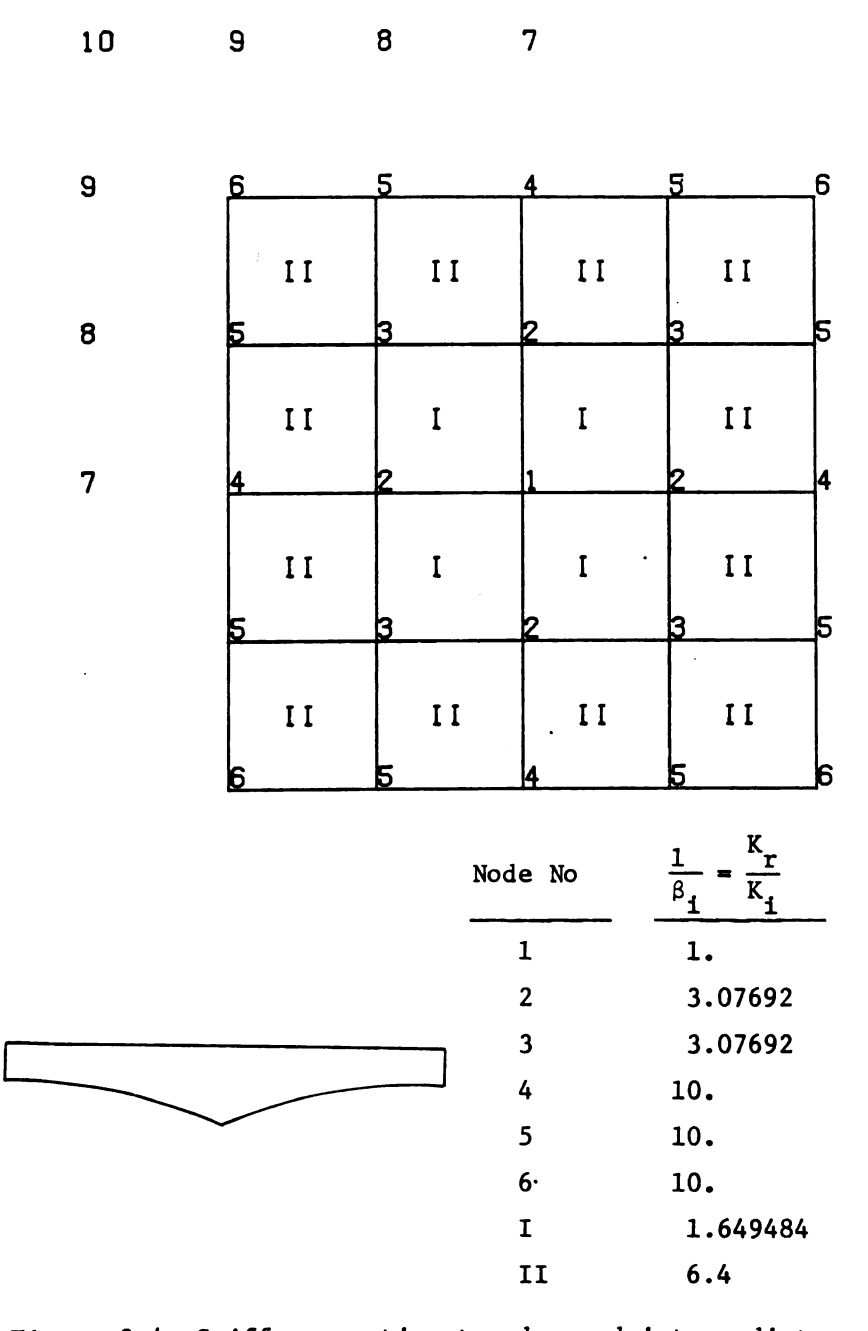


Figure 3.4. Stiffness ratio at nodes and intermediate nodes square plate R = 1/10.

solving the equations, we get:

The membrane resultants can be computed using Equation (2.12)

For example:

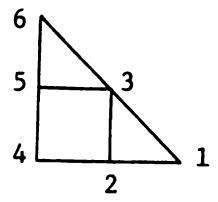
$$N_{x(3)} = (\frac{\partial^2 \varphi}{\partial y^2})_{(3)} = \frac{\varphi_2 - 2\varphi_3 + \varphi_5}{h^2} = \frac{.233482 - 2(.199145) + 3/32}{(\frac{a}{4})^2}$$
 (Na<sup>2</sup>) =

1.136927044N

similarly, stress resultants at each node are calculated; the results for nodes shown, are given in Table 3.1.

Table 3.1 Stress function and stress resultant ratios at each node. Square plate with R = 1/10, v = .25, h = a/4.

Node	Stress function φ/Na <sup>2</sup>	N×/N	Ny/N	Nxy/N
1	.28204873	1.55413	1.55413	0.0
2	.23348206	1.09879	.95865	0.0
3	.100145001	1.13693	1.13693	.03205
4	.12500	1.0	.52857	0.0
5	.0937500	1.0	.67636	0.0
6	0	1.0	1.00	0.0



Equilibrium is satisfied along any section of the plate. For example, along x = .25a, using the block approximation:

$$P = (N_x)_5 (\frac{a}{8})(2) + (N_x)_3 (\frac{a}{4})(2) + (N_x)_2 (\frac{a}{4}) = -.99999999 \text{ Na} \simeq -Na$$

and along x = .5a:

$$P = (Nx)_4(\frac{a}{8})(2) + (Nx)_2(\frac{a}{4})(2) + (Nx)_1(\frac{a}{4}) = -.99999999$$
 Na

which are both very close to in-plane resultant at the edge of the block along x = 0:

$$P = -N \times a = -Na$$

# 3.1.1.b The Same Problem With R = .5

The same square plate is considered except the ratio of stiffness is,  $R = \frac{\text{edge stiffness}}{\text{center stiffness}} = .5$ .

Resulting values of the stress function  $\phi$ , and the calculated in-plane stress resultants at the nodes shown below, are listed in Table 3.2.

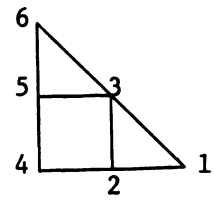


Table 3.2 Stress function and membrane forces (R = .5, h = a/4, v = .25)

Point	Stress function φ/Na <sup>2</sup>	Nx/N	Ny/N	Nxy/N
1	. 26057639	1.19625	1.19625	0.0
2	.22319361	1.04536	.97297	0.0
3	.19052623	1.02574	1.02574	01058
4	.125000	1.000	.8578	0.0
5	.0937500	1.000	.90316	0.0
6	0.00000	1.000	1.000	0.00

As in the preceding problem, equilibrium is satisfied along all sections of the plate.

# 3.1.1.c Uniform Stiffness Plate (R = 1)\*

It is anticipated that as the stiffness of the plate approaches uniformity, the solution will converge to the known results for uniform stiffness plate. Thus, this case is considered as a measure of verification. The results shown in Table 3.3, are as expected. The membrane resultant ratios are equal to 1.0 everywhere and shear stress is zero; these are exact values.

<sup>\*</sup>Both E and thickness are uniform all over the plate.

Table 3.3 Stress function and in-plane resultant ratios.

$$(R = 1, h = \frac{a}{4})$$

Point	oint φ/Na <sup>2</sup>		Ny/N	Nxy/N
1	.2500000	1.00	1.00	0.0
2	.21875000	1.00	1.00	0.0
3	.1975000	1.00	1.00	0.0
4	.125000	1.00	1.00	0.0
5	5 .0937500		1.00	0.0
6	.0000	1.00	1.00	0.0

# 3.1.1.d The Same Problem as in 3.1.1.a With R = 10

In contrast to the previous problems, in this case the stiffness is increasing from center to edges and at the edges it is ten times stiffer than at the center. Results are shown in Table 3.4. Equilibrium is satisfied along all sections.

Table 3.4 Stress function and membrane force ratios, square plate

R	=	10,	h	=	<u>a</u>	,	ν	=	. 25
		-			4	-			

φ/Na <sup>2</sup>	Nx/N	Ny/N	Nxy/N
.21667651	.32022	.32022	0.0
.20666961	.78443	1.14660	0.0
.18215623	1.02229	1.02229	03332
.125000	1.00	1.38657	0.0
.09375000	1.00	1.171	0.0
6 .000		1.00	0.0
	.20666961 .18215623 .125000 .09375000	.20666961 .78443 .18215623 1.02229 .125000 1.00 .09375000 1.00	.20666961       .78443       1.14660         .18215623       1.02229       1.02229         .125000       1.00       1.38657         .09375000       1.00       1.171

## Improvement of the solutions

Since this is an approximate method, it is desirable to study the convergence of the solution with increasing numbers of node points (decreasing grid spacing). In this section the same problems are solved using finer grid spacings (h =  $\frac{a}{8} \notin h = \frac{a}{16}$ ). Solutions to all four problems are obtained. The node arrangements are shown in appendices B.1 and B.2.

The convergence of the solution for the case R = 1/10 is shown in Table 3.5 and illustrated in Figure 3.8.

Table 3.5 Convergence of the solution, square plate R = 1/10, v = .25

Grid spacing h/a	φ -values at node 1	by extrap- olation	N, at node 1	extrapolation results *	3 pt. extrap- olation
1/4	.28204873		1.55413		
		.27472129		1.59060	
1/8	.27655315		1.58149		1.59026
		.27465677		1.59028	
16	.27513087		1.58809		

<sup>\*</sup> Richardson's extrapolation.

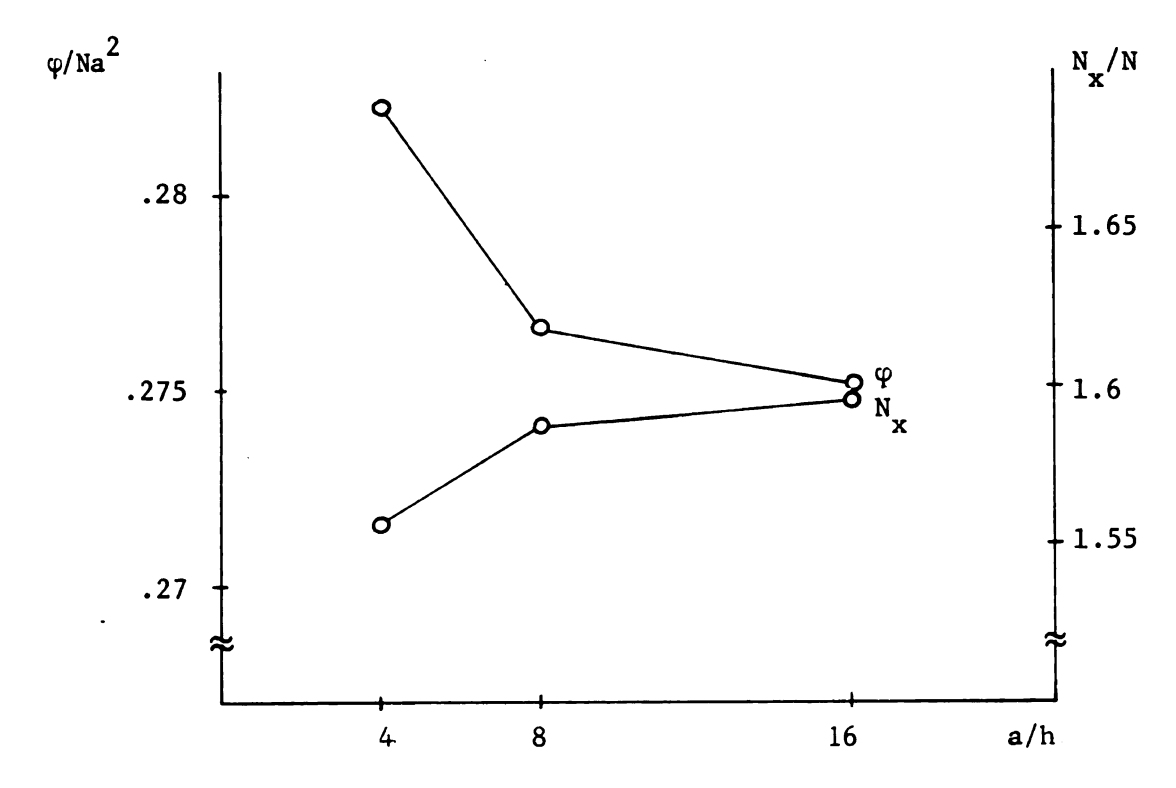


Figure 3.5 Convergence of membrane solution

# 3.1.1.1 Analysis of Results from Membrane Solution.

i) Uniform stiffness plate (R = 1)

Compared to theoretical values, in this case the finite difference solution gives accurate results. The difference operators agree exactly with the usual difference operator for uniform stiffness plate. Since the  $\phi$  function is parabolic in this case, the difference approximations to the second and higher derivatives of  $\phi$  are exact, and the solution is exact, even for  $h=\frac{a}{4}$ . The in-plane stress resultants are uniform

over all the plate and there is no shear stress, as expected. Distribution of  $N_{\rm x}/N$  is shown in Figure (3.6). The displacements vary linearly from the symmetric centerlines (see Figure 3.7), and the strain is constant, which agrees with elasticity theory. The solution obtained with the grid-spacing,  $h=\frac{a}{4}$  is exact, as are solutions with finer grid-spacings.

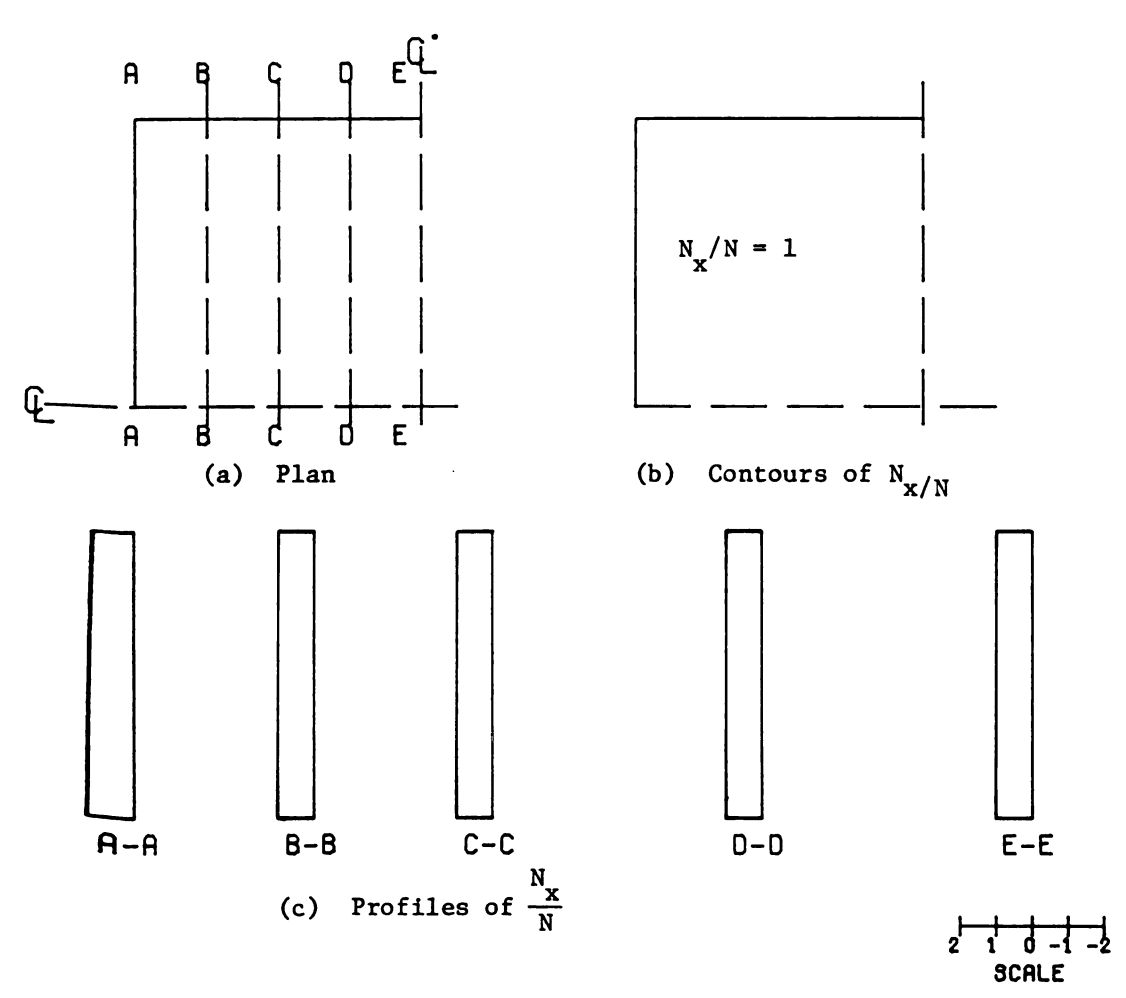


Figure 3.6. Force distribution for undeflected square plate R = 1.

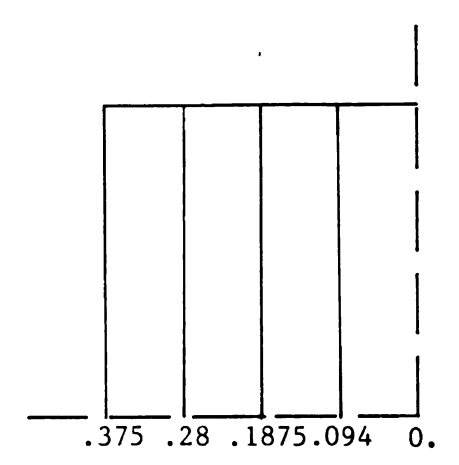


Figure 3.7. Contours of in-plane displacement (U' = U = V = N) for undeflected square plate, R = 1,  $\nu$  = .25.

## ii) Square plate with R = 1/10.

In this case, because of variation in stiffness, the stresses vary over the plate. Thus, the  $\phi$  function is not a smooth, parabolic one as it was in the uniform stiffness case and the solution would be an approximate one. Solutions with finer grid spacing were compared (see Table 3.5) and they show fairly good convergence.

Study of in-plane resultants in Figure (3.8) shows the expected behavior, with a shifting of the load toward the stiffer parts of the plate.

Equilibrium is satisfied along any arbitrary section of the plate. Shear stress is zero at points of symmetry but at nonsymmetric points, because of the load shifting process, there is a small shear force created, as expected.

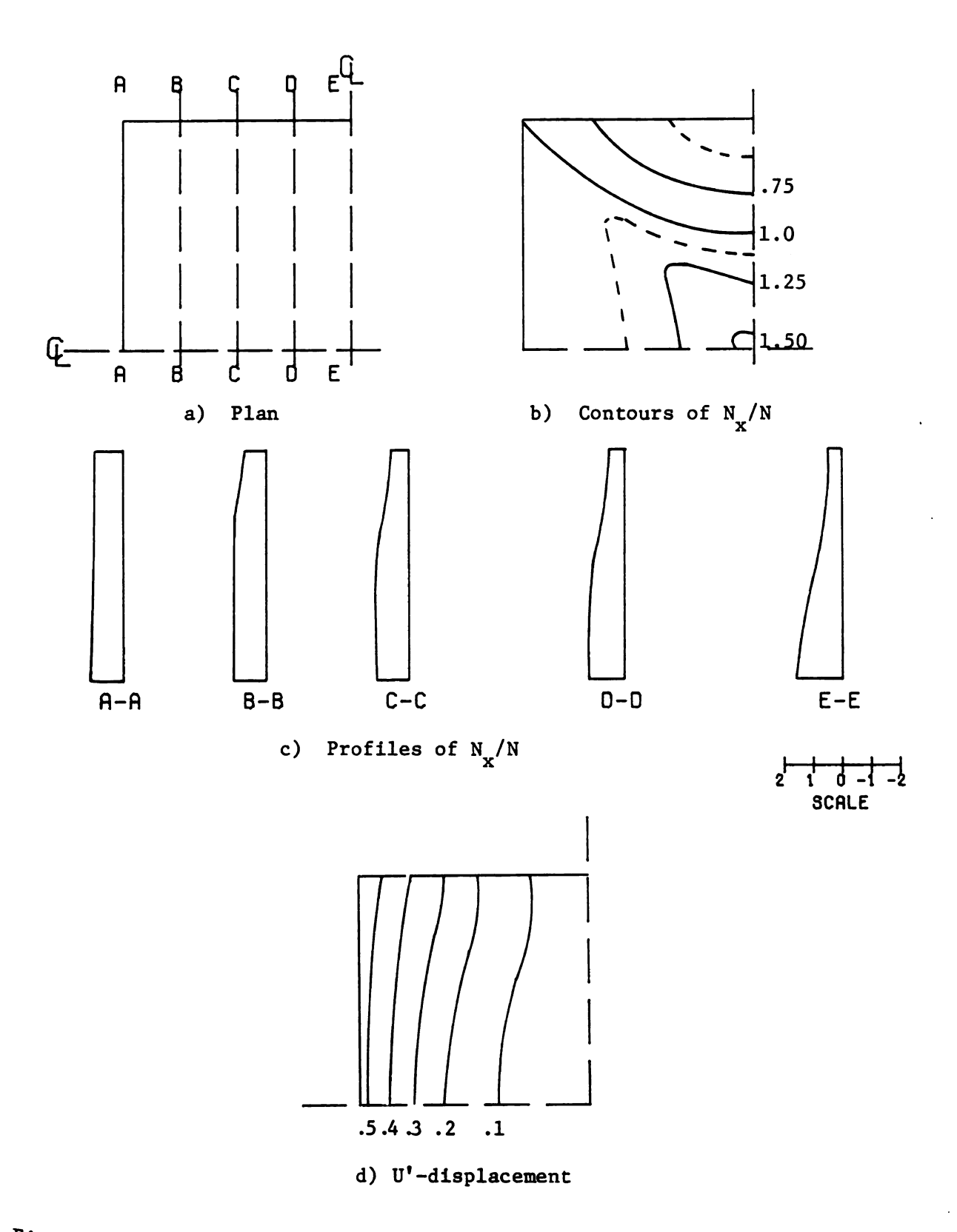


Figure 3.8. Distribution of in-plane force  $(N_x/N)$  and displacement  $(U' = U \frac{K_o}{N})$  square plate, P = 1/10.

In-plane displacement patterns are illustrated in Figure (3.8 d). It is observed that the displacement normal to the edge is increasing as we approach the corners, at which stiffness is less than at the center. This behavior seems reasonable since there is no displacement restraint along the edges.

## iii) Square plate with R = 1/2

This problem can provide a good check on solutions, because it lies between two previous cases. As we go from the R = 1/10 case to the uniform stiffness case (R = 1), we would expect the solutions to approach the uniform stiffness results. Investigation of the results in Figure(3.9) along with the results found by different grid-spacings and comparing with cases (1) and (ii), indicates:

- a) The convergence as the grid spacing becomes finer
- b) Results for the stresses and displacements trend toward those for the uniform thickness case as R is changed from 1/10 to 1/2.
- iv) Square plate with R = 10.

Solution for this case shows convergence as the grid spacing is decreased, and it also agrees with previous results in that:

- a) Load in the plate shifts toward the edges which are stiffer as illustrated in Figure (3.10).
- b) Displacement normal to the edge is a little larger at center of the edge and decreases toward the corner; (see Figure 3.10 d).

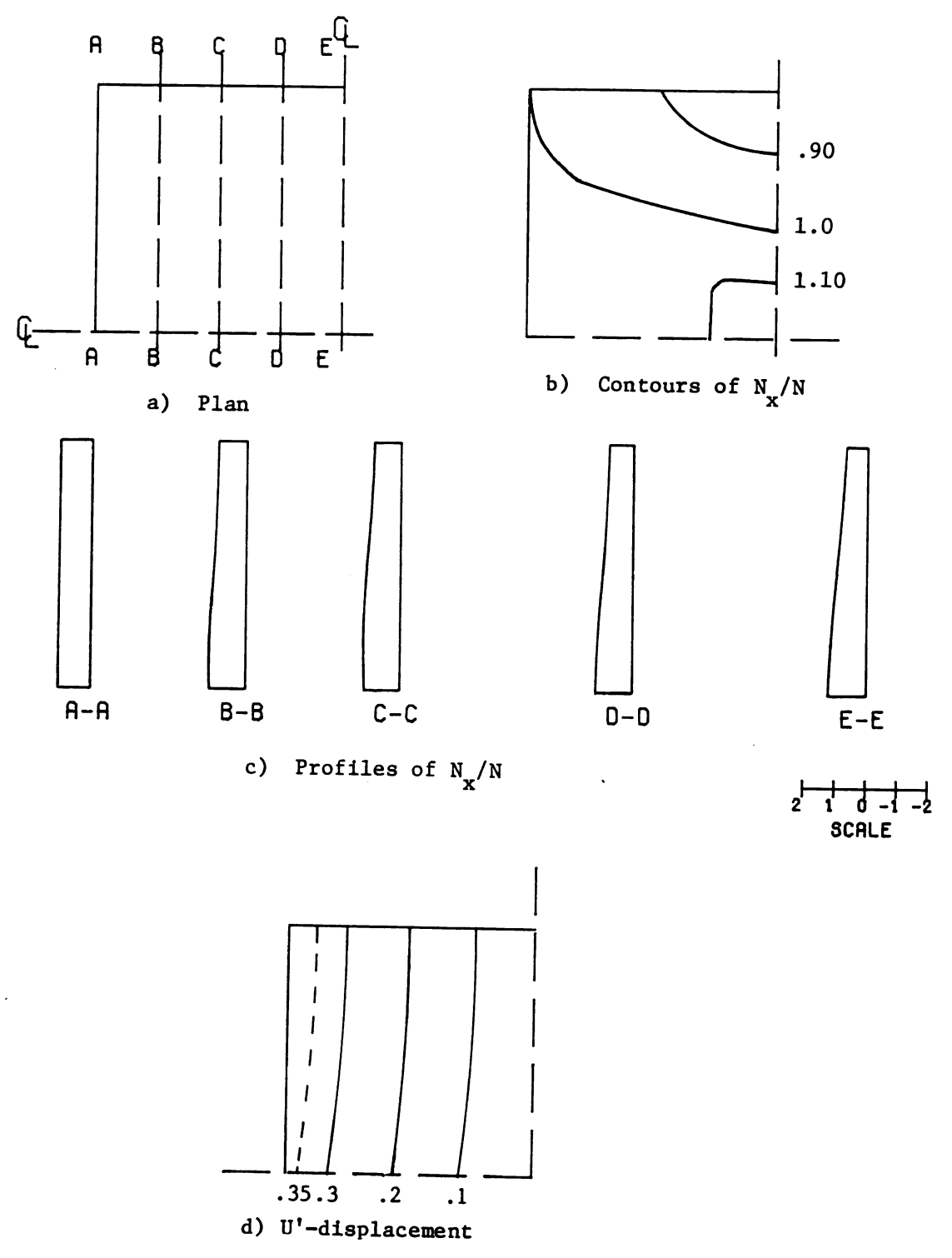


Figure 3.9. Distribution of in-plane force  $(N_x/N)$  and displacement  $(U' = U \frac{K_o}{N})$  square plate, R = 1/2.

-

Estre 3

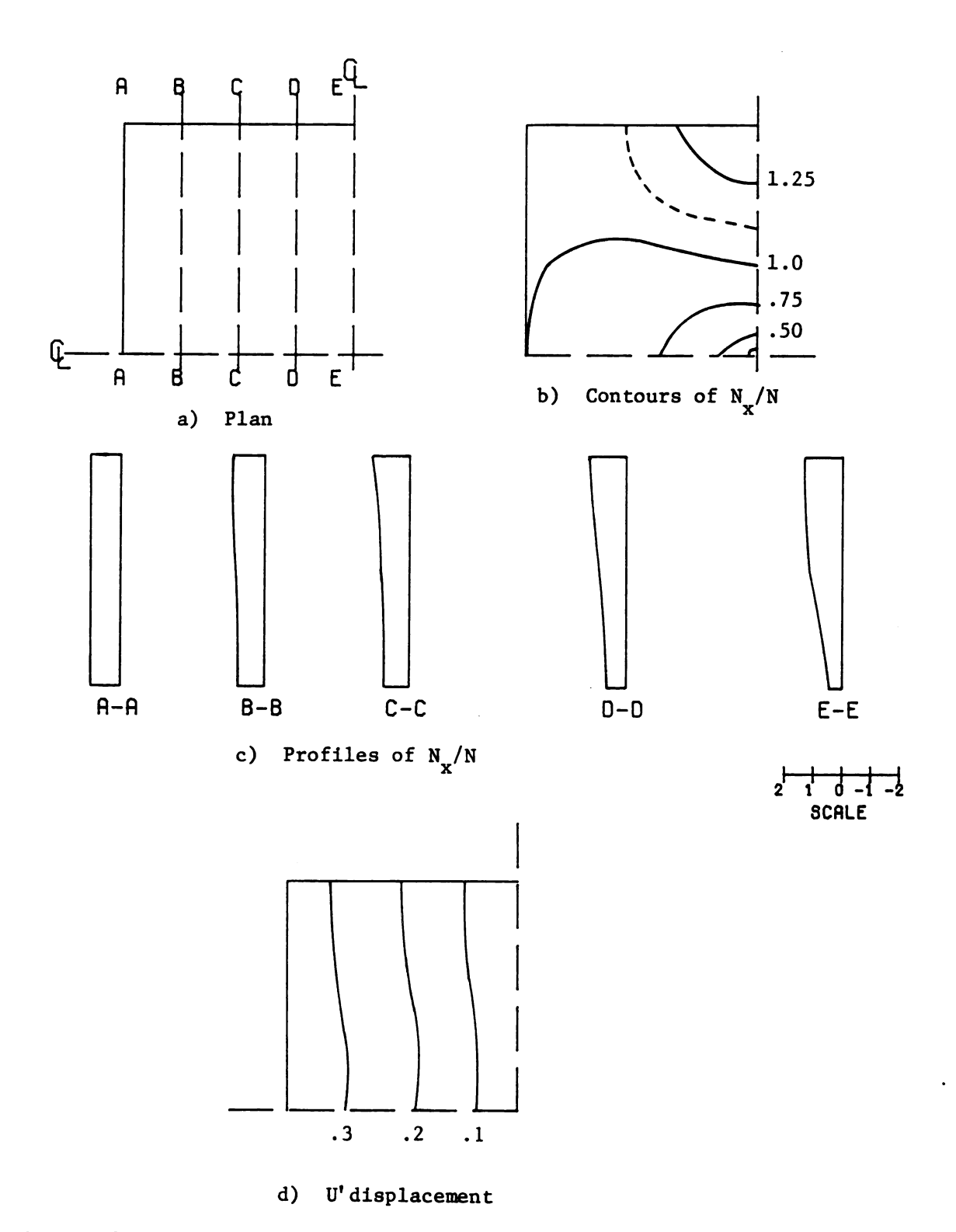


Figure 3.10. Distribution of in-plane force (N  $_{\rm X}/{\rm N})$  and displacement (U' = U  $\frac{{\rm K}_{\circ}}{{\rm N}})$  square plate R = 10.

### 3.1.2 Buckling

To study buckling and determine the critical value of the applied compressive force,  $N_{\rm C_{\rm r}}$ , the equilibrium Equation (2.14) is employed. The left hand side of this equation is approximated by the operator Figure (2.8) and the right hand side is represented by the difference operator Figure (2.9). The stress function,  $\phi$ , values obtained in the membrane solution for the plate with no lateral displacement are used in the equilibrium equation. This is acceptable, because in the stability analysis we are seeking bifurcation of an initially undeflected plate.

# Boundary conditions

In the case of buckling and postbuckling, the out-of-plane displacement, w, has a considerable effect on the solution and out-of-plane boundary conditions must be considered. In the simply supported case, along edge x = 0, we have:

i) 
$$w = 0$$
  
ii)  $M_{x} = -D(\frac{\partial^{2} w}{\partial x^{2}} + v \frac{\partial^{2} w}{\partial y^{2}}) = 0$ 

But  $\frac{\partial^2 w}{\partial y^2} = 0$ , so that (ii) becomes  $\frac{\partial^2 w}{\partial x^2} = 0$ . Using a difference approximation,

$$\frac{\partial^2 w}{\partial x^2} = \frac{w_{i+1} - 2w_i + w_{i-1}}{h^2}$$

we will get at point B (Figure 3.3),

$$\frac{\partial^2 \mathbf{w}}{\partial \mathbf{x}^2} = \frac{\mathbf{w_3} - 2\mathbf{w_B} + \mathbf{w_b}}{\mathbf{h}^2} = 0$$

since 
$$w_B = 0$$
,  $w_b = -w_3$ .

In the case of fixed support, the conditions are:

$$i)$$
  $w = 0$ 

ii) 
$$\frac{\partial \mathbf{w}}{\partial \mathbf{x}} = 0$$

using a central difference approximation for slope we have:

$$\frac{\partial w}{\partial x} = \frac{w_3 - w_b}{2h} = 0 \rightarrow w_b = w_3.$$

# 3.1.2.a Buckling of Plate with R = 1/10.

Let us consider problem a) again (R = 1/10) with simply supported edges and h =  $\frac{a}{4}$ .

In the right hand side of equation (2.14) the  $\,\phi\,$  values have already been obtained for the initially flat plate.

Applying operator Figure (2.8) at each point, and substituting  $\phi$  values in the right hand side, the following eigenvalue problem is obtained.

$$\begin{bmatrix} 14.9375 & -20.52500 & 4.2875 \\ -5.13125 & 10.86875 & -5.5375 \\ 1.071875 & -5.5375 & 6.5725 \end{bmatrix} \begin{pmatrix} w_1 \\ w_2 \\ w_3 \end{pmatrix} = \frac{Na^2}{D_r} \begin{bmatrix} 3.885332 & -.3885332 & 0 \\ -.0686741 & .2571788 & .1198306 \\ -.0040060 & -.1421158 & .2842316 \end{bmatrix} \begin{pmatrix} w_1 \\ w_2 \\ w_3 \end{pmatrix}$$

or: calling 
$$\lambda = \frac{Na^2}{D_r}$$

$$\begin{bmatrix} 14.9375 - .3885332\lambda & -20.52500 + .3885332 \lambda & 4.2875 \\ -5.13125 + .0686741\lambda & 10.86875 - .2571788 \lambda & -5.5375 + .11983.6 \lambda \\ 1.071875 + .004006\lambda & -5.5375 + .1421158\lambda & 6.5725 - .2842316 \lambda \\ \end{bmatrix} \begin{bmatrix} w_1 \\ w_2 \\ w_3 \end{bmatrix} = 0$$

Solving leads to these eigenvalues,

$$\lambda = \begin{cases} 5.20748 \\ 20.42753 \\ 46.71190 \end{cases}$$

or

$$N = \lambda \frac{D_{r}}{a^{2}} = \begin{cases} 5.20749 \\ 20.42753 \\ 46.71190 \end{cases} \frac{D_{r}}{a^{2}}$$

The corresponding eigenvectors are:

To check convergence, the same problem was solved with finer grid spacings,  $(h = \frac{a}{8})$  and  $(h = \frac{a}{16})$ .

The eigenvalues shown in Table 3.6 were obtained. The convergence is fairly good and extrapolation improves the results further.

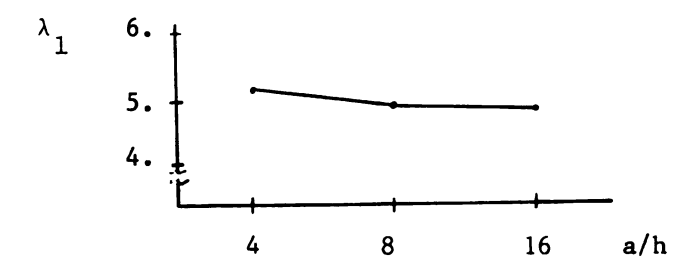


Figure 3.11. Convergence of eigenvalue, R = 1/10.

Table 3.6 Eigenvalues of s-s square plate, R = 1/10, with different grid spacings.

h/a	$\lambda_1$	2 pt. extrapolation	3 pt. extrapolation
1/4	5.20748		
		4.727158	
1/8	4.84724		4.855814
		4.847773	
1/16	4,84764		

The first mode shapes in the three solutions are very close to each other.

# 3.1.2.b Buckling of Uniform Stiffness Plate

As before, a plate with uniform stiffness is considered; the solution can be used for an accuracy test since the exact solution is known. The first eigenvalue obtained using different grid spacings is tabulated below and compared with the exact solution.

Table 3.7 Comparison of first eigenvalues of different solution (R = 1)

h/a	$\lambda_1$	$\lambda_1$ exact	difference	2 Pt. extrap- olation	3 Pt. extrap- olation
1/4	18.74517	19.7392088	5%		
				19.734057	
1/8	19.48684		1.2%		19.739197
				19.738873	
1/16	19.67587		.3%		

It ca

giver

The s

fere:

well the

30 CU

the n

ætho

Vere

fine

to 50

āīe ]

It can be seen that the results are very close to the exact values given in Reference (44);

$$N_{cr} = 2\pi^2 \frac{D}{a^2}$$
 or,  $\lambda_1 = \frac{Na^2}{D} = 2\pi^2 = 19.7392088$ 

The solution is satisfactorily converging to the exact value. Three point extrapolation results in an error of less than  $10^{-6}$ .

Table (3.8) shows the critical loads obtained for two different loading cases and gives comparison with previous work as well as exact values. It can be seen that even with 8 x 8 nodes the results are satisfactorily within engineering accuracy. More accurate results can be obtained by extrapolation. In Table 3.8, the results given by Clough and Felippa are obtained by the finite element method and Dawe used the "discrete element displacement method", which in principle is the same as finite element method.

Eigenvalue problems for other cases (R = 10, and R = 1/2) were solved, and the convergence was examined with increasingly finer grids. Details will be discussed later.

# 3.1.2.1 General Buckling

So far, the problem was considered symmetric with respect to both centerlines and the diagonals. Therefore, the solutions are limited to symmetrical modes of buckling only and nonsymmetrical

Table 3.8 Critical loads of simply supported square plate,  $\frac{*}{cr} = \frac{cr}{\tau^2} = \frac{2}{r}$ , R = 1, v = .333

Loading case	Mesh size	Present	By Extrap-	Dawe (15)	Clough and	Classical
	h/a	Results	olation		Felippa (11)	Solution
Uniform Uniaxial	1/4			3.978	4.126	
Compression	1/8	3.96		3.993	4.031	7.
	1/16					
Uniform Bi-axial	1/4	1.89928		1,989		
Compression			1.99948			
	1/8	1.974430		1.997		2.
			1.99999999			
	1/16	1.9936				
			2.000024*			

\*
Result of 3-point extrapolation

modes are absent. This means that  $\lambda_2$  in this solution is not the eigenvalue corresponding to the second mode, but it represnts the eigenvalue corresponding to the second symmetric mode of buckling. In this particular case the 2nd symmetric mode corresponds to the 5th general buckling mode.

To obtain more accurate results, the plate was considered without imposing any symmetry. Thus, all possible degrees of freedom were allowed, within the restrictions imposed by the choice of grid spacing. The solution for each case was obtained and the buckling modes and corresponding critical loads are studied in the next section.

## 3.1.2.1.a General Buckling of Square Plate with R = 1/10.

i) Simply-supported boundaries.

Problem a is solved for general buckling (no symmetry imposed) with h = a/8 and assuming simple support along all edges. The first few modes of buckling and the corresponding eigenvalues are shown in Figure (3.12)

ii) Clamped edge.

The same problem as in (i), but with all edges clamped, was solved. The first six modes of buckling and the corresponding eigenvalues are shown in Figure (3.13).

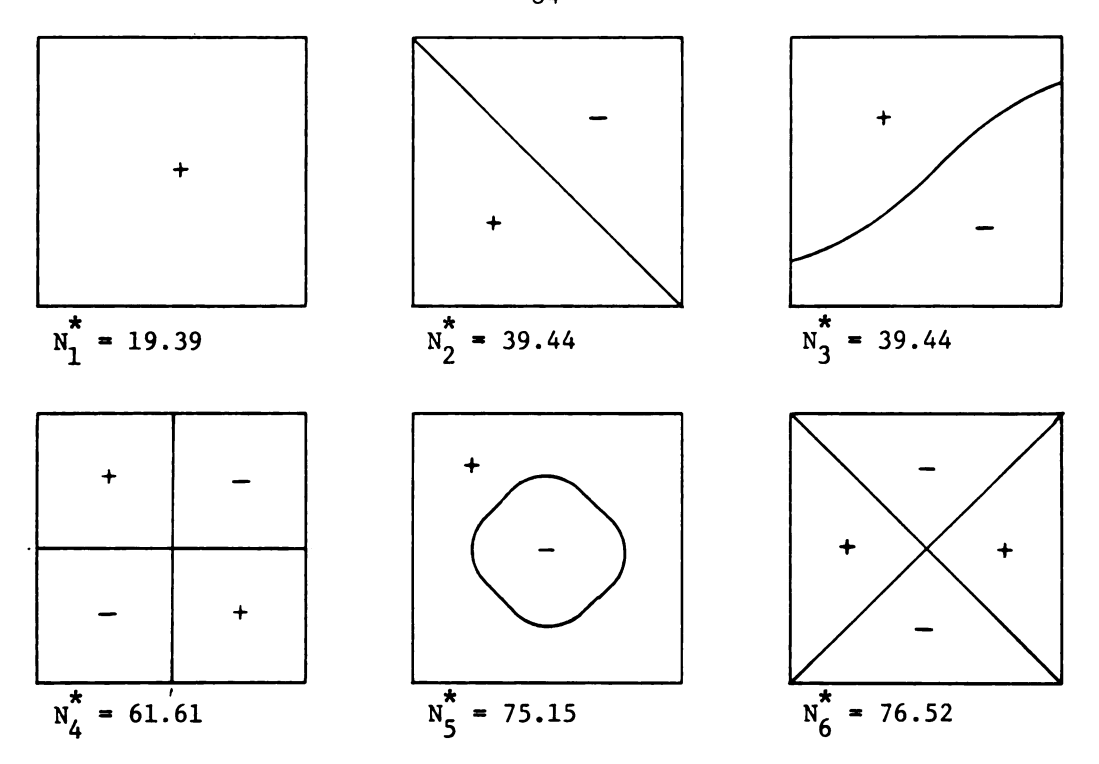


Figure 3.12. Modes of buckling of square plate, R = 1/10, simply supported.

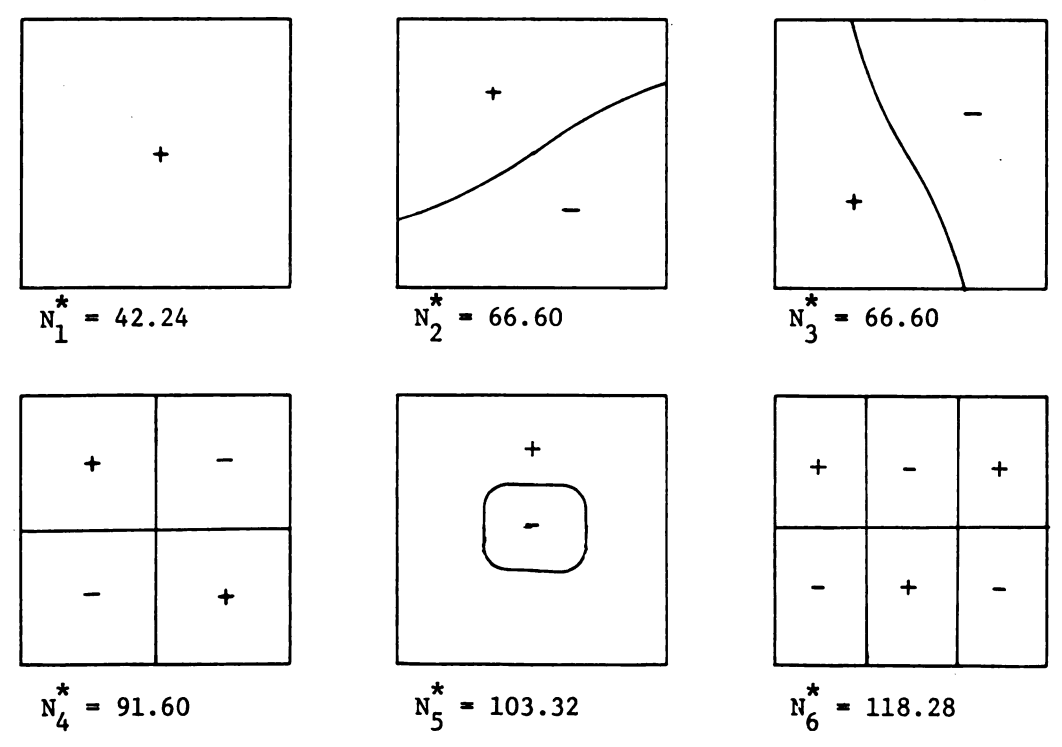


Figure 3.13. Modes of buckling of square plate, R = 1/10, clamped,  $(N^* = Na^2/D_o)$ .

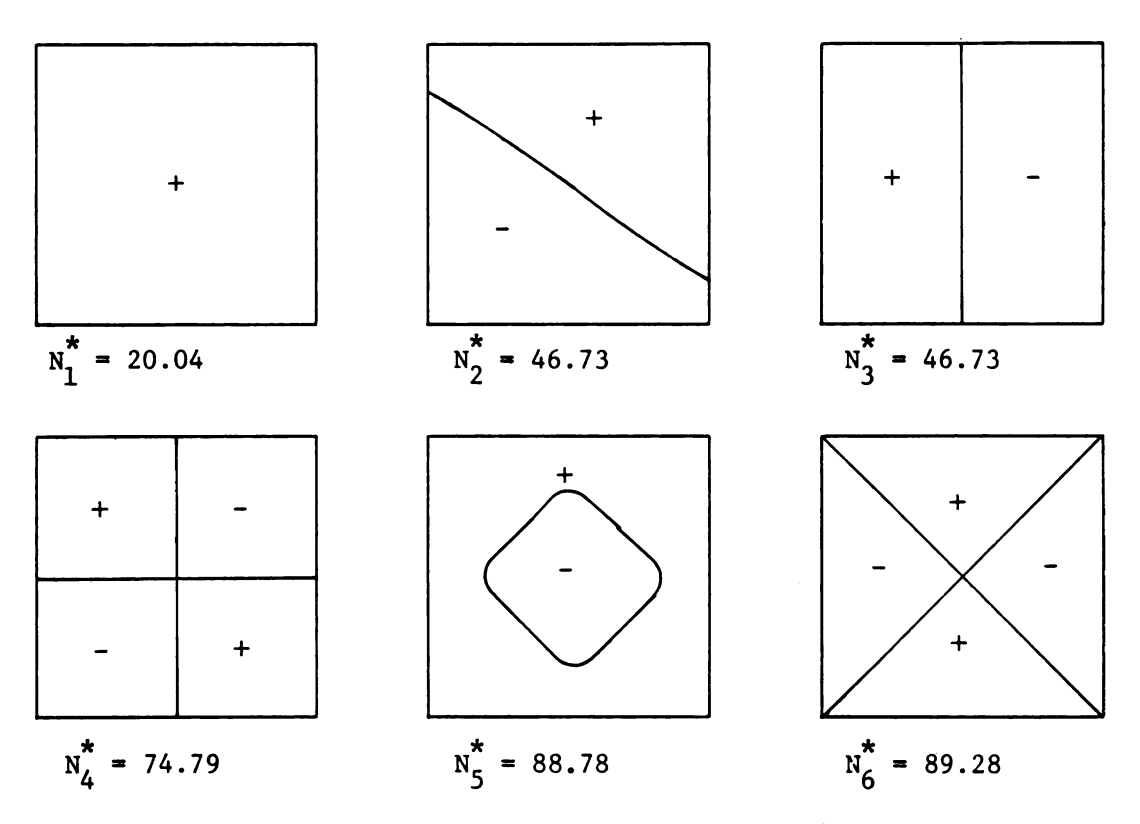
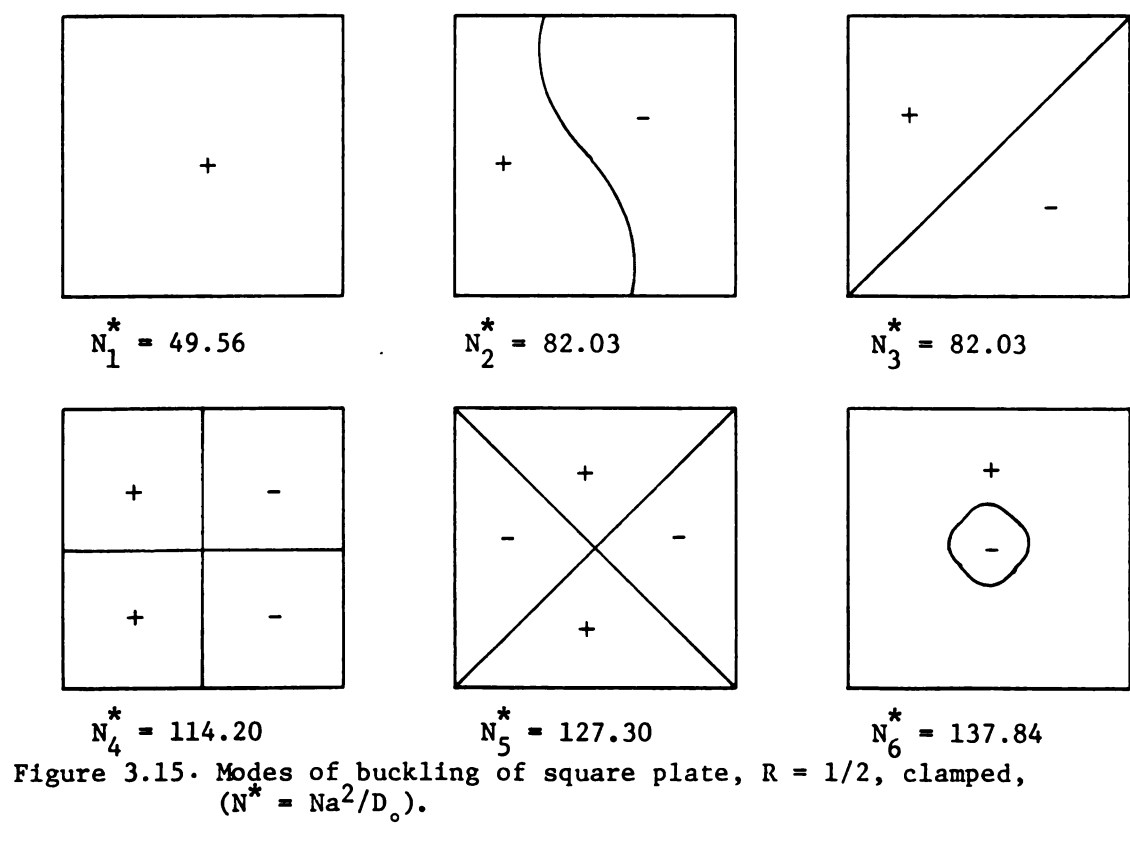


Figure 3.14. Modes of buckling of square plate, R = 1/2, simply supported.



			<del>.</del>
			;

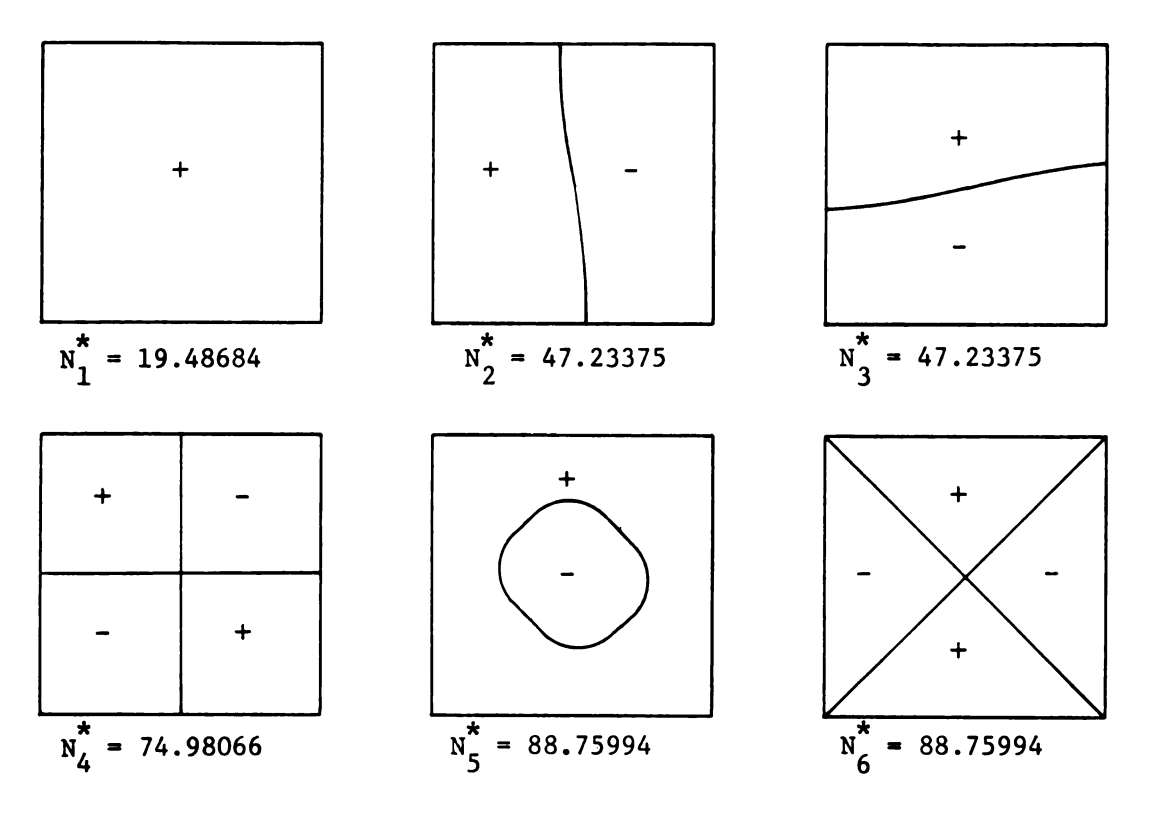


Figure 3.16. Modes of buckling of square plate, R = 1, simply supported.

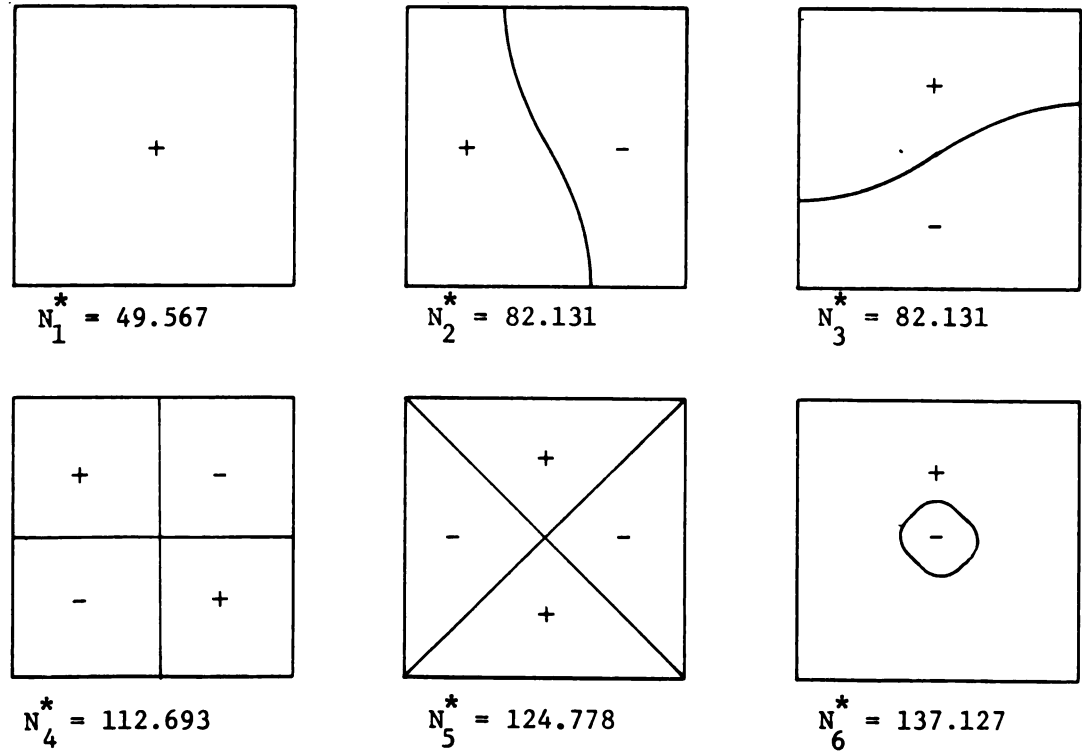


Figure 3.17. Modes of buckling of square plate, R = 1, clamped,  $(N^* = Na^2/D_o)$ .

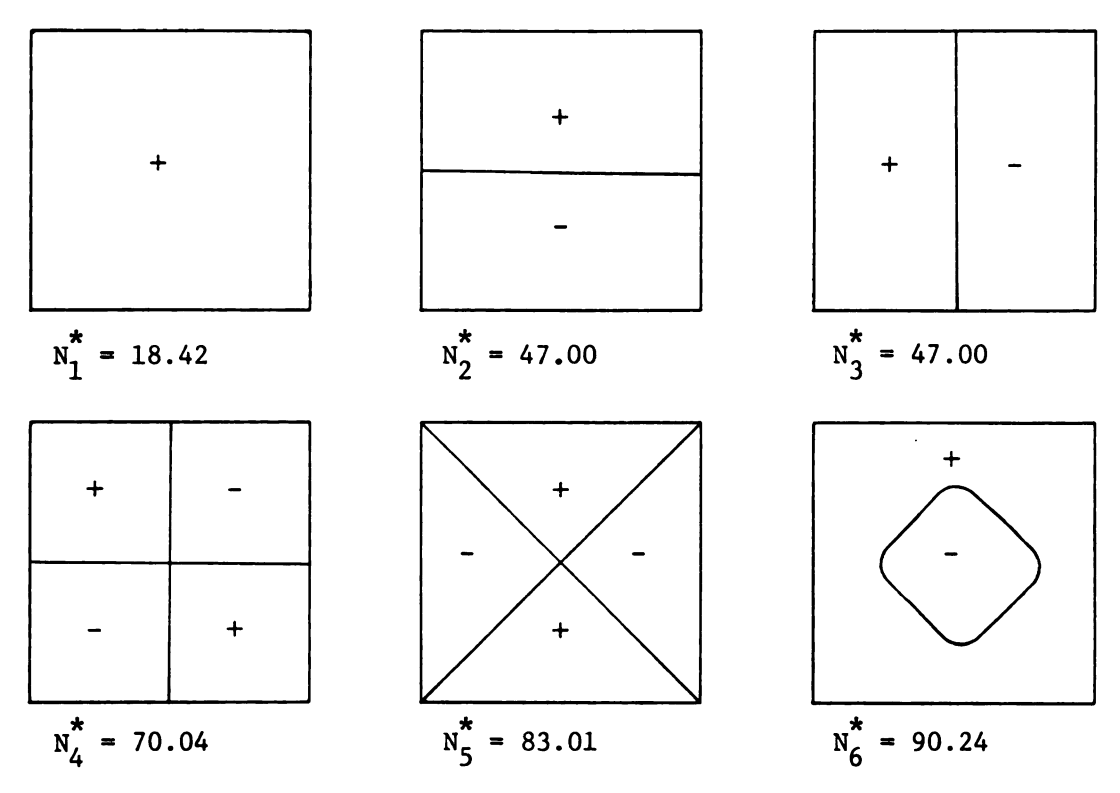


Figure 3.18. Modes of buckling of square plate R = 10, simply supported.  $\hat{\chi} = i \hat{\epsilon}$ 

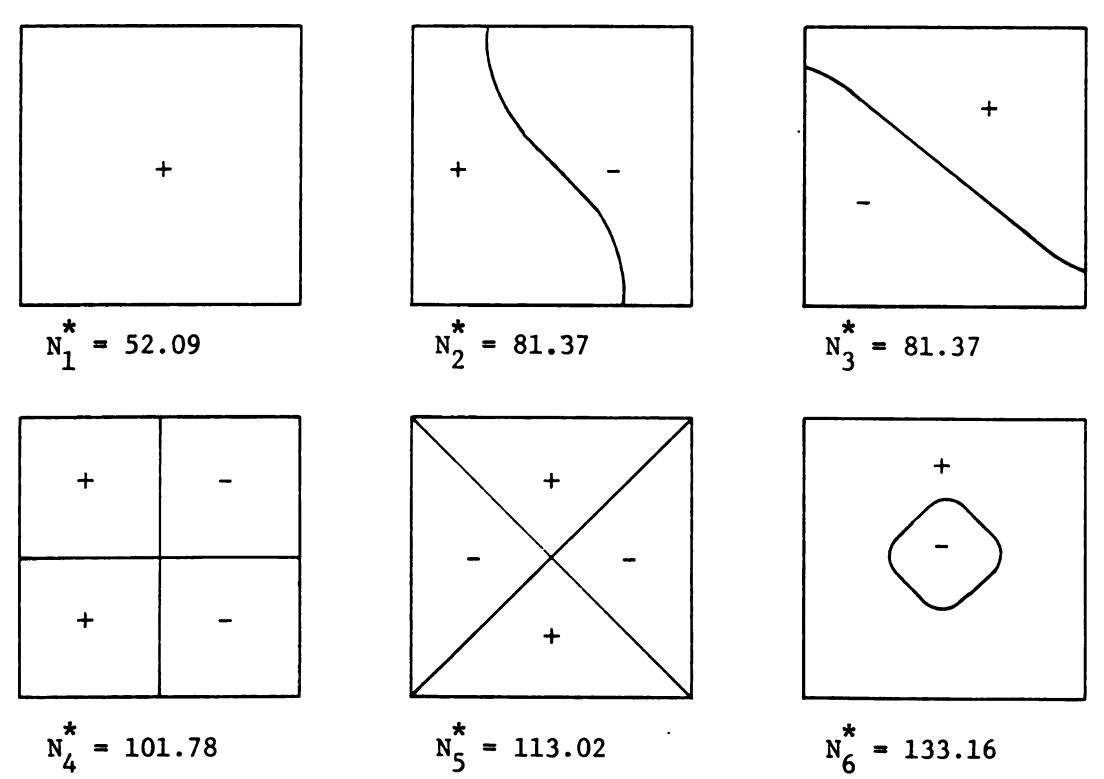


Figure 3.19. Modes of buckling of square plate, R = 10, clamped,  $(N^* = Na^2/D_o)$ .

# 3.1.2.1(b,c,d)

The plates with R = 1/2, R = 1 and R = 10 were solved for both simply supported and clamped boundaries; the buckling modes and critical loads are illustrated in Figure (3.14) through (3.19).

#### 3.1.2.2 Analysis of the Results

#### A. Simply-supported edges:

i) Uniform stiffness plate.

As discussed earlier, the critical load obtained for this problem agrees very well with the exact solution. Modes of buckling based on theoretical solutions are combinations of one or more half-sine waves in each direction. The first mode shape is one half-sine wave in each direction, x and y.

The first mode obtained by the difference solution was examined and the deflected plate after buckling was found to consist exactly of one half-sine waves in both directions. First mode deflected shapes are shown on Figure (3.20).

The second and third modes had two half-sine waves in one direction and one half-sine in the perpendicular direction.

ii) Square plate with R = 1/10.

If we investigate mode shapes and critical loads and compare with the uniform stiffness case, the following

# properties are observed:

- First mode of buckling is not a half-sine shape, but it is flatter at the center where the plate is stiffer and more curvature appears near the edges where the stiffness decreases. This phenomenon could be predicted, based on the nature of the plate.
- 2. In the higher modes, in contrast to the uniform stiffness case, in which the modes are formed by two or more half sine waves in one or two directions, there is a flat region around the stiff center of the plate and larger bending near the edges. See Figure (3.20).
- 3. The second eigenvalue in the uniform stiffness case is about 2.42 times the first one, while in the present case the ratio of second to first eigenvalue is 2.03. This can be interpreted as follows:

The first mode shape has greater curvature in the central region, while the second mode has zero curvature in the center. Therefore, it is expected that plates with more flexible edges correspond to lower second eignevalue.

## iii) Case R = 1/2.

Since this problem lies between the two previous cases, mode shapes are something in between which supports the aforementioned ideas. The ratio of second to first eigen-

values is 2.33, which lies between 2.44 for case (i) and 2.03 for case (ii).

# iv) Case R = 10.

In this case, the variation of stiffness is reversed, with the plate being stiffer near the edge. Investigation of the mode shapes indicates more bending in the less stiff central region and flat curvature near edges where the plate is stiffer, supporting the ideas introduced above.

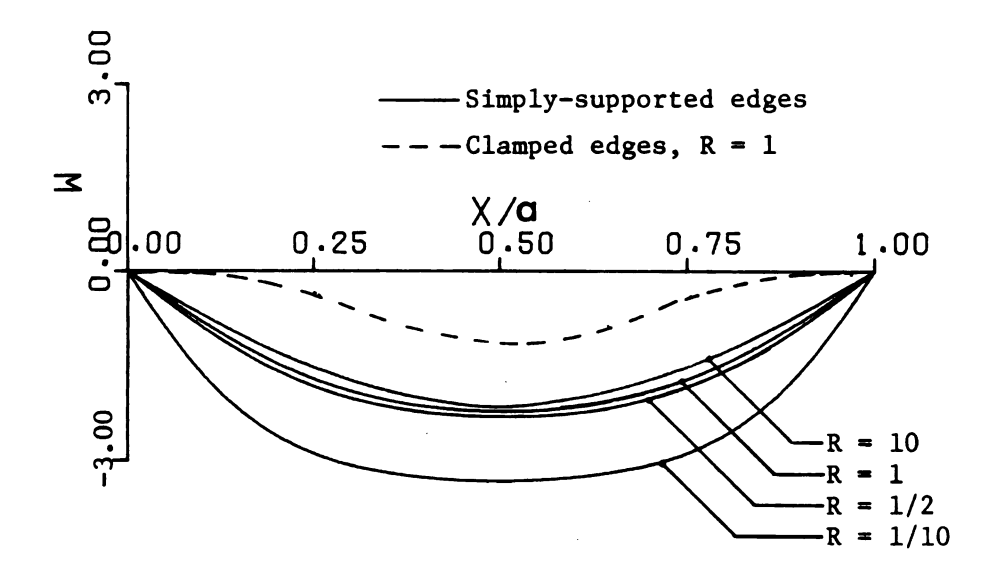


Figure 3.20. Deflected shape for s-s and clamped plate.  $(N = 2.40 N_{\rm cr})$ 

# B. Clamped Boundaries.

i) Uniform stiffness plate.

The first eigenvalue is found to be 49.56763 which is very close to the exact value, obtained by Levy (28), of  $5.037\pi^2 = 49.71319$ .

Table 3.9 shows convergence and accuracy of the results, and gives comparison with some previous works and the exact value. Extrapolation of the results shows an accuracy of about .2%.

Table 3.9. Critical load  $\overline{N}^* = N_{cr} \frac{a^2}{\pi 2D}$  of clamped square plate under bi-axial uniform load, R = 1, v = .316.

Grid-spacing (h/a)	<sup>λ</sup> 1	Extrapolation	Levy (28)	Clough & Felippa	Classical Solution
1/4				5.625	
1/8	5.02225	·	5.037	5.399	5.31
		5.29921			
16	5.22997				

The first buckling mode agrees almost exactly with the theoretical mode shape (1-  $\cos \frac{2mx}{a}$ ), for m = 1. See dashed curve in Figure (3.20).

ii) Case R = 1/10.

Similar to the s-s case, in the central region the plate remains flat and sharper curvature occurs near the edges.

iii) Case R = 1/2.

As anticipated, results obtained for this problem lie between cases (i) and (ii) supporting the validity of the solutions. iv) Case R = 10.

As before, sharp curvature is observed in the central region of the plate due to smaller stiffness of that region.

ĵ**.**1.3

3.1.3.

after

be in There

be emp

second

and t

the e

to ti

large

tech

is g

Step

#### 3.1.3 POSTBUCKLING

### 3.1.3.1 General Procedure

As discussed in the preceding chapter, a plate will stabilize after first buckling. Immediately after buckling, the plate would be in a state of stable equilibrium with moderately large deflection. Therefore, the large deflection theory discussed in chapter 2 can be employed to study postbuckling behavior of the plate up to the secondary buckling point.

In this section, the procedure followed will be discussed and the results will be analyzed.

For a solution to the large deflection behavior of a plate, the equilibrium and compatibility conditions must be satisfied; both equations are coupled in  $\,w\,$  and  $\,\phi\,$ . In this case, in addition to the variation in stiffness, geometrical nonlinearity caused by large deflection will also be involved.

To solve these coupled, nonlinear equations, an iterative technique is employed. A schematic flow chart of the procedure is given in Figure (3.21). The steps of the procedure in Figure (3.21) are as follows:

Step 1 - Solve the equilibrium equation (2.14)

The left hand side is approximated by the operator of Figure (2.8), which will be applied at each node to form the matrix [Aw]. To calculate the right hand side of this equation, initial values for  $\phi$  and w are needed. w is assumed consistent with the first buckling mode shape, and the

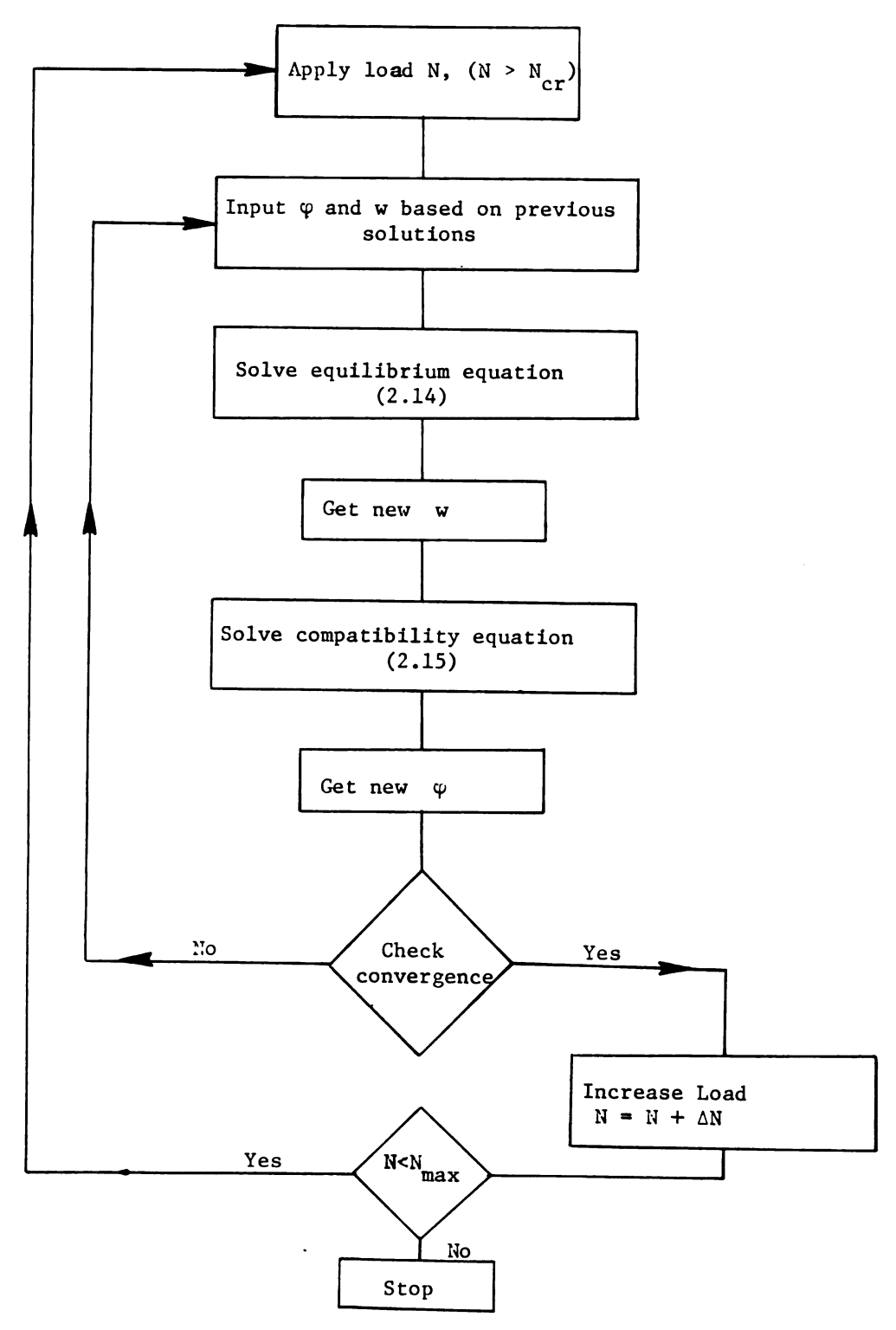


Figure 3.21. Flow chart of iterative procedure.

 $\phi$  values calculated for the undeflected plate are used. Second derivatives of  $\phi$  and w can be approximated by finite differences to obtain the known vector  $\{Q_1\}$ . Then the linear system of equations,  $[Aw]\{w\} = \{Q_1\}$ , is solved and the new values of  $w_1$  calculated.

#### Step 2 - Solve compatibility equation

To solve compatibility equation (2.15), the difference operator, Figure (2.10), which represents equation (2.15), is applied at each node and matrix [A] formed. The right hand side of this equation includes derivatives of w only. The values of  $\{w\}$  computed in step 1 are used along with the finite difference approximation to the derivatives to form the right hand side vector,  $\{B\}$ . The linear system of equations  $[A]\{\phi_1\} = \{B\}$  is solved, resulting in new values for the stress function,  $\phi_1$ .

Step 3 - Taking the new values of  $\ w_1 \$  and  $\ \phi_1$ , steps 1 and 2 are repeated. Step 4 - Convergence

After each iteration, the new values are compared with the old ones. If they are close enough, the iteration will be stopped and the last computed values of  $\phi$  and w will be accepted as the final solution for the given load. If the new values are not satisfactory, the iteration procedure will continue. The convergence was accelerated by using the convergence-inducing technique using 3 successive values, as discussed in reference (53) and it proved to be very useful.

Step 5 - The applied load is increased by a small amount,  $\Delta N$ , and steps 1 to 4 repeated again to get the solution corresponding to load  $N + \Delta N$ .

The above iterative procedure was continued until the applied load approached the second critical load. Near the second critical load, the equilibrium approaches instability and it was observed that the solution would not converge.

More details of the numerical solutions are discussed in the following sections.

### 3.1.3.2 Numerical Solutions

In this section some problems will be solved and the results analyzed.

a) Square plate with R = 1/10, h = a/8A square plate with  $R = \frac{D_{edge}}{D_{center}} = 1/10$ subject to an in-plane load, N, on all four edges,
was considered. A grid spacing of  $h = \frac{a}{8}$  was first
considered and later the problems were solved with the grid spacing of  $h = \frac{a}{16}$  for more accuracy.

The first critical load was found in (3.1.2 a) to be  $N = 4.84724 \frac{Dr}{a^2} \text{ and the } \phi \text{ values are known from Table}$  (3.1). A deflected shape, w, was assumed based on the first mode shape obtained from the buckling solution.

Initially, N = 5.  $\frac{D_r}{2}$  was assumed; this is slightly above the critical load. The transverse load, q, was taken to be zero.

The iteration was continued until the new values of  $\phi$  and w differed from the previous values by not more than a predetermined tolerance of .5%;  $(\left|\frac{w_1-w}{w}\right| \le .005)$ .

The last values of  $\phi$  and w were accepted as converged values and based on them the in-plane forces and displacements, as well as the bending moments and bending stresses, were computed.

In the very first step, convergence depends greatly on first input values; in the choice of these, experience will play a major role. In the following steps, convergence was achieved after about ten to twenty iterations - depending on the size of load increment. In this case, the load increments were taken as  $.5\frac{D_r}{a^2}$ , which is ten percent of initial load. Variation with load of the lateral deflection, w; in-plane displacement, umembrane force, N and bending moment, M, are plotted in Figure (3.22).

At the end of each step, having  $\phi$  and w at each node, we can calculate in-plane stress resultants from the difference approximations of equations (2.31) and

the bending moments from the difference approximations of equations (2.35).

So far, we have enough information at each node to illustrate the behavior of in-plane forces, bending moments and principal stress; they are plotted along the centerline of the plate in Figure (3.23), for three different load levels. The variation of maximum principal stress with load increase is also plotted in 3.23 d.

Contours of the in-plane force ratio,  $\frac{N}{X}$ , at the three different levels of loading are shown on Figure (3.24), and the distribution along various sections of the plate is shown on Figure (3.24 e). The variation of the in-plane force at the plate center with load increase can be seen on Figure (3.22 c).

It should be noted that  $\underset{y}{N}$  can be determined from  $\underset{x}{N}$  plots by considering symmetry.

To investigate in-plane displacements, equations (2.33) and (2.34) can be used.

We have already determined  $N_x$  and  $N_y$ , and the derivatives of w can be easily obtained by difference approximations; we are thus able to compute  $u_x = \frac{\partial u}{\partial x}$  and  $v_y = \frac{\partial v}{\partial y}$  at each node. Then  $(\frac{\partial u}{\partial x})_1 = (bu)_1$  and  $(\frac{\partial v}{\partial y})_1 = (bv)_1$ , where the right hand sides (bu) and (bv) are computed constant values. Applying the difference operator to the left hand sides will give:

$$[AU] \{u\} = \{bu\}$$

$$[Av] \{v\} = \{bv\}$$

In order to obtain a solution to these equations, we need to know some boundary values of u and v.

In this case, we will take advantage of symmetry. Since the geometry and the loading is symmetric, we can conclude the following (see Figure 3.3):

- i) Because of symmetry in x, the u displacements along the axis  $x = \frac{a}{2}$  will be zero.
- ii) Because of symmetry in y, the v displacements along axis  $y = \frac{a}{2}$  will be zero.
- iii) Symmetry about diagonals implies that u = v along the diagonal, x = y, at nodes 1, 3, and 6 in Figure (3.4).

Taking advantage of these assumptions enables us to solve a system of linear equations and obtain the  $\, u \,$  and  $\, v \,$  values for each node.

The patterns of u displacements at each load step and the contours of equal displacements are given in Figure (3.25). The v displacement behavior can be easily visualized considering symmetry.

The variation of in-plane displacement with load at some specific points is illustrated in Figure (3.22 b).

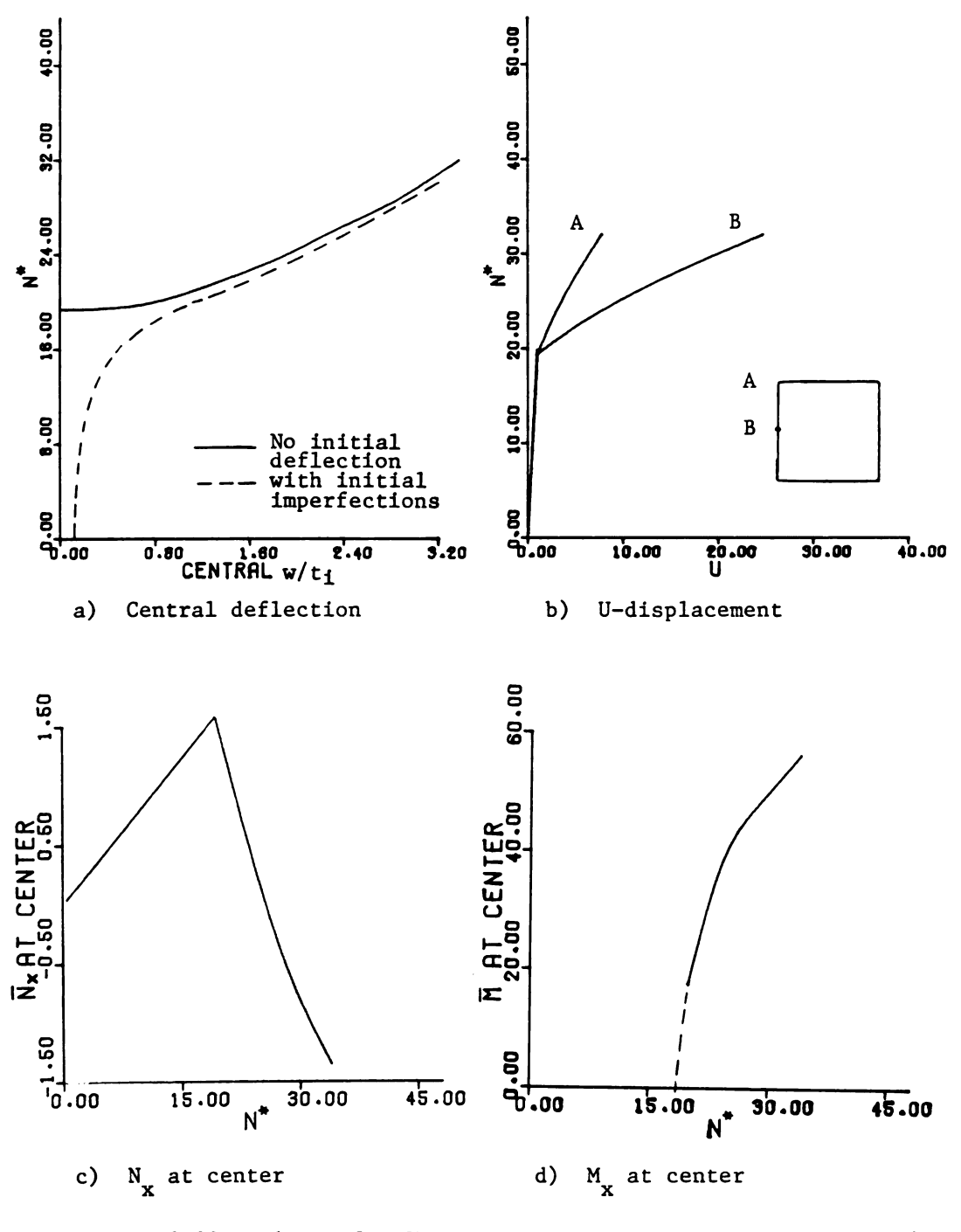


Figure 3.22. Plots of w, U, N<sub>x</sub>, and M<sub>x</sub>; square plate, s-s, R = 1/10

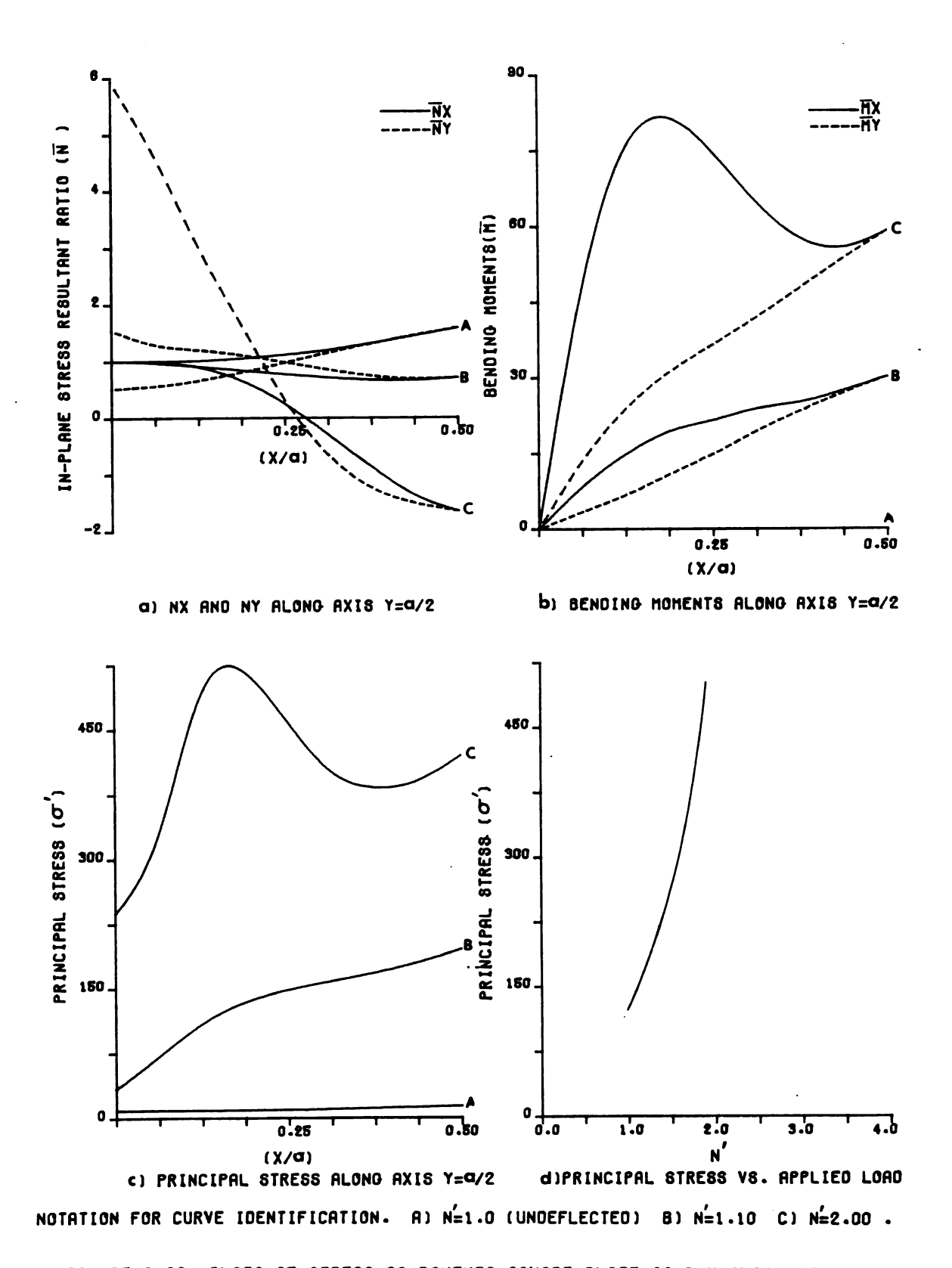


FIGURE 3.23. PLOTS OF STRESS COMPONENTS.SQUARE PLATE.SIMPLY SUPPORTED.R=1/10.

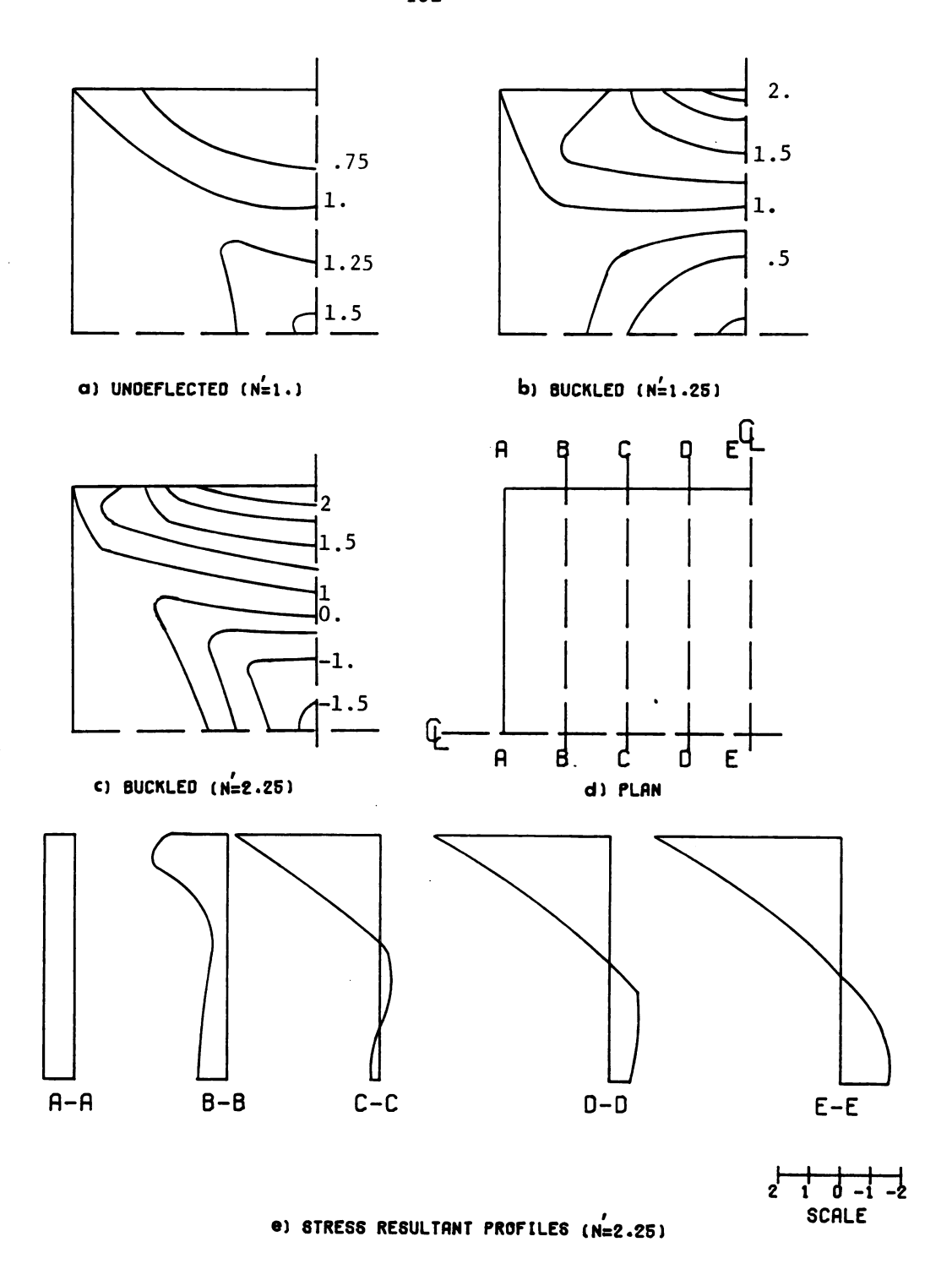


FIGURE 3.24. CONTOURS OF IN-PLANE FORCE(NX) AND PROFILES OF NX AT SPECIFIED SECTIONS FOR LOAD 2.25 TIMES THE CRITICAL LOAD, SIMPLY SUPPORTED.R=1/10

To compare the behavior of an imperfect plate, a small initial deflection was imposed by applying a small transverse load, q, at node 1 only. The plot of w vs load is shown in Figure (3.22 a).

Convergence of the solution was checked by solving the problem using two different grid spacings (h/a = 1/8 and h/a = 1/16) and the results proved to be very close. For example, corresponding to N = 1.5N<sub>cr</sub> the central deflection was found to be 3.335299 for h =  $\frac{a}{8}$  and 3.3735 for h =  $\frac{a}{16}$  a difference of only 1%. For more accurate results in all succeeding analyses, solutions with h =  $\frac{a}{16}$  are given.

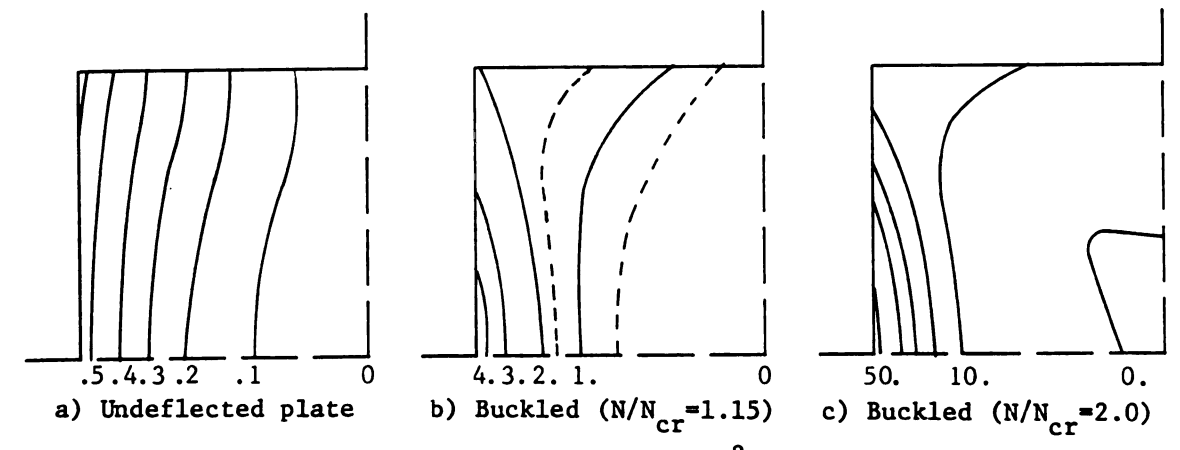


Figure 3.25. In-plane displacement  $(U = ua/t_1^2)$ , square plate, simply-supported, R = 1/10.

b) Square plate with uniform stiffness, R = 1.
As before, this problem, for which solutions have already been published, is undertaken in order to investigate
the accuracy of the difference method.

Just as in problem (a), the iteration procedure was followed, starting with the load  $N = 20 \frac{Dr}{a^2}$ , which is slightly above the critical load,  $N_{cr} = 19.48 \frac{Dr}{a^2}$ . The load increment was taken as 2.5, which is about 12.5% of the initial load and the tolerance range was taken as .5%. Convergence was usually achieved after 7 or 8 iterations.

Graphs of the w and u displacements versus load are given in Figure (3.26).

Plots of the membrane forces, bending moments, principal stress along the centerline  $(y = \frac{a}{2})$ , and principal stress versus load are shown in Figure (3.27).

For further illustration, the contours of in-plane force ratio,  $\frac{N}{N}$  and its distribution along various sections of the plate are shown in Figure (3.28). Figures (3.26 c) and (3.26 d) show the variation with load of membrane force and bending moments at the center of the plate. In-plane displacement, u, is illustrated by the contours in Figure (3.29).

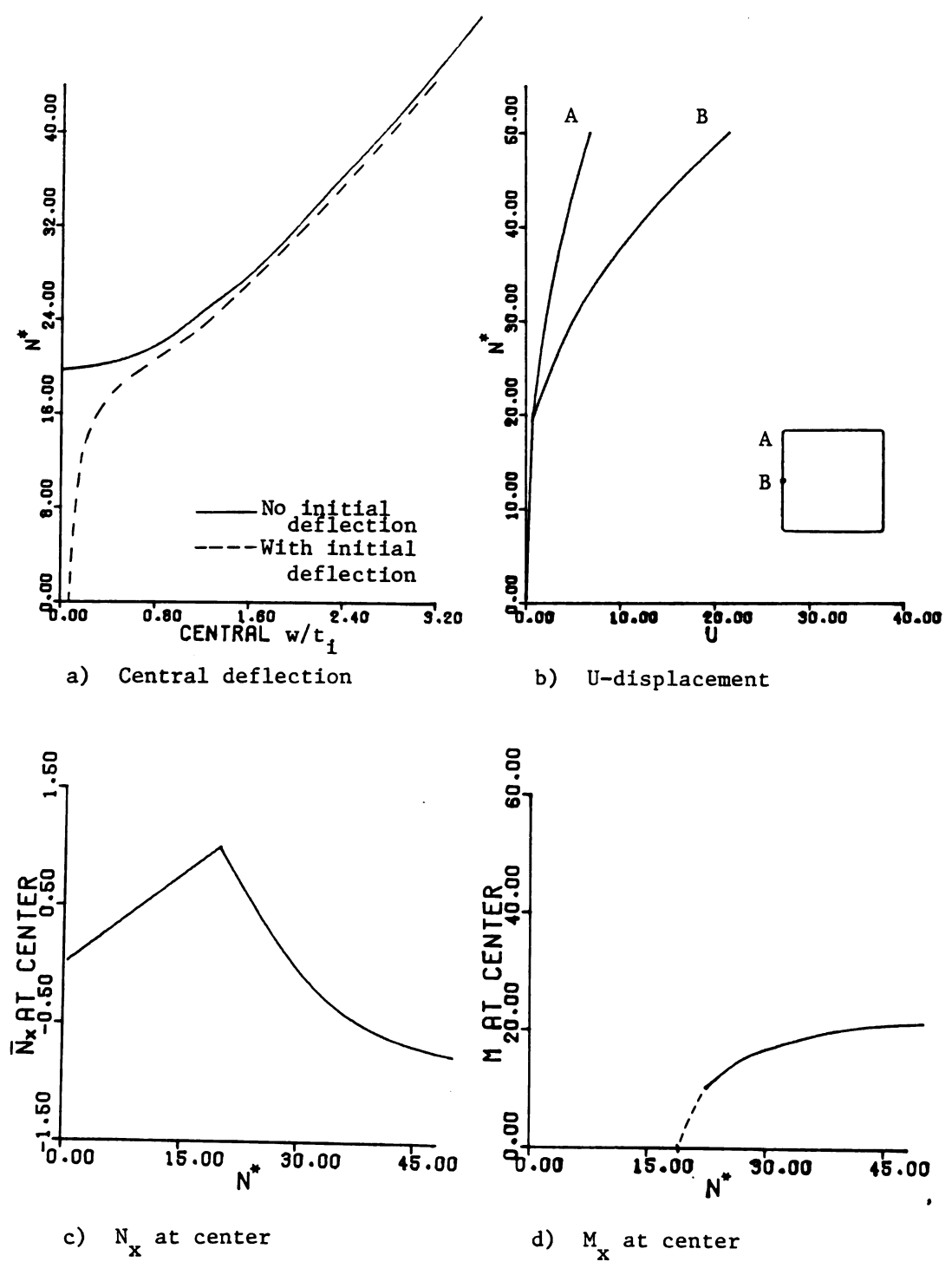
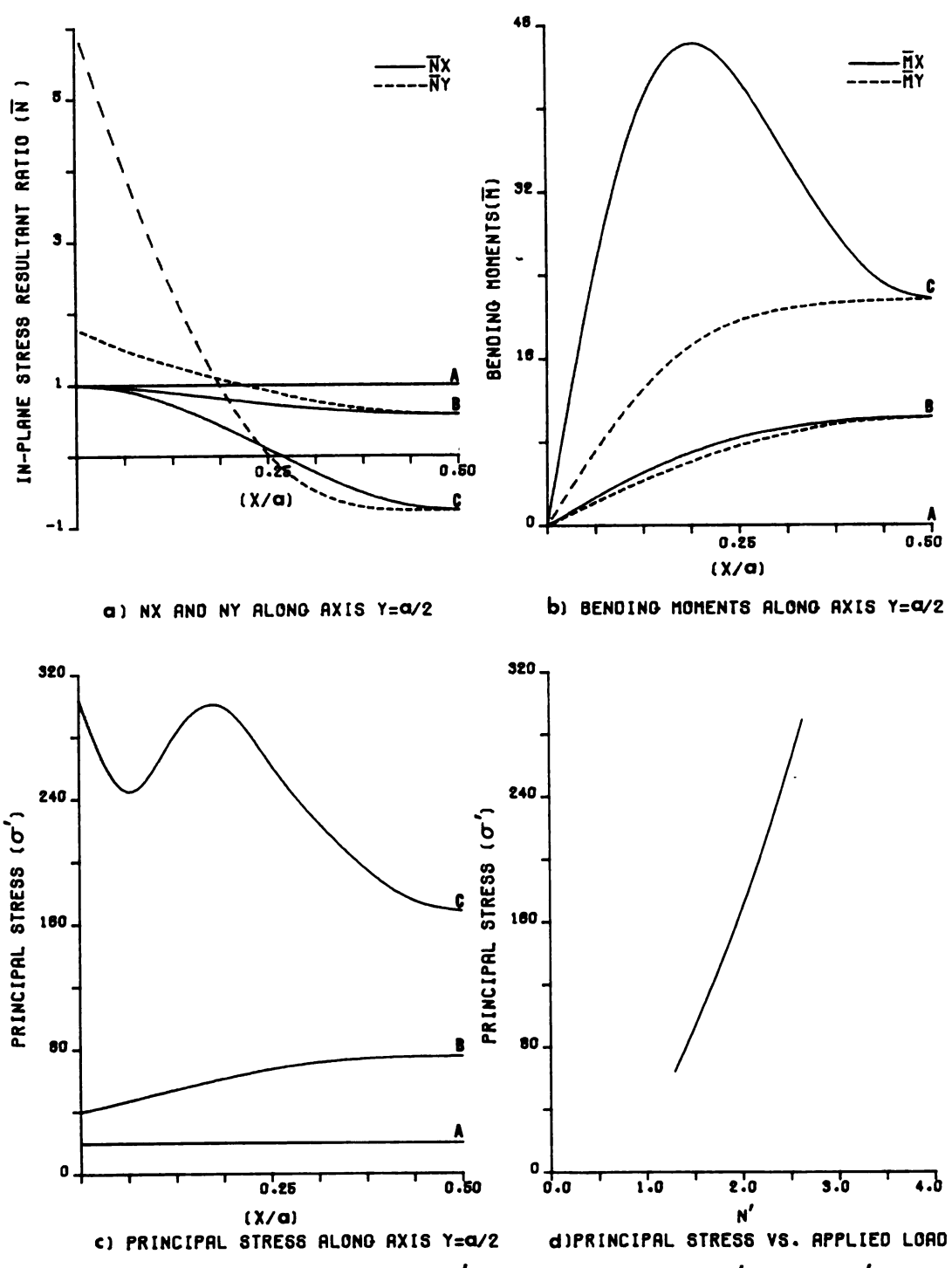


Figure 3.26. Plots of w,U,N, and M, square plate, s-s, R = 1

F



NOTATION FOR CURVE IDENTIFICATION. A) N=1.0 (UNDEFLECTED) B) N=1.10 C) N=2.50 .

FIGURE 3.27. PLOTS OF STRESS COMPONENTS. SQUARE PLATE. SIMPLY SUPPORTED. R=1 .

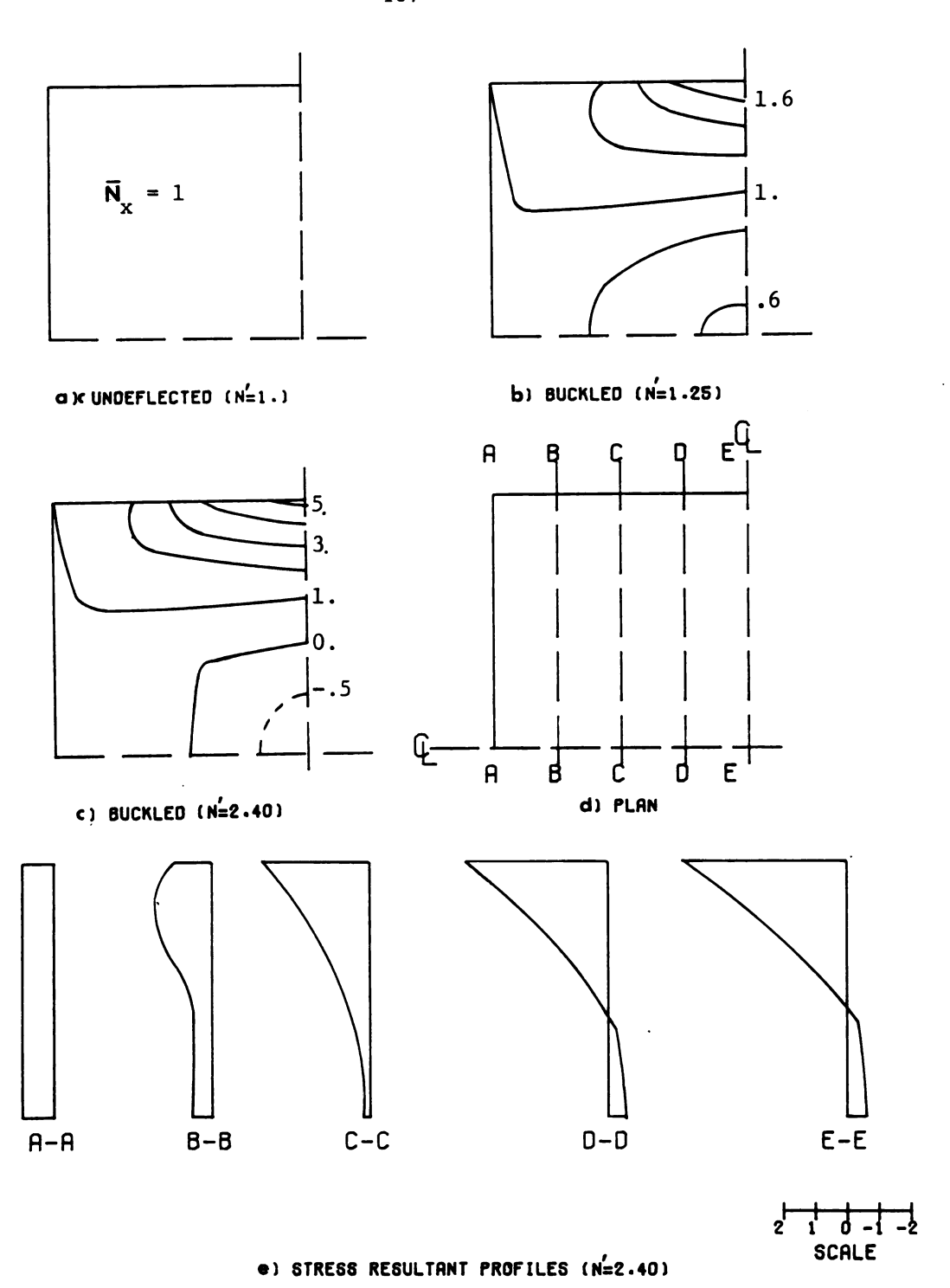


FIGURE 3.28. CONTOURS OF IN-PLANE FORCE(NX) AND PROFILES OF NX AT SPECIFIED SECTIONS FOR LOAD 2.40 TIMES THE CRITICAL LOAD.SIMPLY SUPPORTED,R=1 .

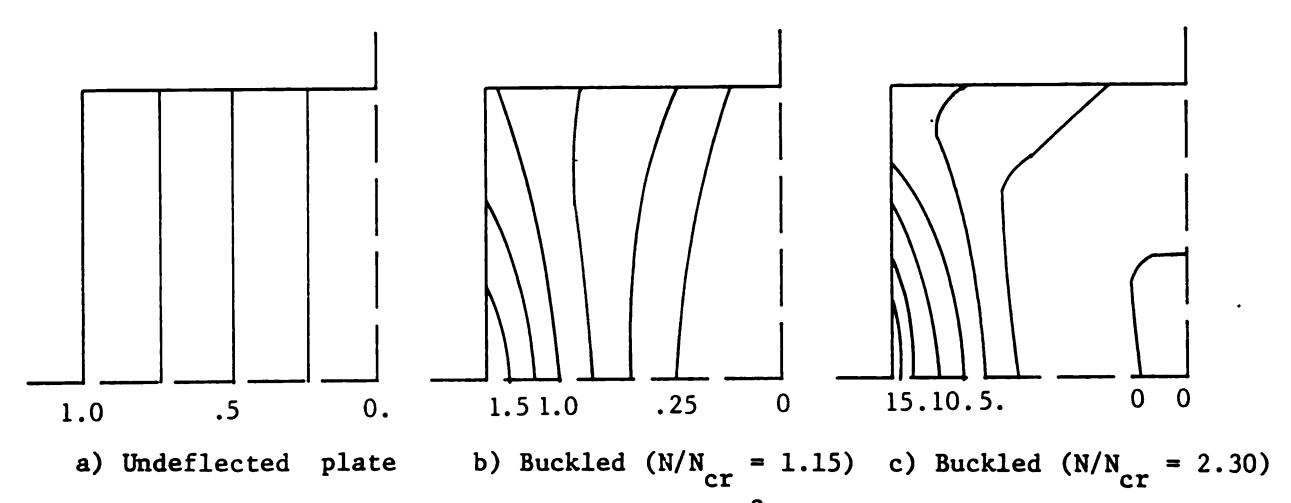


Figure 3.29. In-plane displacement ( $U = ua/t_i^2$ ), square plate, simply-supported, R = 1.

## Comparison of the results

In order to compare the results obtained by the iterative difference method with some currently available results, a square plate under uniform lateral load, q, was solved, and the results compared with those of Kaiser [26] and Basu [5].

Figure (3.30) demonstrates the very close agreement with the previous works.

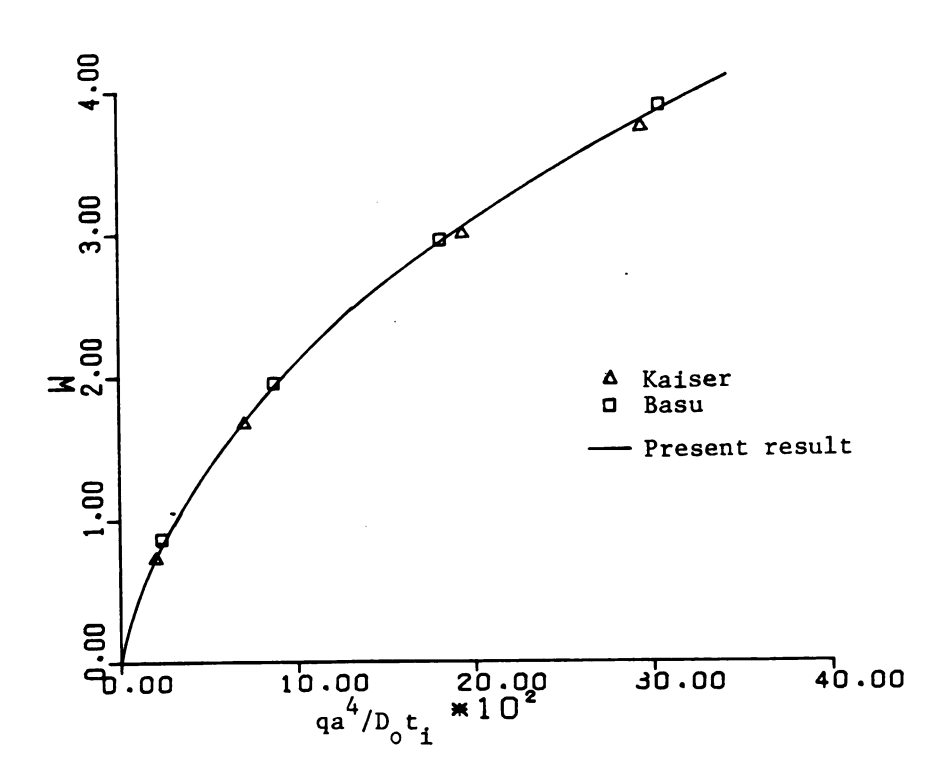


Figure 3.30. Square plate under uniform load, boundary free of any in-plane force, simply supported  $\nu$  = .316.

c,d) R = 1/2 and R = 10.

Problems c and d were also solved similarly and corresponding graphs are illustrated in Figures (3.31) to (3.38).

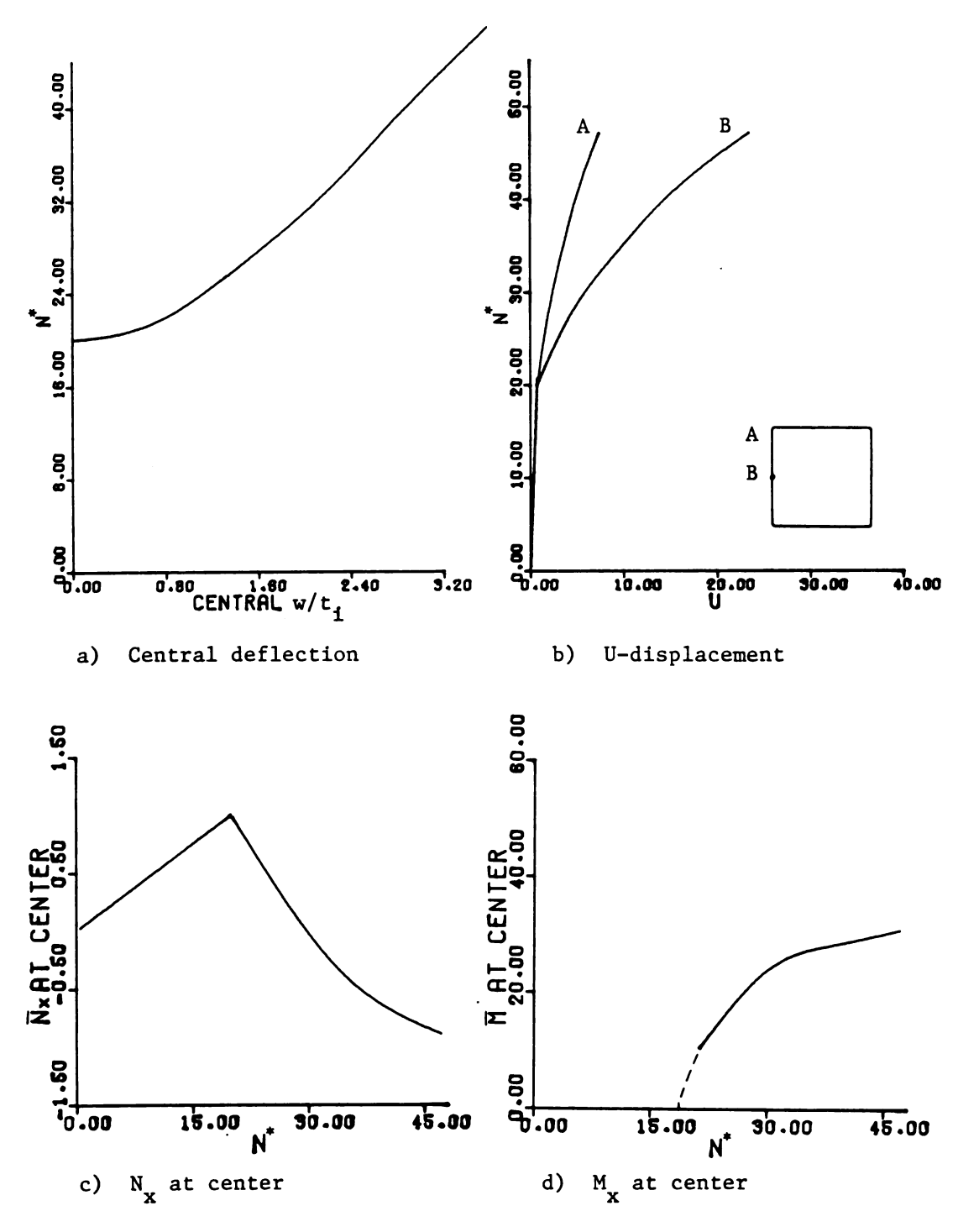


Figure 3.31. Plots of w,U,N<sub>x</sub>, and M<sub>x</sub>, square plate, s-s, R = 1/2

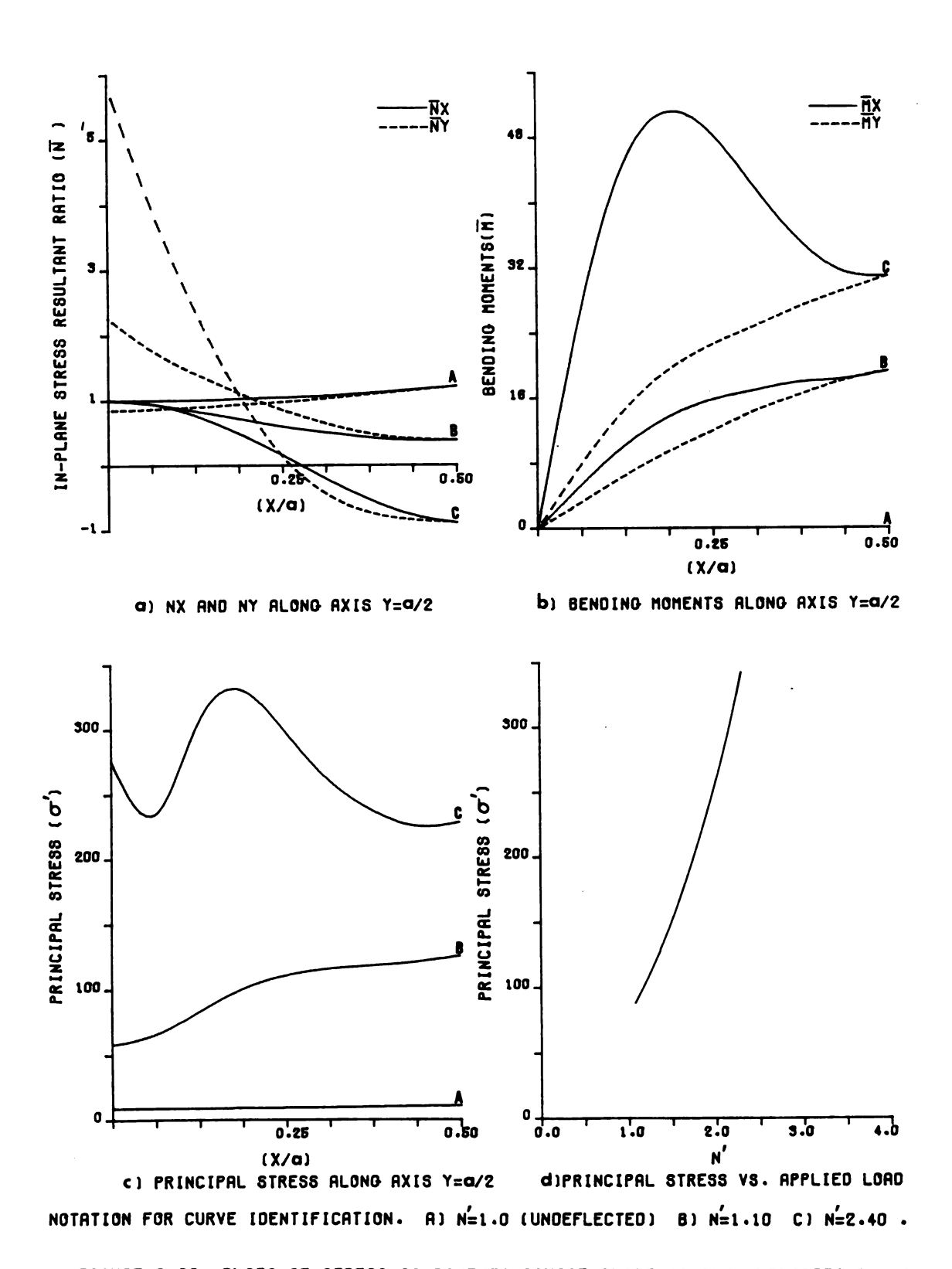


FIGURE 3.32. PLOTS OF STRESS COMPONENTS, SQUARE PLATE, SIMPLY SUPPORTED, R=1/2.

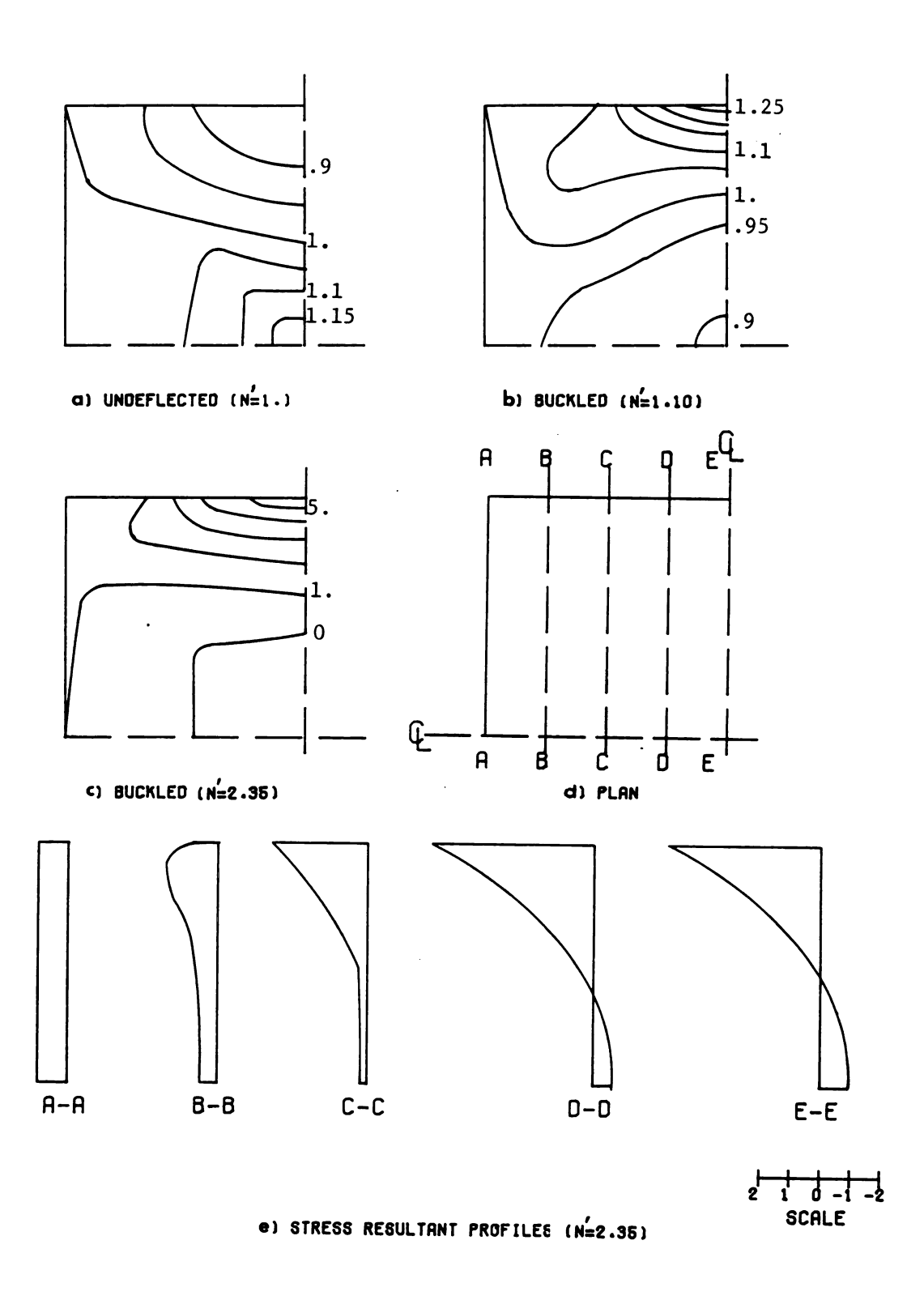
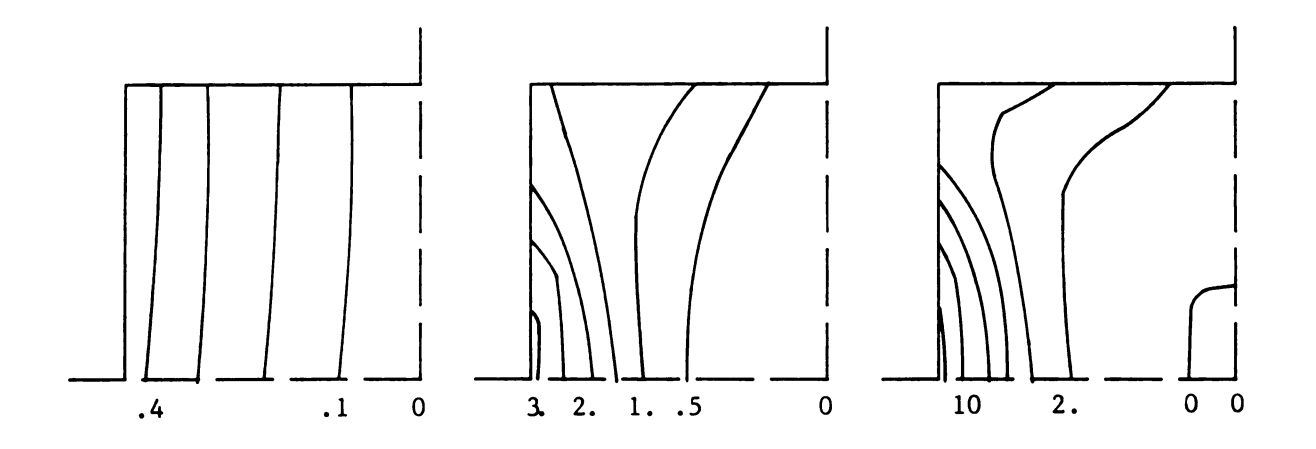


FIGURE 3.33. CONTOURS OF IN-PLANE FORCE(NX) AND PROFILES OF NX AT SPECIFIED SECTIONS FOR LOAD 2.35 TIMES THE CRITICAL LOAD.SIMPLY SUPPORTED.R=1/2.



b) Buckled  $(N/N_{cr} = 1.25)$  c) Buckled  $(N/N_{cr} = 2.20)$ Figure 3.34. In-plane displacement (U = ua/ $\xi_1^2$ ), square plate, simplysupported, R = 1/2.

a) Undeflected plate

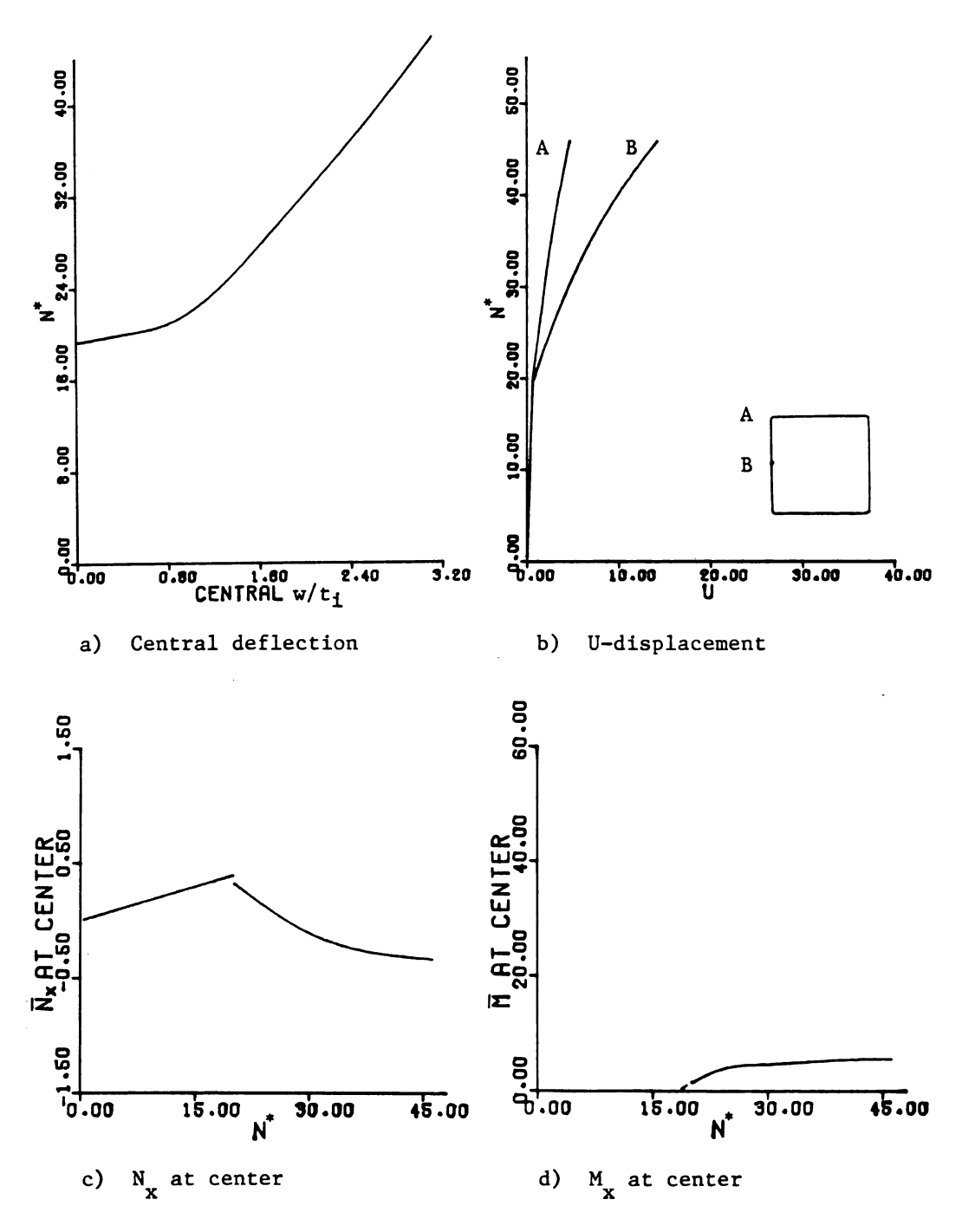


Figure 3.35. Plots of w,U,N<sub>x</sub>, and M<sub>x</sub>, square plate, s-s, R = 10

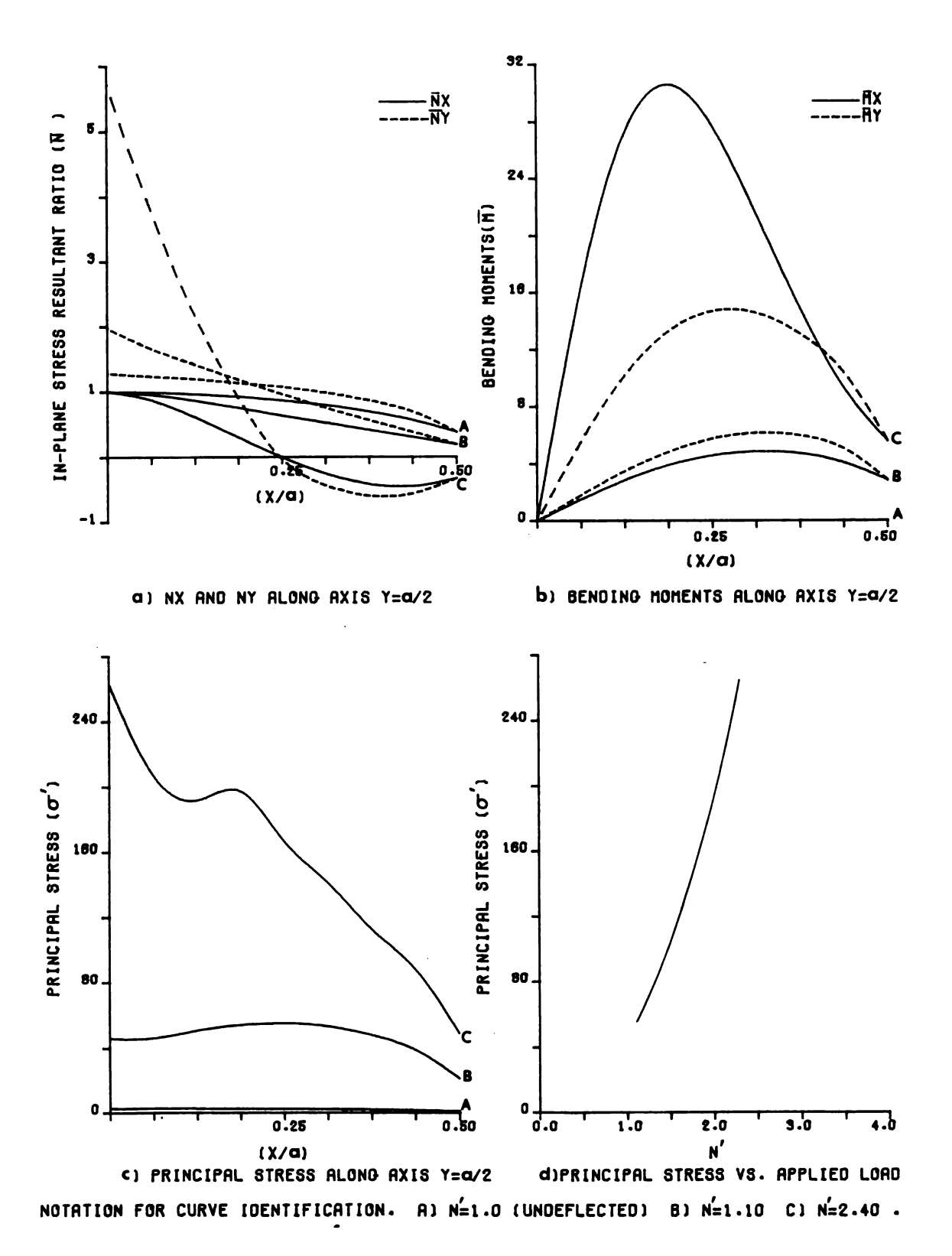


FIGURE 3.36. PLOTS OF STRESS COMPONENTS.SQUARE PLATE.SIMPLY SUPPORTED.R=10 .

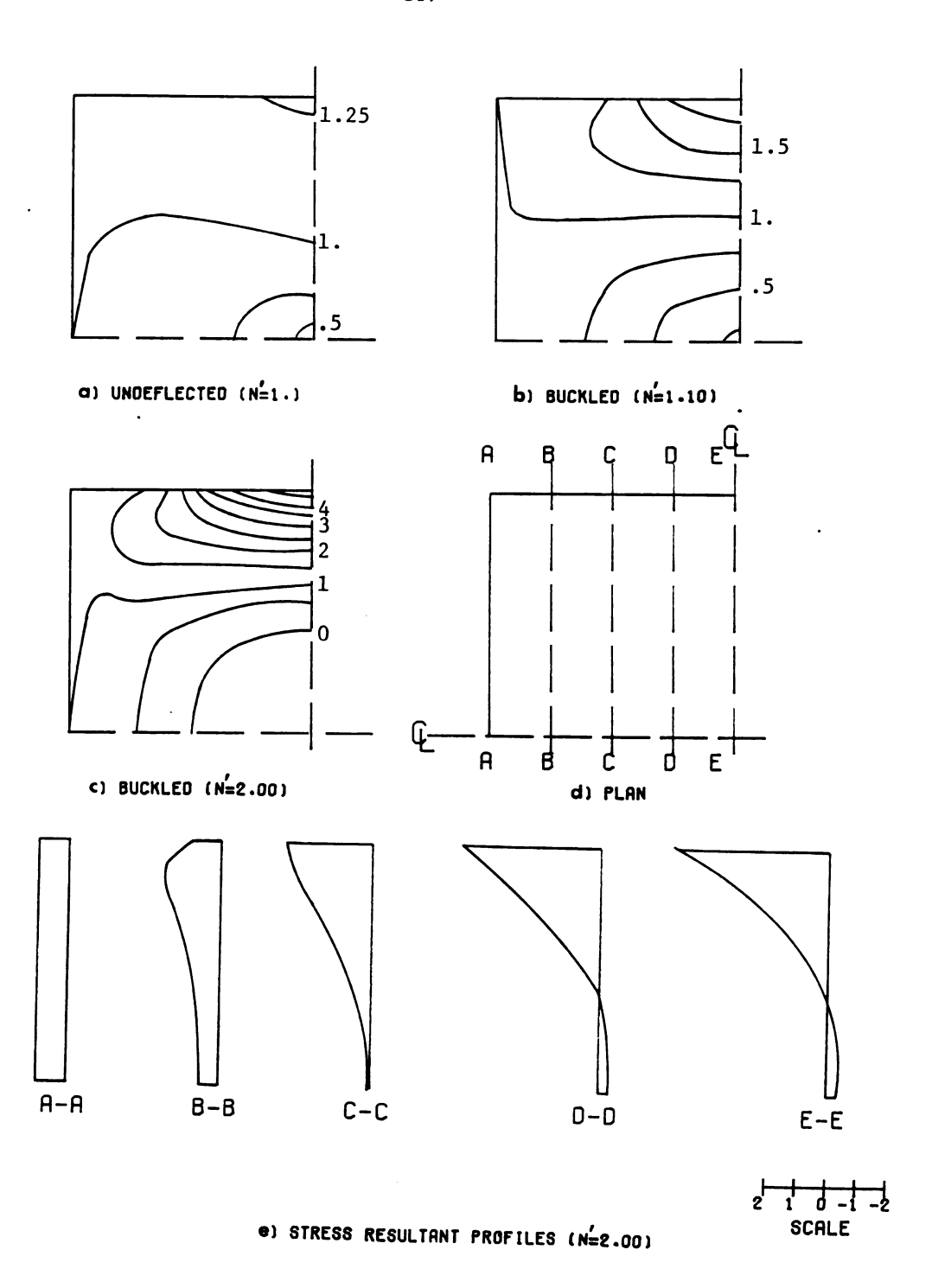


FIGURE 3.37. CONTOURS OF IN-PLANE FORCE(NX) AND PROFILES OF NX AT SPECIFIED SECTIONS FOR LOAD 2.00 TIMES THE CRITICAL LOAD.SIMPLY SUPPORTED.R=10.

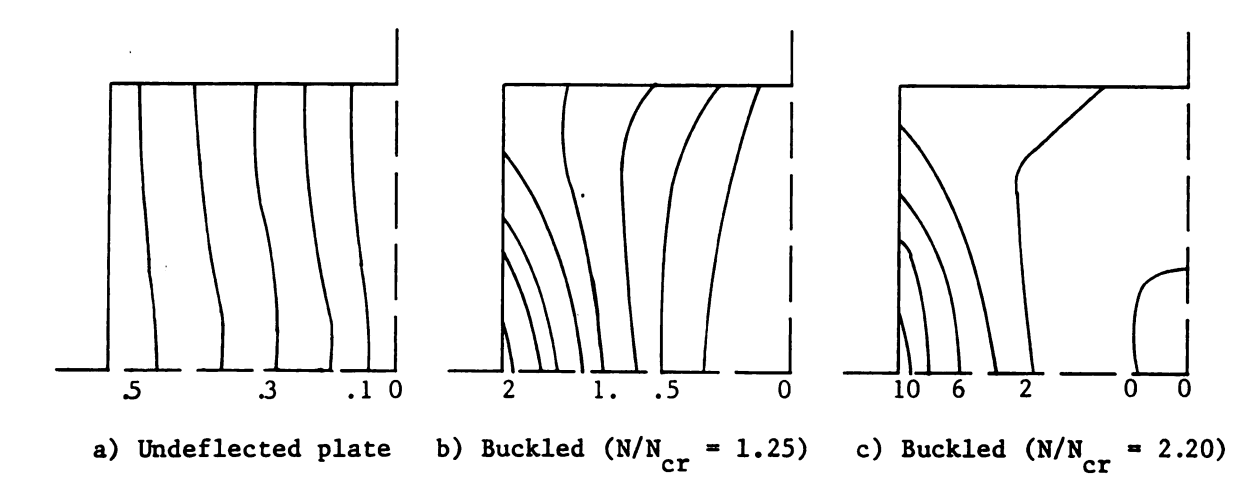


Figure 3.38. In-plane displacement  $(U = ua/t_1^2)$ , square plate, simply-supported, R = 10.

#### 3.1.3.3 ANALYSIS OF POSTBUCKLING RESULTS

#### 3.1.3.3.1 SIMPLY SUPPORTED EDGES

a) Uniform stiffness plate:

### Lateral Deflection

The plot of w-displacement versus edge load, Figure (3.26 a)shows a rapid increase in w immediately after buckling, continuing in a smooth manner.

Consider the plate under combined loading (bending and membrane) and introduce  $\overline{K}_b = \frac{\Delta N}{\Delta w \; center};$  the slope of the curve is the instantaneous stiffness. Before buckling, w at the center of plate is increasing almost linearly. As the critical load is approached, the stiffness,  $\overline{K}_b$ , begins to decrease rapidly. Finally, after passing the buckling range, it increases again and remains almost constant but less than the initial stiffness.

This reaffirms that, in contrast to beams, the plate has the capability of carrying load after buckling, but with a lower equivalent bending stiffness. This behavior is in agreement with previous research and results published.

# Convergence of the Solution

To check variation of the solution with grid spacing, the problem was solved with different mesh sizes and the w results for each solution are shown in Figure (3.39).

Study of the plots leads us to the conclusion that:

- i) the solution converges with decreasing mesh size.
- ii) solution obtained with grid spacing  $h = \frac{a}{8}$  is reasonably accurate for engineering purposes.

Investigation of membrane forces, bending moments, and in-plane displacements also indicates convergence, but the rate of convergence in bending moments is much greater than the others. This is attributed to the fact that the w function is very smooth.

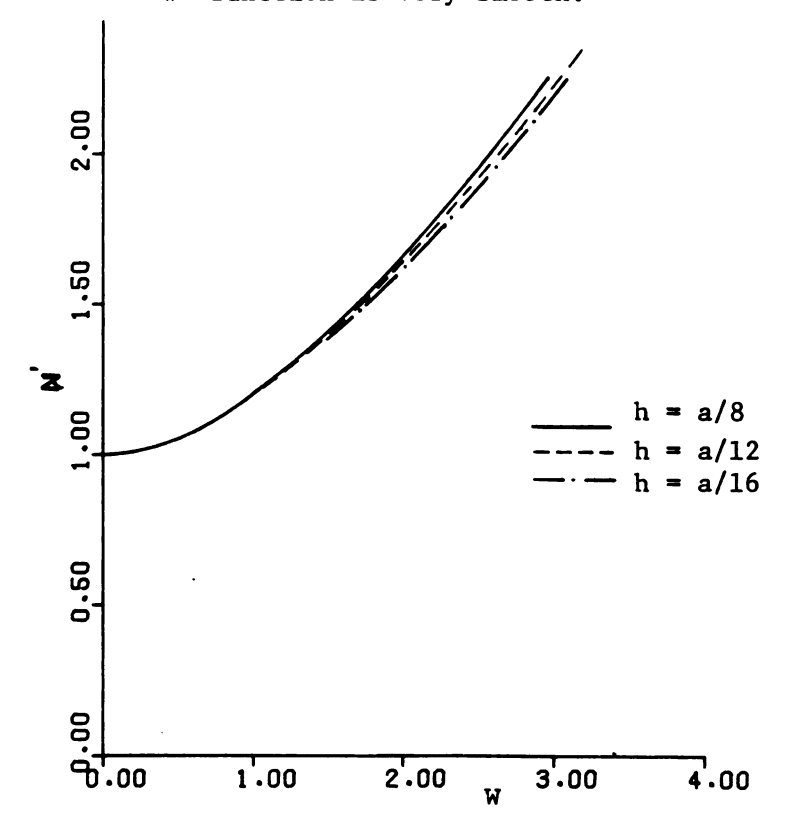


Figure 3.39. Convergence of the solution with mesh size.

#### In-Plane Stress Resultants

In the uniform stiffness plate, because of symmetry in loading (hydrostatic), N and N are equal to N everywhere before buckling.

After buckling, there is a change in distribution of the in-plane resultants as illustrated in Figure (3.26), which shows a tensile stress resultant at the center of the plate. This can be explained as follows: due to buckling, the plate will deflect a large amount - especially in this case with free in-plane displacement and no restraint on lateral slope. In this deflected position, the plate is analogous or similar to a shallow spherical shell with horizontal load applied all around the edges.

The variation of membrane resultants

agrees, qualitatively, with that of a shell. Shell analysis shows that, due to this type of loading,  $N_{\phi}$  (which is analogous to  $N_{\chi}$ ) along the axis,  $y=\frac{a}{2}$ , has its maximum near the edge, decreases towards the center and sometimes becomes tensile at points far from the edge as discussed in reference (7).

 $N_{\theta}$ , the membrane resultant in the direction of the parallels, will be the major load carrying element and will have values much greater than  $N\phi$ , the meridional resultant, near the edge. In this case,  $N_y$  along the axis y=a/2 is the counterpart of  $N_{\theta}$  in a shell and shows similar behavior.

Equilibrium was examined along different arbitrary sections

In us to

and the results were very good.

Referring to the paper by Kennedy and Prabhakara [27], although the conditions are different, their results show the existence of a tensile force at the center of a plate under edge compression. Figure (3.26 c) illustrates the variation of the membrane resultant  $N_{\rm x}$  at the central point. It shows that before buckling, in a flat plate or the small deflection case, the compressive in-plane resultant is increasing in proportion to the applied load. After buckling, however, it will start to decrease (sharply in a flat plate and smoothly in the small imperfection case) with an increase in the edge load and subsequently the deformation behavior of the plate is similar to that of a shallow shell.

# **Bending**

Since the bending moment is a function of curvature, immediately after buckling, when considerable deflection occurs, bending moments will be developed within the plate. The Figure (3.27 b) shows the variation of moment along the centerline, y = a/2, corresponding to different loading stages. At the beginning, maximum  $M_{\chi}$  is at center, but as the deflection increases and a flat region is formed around the center, the location of  $M_{\chi}$  maximum shifts toward the edges.

This phenomenon was studied by W.A. Bradley, (author's adviser), using a frame-work approximation (or analogy) and the behavior proved to be qualitatively in agreement with the above result.

#### Principal Stress

Due to dependence of principal stress on both in-plane forces and bending moments, it is varying with load both in distribution and magnitude. Since maximum stress is one of the major keys to design problems, the maximum principal stress is plotted versus load and the point at which the maximum is located is shown on Figure (3.27 c). It is seen that due to edge loads appreciably above critical load, the maximum principal stress is located at the middle point of the edges in the postbuckling range, while in membrane analysis it is uniform all over the plate.

#### Note

The principal stress is a function of both membrane and bending stresses and these two are functions of thickness in different degree. Thus, the principal stress would vary with reference thickness and the values given here are valid only for this case, (i.e., unit thickness plate with E varying).

#### In-Plane Displacements

Study of graphs (Figure 3.29) shows that before buckling, displacements are linear as expected (constant strain).

However, after buckling, geometrical nonlinearity caused by w introduces some changes in their patterns. As illustrated in (3.29), along edge x = 0, the u displacement (normal to the edge) is increasing from the corner towards

the center, which is consistent with lateral bulging. The v displacement along the x=0 edge (same as the u displacement along the y=0 edge) shows larger compressive strain at center and smaller strain near corner; this is caused by the considerable compressive membrane force in this direction near the middle of the edge.

The in-plane displacement is illustrated in (3.26). It shows that:

Before buckling, the edge displacement is linear with respect to applied load.

After buckling, the rate of in-plane displacement u, will increase at the corners. Define  $\frac{\Delta N}{\Delta u} = \overline{K}_m$ , the equivalent in-plane stiffness; it will decrease with increase in deformation. Also, there will be much greater reduction in  $\overline{K}_m$  at the middle of the edge (x=0, y=a/2), than at the corner.

#### b) Variable stiffness plate R = 1/10

#### Lateral Deflection

According to graph (3.40), in this case the lateral deflection w, follows the same pattern as in the uniform stiffness case. However, when the lateral deflection gets moderately large, a wide flat region occurs at the center where the plate is stiffer and there is sharper curvature near the edges, because of the smaller stiffness.

#### Membrane Resultants

Study of Figure (3.22, 23, 24) shows similar behavior in membrane resultant as for case (a) the uniform stiffness plate.

### Bending

Figure (3.23.b) shows bending moment behavior similar to that of the uniform stiffness plate. The only noticeable difference is that the location of the maximum  $M_{\chi}$  moment is closer to the edge because of the greater curvature near the edge, although the moment is a function of stiffness as well as curvature.

## Principal Stress

The maximum principal stress is found to be located at a point close to the edge in the postbuckling range; whereas, before buckling and during the first stages of postbuckling, the maximum stress was at the center.

## In-Plane Displacements

The graphs of Figure (3.25) show that along the edges, the displacement normal to edge is almost constant, as in the uniform stiffness case. As we move towards the center, however, we observe a change in the pattern which can be explained on the basis of the force distribution and the stiffness. Along sections parallel to y, near the center  $x \approx a/2$  and moving toward the edges, the reduction in stiffness

is greater than the reduction in the membrane forces.

Therefore, there is less displacement at the center and larger displacement near the edge.

As a quantitative example, as seen in Figure (3.24.a), along the section,  $x = \frac{a}{4}$ , at point  $(x = \frac{a}{4}, y = \frac{a}{2})$ ,  $N_x = 1.12N$ , and the in-plane stiffness Et = .325(ET)<sub>r</sub>. At point  $(x = \frac{a}{4}, y = 0)$  on the edge,  $N_x = .64$  while Et = .1(Et)<sub>r</sub>. Thus:

$$\epsilon_{x} = \frac{N_{x}}{Et} = \frac{1.12N}{.325(Et)_{r}} = 3.446 \frac{N}{Et_{r}}$$
 at point  $(\frac{a}{4}, \frac{a}{2})$ 

$$\varepsilon_{x} = \frac{N_{x}}{Et} = \frac{.64 \text{ N}}{.1 \text{ Et}_{r}} = 6.4 \frac{N}{Et_{r}}$$
 at point  $(\frac{a}{4}, 0)$  on the edge

(Note: Poisson's ratio will not cause a major change.)

After buckling, there is also a change in displacement normal to the edge, similar to that explained in case (a).

c) R = 1/2

This case is between cases (a) and (b); thus, we expect the results to be so. All results obtained do lie between the two previous cases and exhibit behavior already explained.

d) R = 10

#### Lateral Deflection

The graph of Figure (3.35a) shows the general behavior of the center deflection to be similar to that of the uniform stiffness case; for the lateral deflection along the center line,

Figure (3.40) shows an expected difference compared to previous cases, in line with the stiffness variation. There is greater curvature in the central region in contrast to case (b), which has a flat region in the center.

### Membrane Resultants

The overall effect of large deflection after buckling is similar to that in previous cases.

## Principal Stress

The maximum principal stress always occurs at the middle point of the edges.

## Bending

Studying graph (3.36 b), we observe that  $M_{\mathbf{x}}$  maximum, occurs at a point closer to the center, where considerable curvature takes place.

In contrast to previous cases,  $\frac{M}{y}$  reaches its maximum not at the center but at some midpoint. This is because the stiffness is minimum there and  $\frac{M}{y}$  is a function of both D and curvature, although the curvature in y-direction is maximum at the center.

## In-Plane Displacement

Before buckling, in contrast to case (b), we observe a smaller u-displacement in the vicinity of the centerline  $(y = \frac{a}{2})$ . This is consistent with the in-plane force distribution and the stiffness distribution as calculated in case (b).

After buckling, the in-plane displacements due to N are increased by the effect of large lateral deflection; also, the region having more closely-spaced contours is moved away from the center toward the edge.

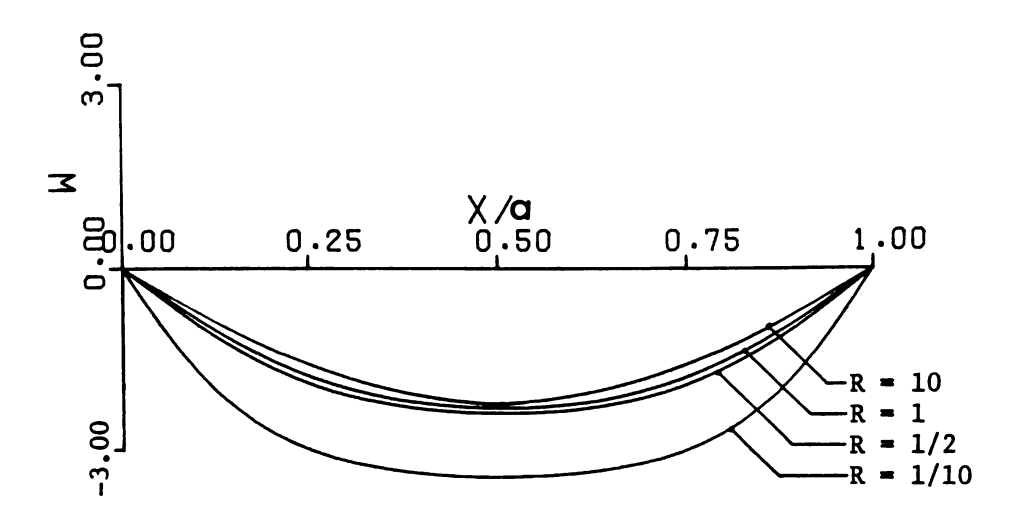


Figure 3.40. Deflected shape for various R values.

Simply-supported edge;  $N/N_{cr} = 2.40$ .

## 3.1.3.3.2 CLAMPED EDGES

The same stiffness variations discussed for plates with simply-supported edge are considered in this section, but for plates with clamped edges. The corresponding plots are given in Figures (3.41) to (3.56), which show the displacements and stress resultants. The behavior is largely similar to that for the simply-supported plate; notable differences are mentioned in the following.

### In-plane Stress Resultant

Overall behavior of the in-plane forces is similar, but in the simply-supported case they decrease more rapidly at the center. For example, compare Figure (3.26c) with (3.45c) for the uniform stiffness plate. The plate with simple support shows a much greater drop in  $N_{\rm X}$  at the center corresponding to edge load of two times the critical load.

#### Bending Moments

Bending moments exhibit the greatest differences between clamped and simply-supported boundary conditions. Their magnitudes and distributions are appreciably different as a comparison of Figures 3.22 d and 3.23 b with Figures 3.41 d and 3.42 b, for example, shows.

# In-plane Displacements

The in-plane movement of the plate in the postbuckling range follows almost the same patterns for the simply-supported and clamped cases. However, the plate with clamped edges undergoes smaller displacement along the edges. Compare Figures (3.25) and (3.44).

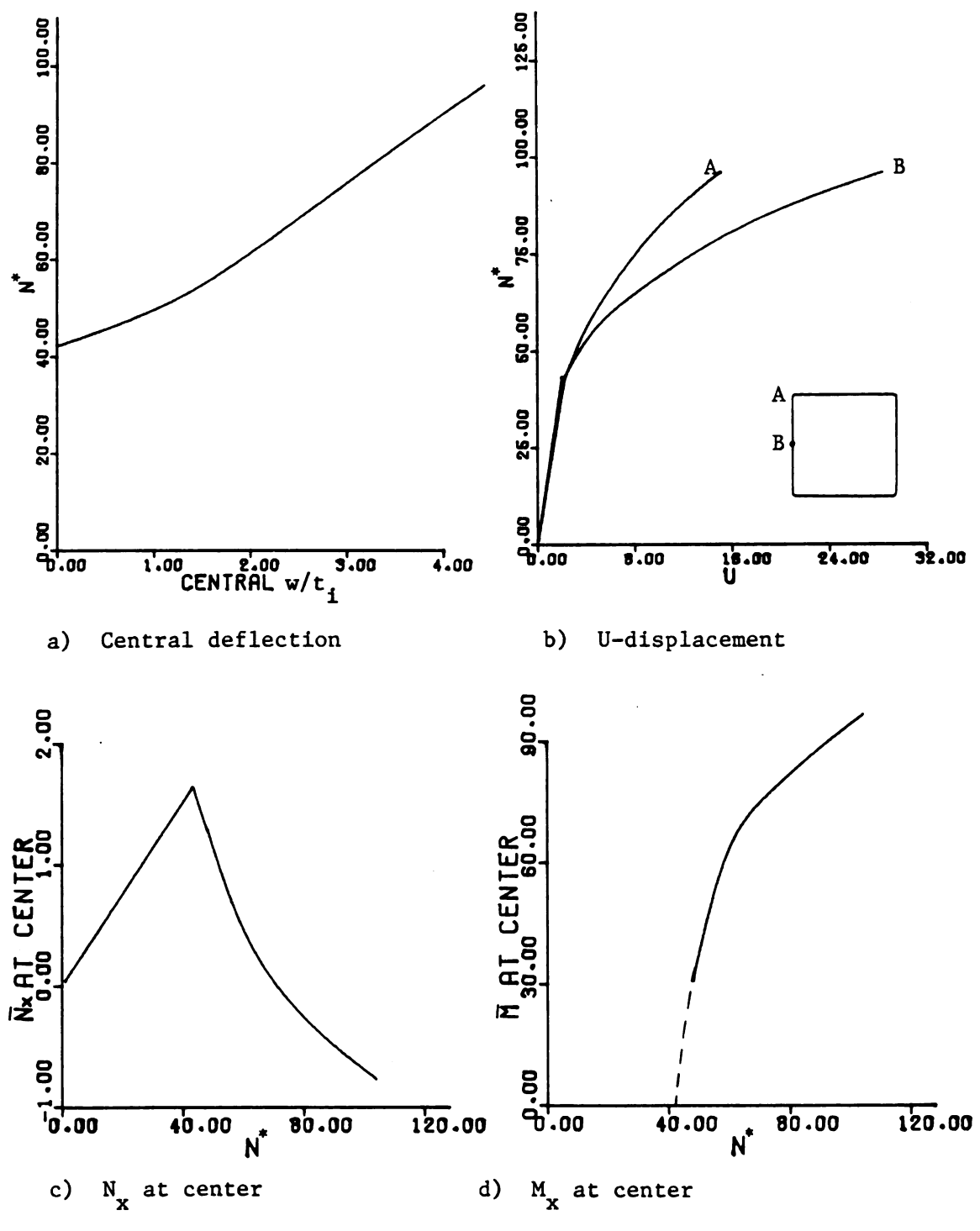
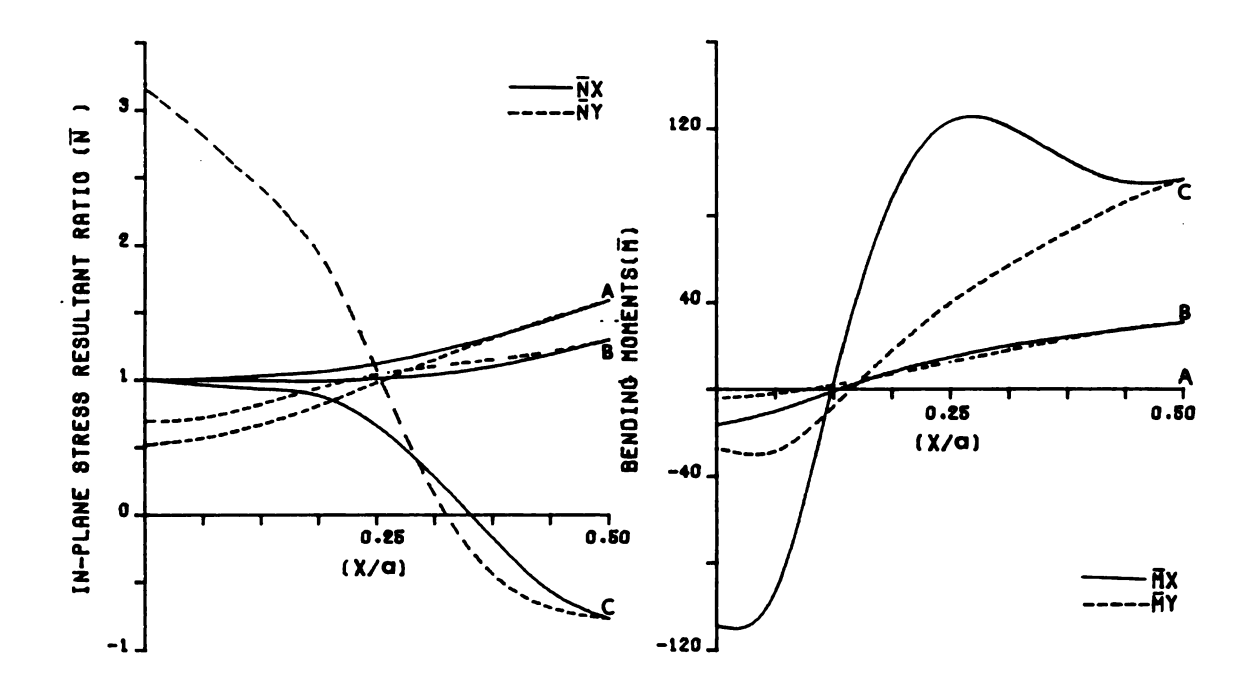
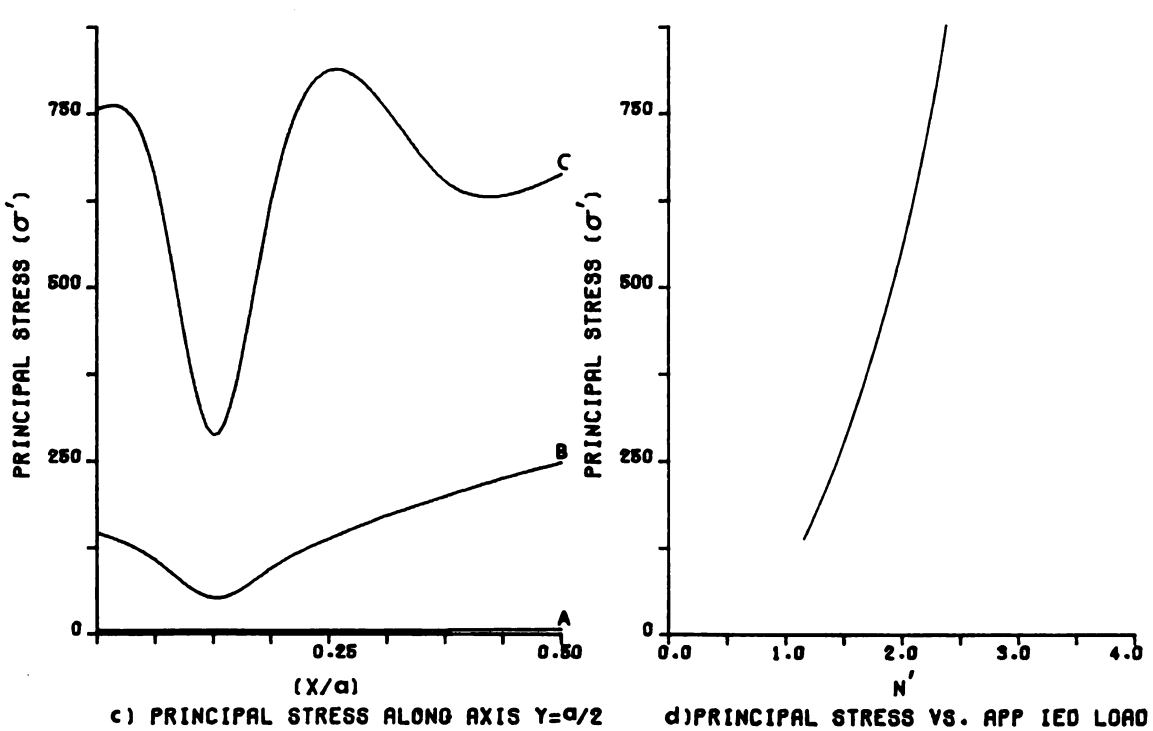


Figure 3.41. Plots of w,U,N<sub>x</sub> and M<sub>x</sub>, square plate, clamped, R = 1/10



a) NX AND NY ALONG AXIS Y=Q/2





NOTATION FOR CURVE IDENTIFICATION. A) N=1.0 (UNDEFLECTED) B) N=1.10 C) N=2.50 .

FIGURE 3.42. PLOTS OF STRESS COMPONENTS.SQUARE PLATE.CLAMPED. R=1/10 .

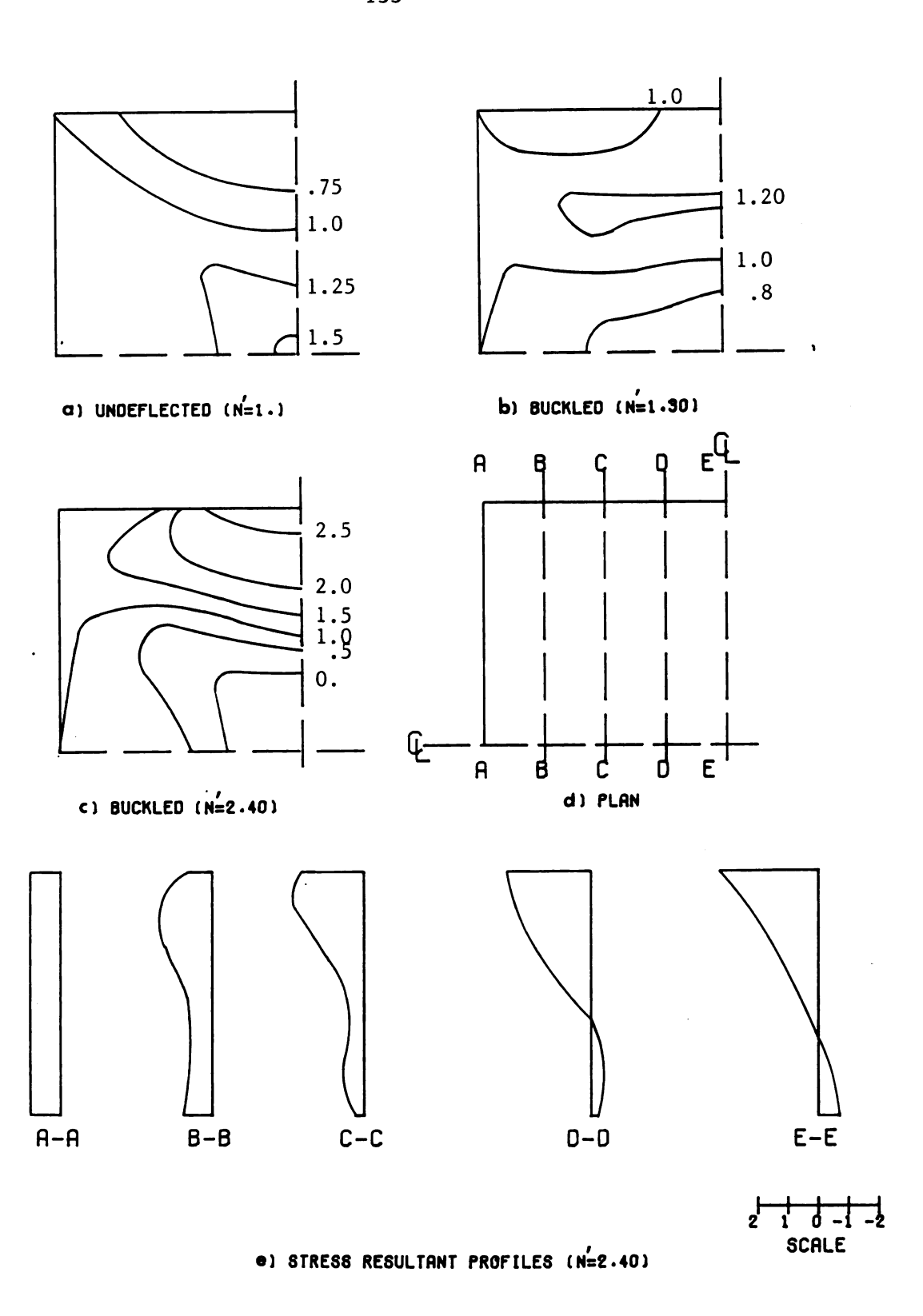
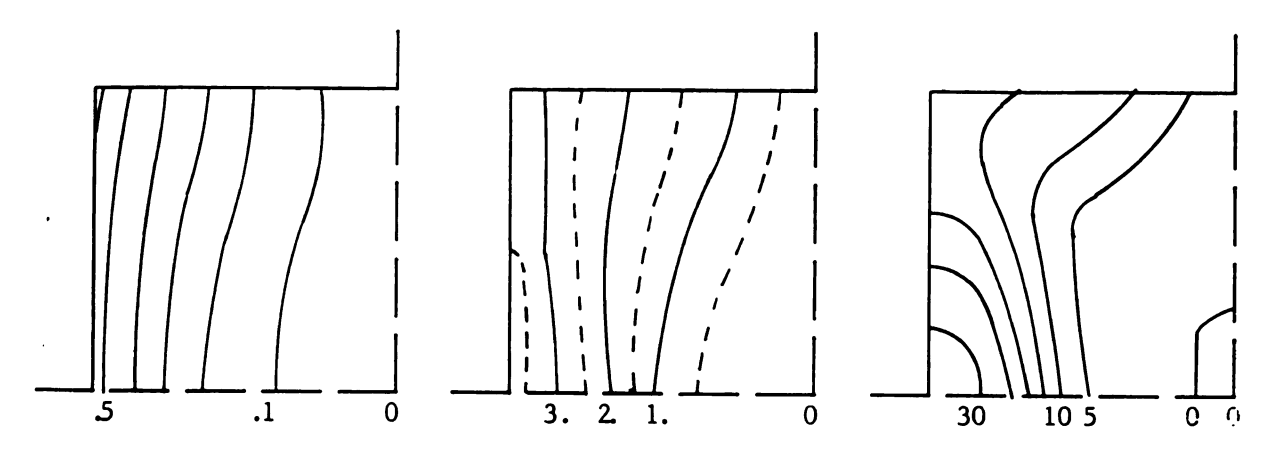


FIGURE 3.43. CONTOURS OF IN-PLANE FORCE(NX) AND PROFILES OF NX AT SPECIFIED SECTIONS FOR LOAD 2.40 TIMES THE CRITICAL LOAD.CLAMPED. R=1/10.



- a) Undeflected plate
- b) Buckled  $(N/N_{cr} = 1.25)$  c) Buckled  $(N/N_{cr} = 2.25)$

Figure 3.44. In-plane displacement ( $U = ua/t_1^2$ ), square plate, clamped edges, R = 1/10.

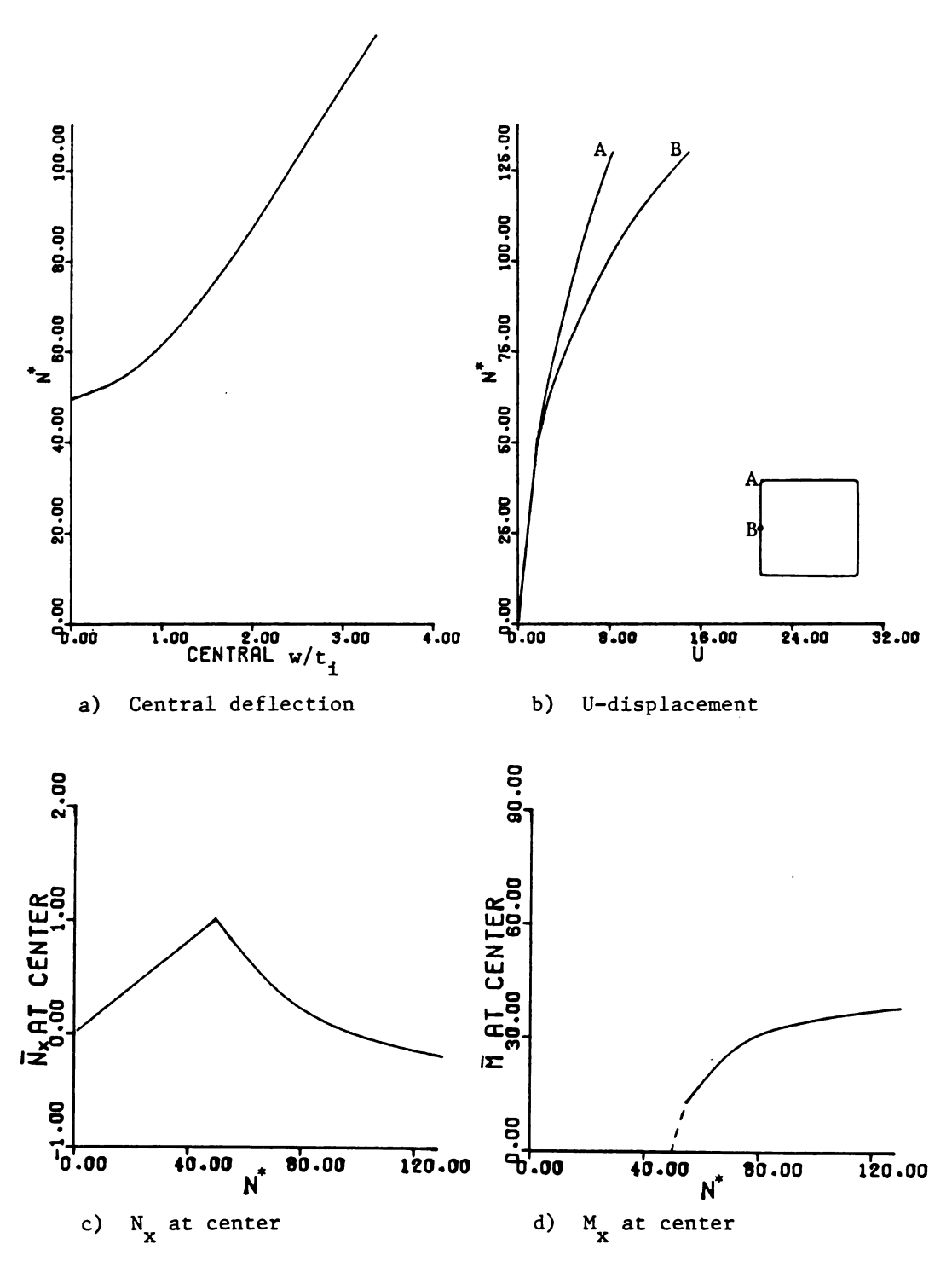
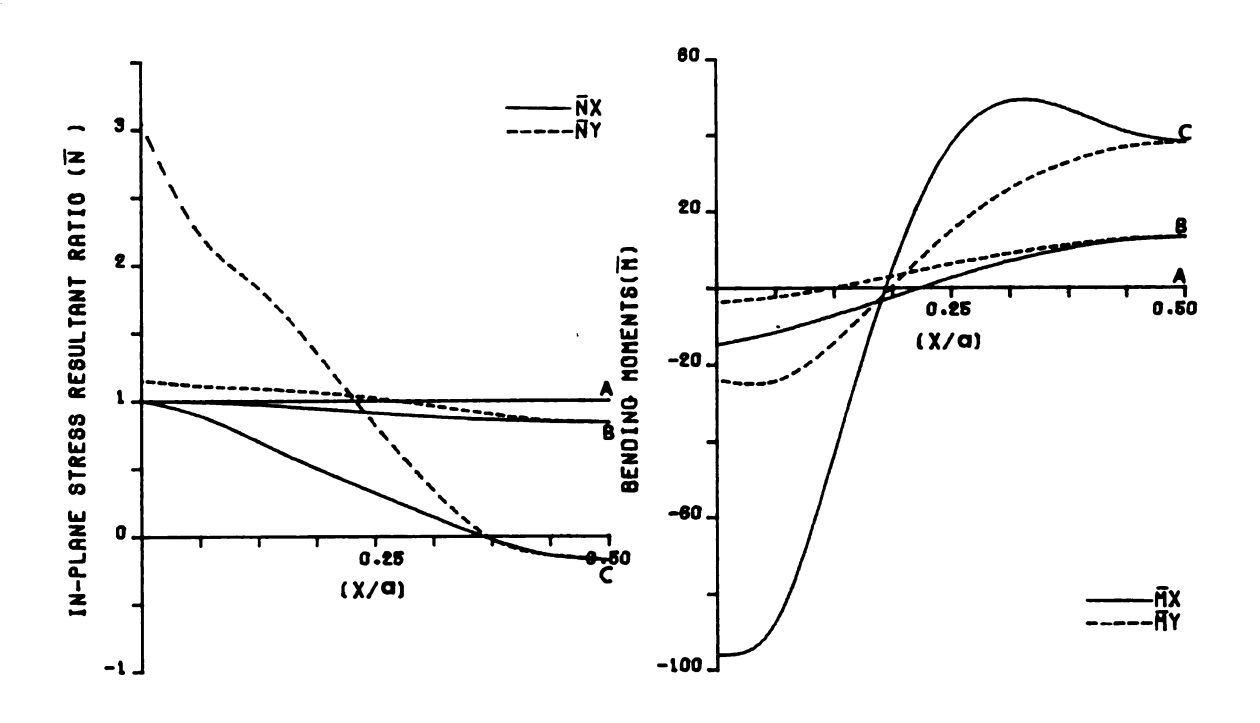
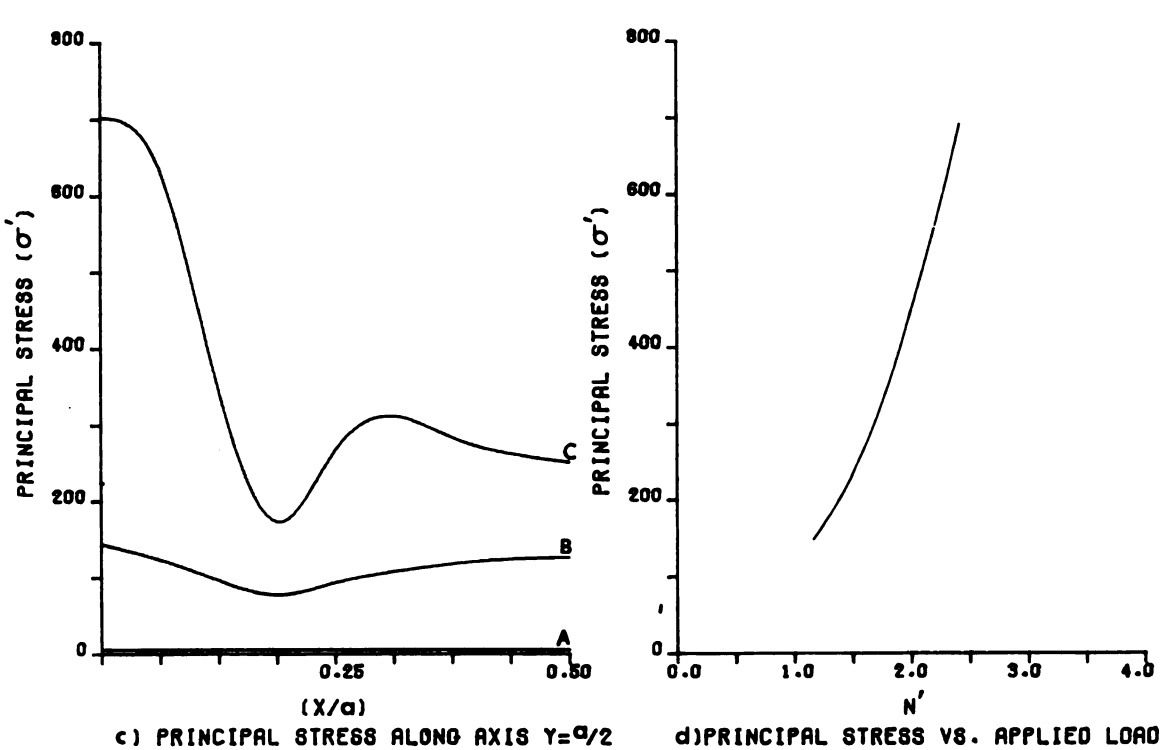


Figure 3.45. Plots of w,U,N<sub>x</sub>, and M<sub>x</sub>, square plate, clamped, R = 1









NOTATION FOR CURVE IDENTIFICATION. A) N=1.0 (UNDEFLECTED) B) N=1.10 C) N=2.50 .

FIGURE 3.46. PLOTS OF STRESS COMPONENTS, SQUARE PLATE, CLAMPED, R=1.

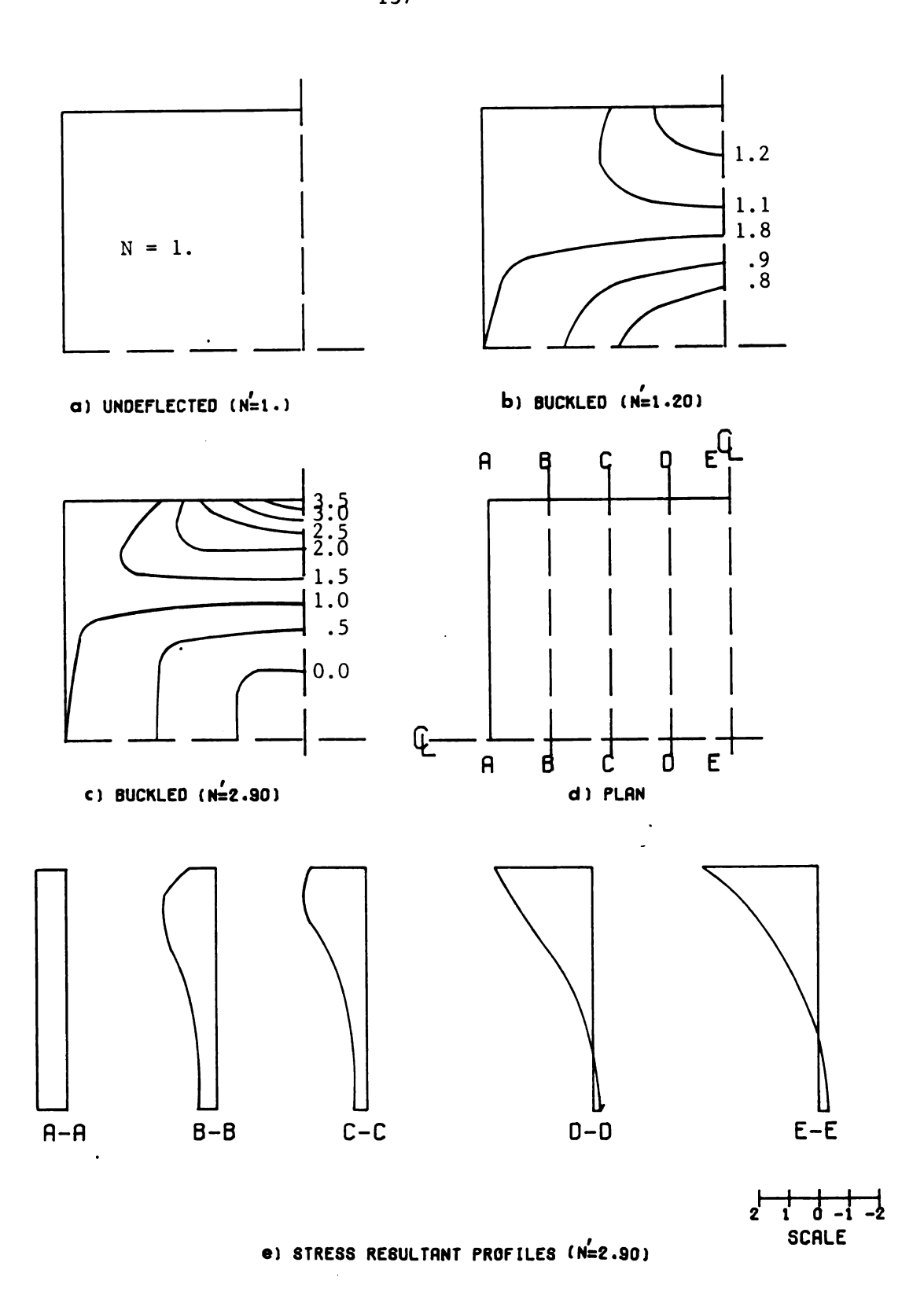


FIGURE 3.47. CONTOURS OF IN-PLANE FORCE(NX) AND PROFILES OF NX AT SPECIFIED SECTIONS FOR LOAD 2.90 TIMES THE CRITICAL LOAD.CLAMPED. R=1.

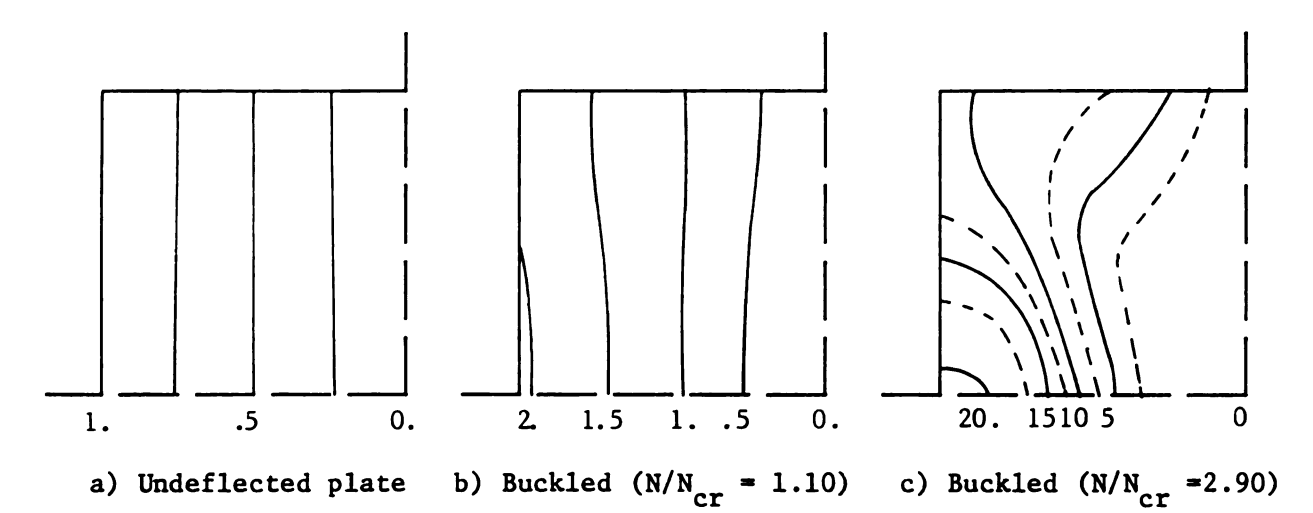


Figure 3.48. In-plane displacement ( $U = ua/t_1^2$ ), square plate, clamped edges, R = 1.

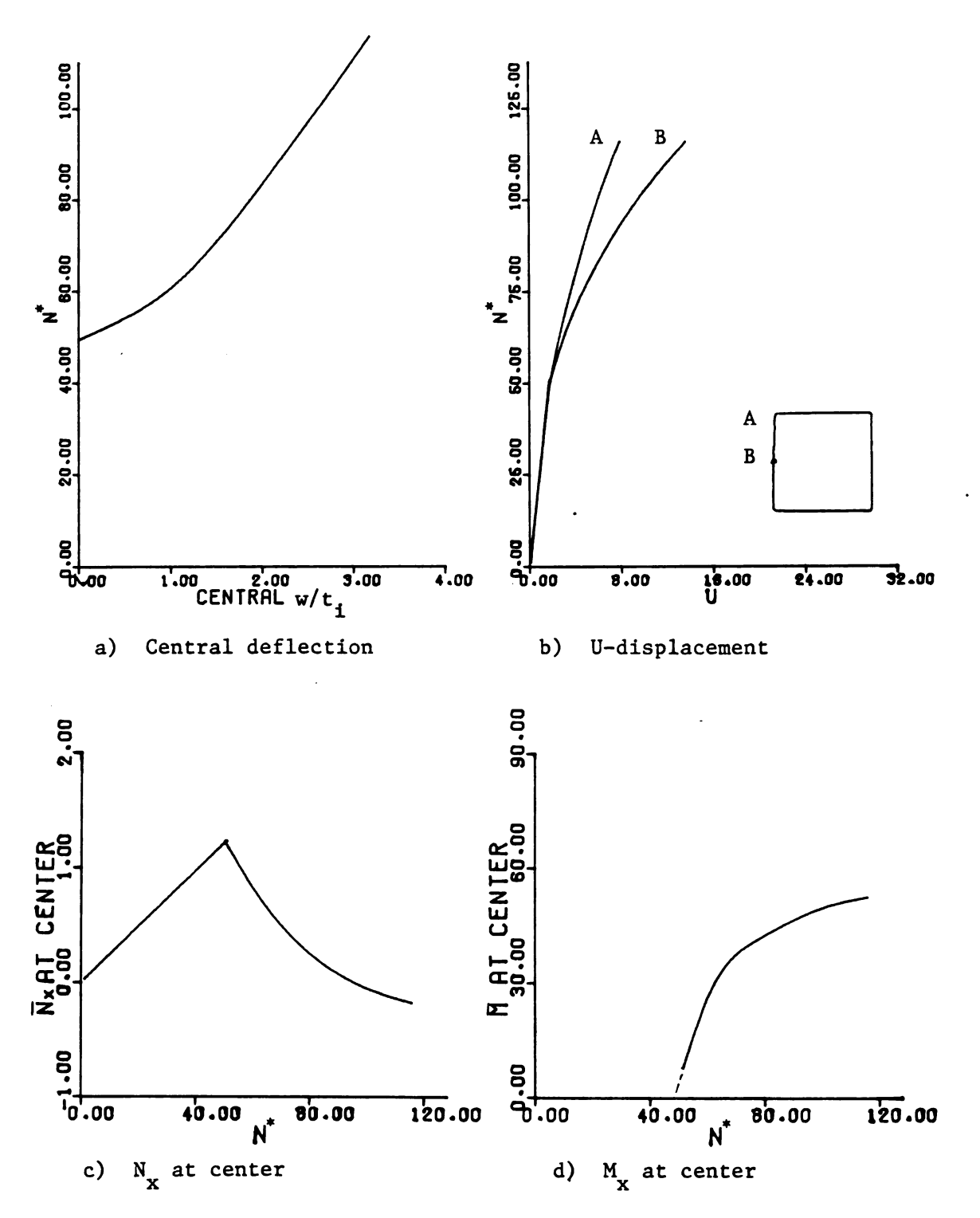
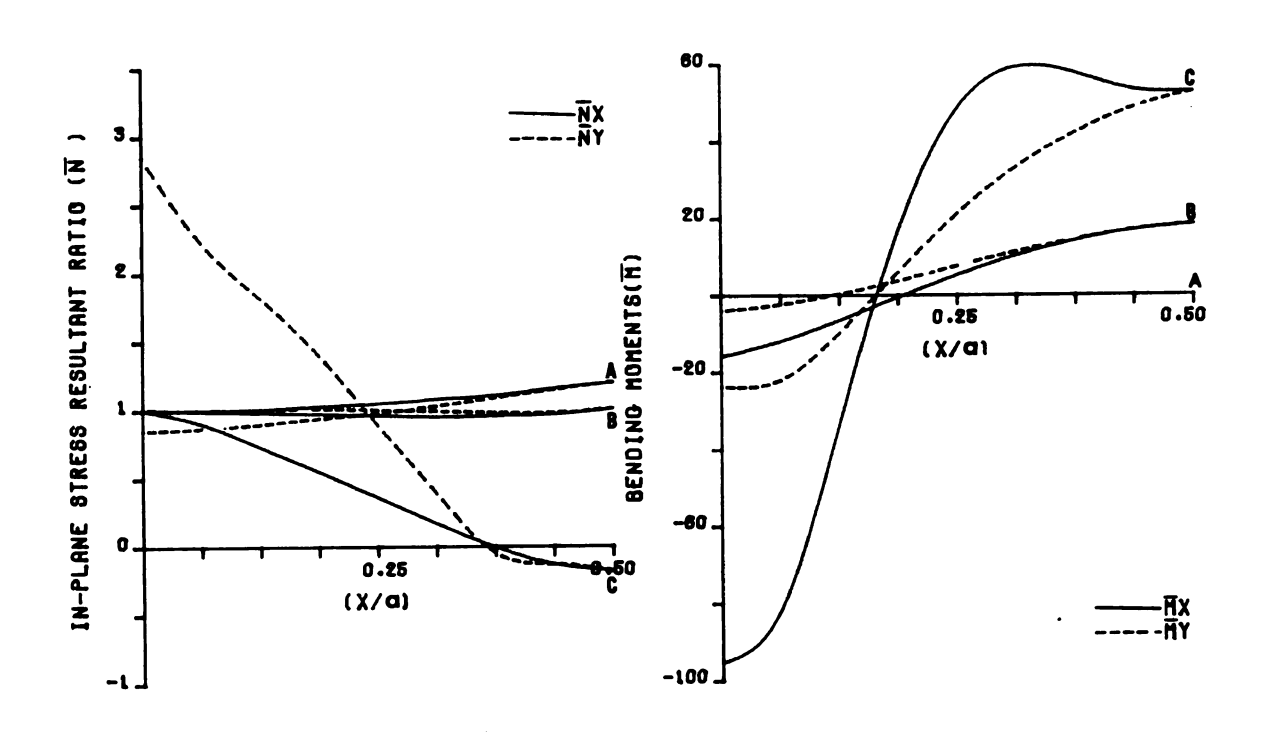


Figure 3.49. Plots of w,U,N, and M, square plate, clamped, R = 1/2



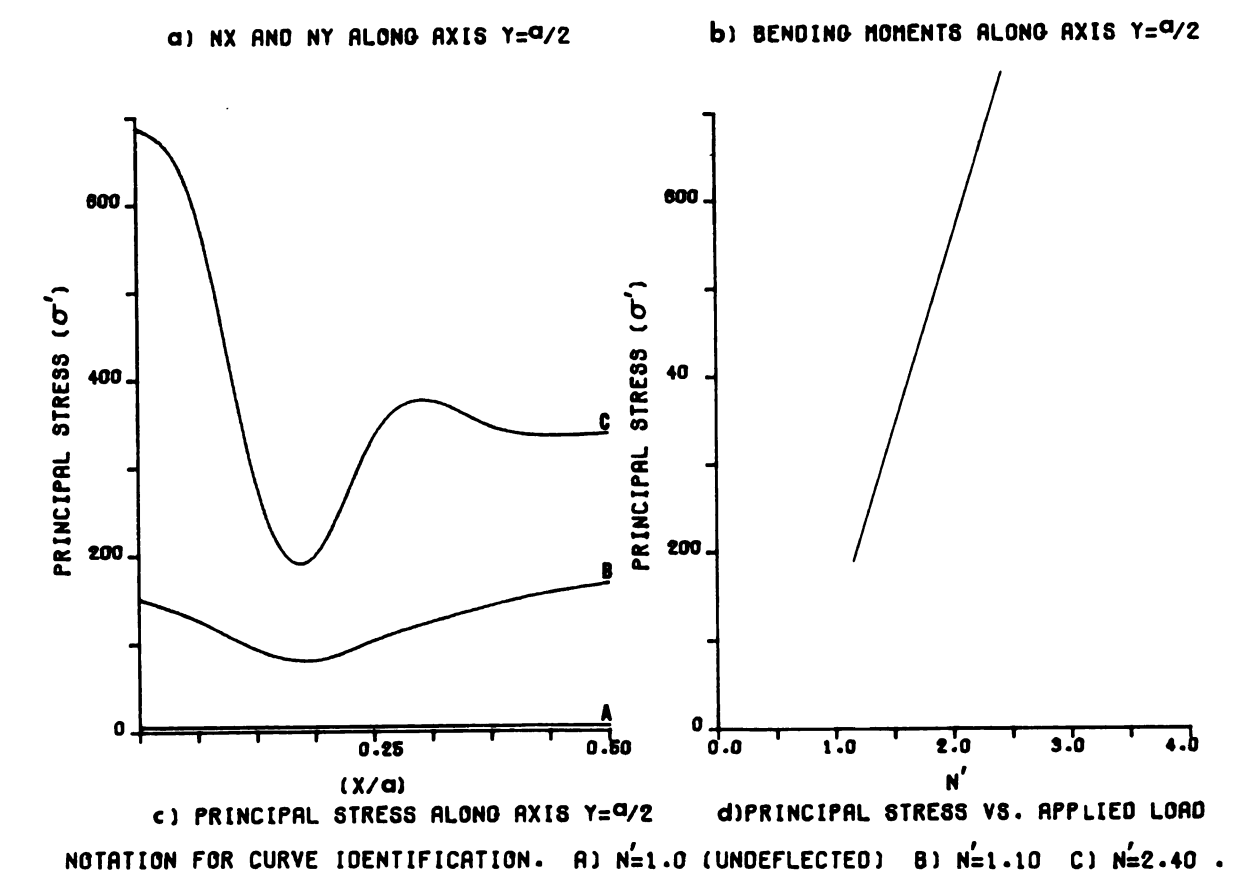


FIGURE 3.50. PLOTS OF STRESS COMPONENTS.SQUARE PLATE.CLAMPED. R=1/2 .

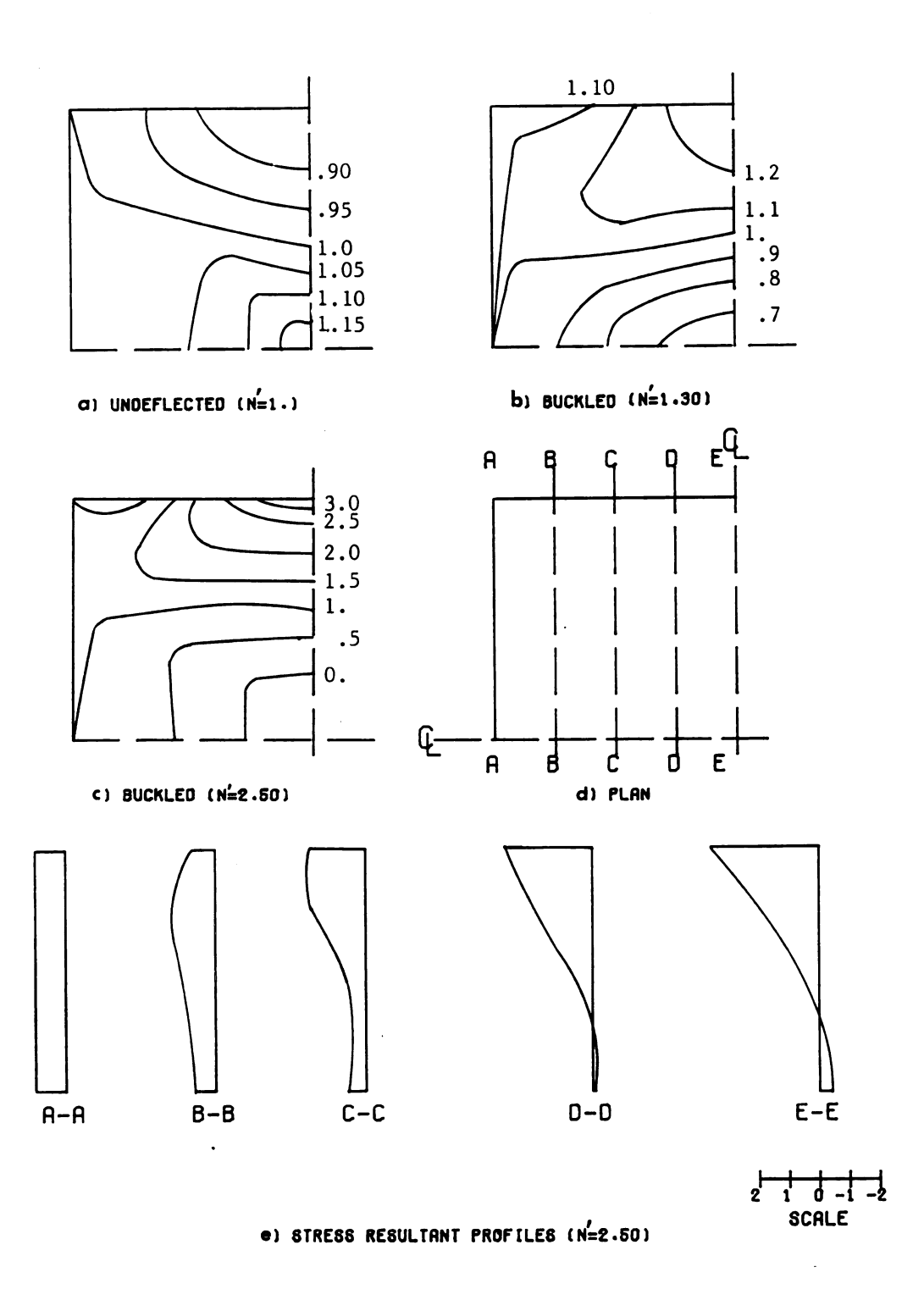


FIGURE 3.51. CONTOURS OF IN-PLANE FORCE(NX) AND PROFILES OF NX AT SPECIFIED SECTIONS FOR LOAD 2.50 TIMES THE CRITICAL LOAD.CLAMPED. R=1/2.

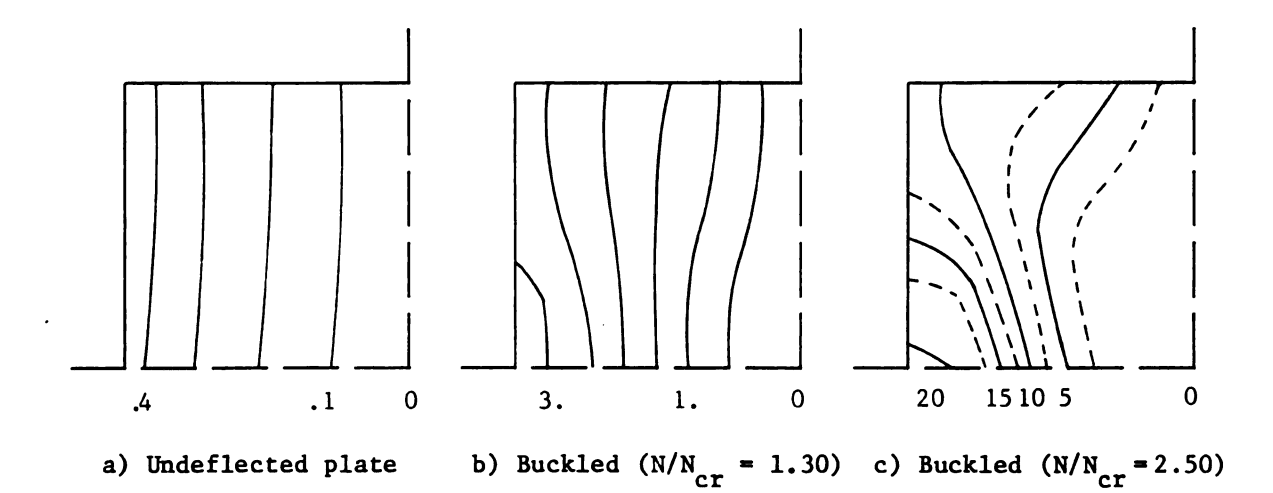


Figure 3.52. In-plane displacement ( $U = ua/t_i^2$ ), square plate, clamped edges, R = 1/2.

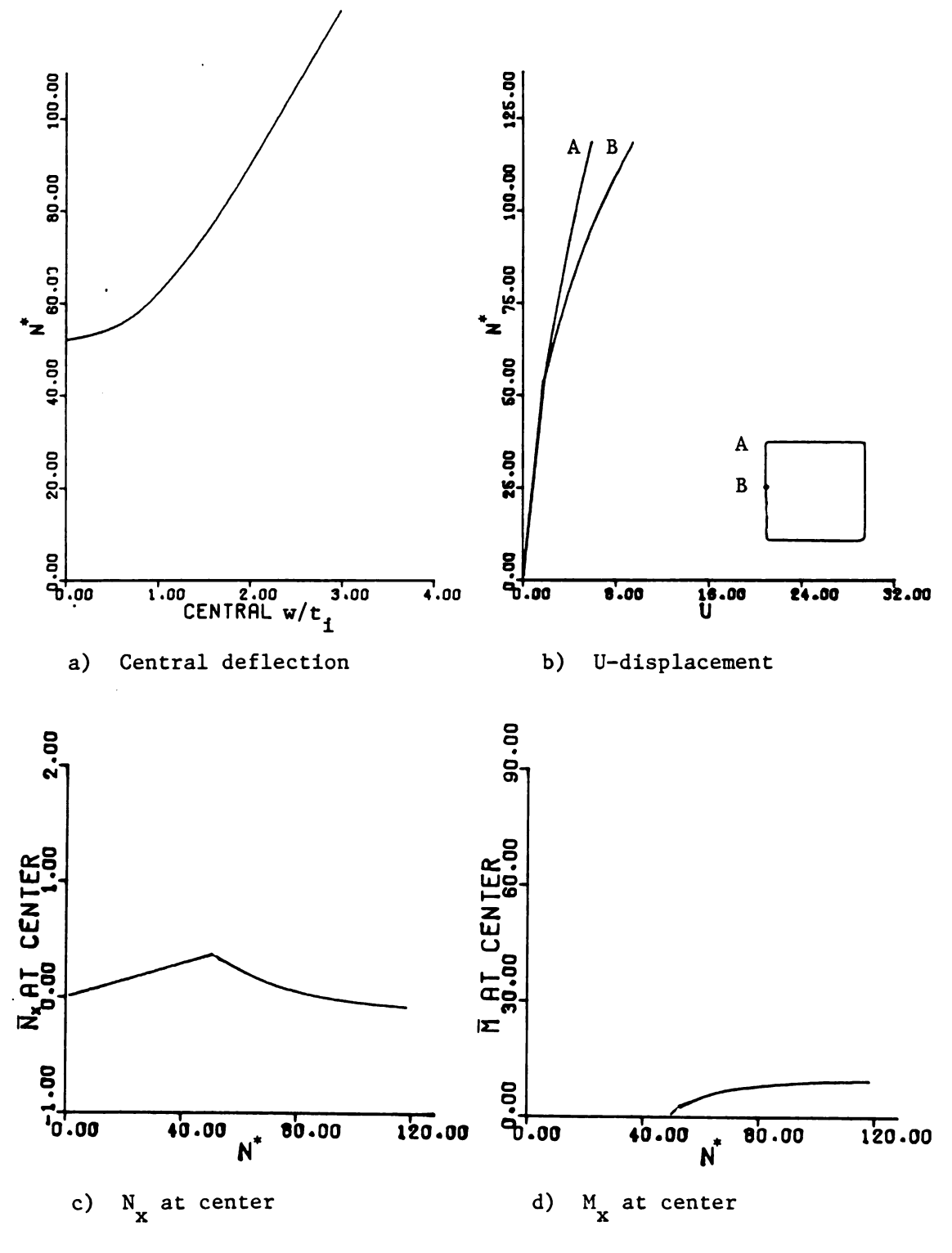
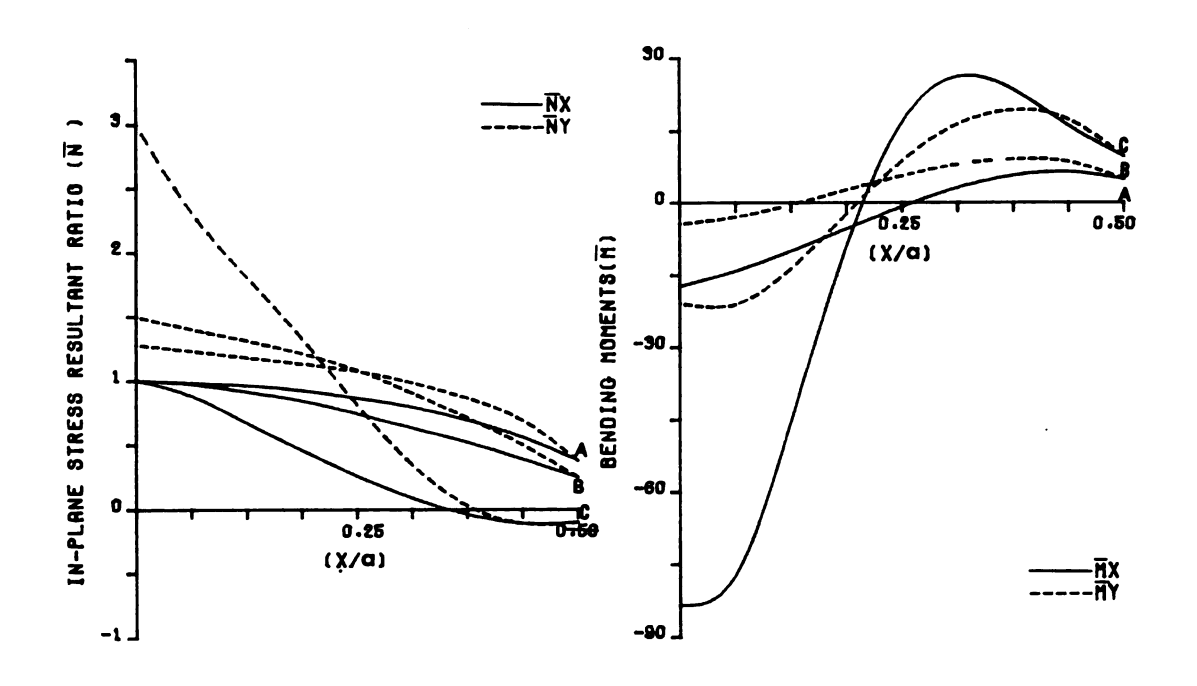
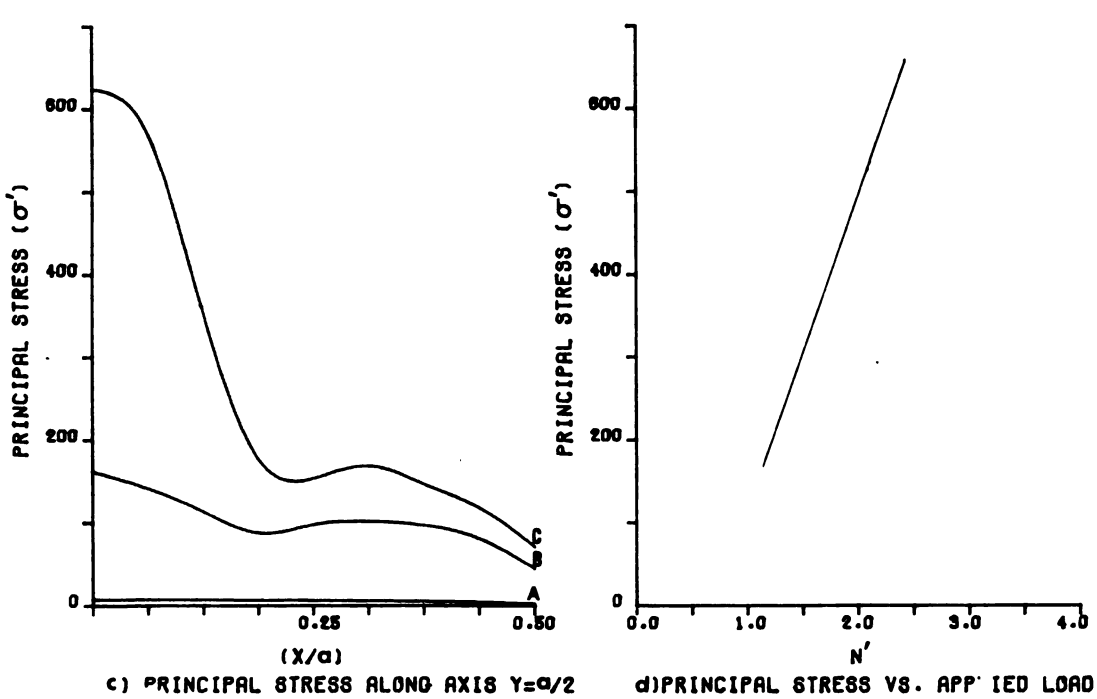


Figure 3.53. Plots of w,U,N $_{x}$ , and M $_{x}$ , square plate, clamped, R = 10



a) NX AND NY 9LONG A/IS Y=4/2





O PRINCIPAL STRESS ALONG AXIS Y=9/2 d)PRINCIPAL STRESS VS. APP IED LOAD NOTATION FOR CURVE IDENTIFICATION. A) N=1.0 (UNDEFLECTED) 8) N=1.10 C) N=2.40 .

FIGURE 3.54. PLOTS OF STRESS COMPONENTS. SQUARE PLATE. CLAMPED. R=10 .

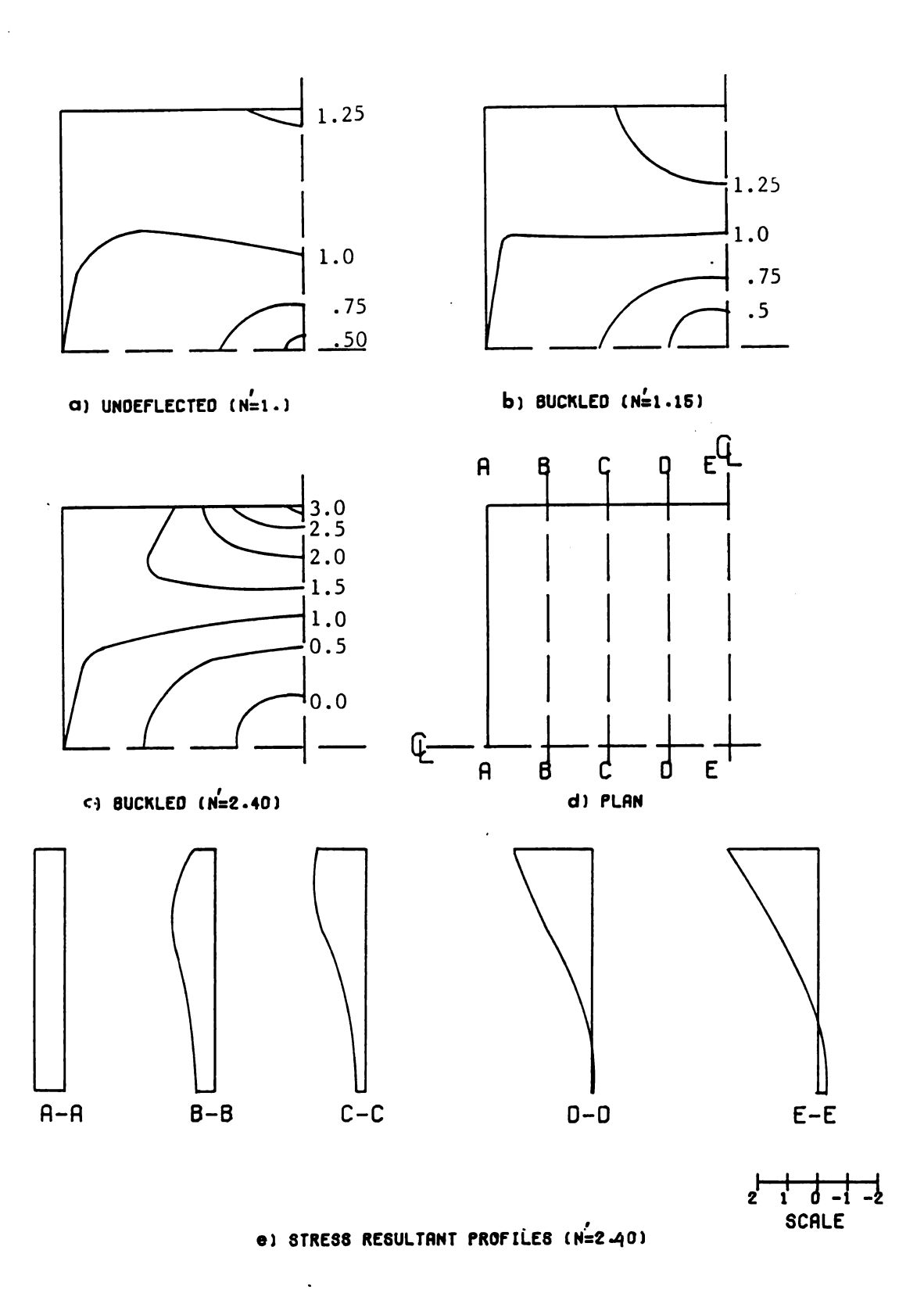


FIGURE 3.55. CONTOURS OF IN-PLANE FORCE(NX) AND PROFILES OF NX AT SPECIFIED SECTIONS FOR LORD 2.40 TIMES THE CRITICAL LORD.CLAMPED. R=10.

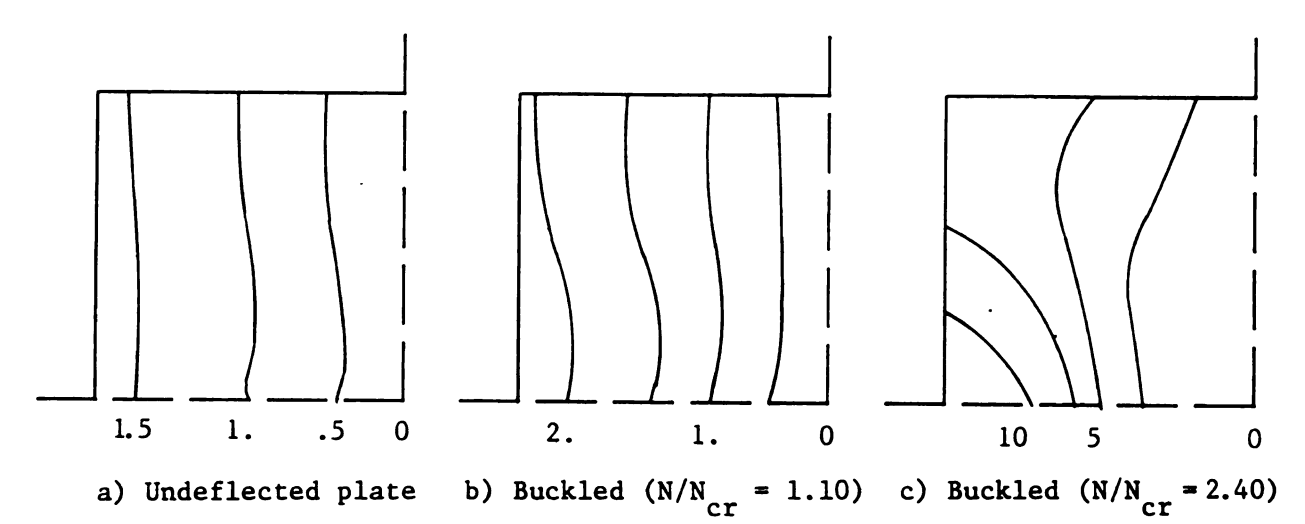


Figure 3.56. In-plane displacement ( $U = ua/t_i^2$ ), square plate, clamped edges, R = 10.

## 3.1.4 OPTIMIZATION

The main purpose of this study is to investigate the application of the difference method to the variable stiffness plate.

The goal is to design a plate with a stiffness variation such that it be optimum in some respect.

For example, we may be concerned with weight or the amount of material used, as is the case in most space structures, aircraft, etc. In these cases, we are seeking the form of variation in thickness of the plate for which the plate will be most efficient from the point of view of either stress or displacement. Following are some examples:

- a) In case of a flat plate (membrane solution), we may want to use a certain volume of material to construct a plate which will result in minimum in-plane displacement at some edge point, or ir a minimum stress at some point. It might also be desired that due to nonuniform load, the stress be almost equal everywhere, or the maximum stress be minimized.
- b) In stability analysis, we may want to utilize a constant amount of material to achieve maximum critical load, or to minimize the center deflections immediately after buckling.
- c) In the postbuckling range, there is the possibility of many different forms of optimization. For example, corresponding to some combination of lateral and edge

loads within some range, we may wish to maintain an almost uniform principal stress to prevent local yielding. Also, it may be desirable to minimize the central deflection.

## OPTIMIZATION EXAMPLE 1

Consider the square plate of Figure (3.57) with thickness varying from the edge toward the center as shown. We want to find the optimal slope (ratio of  $\frac{\text{te}}{\text{tc}}$ ) so that the critical load under biaxial compression be maximum for a

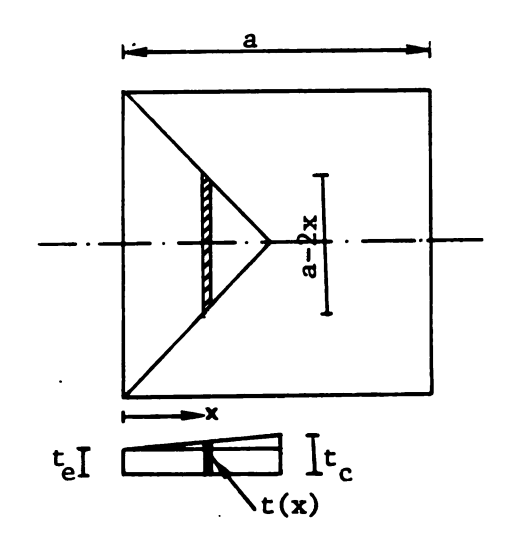


Figure 3.57.

constant amount of material.

For a square plate of thickness, t, and sides, a, the total volume of material used is

$$\bar{v} = a^2 t$$
.

For a variable thickness plate, if the variation in thickness is linear, the thickness t(x) at point x is

$$t(x) = t_e + \frac{t_c - t_e}{a/2} x$$

where

t = thickness at center

		ļ.

t = thickness along the edges

Let  $\frac{t_e}{t_c}$  = RT= Ratio of edge thickness to thickness at center. Then:

$$t(x) = t_c[RT + (1-RT)\frac{2x}{a}]$$

and the volume is

$$\overline{v} = 4 \int_{0}^{\frac{a}{2}} (a-2x) t_{c} (RT + \frac{2x}{a} - RT \frac{2x}{a}) dx$$

$$\overline{v} = 4a^{2} t_{c} (\frac{1+2RT}{12}) = \frac{a^{2} t_{c}}{3} (1+2RT).$$
 (1)

If the volume is limited to the original value, then

$$t_{c} = \frac{3\overline{v}}{a^{2}(1+2RT)}; \text{ for } \overline{v} = a^{2}t_{i} \quad (t_{i} = \text{ unit thickness})$$

$$t_{c} = \frac{3t_{i}}{(1+2RT)} \quad (ii)$$

To maintain a constant volume, the center thickness must vary with ratio RT, according to equation (ii).

For example:

RT 
$$t_c/t_i$$
  $\overline{v}$ 

.1 2.5  $a^2T_i$ 
 $\frac{1}{2}$   $\frac{3}{2}$  "

1. 1. "

2 .6 "

10  $\frac{1}{7}$  "

It is evident that as the ratio, RT, and the center thickness,  $t_c$ , change, the in-plane and flexural stiffness of the plate at each node will change.

A subprogram is provided to compute center thickness and stiffness at each node in each trial for a given RT.

The buckling problems were solved for a family of given ratios, and the variation of critical load with ratio RT, is shown in Figure (3.58). In this problem the plate is simply supported along all edges and  $\nu = .316$ .

Graph (3.58 a) indicates that the maximum critical edge load for a given volume of material occurs with RT  $\simeq$  .2. To find a more accurate value, the trial is continued with finer intervals between RT = .15 and RT = .25. The larger scale graph (3.58 b) shows that the maximum critical load is  $(N_{cr}^*)_{maximum} = 25.66$ , corresponding to RT=  $\frac{t_e}{t_c}$  = .22. Thus, consider a simply supported square plate under bi-axial compression.

From the stability point of view, the minimum material can be used if RT = .22 for the linear thickness variation introduced in Figure (3.57). An increase of  $\frac{25.66-19.48}{19.48}$  = 31.6% over the buckling load for a uniform thickness plate of the same volume results.

#### Note

- i) The result obtained above is not the absolute optimum. For the given amount of material, a still greater critical edge force could no doubt be obtained with a thickness variation other than linear. This form was used for practical simplicity.
- ii) For other types of loading or boundary conditions, appropriate forms could be proposed and analyzed by trial.

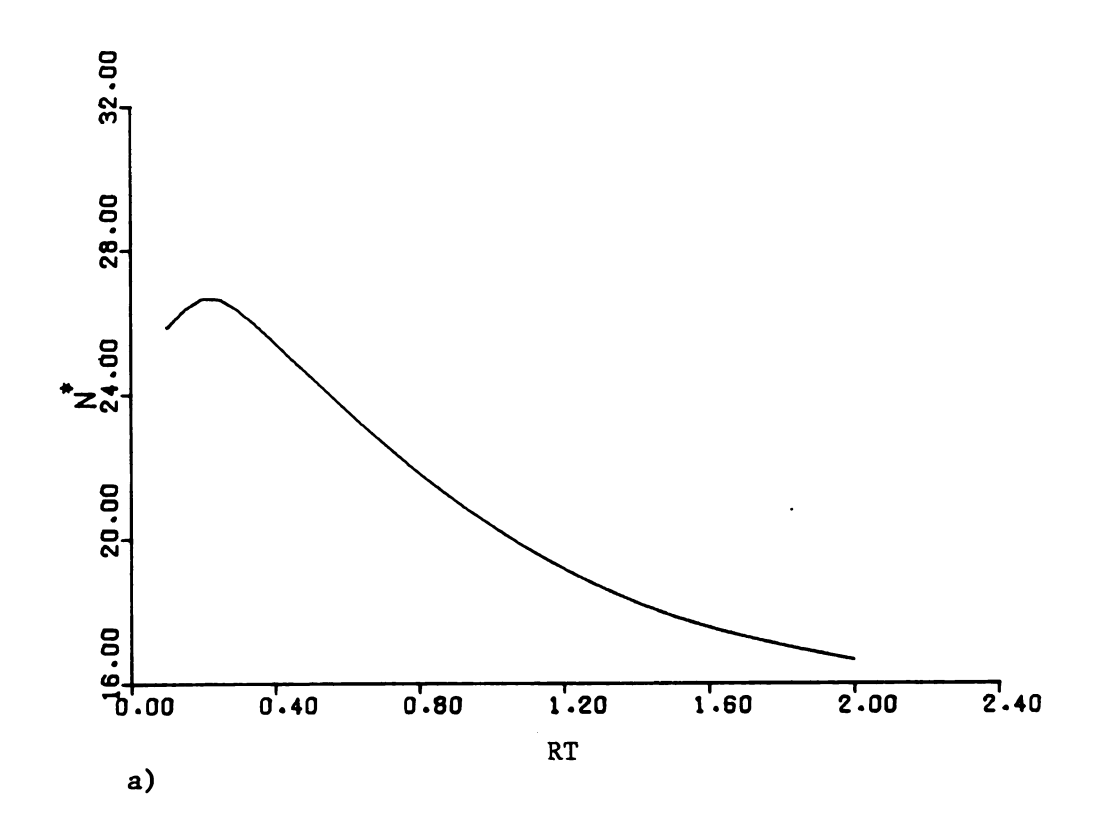
## EXAMPLE 2

The plate in this example is the same as in example 1, but with clamped edges; results are shown in Figure (3.59).

In this case, the maximum critical load is found for an RT of approximately 0.8.

Figure (3.59 b) is obtained by taking finer intervals ( $\Delta RT = .01$ ) between .6 and .8. This graph indicates the maximum critical load is  $(N_{cr}^*)_{max} = 473.962$ , corresponding to RT = .71.

The results show an increase of  $\frac{51.20-49.56}{49.56} = 3.3\%$  over the plate of uniform thickness. In the case of fixed support, from the stability point of view, it is not worthwhile constructing a plate of variable thickness. The effect of variation in thickness on other aspects of the problem such as internal forces, bending moments and lateral deflection will be analyzed later in this chapter.



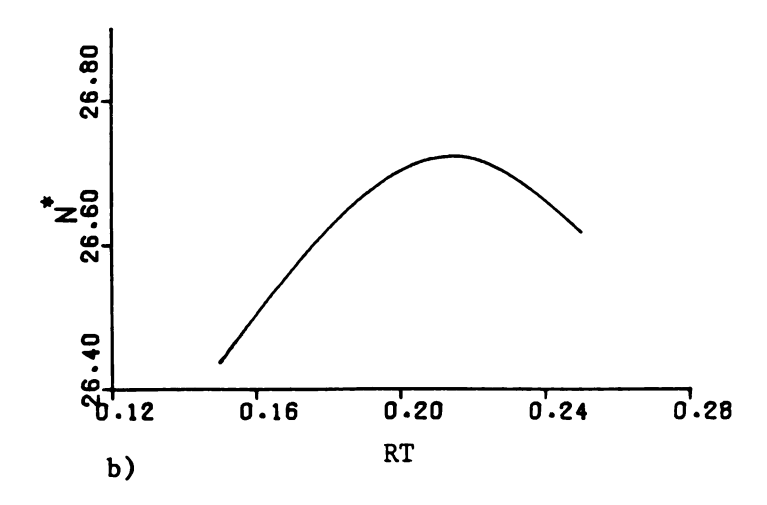
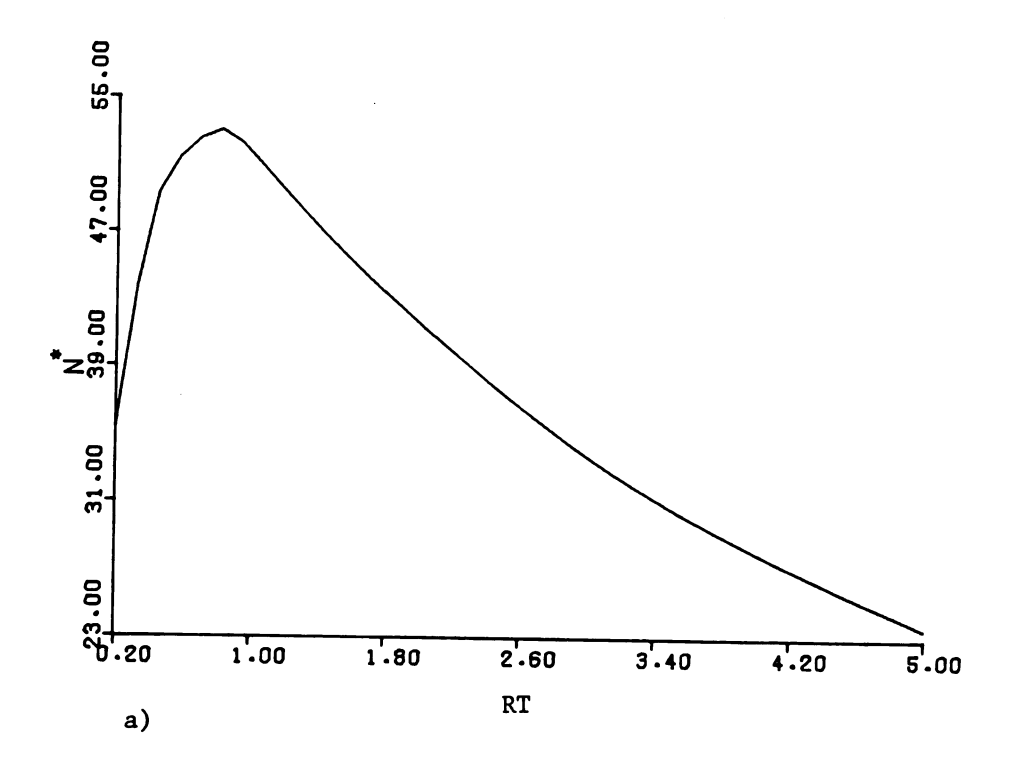


Figure 3.58. Critical load vs RT, for a simply supported square plate under Bi-axial compression, N.



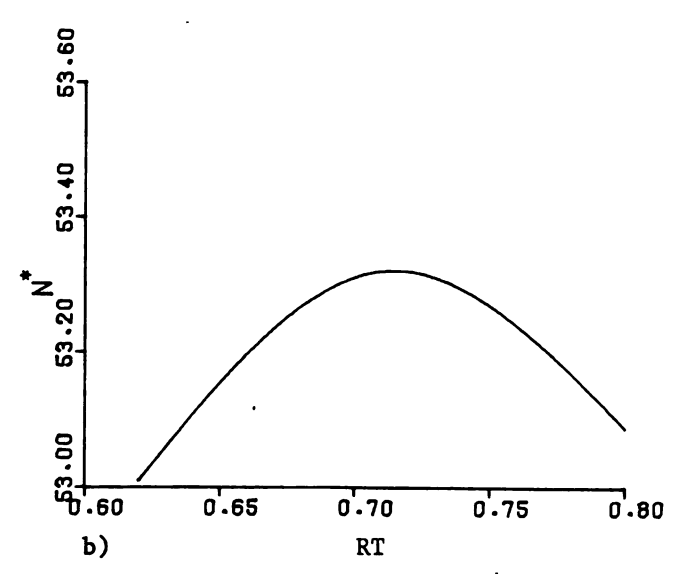


Figure 3.59. Critical load vs RT =  $\frac{t_e}{t_c}$ , for square plate of constant volume under Bi-axial compression; clamped edges.

#### 3.1.5 SUMMARY

In Section 3.1 a method was developed for force boundary condition problems, and the related computer program was applied to a variable stiffness plate and the results were discussed extensively.

It seems necessary to emphasize that the plates discussed in Section 3.1.1 through 3.1.3 have uniform thickness with varying E, so that patterns of membrane and bending stresses follow exactly the pattern of in-plane forces and bending moments respectively. Solutions to similar problems are not available in the literature; however, comparison with the uniform stiffness plate, as a special case, supports the accuracy of the solutions. Convergence of the solutions with an increasing number of nodes strengthens confidence in the method.

In Section 3.1.4 the weight-saving advantage of a variable thickness plate, from the stability point of view, was demonstrated as an example. However, one can apply the optimization to any possible aspects of stress or strain as desired.

Figure (3.60) shows variation of central deflection with load for all cases. The graphs show that the plates with less stiff edges undergo larger lateral deflection because, in the postbuckling range, the main portion of the in-plane load is carried by portions of the plate near the edges.

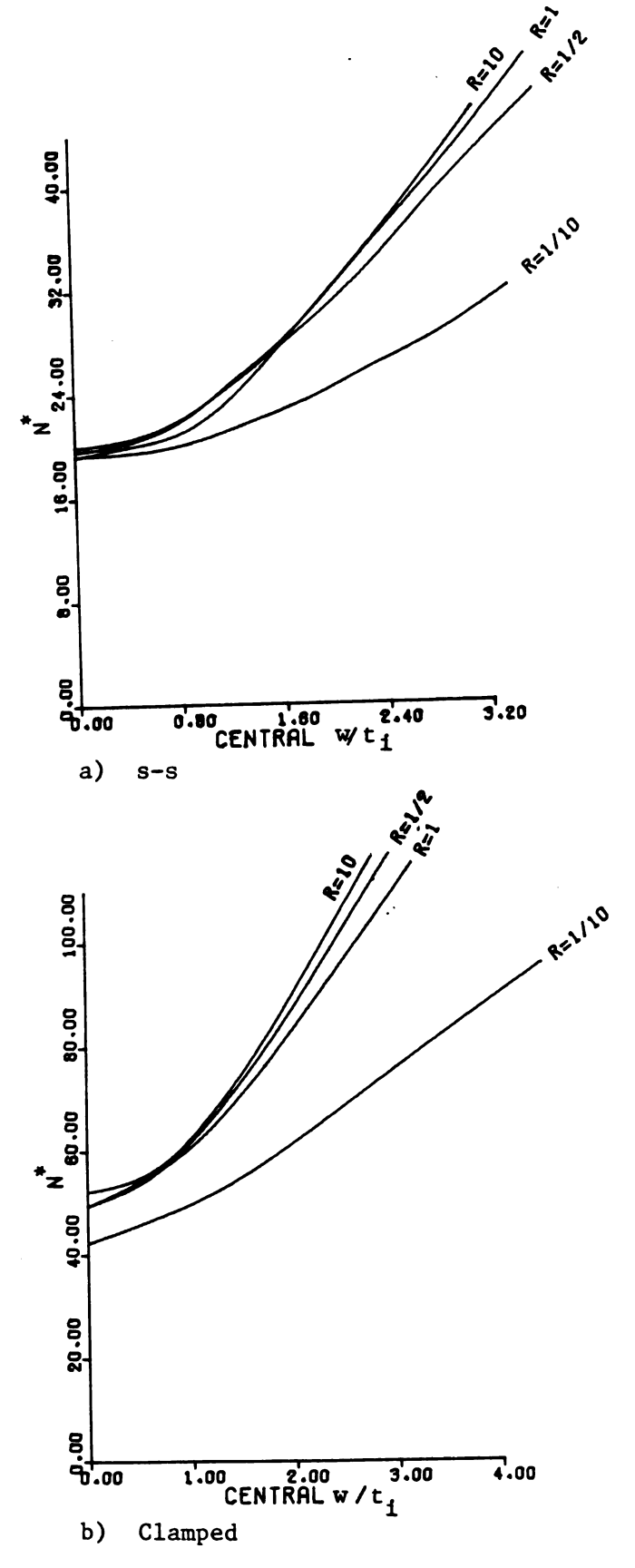


Figure 3.60. Central deflection for different R values, s-s and clamped edges.

#### 3.2 DISPLACEMENT BOUNDARY CONDITION

In this section, problems with specified in-plane displacements along the boundaries will be considered.

A computer program has been developed to solve this type of problem based on the procedure discussed in section 2.3.

Plates with uniform thickness are analyzed, as well as variable thickness plates. The results are compared with previous works or exact solutions when they are available. As an example, optimization of the thickness variation, from the stability point of view, is also considered.

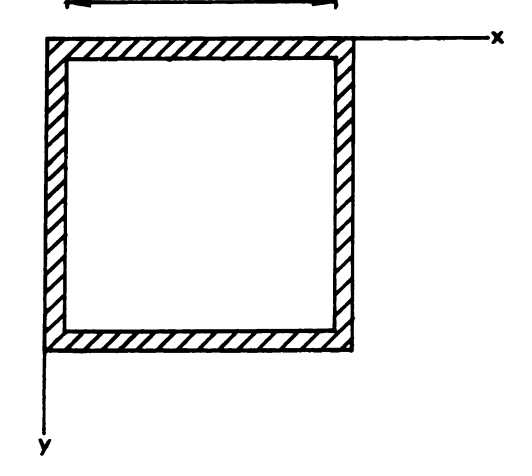
# a - Geometry and Loading Conditions

For an example, let us take a plate under uniform edge displacement due to thermal load, and examine the membrane, buckling, and postbuckling behavior of plates of different thickness variation, with both simply-supported and clamped boundaries. Figure (3.61)

shows a plate, surrounded by a rigid frame that undergoes a temperature change of either expansion or contraction.

The strain in the frame will impose a state of displacement on the plate edges.

The strain in the frame is



 $\varepsilon = \alpha_{T}(\Delta T)$ 

Figure 3.61. Plan

where  $\alpha_T^{-}$  coefficient of thermal expansion of the frame and  $\Delta T$  = temperature change.

#### Note

- i) It is assumed that the effects of the reaction forces of the plate edges are negligible, so that the stresses created within the frame have negligible effect on the strain and displacements of the frame.
- ii) Because of symmetry, we analyse only a quadrant of the plate.

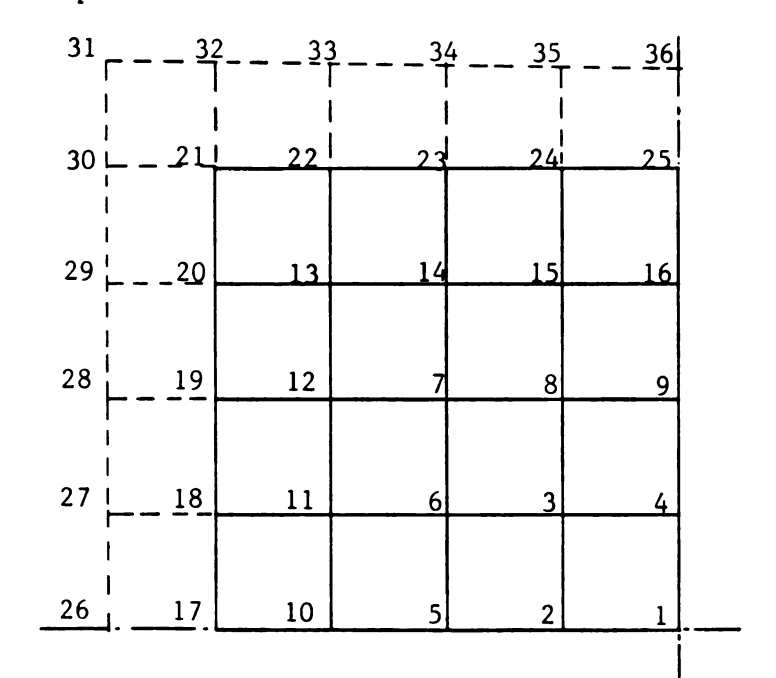


Figure 3.62. Node arrangement, square plate, h = a/8

Since, because of symmetry, the centerlines of the plate will not move, displacements enforced along the edges will be as follows:

1 - Along edge x = 0, u displacement would be constant and equal to  $-\frac{\alpha}{2}T$  a  $\Delta T$ .

2 - Because of constant strain (in frame), the v-displacement along x-edge will be linear with respect to  $y, \text{ so that } v = {}^{\alpha}_{T} \Delta T (y - \frac{a}{2}).$ 

The boundary displacements are tabulated in Table (3.10).

Table 3.10. Boundary displacement for square plate of Figure 3.62

	. ~		
Point	$u/-\frac{a\alpha_T^{\Delta T}}{2}$	$\mathbf{v}/-\frac{\mathbf{a}\alpha_{\mathbf{T}}\Delta\mathbf{T}}{2}$	
17	1.	0.	
18	1.	.25	
19	1.	.5	
20	1.	.75	
21	1.	1.	
22	.75	1.	
23	.5	1.	
24	.25	1.	
25	0.	1.	

Based on the given data, the problem is solved and the results analysed step-by step in the following pages.

#### 3.2.1 MEMBRANE SOLUTION

In the solution for in-plane forces and displacements, assuming zero w-displacement, the in-plane equilibrium equations can be approximated by finite differences to obtain a set of linear equations in u and v. (See equation (2.43)).

The equations are solved and in-plane forces and displacements lead us to following conclusions.

a) In case of a uniform thickness plate, the equilibrium equations (2.16) and (2.17) are linear differential equations, and in this symmetric case the solution leads to exact values of membrane stress resultants and displacements, even with very coarse mesh sizes.

The theoretical solution predicts constant strain in both directions.

$$\varepsilon_y = \varepsilon_x = \frac{-u_o}{a/2} = \frac{-2u_o}{a}$$
 (For  $(x,y) < \frac{a}{2}$ )

and the in-plane stress resultants are

$$N_{y} = N_{x} = \frac{Et}{1-v^{2}} \left[\varepsilon_{x} + v\varepsilon_{y}\right] = \frac{Et}{1-v^{2}} \left[(1+v)\left(\frac{-2u_{o}}{a}\right)\right] = \frac{-2Et}{(1-v)} \frac{u_{o}}{a}$$

$$N_{x}^{*} = N_{x} \frac{a^{2}}{D_{o}} = \frac{-2Et_{i}}{(1-v)} \frac{u_{o}}{a} \left(\frac{a^{2}(1-v^{2})12}{Et_{i}^{3}}\right) = -(1+v)(24) \frac{u_{o}a}{t_{i}^{2}}$$
or, calling  $\frac{u_{o}a}{t_{i}^{2}} = U_{o}$ 

$$\frac{N_{x}^{*}}{U_{o}} = -24(1+v)$$
and for  $v = .316$ ,  $\frac{N_{x}^{*}}{U_{o}} = 31.58$ 

Similarly,

$$\frac{N^*}{U_0} = -31.58$$

$$N_{xy} = 0$$

and

$$u = u(x) = \varepsilon(\frac{a}{2} - x) = \frac{2u_o}{a} (\frac{a}{2} - x)$$

$$v = v(y) = \varepsilon(\frac{a}{2} - y) = \frac{2v_o}{a} (\frac{a}{2} - y)$$

These values agree exactly with the solution obtained with the computer program listed in Appendix C. Contours of the membrane force,  $N_{\rm x}$ , the principal stress and U-displacement are shown in Figure (3.63).  $N_{\rm y}$  and v-displacement can be obtained considering symmetry.

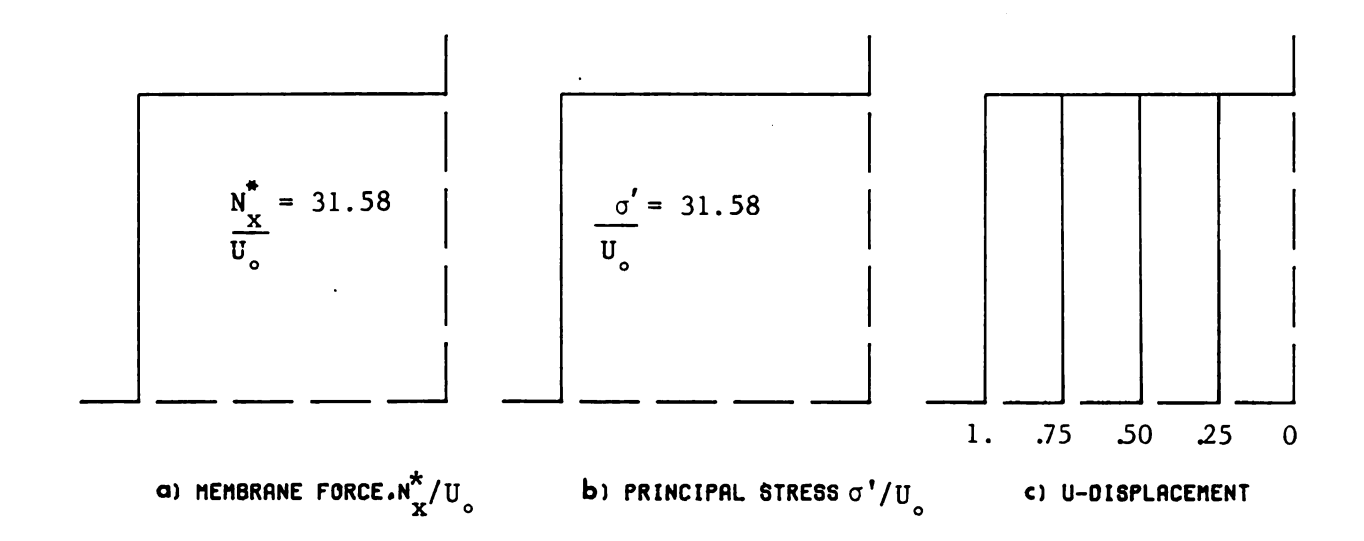


FIGURE 3.63. CONTOURS OF MEMBRANE FORCE, PRINCIPAL STRESS, AND U-DISPLACEMENT UNDEFLECTED SQUARE PLATE. RT=1.

#### SOLUTION OF PLATES WITH VARIABLE THICKNESS

To observe the behavior of a variable thickness plate, two different problems were solved. One with RT = .25, and the other had RT = 2, and the results studied. Parameter  $RT = \frac{\text{edge thickness}}{\text{center thickness}}$  is the thickness ratio.

# b) Square plate with RT = 1/4

Figure (3.64) illustrates membrane forces, principal stresses and in-plane displacements; from the figures, we can conclude the following.

- i) Figure (3.64 a) shows shifting of the load carrying toward the center where the plate is thicker. The shifting of the load becomes greater as we move toward the center, and it is nearly uniform along the edge.
- ii) Although there are larger in-plane stress resultants in the central region, because the thickness is large, the stress is smaller. Figure (3.64 b) shows the principal stress within the plate. It is observed that the minimum stress exists at the center and it becomes larger toward the thin edges.
- iii) In Figure (3.64 c), the wide-spacing of contours of inplane displacement U in the central region, indicates small strain corresponding to smaller stress in that region.

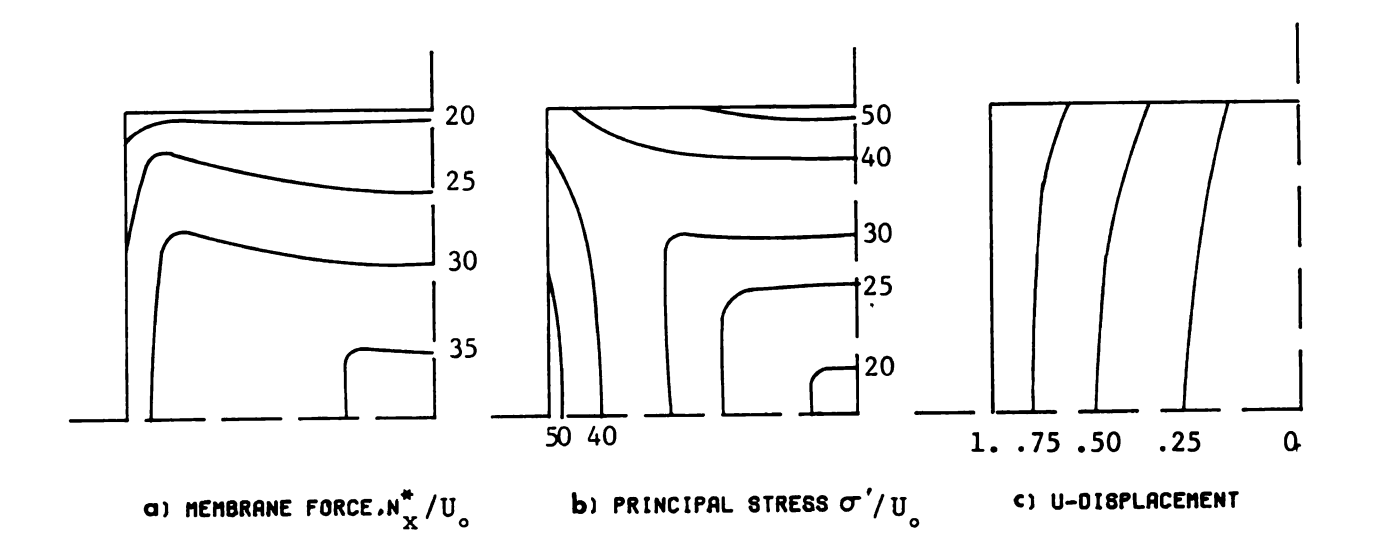


FIGURE 3.64. CONTOURS OF MEMBRANE FORCE.PRINCIPAL STRESS.AND U-DISPLACEMENT UNDEFLECTED SQUARE PLATE, RT=1/4

# c) Square plate with RT = 2.

The same problem is considered except with  $R_{T} = \frac{\text{edge thickness}}{\text{center thickness}} = 2$ . and the results obtained are shown in Figure (3.65). This leads to the following conclusions.

- Supporting discussion of the preceding section, less load is carried by the thin central region, and as we move toward the edges, more load is transmitted.
- ii) Figure (3.65 b) shows larger stresses in the central region.
- iii) Contours of in-plane displacements are consistent with part (ii); i.e., larger strain occurs in the central region, due to larger stresses.

Clearly, the out-of-plane support condition has no effect on the membrane solution of the plate.

It should be noted that Figures (3.63), (3.64) and (3.65) correspond to plates with RT = 1, 1/4 and 2, respectively, but with thickness such that total material volume is the same in each case.

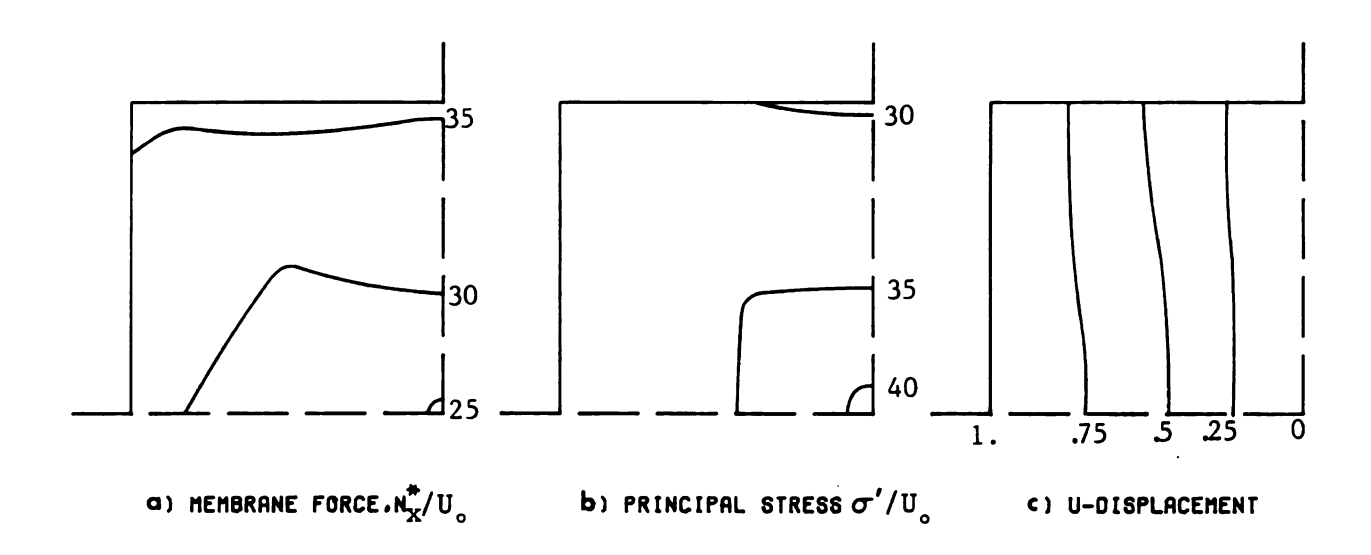


FIGURE 3.65.CONTOURS OF MEMBRANE FORCE.PRINCIPAL STRESS.AND U-DISPLACEMENT UNDEFLECTED SQUARE PLATE. RT= 2.

## 3.2.2 BUCKLING SOLUTION

As is discussed in Section (3.1), the buckling solution is based on the eigensolution of the out-of-plane equilibrium equation (2.40). On the right hand side of this equation, the effect of w on in-plane forces is considered to be zero. Thus, in the matrix [Bw] of Equation (2.49), the in-plane forces obtained from the membrane solution of the unbent plate will be used. The eigenproblem will be solved, giving the critical edge displacements and the corresponding buckled mode shapes.

Following are solutions to some stability problems.

#### 3.2.2.1 Convergence Check and Comparison

In order to check the convergence and consequently the accuracy of the buckling solution, a uniform thickness plate (problem 3.2 a) was solved using different mesh sizes. The critical loads obtained in each solution are shown in Table (3.11) for s-s boundaries. Also, the values of critical displacements are compared to exact values.

Convergence of the solution is graphically illustrated in Figure (3.66) for s-s boundaries.

Table (3.12) and graph (3.67) show the convergence pattern of critical displacement for the case of boundaries fixed against out-of-plane displacement.

The convergence tables show that the result obtained using  $h=\frac{a}{3}$  in the simply supported case and  $h=\frac{a}{12}$  in the clamped case are sufficiently accurate for engineering purposes.

More accurate results can be predicted by extrapolation.

The critical edge displacement obtained from extrapolation of the last 3 lines has an accuracy of .000016 in the simply-supported case and .0013 in case of clamped edges, compared to exact results.

Table 3.11 . Critical displacements for a simply-supported plate using different mesh sizes. Uniform stiffness plate.  $\nu \, = \, .316 \, .$ 

Mesh size (h/a)	Present solution U Ĉr	Exact (1)	Difference %	Two point extrap- olation	3 point extrap- olation
1/4	.5935		5		
				. 6248	
1/8	.61698		1.2		.624972
		. 62497		.62495	
$\frac{1}{12}$	.62141		5		.62498
				.624975	
$\frac{1}{16}$	. 62297		.3		

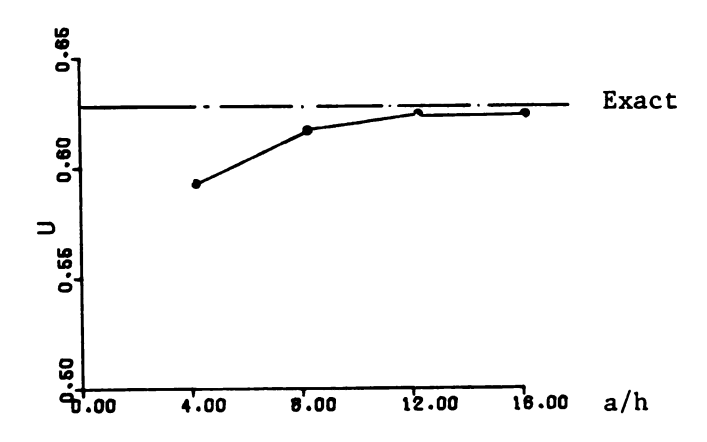


Figure 3.66. Convergence of buckling solution.

Table 3.12. Critical displacements for a clamped square plate using different mesh sizes. Uniform stiffness.  $\nu$  = .316.

Mesh size (h/a)	Present Solution Ugr	Exact (1)	Difference %	2 point extrap- olation	3 point extrap-
$\frac{1}{4}$	1.34062		19.2		
				1.6456	
$\frac{1}{8}$	1.56939		5.4		1.65620
		1.6593		1.6550	
$\frac{1}{12}$	1.61697		2.5		1.65709
				1.6566	
$\frac{1}{16}$	1.6343		1.5		

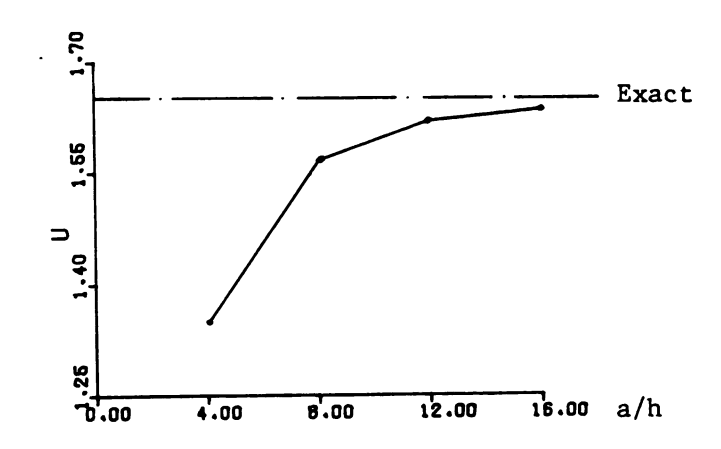


Figure 3.67. Convergence of buckling solution.

<sup>(1)</sup> The exact value of critical displacement is derived on page 167.

buc pla all

for

bu

tì

1

Since it is assumed that the plate is perfectly flat before buckling, the in-plane displacements are linear within the entire plate (constant strain), and the membrane forces will be the same at all points. Thus, critical displacements can be related to edge forces as

along x-edges

$$\varepsilon_{\mathbf{x}} = \frac{1}{Et} \left[ \mathbf{N}_{\mathbf{x}} - \mathbf{v} \mathbf{N} \mathbf{y} \right]$$

but in this case

$$(\varepsilon_x)_{cr} = \frac{-u_{cr}}{a/2}$$
, and  $N_x = N_y = N_{cr}$ 

therefore

$$u_{cr} = \frac{-a}{2Et} [1-v]N_{cr}$$

For s-s square plate under bi-axial compression  $N_{cr} = \frac{2\pi^2 Dr}{a^2}$ . [see Table 3.8]

Thus

$$u_{cr} = \frac{\pi^{2}}{a} \frac{D}{Et} (1-v) = \frac{\pi^{2}t^{2}}{12a(1+v)};$$

$$u_{cr} \frac{a}{t^{2}} = \frac{.822467}{1+v};$$

$$U_{cr} = \frac{.822467}{1+v} \quad \text{or for } v = .316, U_{cr} = .62497$$

similarly, considering  $N_{cr} = 5.31 \frac{\pi^2 Dr}{a^2}$  for clamped boundaries

$$U_{cr} = 1.6593$$
 for  $v = .316$ 

to

alo

is

a:

dı

a

t

ī

### EXAMPLE 1

To further check the accuracy of the method, the solution to problem (9.13) of Reference (44) is examined. In this example, along the edges x = 0, and x = a, the u-displacement is prevented. y-direction, constant strain,  $\varepsilon$ , is assumed. Therefore,  $v = \varepsilon(\frac{a}{2} - y)$  and assuming that centerlines of the plate coincide with axes of symmetry during deformation,  $(\varepsilon = \frac{-v}{a/2})$ .

No u-displacement is allowed along edges y = 0, and y = a, and with regard

Figure 3.68. Plan

to out of plane displacements, all edges are taken as simply supported.

The boundary data are tabulated below. For the node arrangement, see Figure (3.62).

<u>Node</u>	u	v	W	
17	0	0	0	
18	0	.25v <sub>°</sub>	0	
19	0	.5 v <sub>°</sub>	0	
20	0	.375v <sub>°</sub>	0	
21	0	v <sub>o</sub>	0	
22	0	$\mathbf{v}_{o}$	0	
23	0	v <sub>o</sub>	0	
24	0	v <sub>o</sub>	0	
25	0	v <sub>o</sub>	0	

The

٠,

an

e c

 $\frac{a}{2}$ 

of

\_

Using the data for input, the buckling solution was obtained. The critical uniaxial edge displacement was found to be  $v = 1.23033 \frac{t^2}{a}.$ 

This is to be compared to Timoshenko's results (44), obtained by an energy method. Remember that he was taking the total edge strain to be  $e_y$ , while in our case the compressive strain  $e_{cr} = \frac{2v_0}{a}$ ,  $e_{cr} = \frac{2v_0}{a}$  or  $e_{cr} = \frac{2v_0}{a}$ .

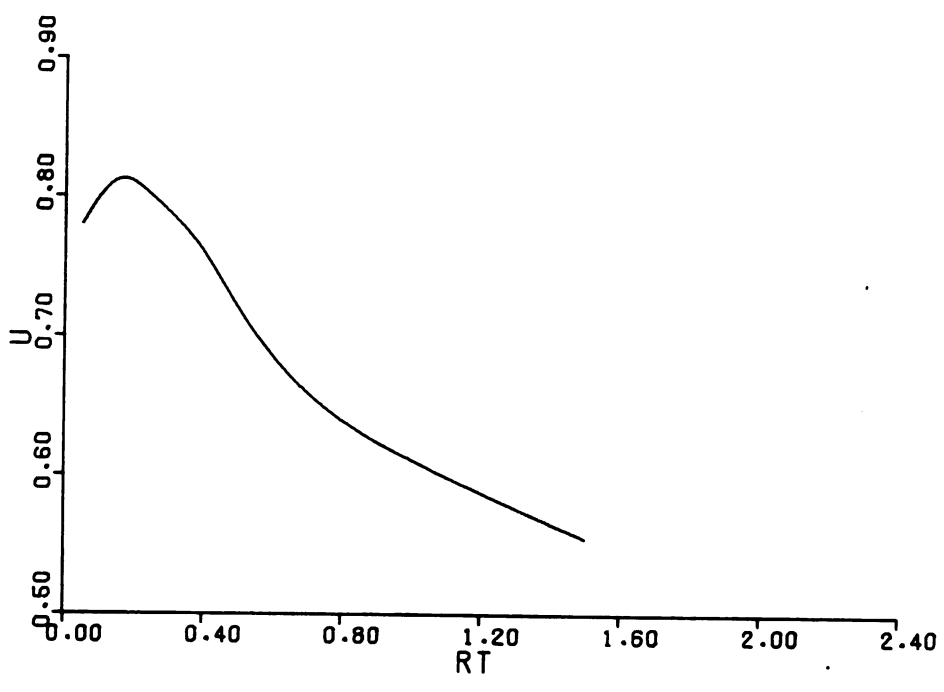
Timoshenko found  $e_{cr} = .632 \, \frac{h^2}{a^2}$  but he used a plate

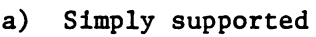
of sides  $2a=\overline{a}$  and thickness h. By substituting t for h, and  $\frac{\overline{a}}{2}$  for a in Timoshenko's result it becomes  $e_{cr} = .632 \frac{h^2}{a^2} = .632 \frac{t^2}{(\overline{a}/2)^2} = 2.528 \frac{t^2}{a^2}$ . The results differ by 2.6%, fairly close for such a coarse mesh size  $(h = \frac{a}{8})$ .

## 3.2.2.2 Optimization Analysis

Using the same data as in problem 3.2.a, and solving for the eigenvalues, two series of solutions are obtained for simply-supported and for fixed out-of-plane boundary conditions-considering different thickness variations. The variation in thickness is taken to be linear, as in Section 3.1.4. The variation in thickness is to be optimized in order to give the greatest edge displacement at buckling for a given volume of material.

In the case of the simply-supported edge, Figure (3.69 a) shows that the optimum variation corresponds to  $RT = \frac{\text{edge thickness}}{\text{center thickness}} = .15, \text{ with an increase in buckling displacement}$ 





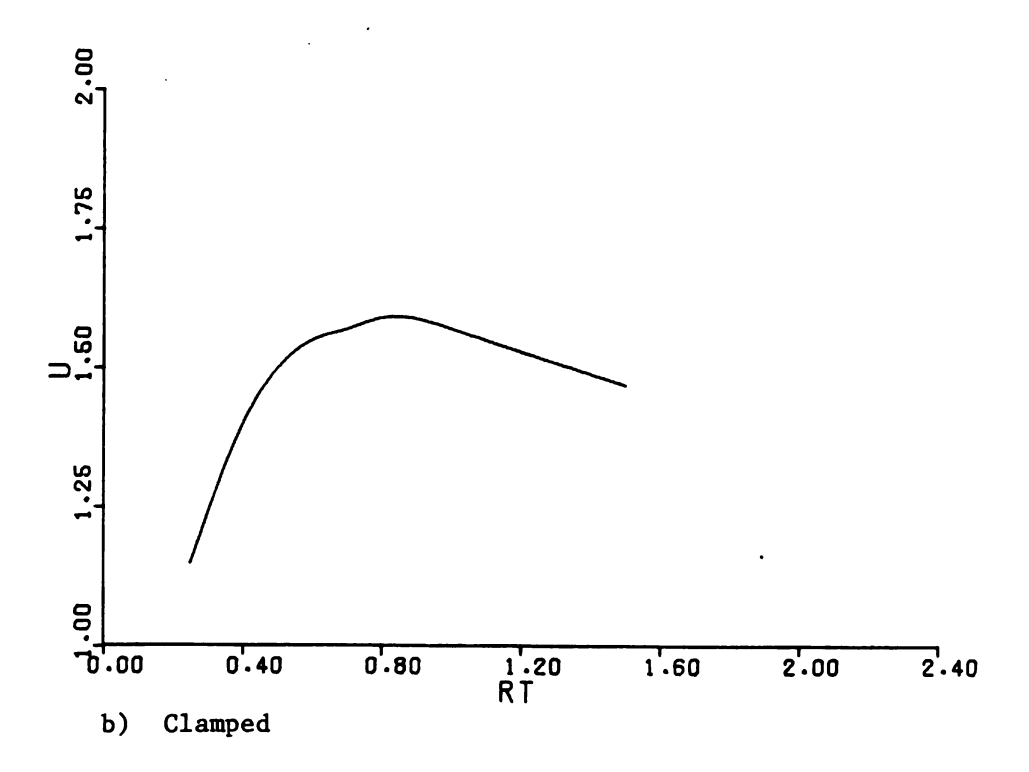
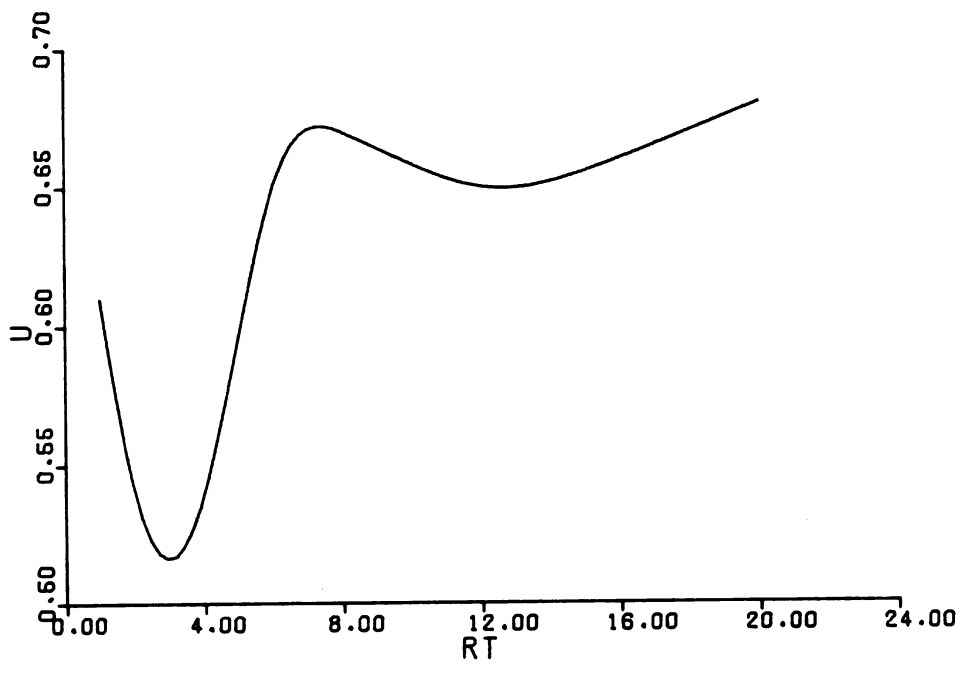
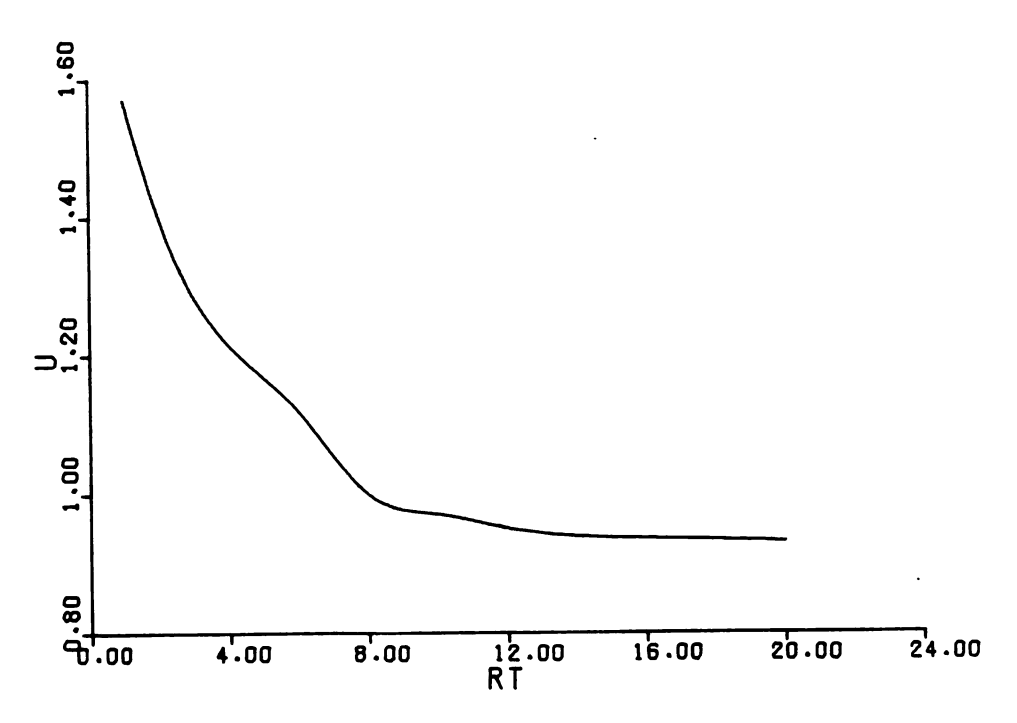


Figure 3.69. Variation of critical displacement versus RT.



a) Simply supported



The Part Carbon Below a William Commence

b) Clamped

Figure 3.70. Variation of critical displacement versus RT.

of  $\frac{.81199 - .6116}{16116}$  = 33% with respect to uniform thickness plate of the same volume.

Figure (3.69 b) illustrates the variation of critical displacement with respect to thickness variation for a clamped square plate. The maximum critical displacement can be achieved if the edge thickness is .85 times the center thickness with an increase of  $\frac{1.589-1.569}{1.569} = 1.2\%$  over the critical edge displacement for the plate of uniform thickness.

To check the buckling behavior of the plate, within a wider range of variation in thickness, the critical displacement for different RT values up to 20 is obtained and plotted in Figure (3.70 ); the plot shows a decrease in critical displacement all the way up to RT = 20.

Note: Examination of mode shapes shows that as the center of the plate gets thinner, beyond some point, the buckling mode associated with the lowest critical displacement is not a single concave shape. The buckling mode corresponding to the lowest eigenvalue for a clamped plate with RT > 2.2 consists of more than one buckled wave. These results are not shown in this thesis.

#### 3.2.2.3 Analysis of Buckling Modes

In this section, the shape of buckling modes will be reviewed and compared with the exact shape in those cases where the exact solutions are available.

Up to this point, all solutions were based on the assumption of symmetry about both axes of the plate. Thus, only a quarter of the plate was considered.

Therefore, the nonsymmetric modes are missing. To obtain all modes of buckling, a solution is obtained by considering every node as an independent degree of freedom, from the out-of-plane displacement point of view, while symmetry and anti-symmetry in u and v are assumed, as before. Solution for the simply-supported plate of uniform thickness shows the first mode shape to consist of half-sine waves in both directions, and the second mode to consist of two half-sine waves in one direction and one in the perpendicular direction.

The first few mode shapes for the simply-supported plate are shown in Figure (3.71) and for damped edges in Figure (3.72).

The Control of the Co

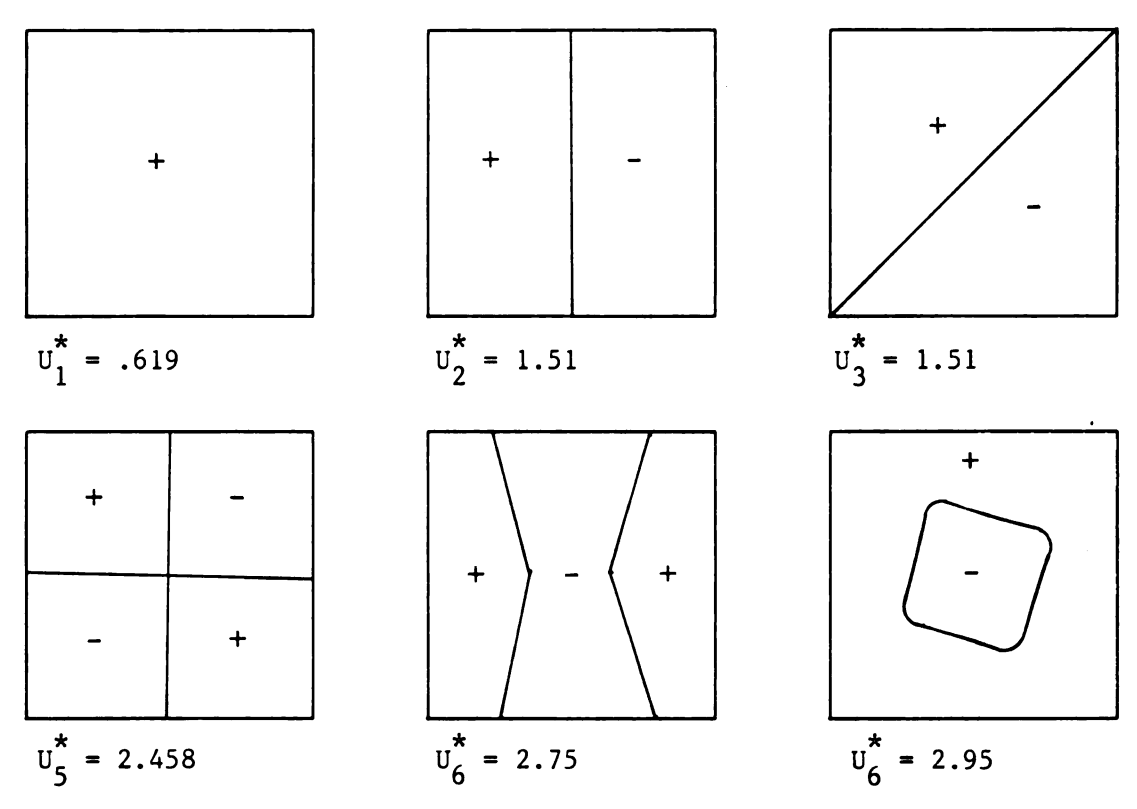


Figure 3.71. Buckling modes of simply supported square plate, RT = 1.

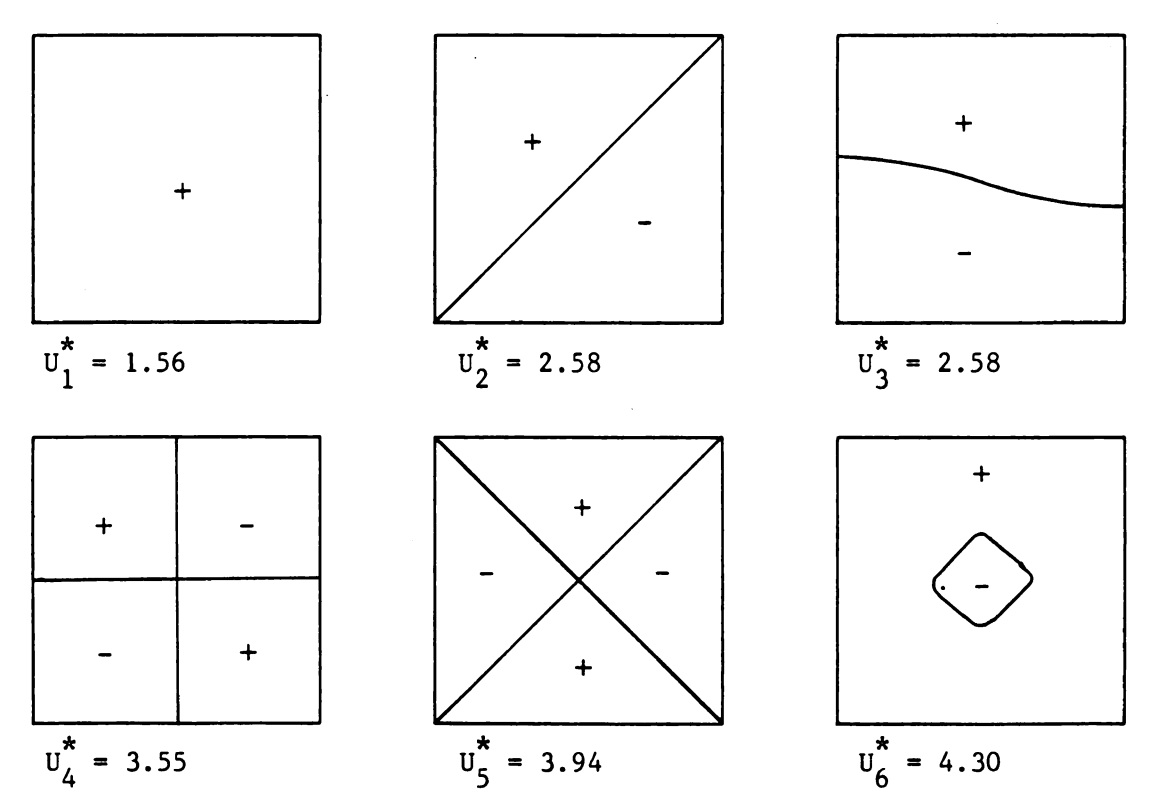


Figure 3.72. Buckling modes of clamped square plate, RT = 1.

#### 3.2.3 POSTBUCKLING

In this section, a study is made of the postbuckling behavior of uniform and variable thickness plates under uniform bi-axial edge displacement compressed beyond the critical displacement. Convergence of the solution is examined by solving the problem with different mesh sizes. Variation of in-plane forces as well as in-plane displacements is also studied.

# 3.2.3.1 Uniform Thickness Plate, s-s Boundaries

A simply-supported uniform thickness plate is compressed beyond the critical displacement and the solution is obtained. Following are some results from the solution.

## a) Convergence of the solution

The problem is solved, successively taking h/a = 1/4, 1/8, 1/12 and 1/16, and the results are compared. Table (3.13) shows the central deflection of the plate due to edge displacements of 1.26  $\frac{t^2}{a}$ , which is almost two times the critical displacement.

Table 3.13.	Convergence of	postbuckling	solution	with mesh	size
-------------	----------------	--------------	----------	-----------	------

Mesh size (h/a)	W-center	Difference %	Extrapolation	N*-center	M -center
$\frac{1}{4}$	.96795			-118.99	100.80
		9.7	.853016		
1/8	.88175			-130.17	98.55
		1.5	.8643366		
$\frac{1}{12}$	.86869	·		-132.98	98.27
		.1	.8701166		
1/16	.86976			-136.74	98.88

Review of Table (3.13) indicates that the solution obtained by only 8 x 8 nodes is satisfactorily close to the converged solution, keeping in mind that the accuracy of the iterative solution is set to be one percent. The difference for mesh sizes finer than 8 x 8 is small. The results can be improved by extrapolation.

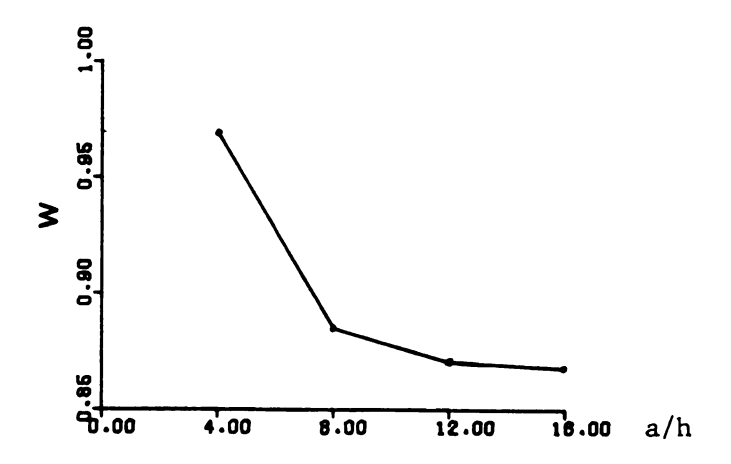


Figure 3.73. Convergence of center-deflection, s-s square plate.  $(\mathtt{U} = \mathtt{2} \ \mathtt{U}_{\mathtt{cr}})$ 

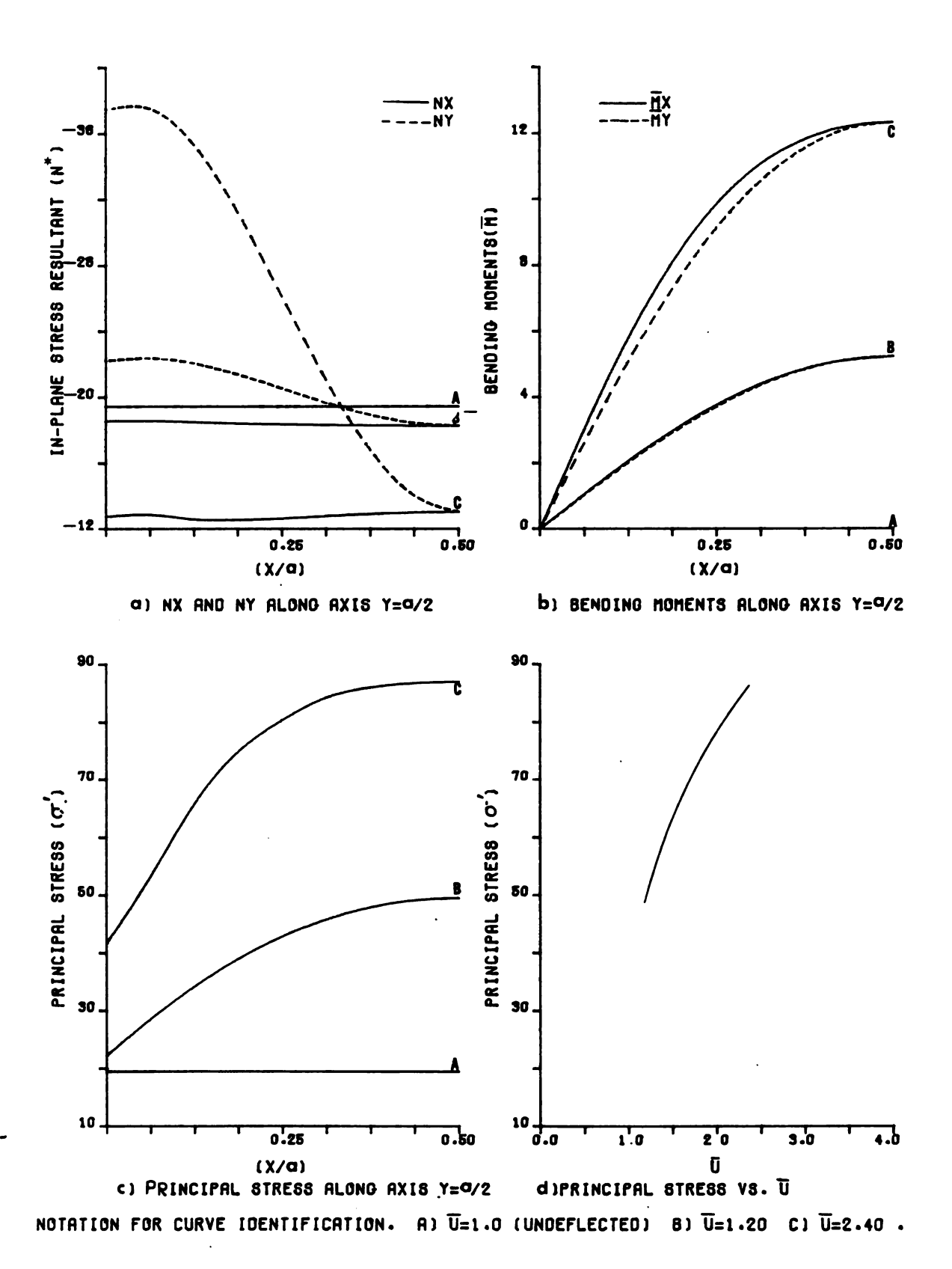


FIGURE 3.74. PLOTS OF STRESS COMPONENTS, SQUARE PLATE, SIMPLY SUPPORTED. RT=1 .

### b) Stress Analysis

The distribution of the membrane forces will change as the lateral deflection becomes larger.

Also, the bending moments will vary with variation of the deflected shape of the plate.

Graphs of Figures (3.74 a) and (3.74 b) show the variation of center-line membrane forces and bending moments as the edge compression varies. Study of these graphs leads to the following conclusions.

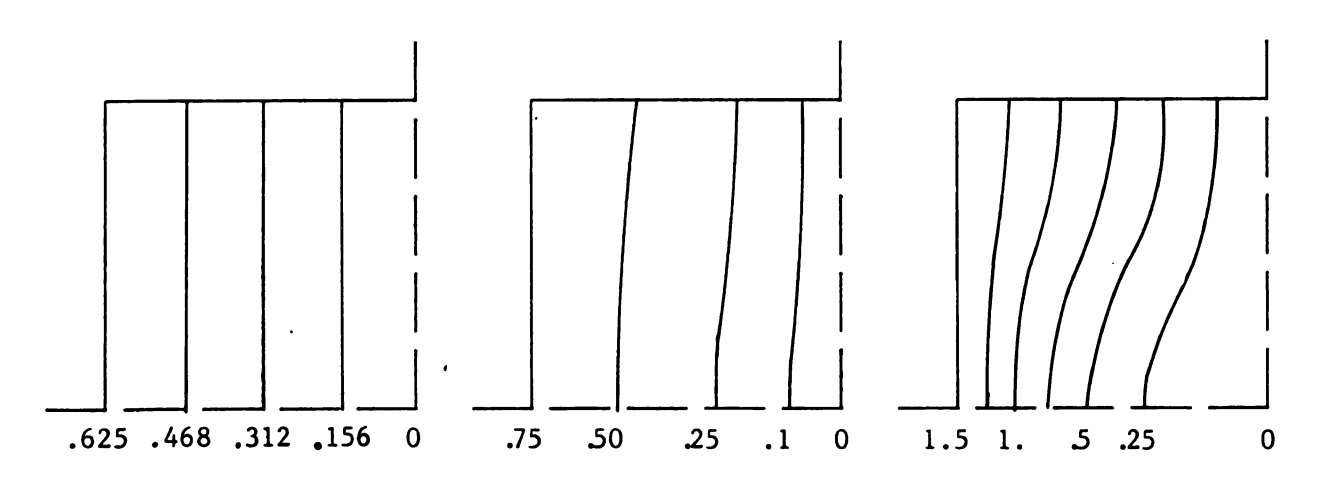
- i) As the center of the plate deflects transversely, the in-plane load shifts with more of the load being carried by the portion of the plate near the edges.
- ii) The bending moment, which is maximum at the center, is increasing with the increase in deflection w.
- iii) Along the centerline parallel to x, the membrane force  $N_y$  is increasing toward the edge, while  $N_x$  is almost constant.
- iv) Bending moments  $M_{x}$  and  $M_{y}$  both are maximum at the center and diminish to zero along the edges, as expected.

# c) <u>In-plane displacements</u>

The distribution of in-plane displacements in the plate is shown in Figure (3.75) at different stages of loading.

Analysis of these leads to the following conclusions:

- i) Before buckling, the plate is perfectly flat. Since there is no w effect, in-plane displacements are linear, as expected.
- ii) After buckling, the plate will undergo more contraction near the edges and the central region carries less compressive load; less in-plane displacement occurs there.
- iii) As the load increases this phenomenon becomes more visible, so that at large edge displacements, the curves show very little u and v displacement in the central regions.



a) Undeflected (U/U<sub>cr</sub>=1.0) b) Buckled (U/U<sub>cr</sub>=1.20) c) Buckled (U/U<sub>cr</sub>=2.40) Figure 3.75. In-plane displacement (U = ua/t<sub>1</sub><sup>2</sup>), square plate, simply-supported, RT = 1.

# d) simply-supported, square plate, loaded by uniform normal pressure

To check the reliability of the method by comparing with previous results, a problem similar to one presented by Levy is considered. In Reference (29), Levy has solved a square plate under a uniform normal pressure, with zero in-plane displacement along the edges. Levy applies the large deflection equations and uses the series expansion method.

In this section, a solution is obtained for the same problem to compare with Levy's. The plot of (3.76) shows the variation of w with lateral load as determined by Levy and by the difference method.

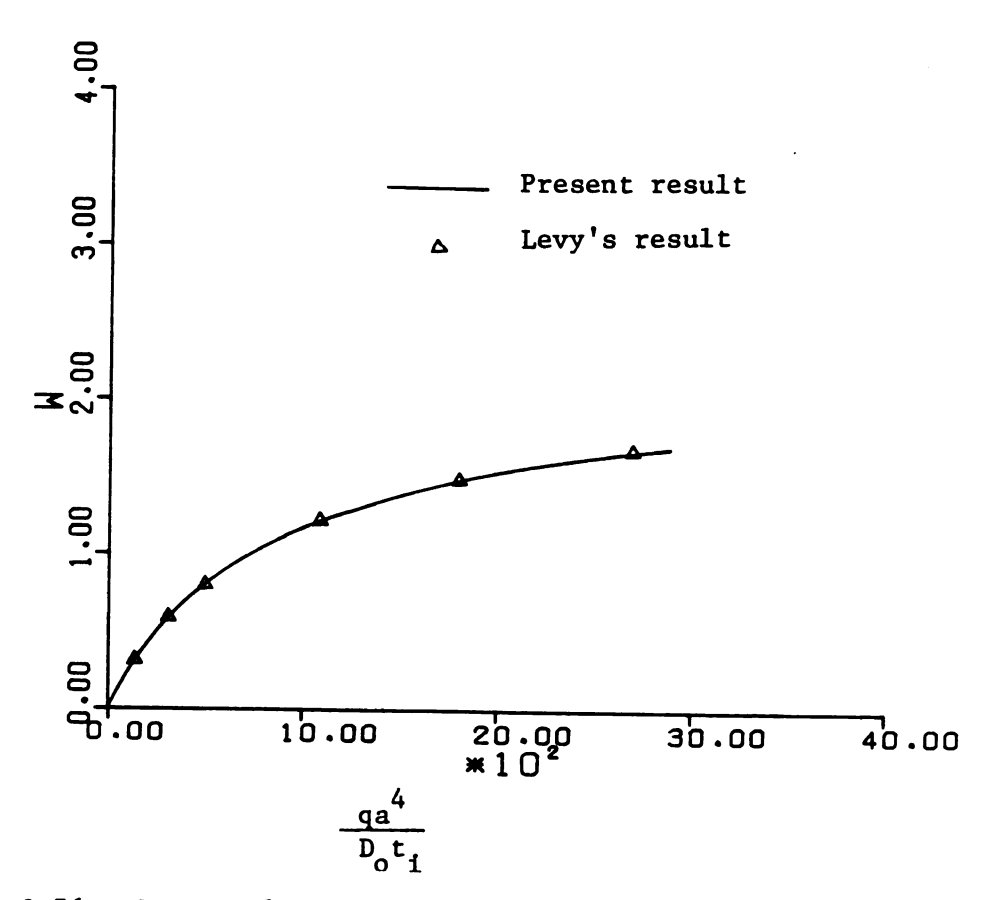


Figure 3.76. Square plate under uniform lateral load; no in-plane displacements on boundary;  $\nu = .316$ .

## 3.2.3.2 Simply Supported Square Plate of Variable Thickness

To study the variable thickness plate, a solution was obtained for two different cases. In the first,  $RT = \frac{\text{edge thickness}}{\text{center thickness}} = \frac{1}{4}$ , for which the membrane stiffness at the edge is  $\frac{1}{4}$  that at the center, while the flexural stiffness at the edge is  $\frac{1}{64}$  of the center stiffness. In the second, RT = 2, with the edge flexural stiffness being  $\frac{1}{8}$  of the central stiffness. These two opposite variations are chosen so that the results, along with those for the uniform thickness plate, would give an idea about the effects of variation in thickness. The discussion follows.

Figure (3.77) shows the central deflection of the plate with variable thickness and also the result for a uniform thickness plate. Comparison of the three plots leads to the conclusion that, corresponding to the same edge compression, less deflection occurs in the plate with  $RT = \frac{1}{4}$  and the plate with RT = 2 undergoes larger deflection. It should be noted that all these plates contain the same volume.

This behavior is expected because, in a simply-supported plate, more bending is occurring in the central region. Thus, plates with thicker central region will experience less deflection and plates with thin central regions are more likely to have greater curvature and deflect large amounts.

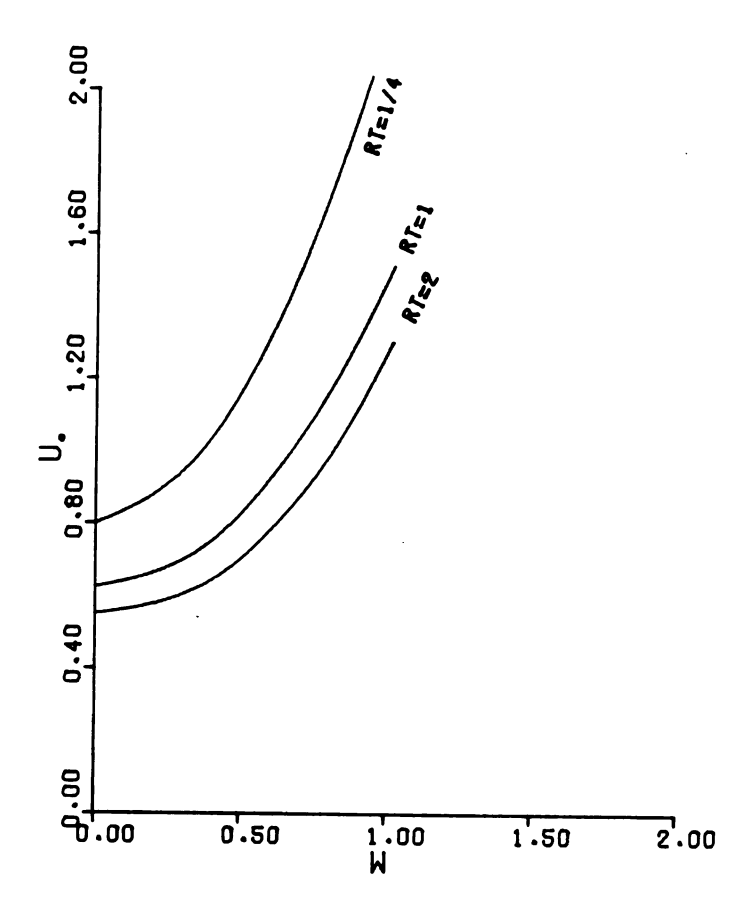


Figure 3.77. Central deflection versus edge displacement for different RT values, simply supported square plate.

## a) Solution Procedure

In (3.2.3.1 a) it was shown that a grid spacing of  $h = \frac{a}{16} \text{ will be accurate enough for engineering design}$  use. Both problems were solved with a grid spacing of  $h = \frac{a}{16} \text{ in determining the results plotted.}$ 

# b) Stress Analysis

Distribution of in-plane forces, bending moments and principal stress, along axes of the plate, are shown in Figure (3.78) for RT =  $\frac{1}{4}$ .

The Graph of N and N shows a decrease in membrane forces with an increase in edge displacement in the central

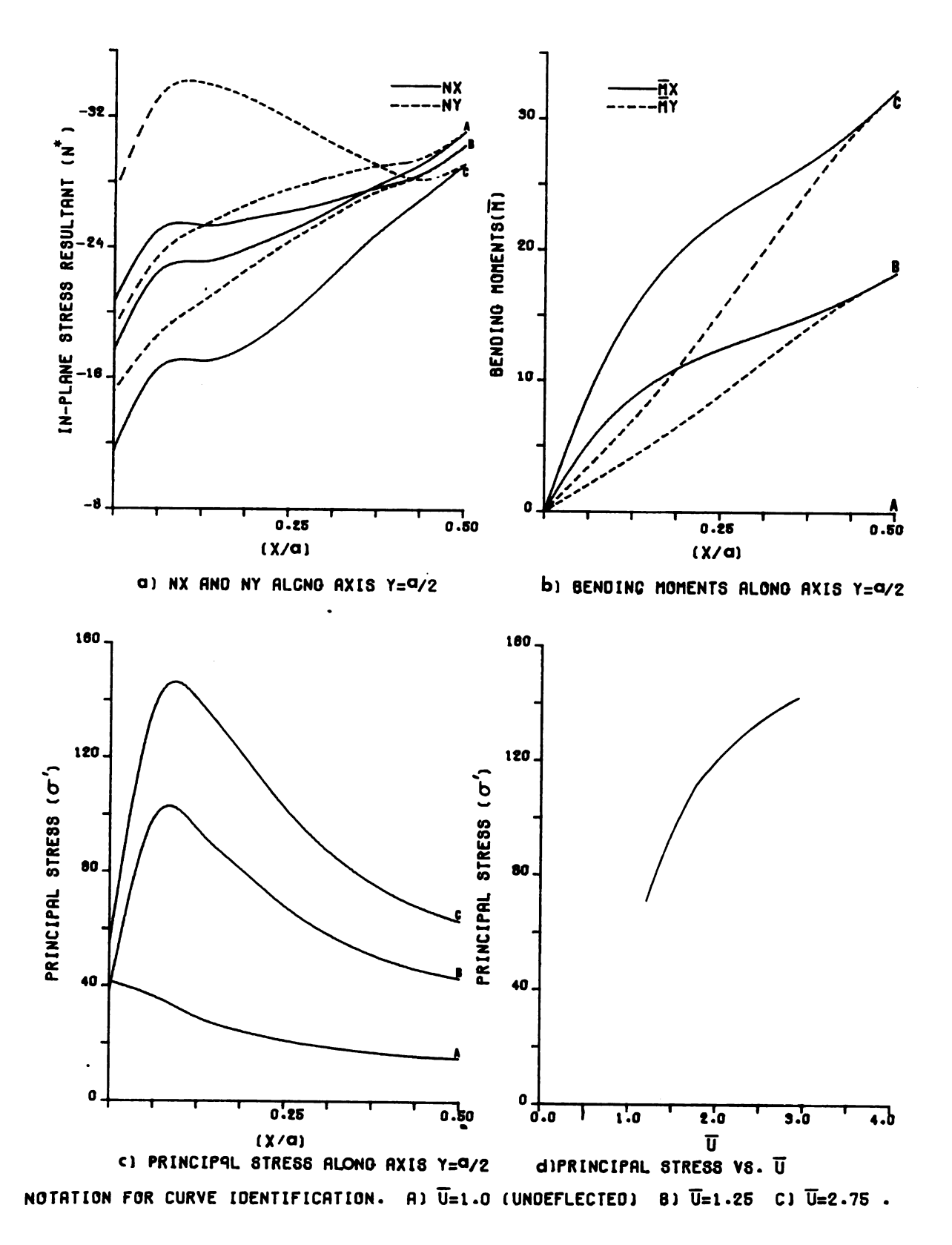


FIGURE 3.78. PLOTS OF STRESS COMPONENTS, SQUARE PLATE, SIMPLY SUPPORTED, RT=1/4.

region, while in a region close to the edge,  $N_y$  is large.

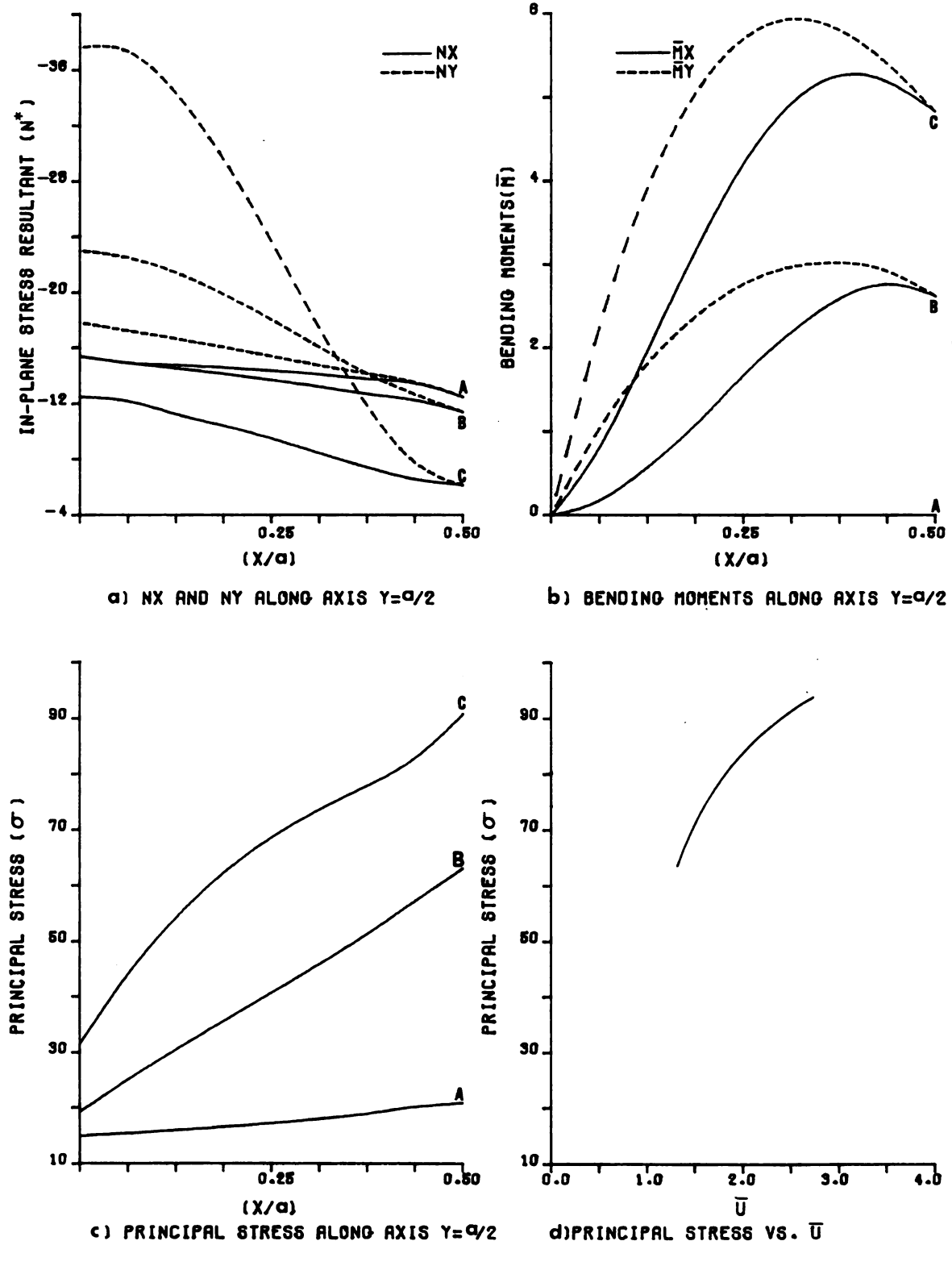
As discussed before, the central region will carry less load because of the transverse deflection and the load will be shifted toward edges.

The moments are maximum at the center and vanish at the edge, but fairly large moments occur at almost halfway from center to edges. This is due to the relatively larger thickness at center. Because most of the bending will occur in the outer region, creating large curvature and resulting in large moments.

Since we are concerned with the state of stress within the plate and not necessarily membrane force or bending moments individually, in Figure (3.78c), the variation of principal stress along the axis of plate is plotted. The curve shows maximum stress occurring approximately at a point  $x = \frac{a}{8}$  on this axis. It should be noted that this stress is also the absolute maximum for the entire plate.

Figure (3.79) show the same variables for a plate with RT = 2.

In this case, because of the thicker edge region, beyond buckling, the membrane load is sharply shifted toward the edges.



NOTATION FOR CURVE IDENTIFICATION. A)  $\overline{U}=1.0$  (UNDEFLECTED) B)  $\overline{U}=1.25$  C)  $\overline{U}=2.20$  .

FIGURE 3.79. PLOTS OF STRESS COMPONENTS. SQUARE PLATE, SIMPLY SUPPORTED, RT=2.

The bending moments have a completely different pattern than for the case  $RT = \frac{1}{4}$ , because the more flexible central region results in maximum curvature and maximum moments in this central region. Also, because of smaller thickness and smaller flexural rigidity, the maximum principal stress is always at the center point. In Figure (3.80) shows the variation of the maximum principal stress with postbuckling edge compression for the different variation in thickness. It can be seen that the least stress occurs for the uniform thickness plate, and the plate with  $RT = \frac{1}{4}$  is subject to largest stress at points away from center.

# c) In-plane Displacements

Contours of the in-plane displacement u, in Figure (3.81) for RT =  $\frac{1}{4}$ , and Figure (3.82) for RT = 2., show a decreasing displacement in the central region due to w deflection and corresponding decrease in membrane forces. In the case of RT =  $\frac{1}{4}$ , we observe very small displacements in the central region, while the more closely-spaced contours in the vicinity of the edge indicate very large strain in this region.

Comparison with the uniform thickness plate shows it to be between these two variations, as expected.

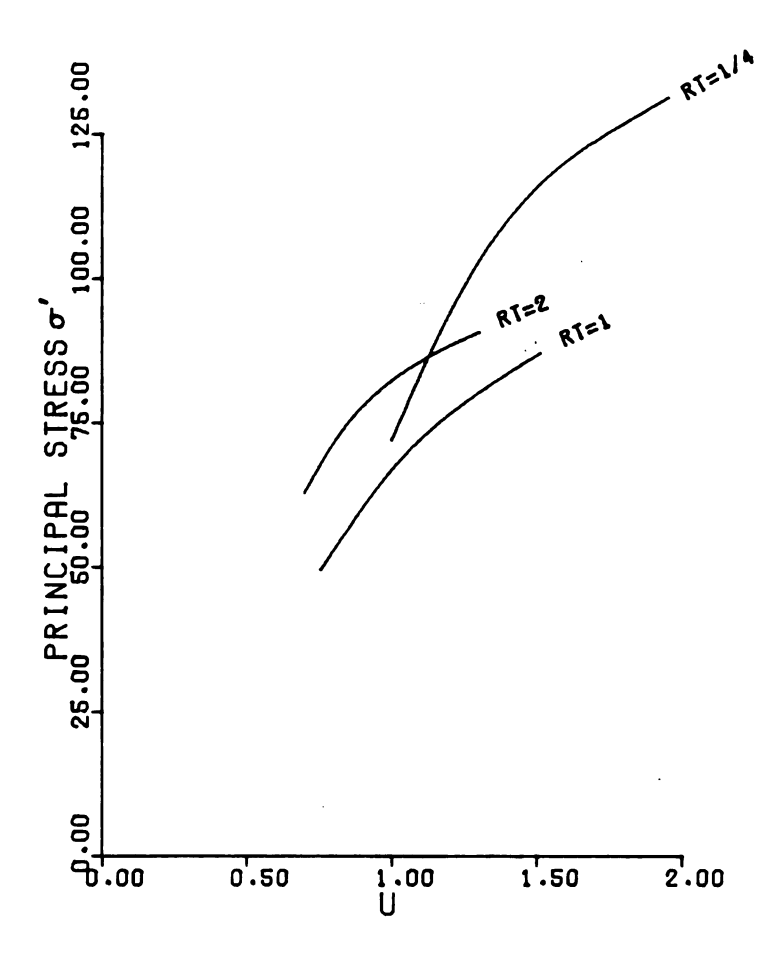
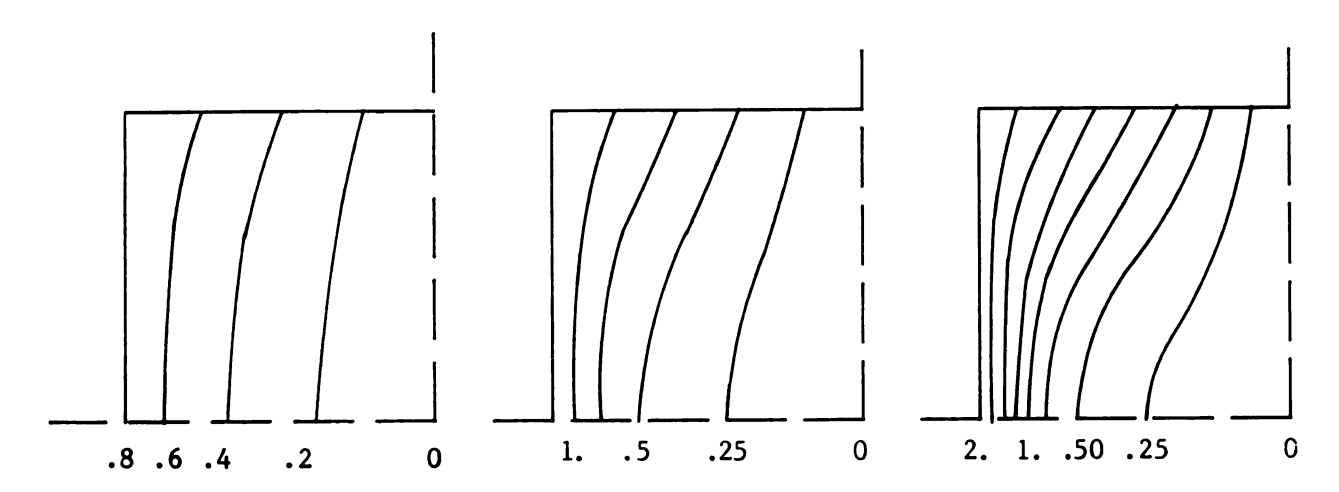
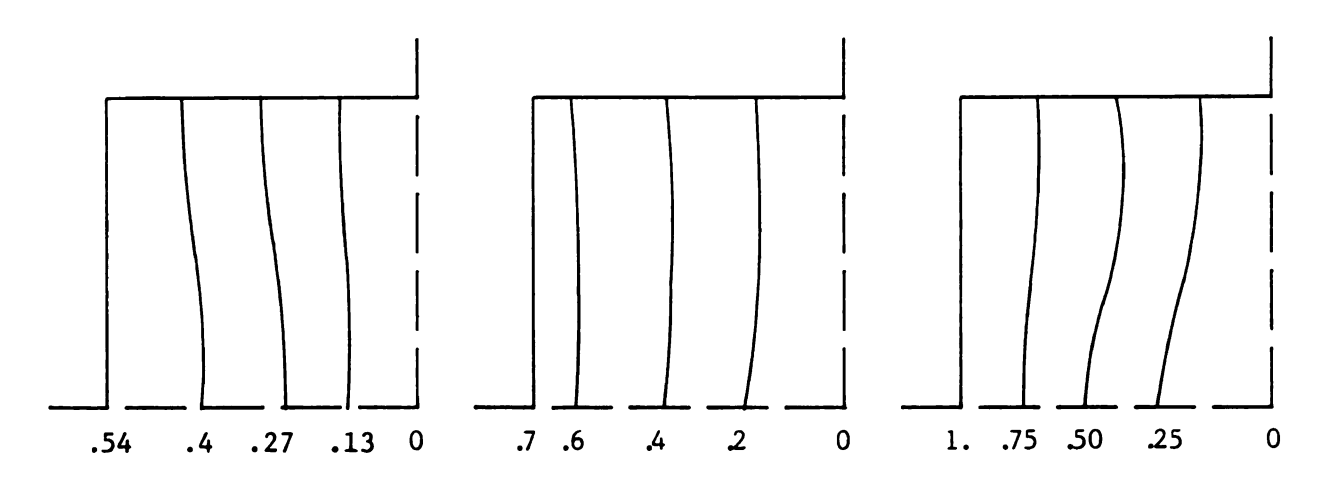


Figure 3.80. Principal stress versus edge displacement for different RT values, simply-supported square plate.



a) Undeflected (U/U<sub>cr</sub>=1.) b) Buckled (U/U<sub>cr</sub>=1.50) c) Buckled (U/U<sub>cr</sub>=2.50) Figure 3.81. In-plane displacement (U=ua/ $t_1^2$ ), square plate, simply-supported,



a) Undeflected (U/U  $_{\rm cr}$  = 1.) b) Buckled (U/U  $_{\rm cr}$  =1.30) c) Buckled (U/U  $_{\rm cr}$  =1.85)

Figure 3.82. In-plane displacement ( $U = ua/t_1^2$ ), square plate, simply-supported, RT = 2.

## 3.2.3.3 Uniform Thickness Plate, Clamped Boundaries

The problem studied in 3.2.3.1 was solved with clamped boundaries, and the results of the solution are as follows.

a) Convergence of the solution.

Table (3.14) presents results for different mesh sizes corresponding to a boundary displacement of  $(\frac{3.2}{1.659} = 1.93)$  times the critical displacement.)

Table 3.14. Convergence of postbuckling solution with grid spacing.

Grid spacing h/a	w-center	Difference %	Extrapolation	N*-center	M <sub>x</sub> -center
1/4	1.9667		·	314.73	295.45
		34.4	1.295366		
1/8	1.4632	·		277.99	263.23
		4.6	1.376613		
1 12	1.39826			289.56	262.96
		2.2	1.357113		
$\frac{1}{16}$	1.3674			285.00	260.576

Considering that the accuracy test of the iterative solution was set at 1% in successive trials, the convergence as illustrated in graph (3.83) is good.

Plot of central deflection with edge compression is shown in Figure (3.84).

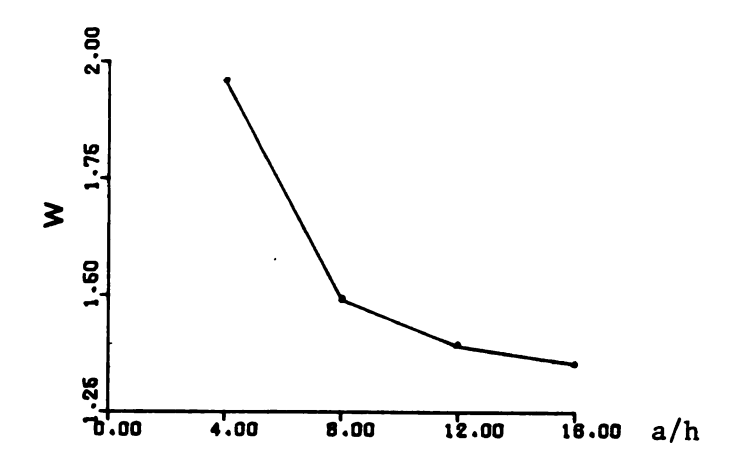


Figure 3.83. Convergence of solution.

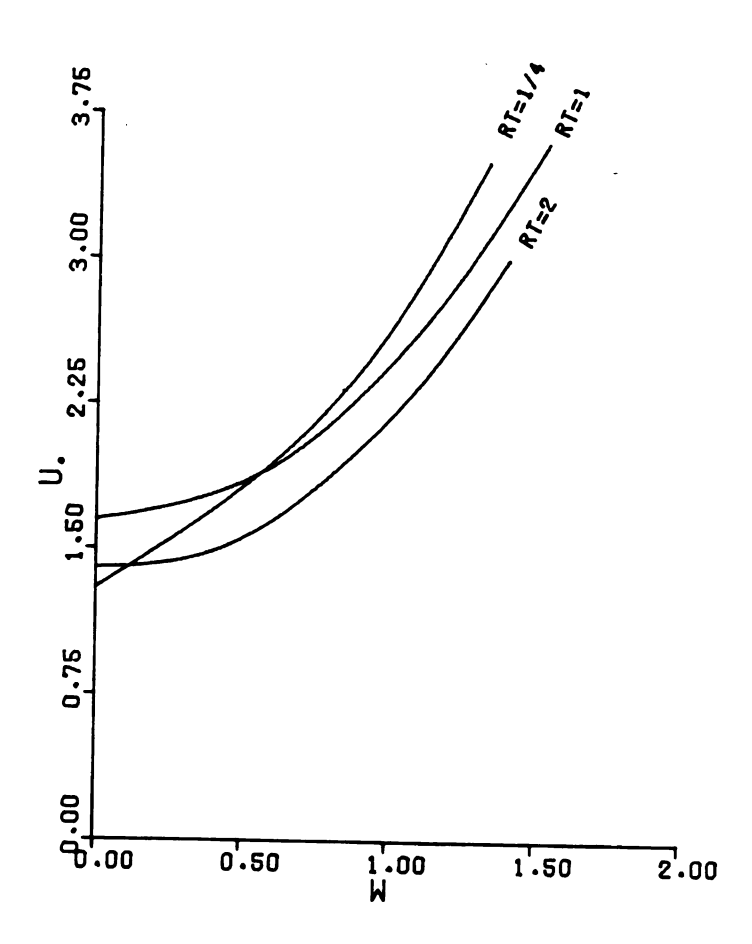


Figure 3.84. Central deflection versus edge displacement for different RT values, square plate, clamped edges.

# b) Stress Analysis

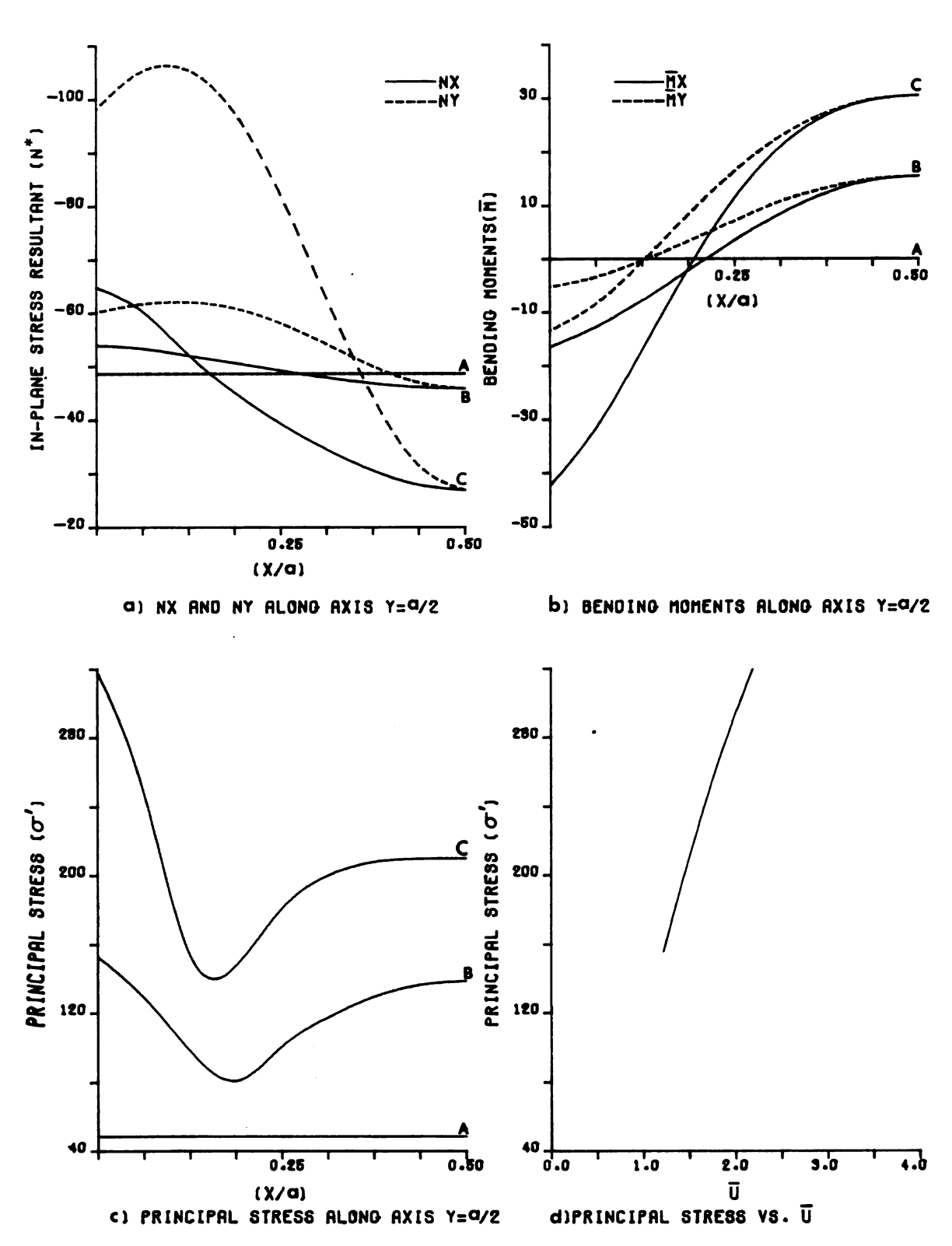
Distribution of membrane forces, bending moments, and principal stress along the axis of the plate, are plotted in Figure (3.85). These figures show:

- Larger membrane force occurs at the edge and the central membrane forces decrease with an increase in postbuckling edge compression.
- ii) Bending moment, M<sub>x</sub>, is positive at the center and along the edge it is negative with an absolute value larger than the central moment for the larger deflection.
- iii) Principal stress is almost equal at center and edge in the early postbuckling stage, increasing on the edge with larger deflection.

#### c) In-plane Displacements

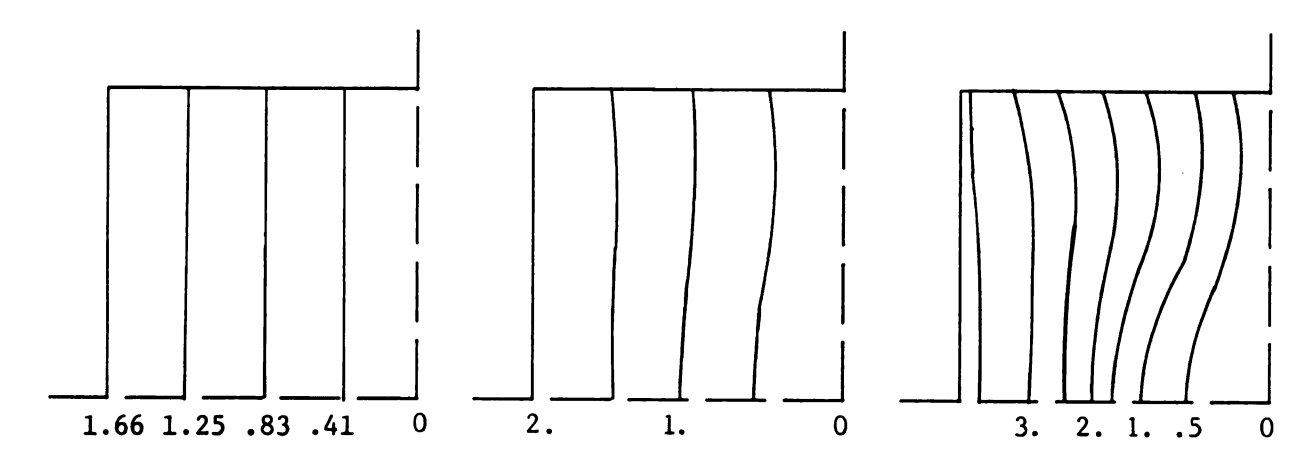
Contours of in-plane displacement, u, shown in Figure (3.86) indicate the following.

- Before buckling, in the flat plate, in-plane displacements are linear everywhere as expected.
- ii) Immediately after buckling, as the deflection starts to increase, the u-displacement tends to decrease in the central region.
- iii) The pattern of displacement is qualitatively similar to that for the simply supported case.



NOTATION FOR CURVE IDENTIFICATION. A)  $\overline{U}=1.0$  (UNDEFLECTED) B)  $\overline{U}=1.20$  C)  $\overline{U}=2.25$  .

FIGURE 3.85. PLOTS OF STRESS COMPONENTS.SQUARE PLATE.CLAMPED. RT=1 .



a) Undeflected (U/U =1.) b) Buckled (U/U =1.20) c) Buckled (U/U =2.2) Figure 3.86. In-plane displacement (U = ua/ $t_1^2$ ), square plate, clamped edges, RT = 1.

# 3.2.3.4 Clamped Plate with Variable Thickness

Again, the plates discussed in Section 3.2.3.2 (RT =  $\frac{1}{4}$ , and RT = 2) are solved with clamped boundaries along all edges.

For comparison, the variation of w with edge compression is plotted in Figure 3.84 for plates with  $RT = \frac{1}{4}$  and RT = 2, along with uniform thickness plate.

It can be seen that in the case of the clamped plate, due to edge displacement appreciably greater than critical displacement, the plate with  $RT = \frac{1}{4}$  undergoes less deflection than either of the plates with RT = 1 and RT = 2. This is similar to the case of simple support, but in the early stages of postbuckling, the plate with RT = 1 has the smaller lateral displacement.

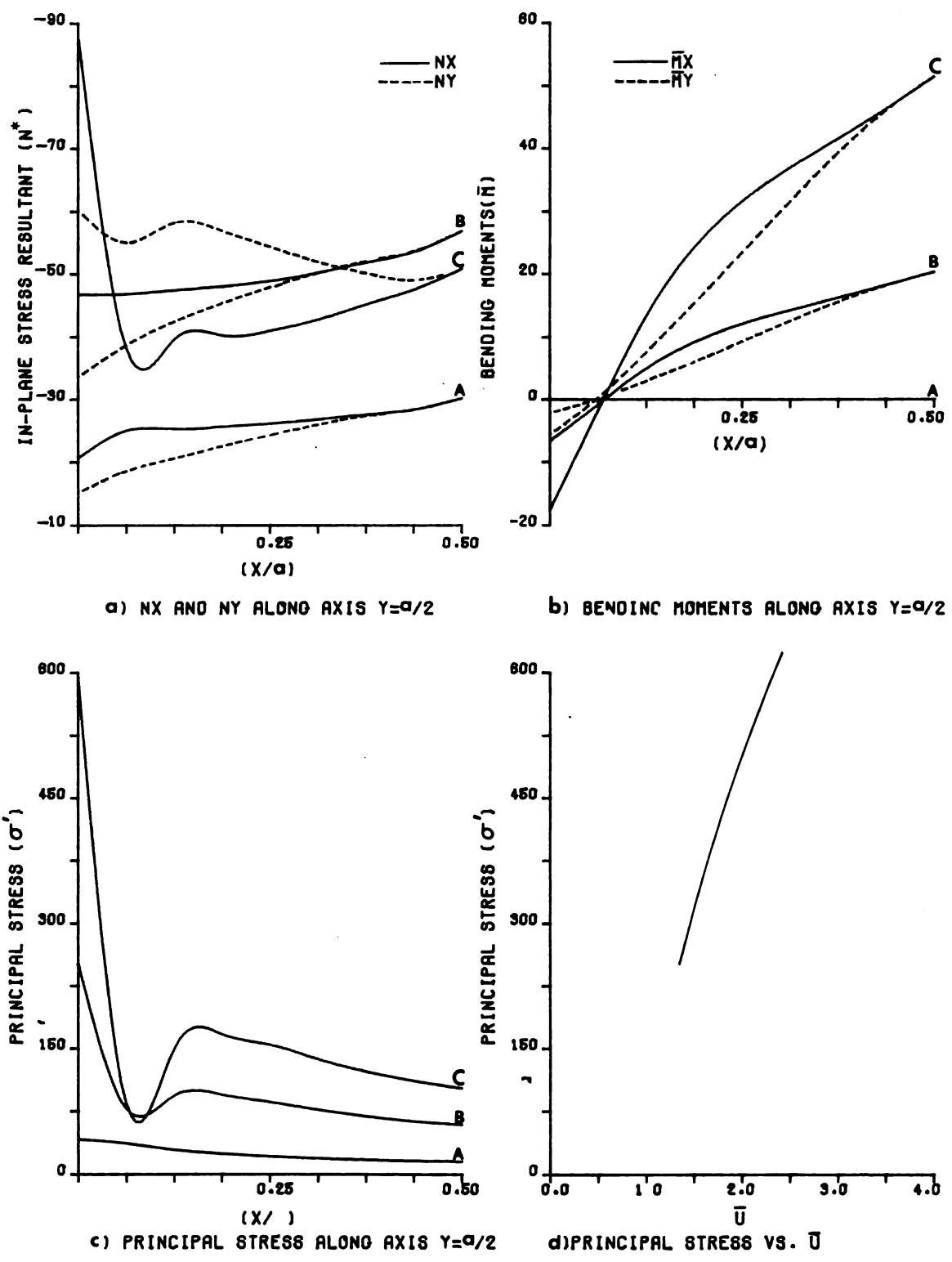
# a) Stress Analysis

Figure (3.87) illustrates the distribution of membrane forces, bending moments, and principal stresses for the plate with RT =  $\frac{1}{4}$ . Analysis leads to the following conclusions:

- i) While the membrane forces are decreasing with increase in edge displacement at the center, these forces increase sharply on the edges.
- ii) Bending moments are maximum at the center, and the negative moments along the edge are small because of small flexural rigidity.
- iii) Principal stress is maximum on the edge and increases with an increase in edge displacement.

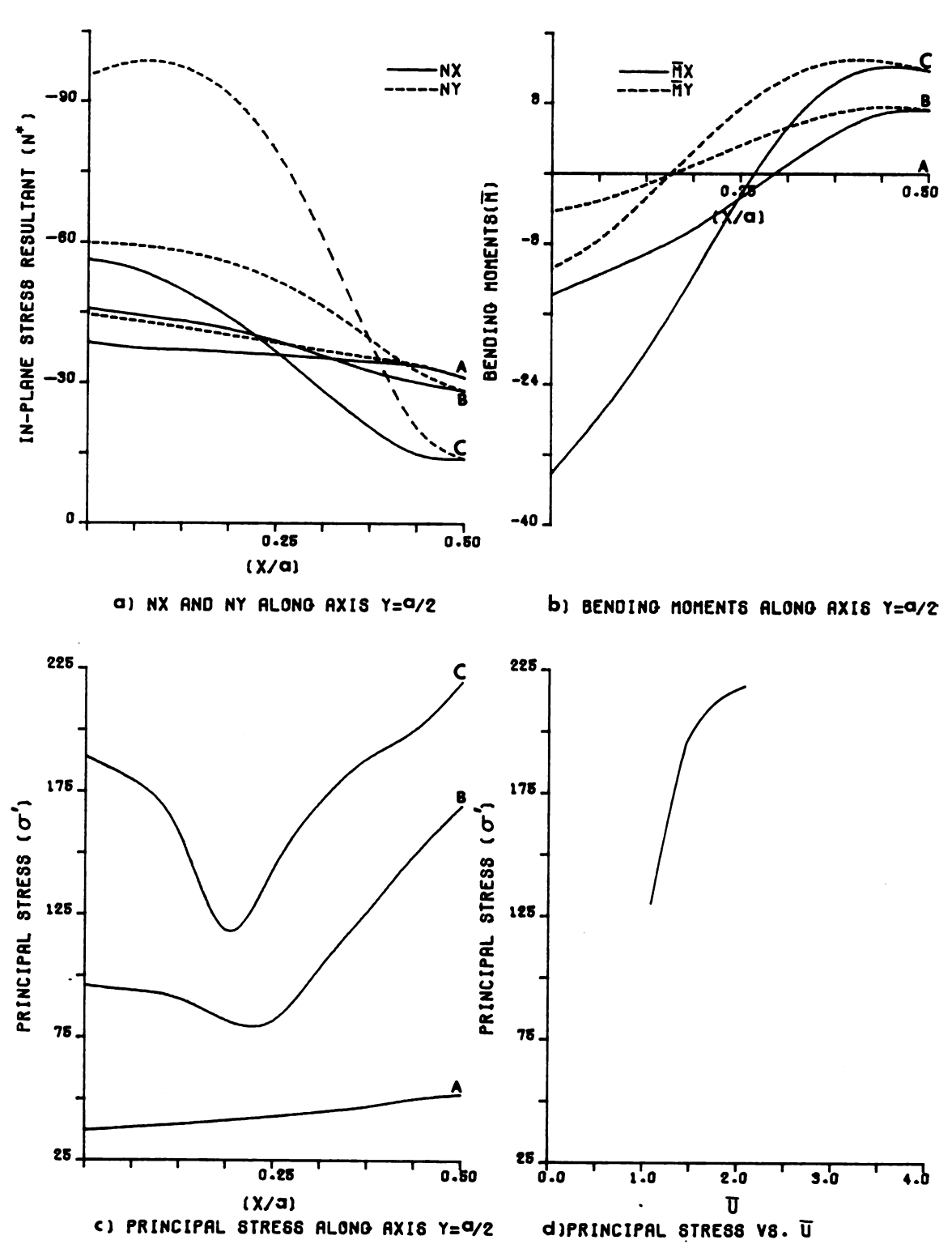
Study of membrane forces, bending moments, and principal stresses for the plate with RT = 2, in Figure (3.88), results in the following observations.

- N decreases in the central region as the edge displacement increases, while it increases sharply near the edge.
- ii)  $N_{\mathbf{x}}$  also decreases at the center and decreases along the edge.



NOTATION FOR CURVE IDENTIFICATION. A)  $\overline{U}=1.0$  (UNDEFLECTED) B)  $\overline{U}=1.30$  C)  $\overline{U}=2.30$  .

FIGURE 3.87. PLOTS OF STRESS COMPONENTS.SQUARE PLATE.CLAMPED. RT=1/4 .



NOTATION FOR CURVE-IDENTIFICATION. A)  $\overline{U}=1.0$  (UNDEFLECTED) B)  $\overline{U}=1.30$  C)  $\overline{U}=2.40$  .

FIGURE 3.88. PLOTS OF STRESS COMPONENTS. SQUARE PLATE. CLAMPED. RT=2 .

- iii) Bending moments increase in magnitude at the center and edges as the edge displacement increases, as expected. The negative moments at the edges are much larger, because the flexural rigidity is larger there.
- iv) The graph of the principal stress shows an increase everywhere as the edge displacement increases, but it is always a maximum at the center of the plate.
  - v) Figure (3.89) shows the variation of maximum principal stress with edge compression, u , for the three different RT values and for plates of constant volume.

It can be seen that the plate with  $RT = \frac{1}{4}$  always undergoes larger stress. Although the uniform thickness plate is less highly stressed than the case RT = 2 for smaller edge displacements, in the higher range of edge compression it is more highly stressed than the plate with RT = 2.

Note: It should be noted that for RT = 1, and RT =  $\frac{1}{4}$ , the maximum principal stress is located at the center of the edge while for case of RT = 2, the location is at the center of the plate.

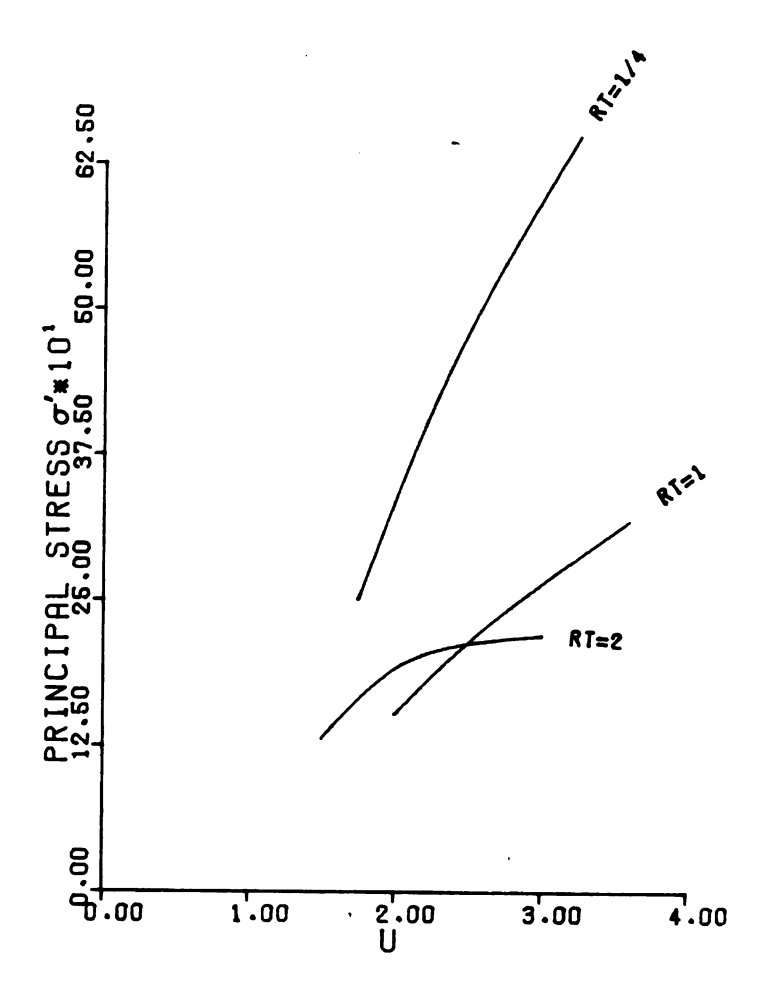
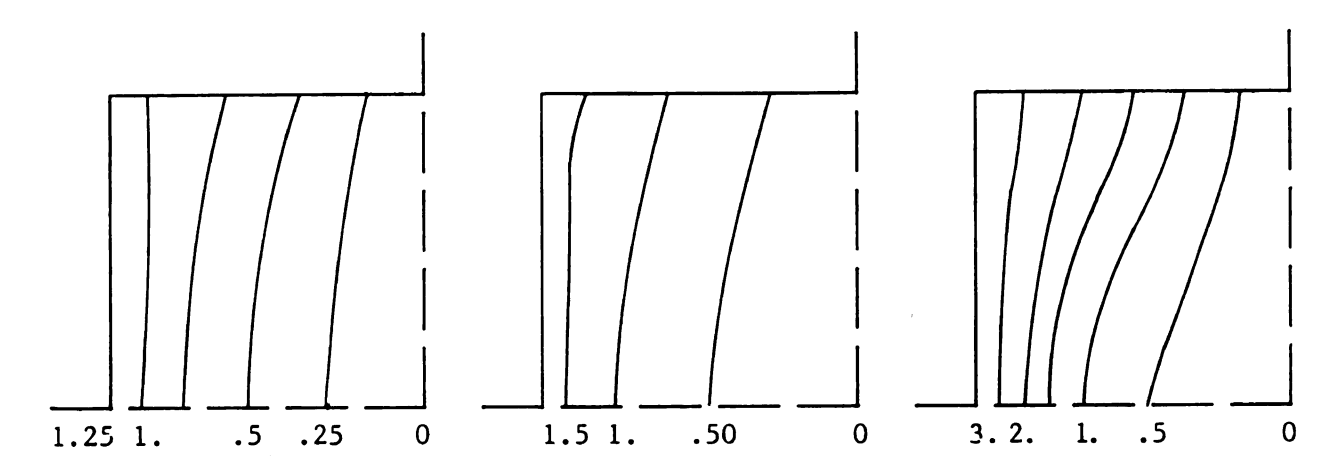


Figure 3.89. Max. Principal stress versus edge displacement for different RT values, square plate, clamped boundaries.

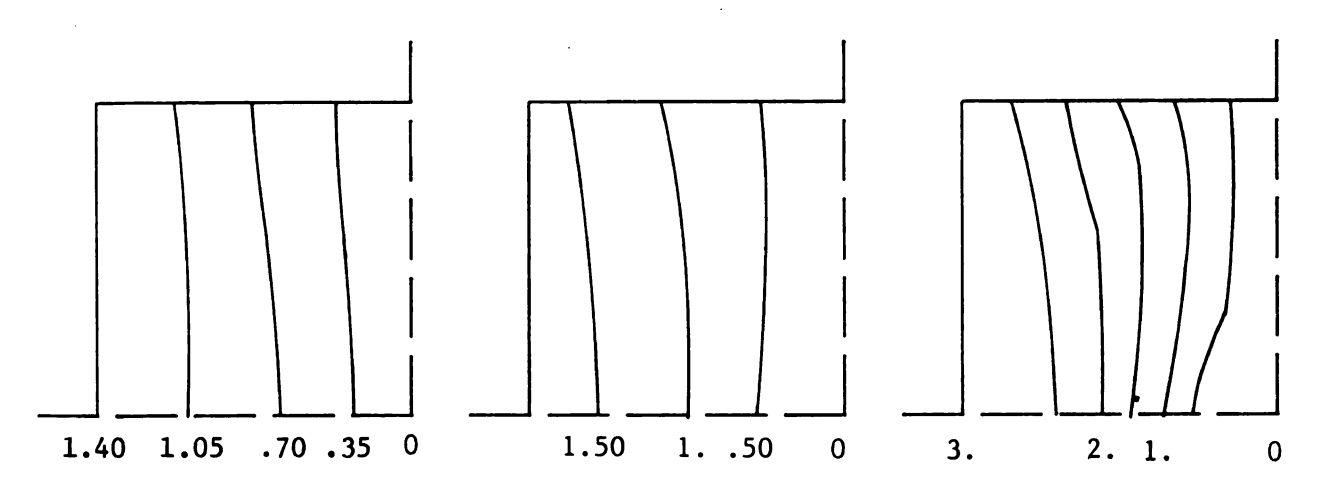
# b) In-plane Displacements

Contours of in-plane displacement, U, are plotted in Figure (3.90) for plate with RT =  $\frac{1}{4}$ , and in Figure (3.91) for plate of RT = 2. These contours show the following:

- i) Before buckling, the contours are exactly the same as those for simple support, because in the undeflected position the out-of-plane boundary condition has no effect on the solution.
- ii) After buckling, as usual, the in-plane displacement in the central region is smaller compared to undeflected case (i.e., the contours are expanding at the center and compacted contours are located away from center toward the edge depending on the RT values.)
- iii) In the case  $RT = \frac{1}{4}$  closer contours are located in the vicinity of the edge, while for the plate RT = 2, because of stiff edges these concentrated contours are seen to be close to the center.
  - iv) The behavior of the uniform thickness plate falls between the cases  $RT = \frac{1}{4}$  and RT = 2.



a) Undeflected (U/U =1.) b) Buckled (U/U cr=1.35) c) Buckled (U/U cr=2.30) Figure 3.90. In-plane displacement (U = ua/t $_{i}^{2}$ ), square plate, clamped, RT = 1/4.



a) Undeflected (U/U = 1.) b) Buckled (U/U = 1.25) c) Buckled (U/U = 2.15) Figure 3.91. In-plane displacement (U =  $ua/t_1^2$ ), square plate, clamped, RT = 2.

#### 3.3 COMPARISON OF TWO METHODS

In order to compare results from the two methods discussed formulation in terms of the stress function or in terms of displacementstwo problems are solved by both methods and compared. Their results
can also be used as a measure of the accuracy of either of the methods.

## a) Simply Supported

- A simply-supported uniform stiffness plate, with
  no restraint on in-plane boundary displacement and
  loaded beyond the critical load was solved using the method
  discussed in Section (2.2) (in terms of φ and w).
   The solution includes in-plane displacements, u
  and v, on the boundary.
- ii) The problem is solved using the method of Section (2.3) (in terms of three displacements, u, v and w), by applying the boundary displacements obtained in (i) as boundary conditions.
- iii) If both methods are correct, we expect (i) and (ii) to result in the same solutions, and they did turn out to be very close. The central deflection (w/t) is .9613 in (i) and .9736 in (ii), with a difference of 1.3%. This is very good agreement. Other components of stress and displacement are also very close.

#### b) Clamped Edges

A uniform stiffness plate with clamped boundaries was also examined in the same way as discussed in part (a). The central deflection (w/t) was found to be 1.67121, using the method of Section 2.2 (i.e., formulation in terms of stress function). It was 1.68578 using the formulation in terms of displacements, with a difference of only .8%. The results are considered to be very good.

#### CHAPTER IV

#### CONCLUSION

#### 4.1 THE PROBLEM SUMMARY

In the preceding chapters, the behavior of variable stiffness plates was studied in the prebuckling and postbuckling range. Instability criteria were also examined. The work used the ordinary finite difference technique. No results for similar variable stiffness plates are available in the literature to confirm the validity of the solutions. However, a uniform stiffness plate was included in each case to serve as a control problem, and the results obtained by the difference method were compared with those of analytical solutions and other published results.

Since the main purpose of varying stiffness is to optimize the plate with respect to some design variables, some optimization examples were presented in the buckling analyses.

In order to provide a better perspective on the change in behavior of plates due to stiffness variation, the different problems considered were assumed to contain a constant mean stiffness or a constant amount of material (see Section 3.1.4). Two different approaches were discussed:

1. Formulating in terms of stress function,  $\phi,$  and the lateral deflection,  $w_{\bullet}$ 

Formulating in terms of three displacement components,
 u, v and w.

First the applicable difference operators were worked out; then the solution procedures were presented in detail. Finally, an increasing number of nodes were used to check the convergence of the solutions and also to provide guidance in selecting an appropriate mesh size to obtain the desired accuracy.

The behavior of different stress and displacement components was illustrated in suitable graphs and the results were analyzed.

In Section (3.1.1), uniform thickness plates with different variations in E were considered, and the behavior of in-plane forces and displacements was analyzed in Section (3.1.1.1). The buckling of those plates was considered in Section (3.1.2.1) and the effect of variation in stiffness on stability criteria was discussed in Section (3.1.2.2). In Section (3.1.3), postbuckling behavior of those plates was examined and the results were analyzed in Section (3.1.3.3). Sections (3.1.4) and (3.2.2.2) deal with optimization of variation in thickness from the stability point of view. The remainder of Section 3.2 shows the effect of variation in thickness (with constant E) on displacement, forces and moments as well as buckling behavior.

# 4.2 CONCLUSION

The comparison of problems solved in Section 3.1 (with free in-plane movement on the boundaries) with those of Section 3.2 (restricted in-plane displacement on the boundaries), shows the great effect of in-plane boundary restraints in the postbuckling state.

Study of figures (3.60), (3.77) and (3.84), leads to the conclusion that the behavior of central deflection due to variation in stiffness is not only dependent on the out of plane boundary conditions but also greatly affected by in-plane boundary conditions.

Figures (3.60), (3.77) and (3.84) show that the trend of central deflection of plates with different variation in stiffness is not the same for all postbuckling ranges. For example, in Figure (3.77), we observe that corresponding to the same load, a simply supported plate with RT = 1 undergoes larger deflection than a plate with RT =  $\frac{1}{4}$ . Study of Figure (3.84) shows that the same plates with clamped boundaries exhibit different behavior. (Although, for highly compressed edges, less deflection is observed for the plate with RT =  $\frac{1}{4}$ , when the edge compression is only slightly above critical displacement, the larger deflection corresponds to plate with RT =  $\frac{1}{4}$ ).

The method and corresponding computer program utilized for force boundary condition (Section 2.2) has been shown to give more accurate results than that developed for the displacement boundary condition (Section 2.3). This is due to the difference in the order of derivatives involved in the formulation. In the force boundary condition formulation, only second and higher order derivatives of the two functions,  $\varphi$  and w, are involved in the equilibrium and

compatibility equations (equation (2.14) and (2.15). The displacement formulation, however, involves first and higher order derivatives of the three functions, u, v, and w. Hence accumulative errors could be expected (In difference approximation equations (2.19), the first error term in the first order derivative includes the third derivative of the function, and the error term in the second derivative includes the fourth derivative of the function, etc.).

Investigation of convergence indicates that for engineering purposes, grid spacings for  $h = \frac{a}{8}$  in the force formulation (see Figure 3.39) and  $h = \frac{a}{12}$  in the displacement formulation (see Table 3.13) are reasonably accurate; more accurate results can be obtained by using finer grids and applying Richardson's extrapolation to the results. Comparison of the results with known values supports the reliability of the solutions.

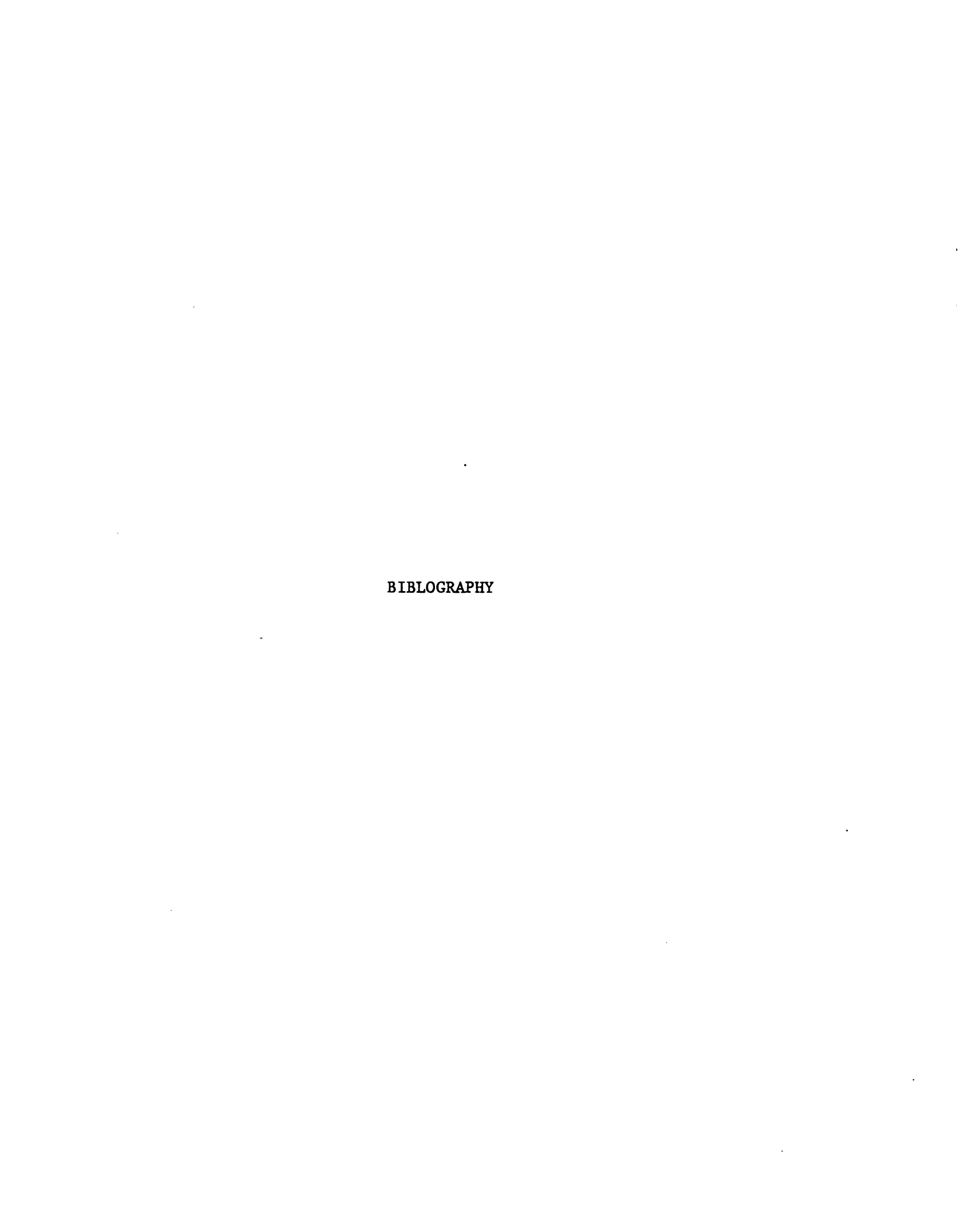
## 4.3 RECOMMENDATIONS

The objective of this work was to examine application of the two formulations in general, and to investigate the behavior of plates with different boundary conditions and stiffness variations. Refinements and extensions of the method which are possible and desirable include:

- Application of improved difference methods involving more accurate approximations to the derivatives.
- Inclusion of more nonlinear terms in the strain components and a study of their effect on the results.
- 3. The difference operators can be revised to make them applicable to orthotropic plates, and the computer program improved so that it can be applicable to orthotropic and nonhomogeneous materials.
- 4. Due to the absence of experimental sources to guarantee the accuracy and practicability of the results, and recognizing the advantages in the use of variable stiffness plates, an experimental study of such plates from the stability point of view and in the postbuckling range should be very useful.
- 5. The computer programs developed here were mainly aimed to solve particular problems. Although they are more general than needed for the problems solved here, for applications to loading and geometry different from the ones presented here, the programs should be used with caution and appropriate changes made. Also, the efficiency of the programs can be improved.

- 6. Application of other methods such as the finite element method using:
  - a) Elements with variable stiffness within the element.
  - b) Constant stiffness within an element but variation of stiffness from element to element.

The boundary integral method might also be considered. Consideration of the same cases and comparing numerical results, convergence, computer cost, etc., would be of interest.



#### **BIBLIOGRAPHY**

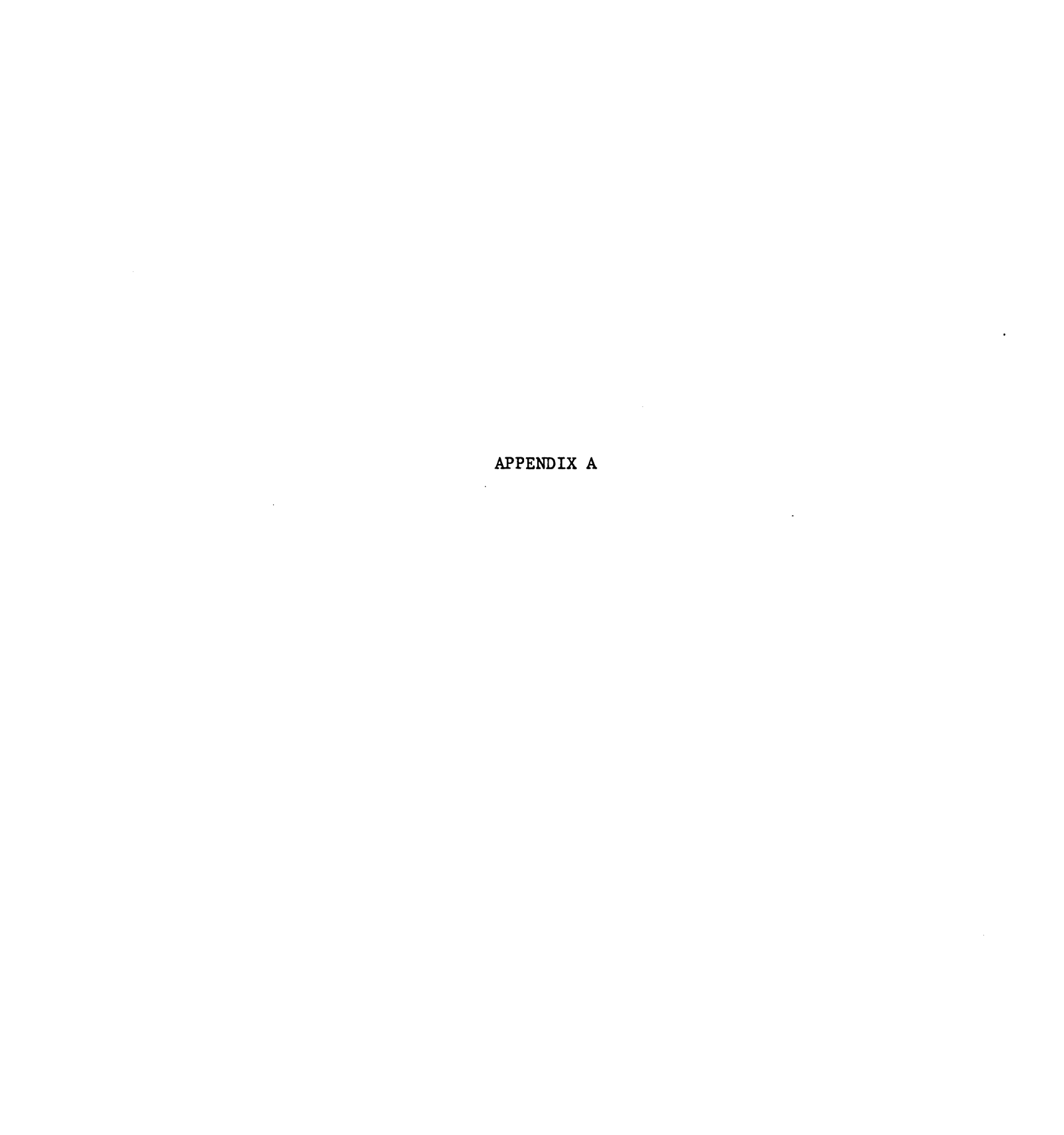
- 1. Aalami, B., and Chapman, J.C., "Large Deflection Behavior of Rectangular Orthotropic Plates and Transverse and In-plane Loads", Institution of Civil Eng. Proceedings 42, pp 347-382 (Mar. 1969).
- 2. Allen, D.N. De G., and Windle, D.W., "The Finite Difference Approach", Stress Analysis, edited by O.C. Zienkiewicz and G. S. Holister, John Wiley and Sons, (1965).
- 3. Altiero, N.J., and Sikarskie, D.L., "A Boundary Integral Method Applied to Plates of Arbitrary Plan Form", Computer and Structures (1979).
- 4. Argyris, J.H., "Energy Theorems and Structural Analysis", Aircraft Eng. 26, 1954, 27, (1955).
- 5. Basu, A.K., and Chapman, J.C., "Large Deflection Behavior of Transversely Loaded Rectangular Plates", Proc. Inst. of Civil Eng. 35, p 79 (1966).
- 6. Bathe, K.J., Oden, J.T. and Wunderlich, W., "Formulation and Computational Algorithms in Finite Element Analysis", MIT Press (1977).
- 7. Billington, D.P., "Thin Shell Concrete Structures", McGraw-Hill (1965).
- 8. Bradley, W.A., "An Alternate Finite Difference Operator for Plates of Variable Stiffness", Int'l Journal for Numerical Methods in Eng. 11, 6, 1044-1048 (1977).
- 9. Brown, J.C., and Harvey, J.M., "Large Deflection of Rectangular Plates Subjected to Uniform Lateral Pressure and Compressive Edge Loading", Journal of Mech. Eng. Science, vol. 11, No. 3, (1969).
- 10. Bryan, G.H. "On the Stability of Plane Plates Under Thrust in it's Own Plane with Application to the Buckling of the Side of the Ship", Proc. London Math. Soc., vol. 22, pp 54-67, (1891).
- 11. Clough, R.W., and Felippa, C.A., "A Uniform Quadrilateral Element for Analysis of Plate Bending", Proceeding of the Second Conference on Matrix Methods in Structural Mechanics, AFFDL-TR-68-150, (Dec. 1969) pp 399-440.
- 12. Coan, J.M., "Large Deflection Theory for Plates with Small Initial Curvature Loaded in Edge Compression", Journal of App. Mech. Tran. ASME, vol. 18 series E, pp 143-150, (1951).

- 13. Colville, J., Beker, E.B., and Eurlang, R.W., "Large Displacement Analysis of Thin Plates", J. Struct. Div., ASCE, vol 59, No.ST3.pp 349-364, (Mar. 1973).
- 14. Conner, J., Jr., Logcher, R.D., and Chan, S.C., "Nonlinear Analysis of Elastic Framed Structures", J. Struct. Div., ASCE, vol. 94, No. ST6, Proc. Paper 6011, pp 1525-1547 (June 1968).
- 15. Dawe, D.J., "Application of the Discrete Element Method to the Buckling Analysis of Rectangular Plates under Arbitrary Membrance Loading", Aeronautics Quarterly, vol. 20, pp 114-128 (1969).
- 16. Dombourian, E.M., Smith Jr., C.V., and Carlson, R.L., "A Perturbation Solution to a Plate Postbuckling Problem", Int. J. Nonlinear Mech., vol. 11, pp 49-58 (1976).
- 17. Euler, L., "De Motu Vibratorio Tympandrum", Novi Commentari Acad. Petropolit., 10, pp 243-260 (1766).
- 18. Galerkin, B.G., "Series Solution of some cases of Equilibrium of Elastic Beams and Plates", (in Russian), Vestnik, Inzhenernov. 1, pp 879-903 (1915).
- 19. Gallagher, R.H., "Geometrically Nonlinear Finite Element Analysis", Proc. Specialty Conference on Finite Element Method in Civil Eng., McGill University, Montreal, Canada; pp 1-33(1972).
- 20. Gallagher, R.H., Lien, S., and Mau, S.T., "Finite Element Plate and Shell Pre-and Postbuckling Analysis", Proceedings, 3rd Air Force Conference on Matrix Methods of Structural Mechanics, Dayton, Ohio, (Oct. 1971) pp 857-879.
- 21. Gass, N., and Taborrok, B., "Large Deformation Analysis of Plates and Cylinderical Shells by a Mixed Finite Element Method", Int. J. for Num. Methods in Eng., vol. 10, pp 731-746 (1976).
- 22. Germain, Sophie, "Recherches Sur La Théorie des Surfaces élastiques", Paris (1821).
- 23. Green, A.E., "On Reissner's Theory of Bending of Elastic Plates", Appl. Math., 7, pp 223-228 (1949).
- 24. Hartz, B.J., "Matrix Formulations of Structural Stability Problems", J. Struct. Div., Proc. ASCE, vol. 91, No ST6, pp 141-157 (1965).
- 25. Jaswon, M.A. and Maiti, M., "An Integral Equation Formulation of Plate Bending Problems", J. Eng. Mech., II (1968).

- 26. Kaiser, R., "Theoretical and Experimental Determinations of Deflections and Stresses in Square Plate Freely Supported at the Edges, with Uniform Load Distributions and Large Deflection", Z. Angew. Math. Mech. 16, 73 (1936).
- 27. Kennedy, J.B., and Prabhakara, M.K., "Postbuckling of Orthotropic Skew Plate Structures", J. Struct. Div., ASCE, pp 1497-1511 (July 1980).
- 28. Lagrange, J. Ann. Chim. vol. 39 pp 149 (1828).
- 29. Levy, S., "Bending of Rectangular Plates with Large Deflections". NACA, TR737, pp 139-157 (1942).
- 30. Maiti, M. and Chakrabarty, S.K., "Integral Equations for Simply Supported Polygonal Plates", Int. J. Mech. Sci., 12 (1974).
- 31. Murray, D.W. and Wilson, E., "Finite Element Postbuckling Analysis of Thin Elastic Plates", AIAA J., vol. 7, No. 10, pp 1915-1920 (1969).
- 32. Murthy, S. D.N., and Sherbourne, A.N., "Nonlinear Bending of Elastic plates of Variable Profile", J. Eng. Mech. Div., Proc. ASCE, 100, EM2, 251-165 (Apr. 1974).
- 33. Neilsen, N.J., Bestemmelse af Spaendinger i plader ved Anvendelse af Differensligninger, Copenhagen (1920).
- 34. Oden, J.T., "Numerical Formulation of Nonlinear Elasticity Problems", J. Struct. Div., ASCE, vol 93, No. ST3 pp 235-255 (June 1967).
- 35. Otter, J.R.H., "Computations for Prestressed Concrete Reactor Pressure Vessels using Dynamic Relaxation", Nuclear Structural Eng., 1, 61 (1965).
- 36. Prabhakara, M.K., and Chia, C.Y., "Postbuckling Behavior of Rectangular Orthotropic Plates", J. Mech. Eng. Sci., vol. 15, No.1, pp 25-33 (1973).
- 37. Ramberg, W., McPherson, A.E., and Levy, S., "Normal Pressure Tests of Rectangular Plates", NACA TN748,pp 349-371 (1942).
- 38. Rushton, K.R., "Dynamic Relexation Solutions of Elastic Plate Problems", J. Strain Analysis.pp 3-23 (1968).
- 39. Rushton, K.R., "Large Deflection of Variable Thickness Plates", Int. J. Mech. Sci., vol 10, pp 723-735 (1968).

- 40. Rushton, K.R., "The Dynamic Relaxation Method used for Stress Analysis", Conf. Recent Adv. Stress Analysis, Royal Aeronaut. Soc. 3, (1968).
- 41. Shye, K.Y., and Colville, J., "Postbuckling Finite Element Analysis of Flat Plates", J. Struc. Div., ASCE, vol. 105, No. ST2, pp 297-311 (Feb. 1979).
- 42. Supple, W.J., "Change of Wave Form of Plates in the Postbuckling Range", Int. J. Solids Structures 6, 1243 (1970).
- 43. Szilard, R., "Theory and Analysis of Plates", Prentice-Hall (1974).
- 44. Timoshenko and Gere, "Theory of Elastic Stability", 2nd edition, McGraw-Hill (1961).
- 45. Turner, M.J., Clough, R.W., Martin, G.C. and Topp, L.J.,
  "Stiffness and Deflections Analysis of Complex Structures",
  J. Aero. Sci., 23 pp 805-823 (Sept. 1956).
- 46. Vlasov, V.Z., "Some New Problems on Shells and Thin Structures", NACA, Tech. Memo. No. 1204 (Mar. 1949).
- 47. Von Kármán, T., "Festigkeitsprobleme im Maschinenbau", vol. IV, Pt. 4, of Encyk. der Math. Wiss., 1910, Art. 27, pp 311-388, ASME Trans. Apm 54-5, vol. 54, No.2 pp 53-57 (Jan. 1932).
- 48. Vos, G.R., "Finite Element Analysis of Plate Buckling and Postbuckling", Ph.D. Thesis, Rice University (1971).
- 49. Wagner, H., "Ebene Blechwändtrager mit sehr Dünnem Stegblech",Z. Flugtech. Motorluftschiffahrt vol. 20, pp 200-306 (1929).
- 50. Wu, B.C., "A New Method for the Solution of Thin Plate Problems", Ph.D. Thesis, Michigan State University (1980).
- 51. Yamaki, N., "Postbuckling of Rectangular Plates with Small Initial Curvature Loaded in Edge Compression", Trans. ASME J. App. Mech., vol. 26,pp 407-414 (1959).
- 52. Yang, T.Y., "A Finite Element Procedure for Large Deflection Analysis of Plates with Initial Deflections", AIAA Journal, vol. 9, No. 8, pp 1468-1473 (Aug. 1971).
- 53. Zienkiewicz, O.C., "Finite Element Procedures in the Solution of Plate and Shell Problems", Stress Analysis, edited by O.C. Zienkiewicz, and G.S. Holister, John Wiley and Sons (1965).





# APPENDIX A

# Finite Difference Operators

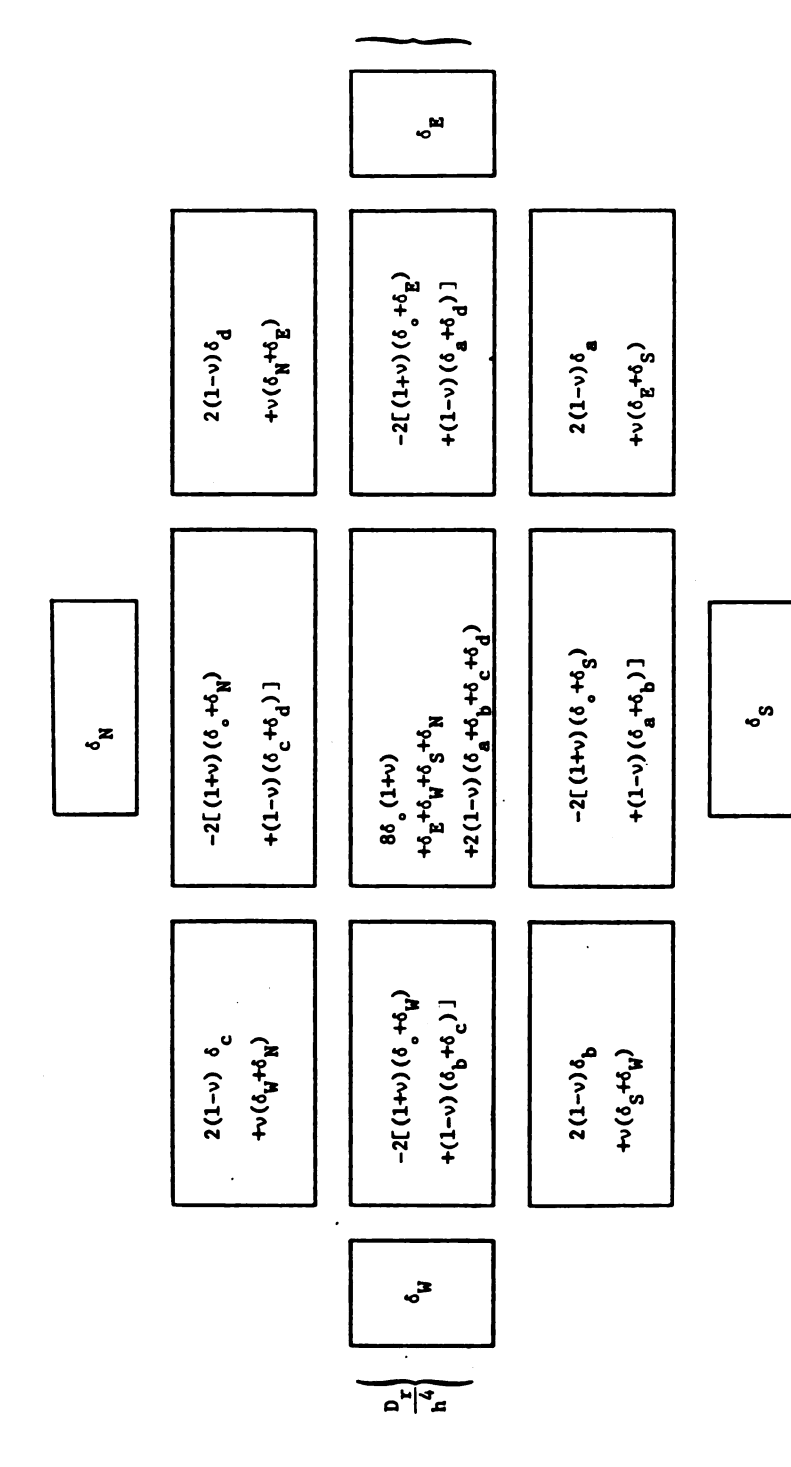
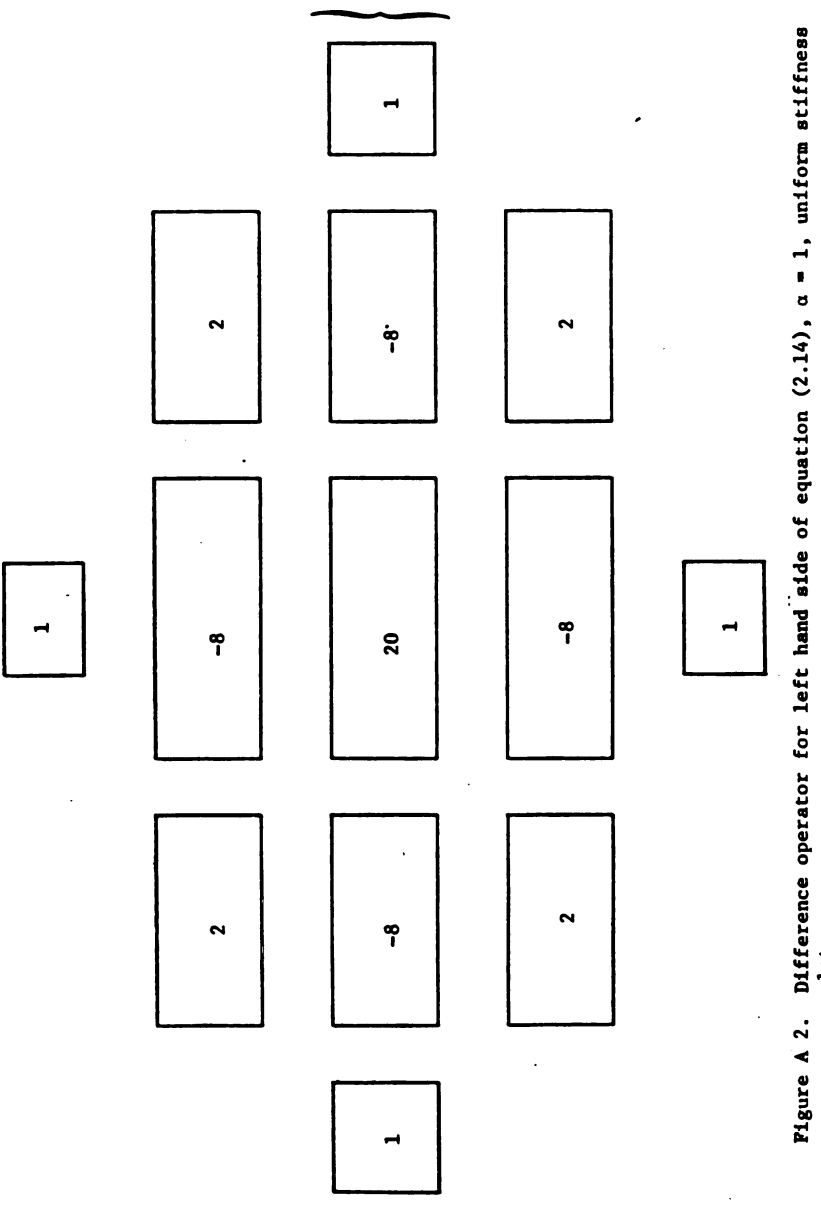


Figure Al. Difference operator for left hand side of equilibrium equation (2.14),  $\alpha$  = 1.



D<sub>T</sub>4n

Pigure A 2. Difference operator for left hand side of equation (2.14),  $\alpha$  = 1, uniform stiffness plate.

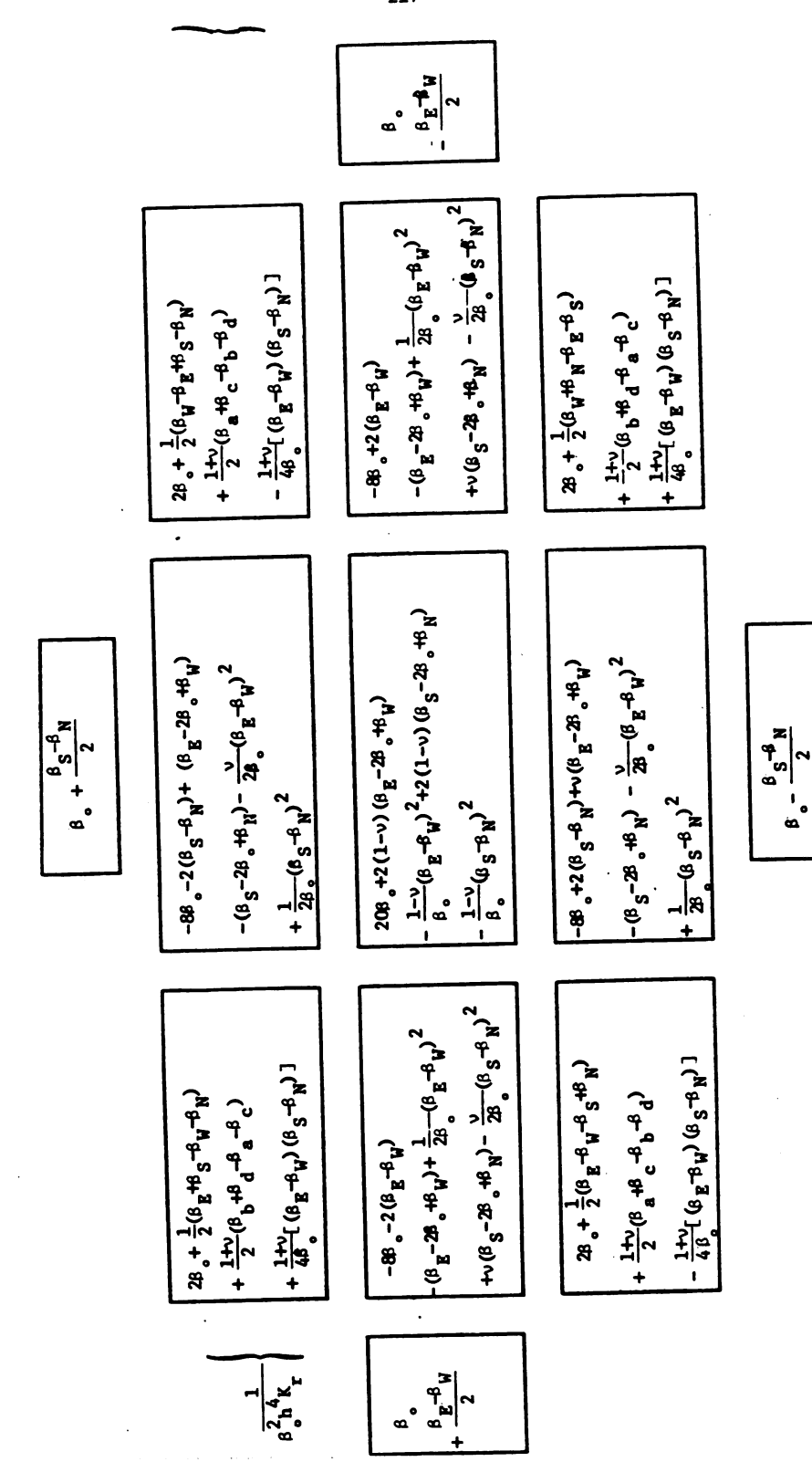


Figure A3. Finite difference operator for left hand side of compatibility equation (2.15),  $\alpha$  = 1.

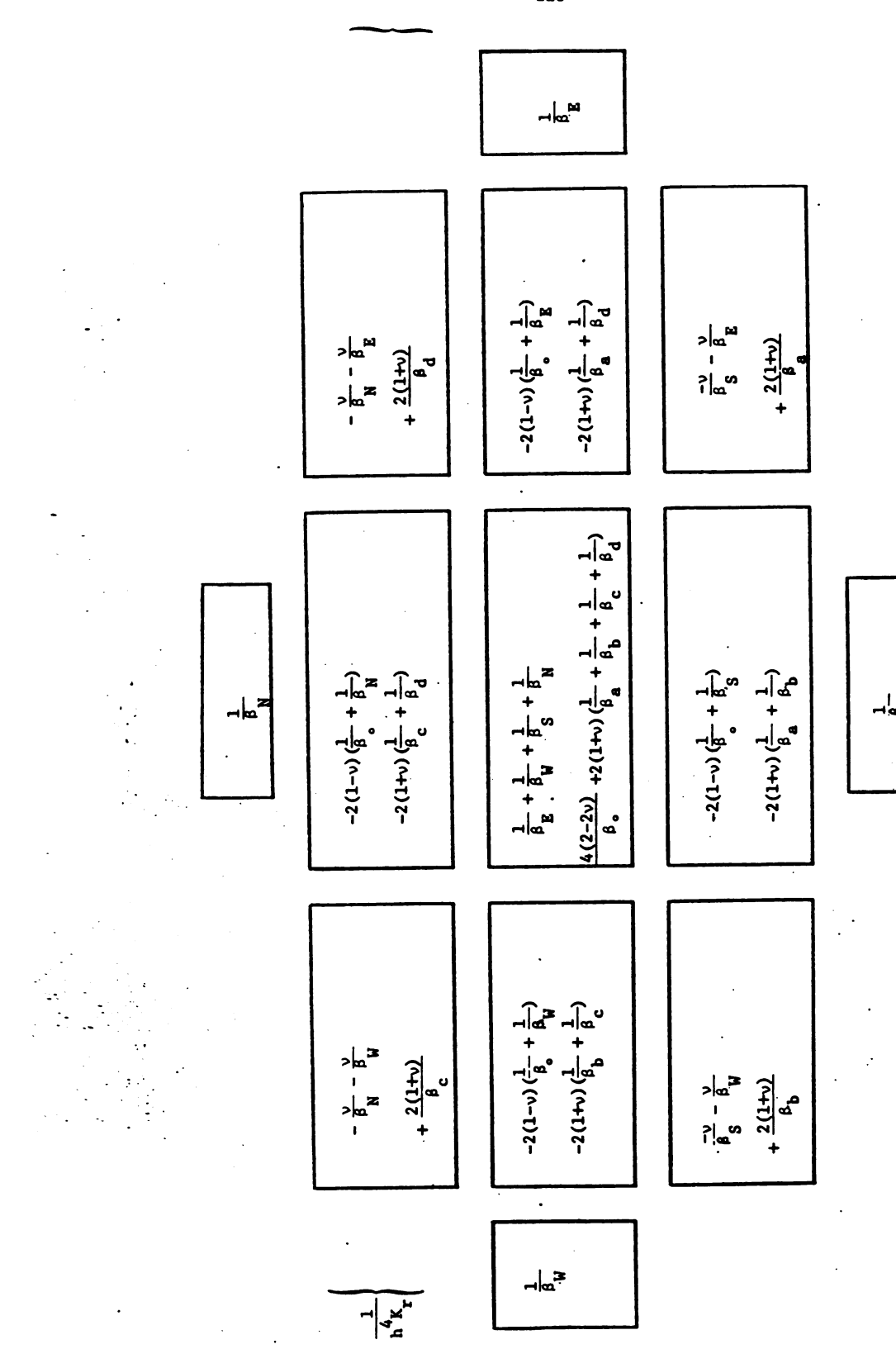


Figure A4. Finite difference approximation of equation (2.29),  $\alpha$  = 1.



## APPENDIX B

The plan and node arrangement on the portion of plate considered in each case is shown. It should be noted that the second rows of exterior nodes are auxiliary nodes for defining the K vector at edge nodes only, and those nodes do not participate in any calculations. Thus, the node number for them could be any number or repetition of previous ones.

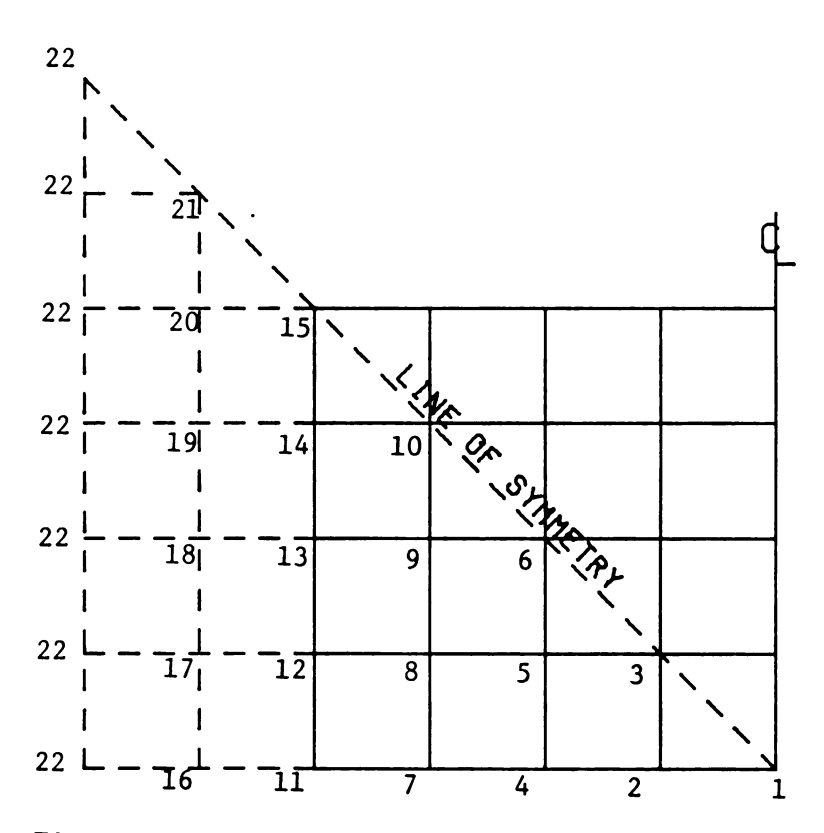


Figure B1. Node arrangement for force boundary condition square plate, h = a/8.

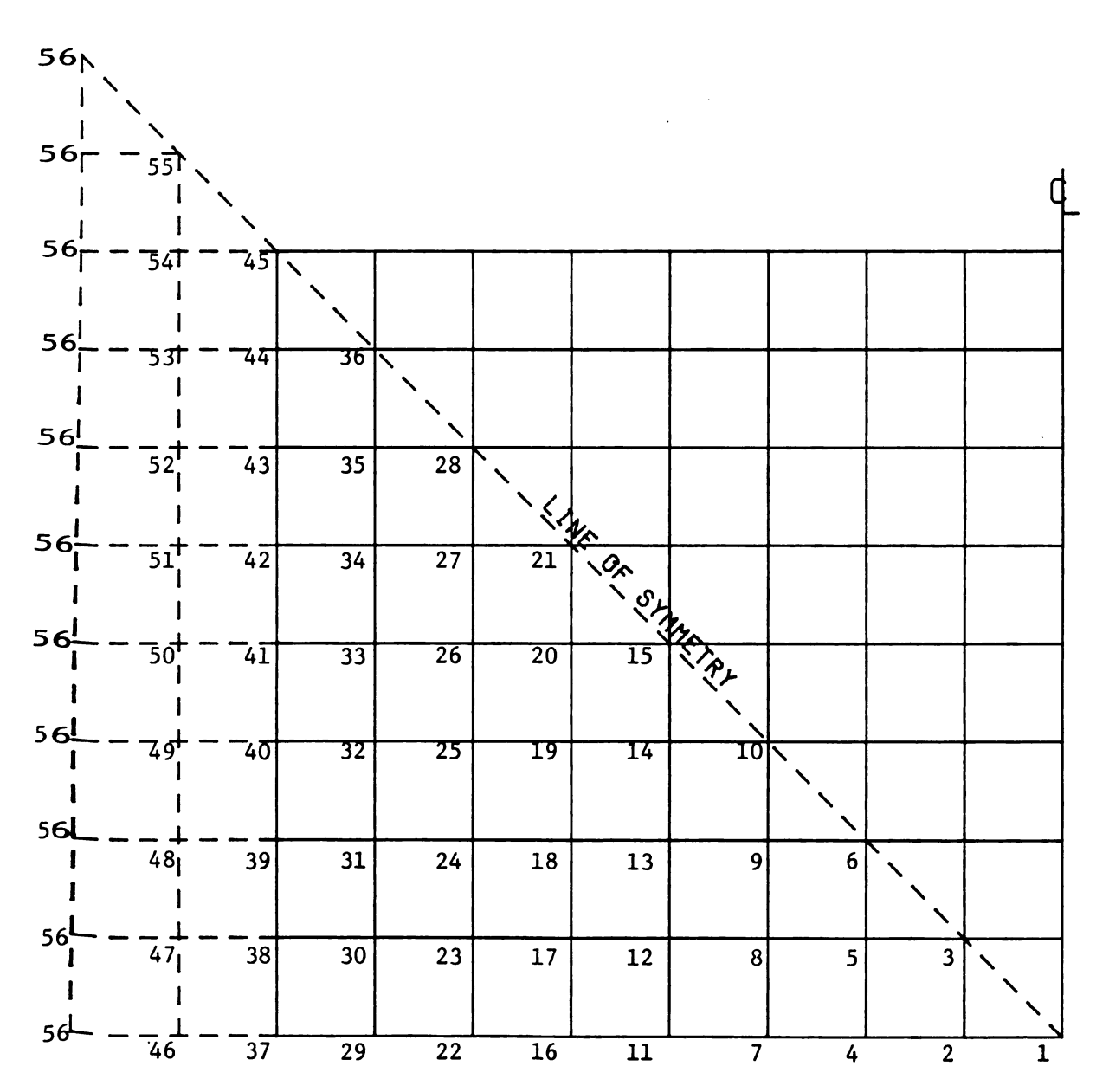


Figure B2. Node arrangement for force boundary condition, square plate,  $h = \frac{a}{16} \ .$ 

65	65_	65,	65,	_6 <u>5</u>	65	65	_ 65, _	_65
1	1	!		1.	1 		1	
65   	57 	<sup>58</sup>   _	<sup>59</sup> ¦ -	- <sup>60</sup> +	_ <del>61</del>	- <del>6</del> 2 -	- 63' - 1	64
65    -	- 5 <del>d</del> -	- <del>- 43</del>	44	45	46	47	48	49
65	1 <u>5</u>	42	31	32	33	34	35	36
65 !	1   54	41	30	21	22	23	24	25
" <b>⊢</b> !	- <del></del> -							
65 <u> </u>	<u> 53  </u> _	40	29	20	13	14	15	16
   65	1 <u>521</u> _	39	28	19	12	7	8	9
     651	   51	38	27	18	11	6	3	4
65	50	37	26	17	10	5	2	1

Figure B3. Node arrangement for displacement boundary condition solution,  $h = \frac{a}{12}.$ 

101	101	101	101	101	101	101	101	101	101	101
101 <u> </u>	-91 +-	-92 <sup>1</sup>	93	<sub>1</sub> - -94  -	_ 95   _ 95	_ 96  -	_ 97 _	    -98 -	<sub> </sub> - _92¦ _	_ 100
101 _	- <sup>90</sup> l	_7 <u>3</u>	74	75	76	77	78 <u></u>	79	- - 80  	81
101	_ <sup>89</sup>	72	57	58	59	60	61	62	63	64
101	_88 _	_71	_56	43	44	45	46	47	48	49
101	87   - 87   -	70	55	42	31	32	33	34	35	36
1 101 L	- 86   -	_69	54	41	30	21	22	23	24	25
101 <del> </del>	85   - 85	68	53	40	29	20	13	14	15	16
101	841 - 841	67	52	39	28	19	12	7	8	9
1 101 <u> </u>	1 _ <u>83</u> 1_	_66	51	38	27	18	11	6	3	4
     101	l l 82 <sub>1</sub>	65	50	37	26	17	10	5	2	1

Figure B4. Node arrangement for displacement boundary condition solution, h = a/16.

### APPENDIX C

#### COMPUTER PROGRAMS

## C.1 DESCRIPTION OF THE PROGRAMS

A listing of the computer programs is presented in this appendix. In the following a brief description of the main programs and subroutines is given.

There are two programs, PLATE 1 and PLATE 2, corresponding to Sections 3.1 and 3.2, respectively. Program PLATE 1 consists of a main program and seven subroutines. Main programs direct the flow of the computations by calling the appropriate subroutines, in addition to reading data and performing minor calculations.

The subroutine FEOPRT computes values of the operator for the compatibility equation (2.30) as well as the contribution of each node considering the node number and the boundary condition. The subroutine AMATRX forms the coefficient matrix [A] by adding the contribution of nodes. It also forms the vector {B}, the right-hand side of compatibility equation (2.15). Formation of the operator for the right-hand side of equilibrium equation (2.22) is accomplished by subroutine WOPRT. The subroutine BWMAT forms the right-hand side of equilibrium equation (2.22) as matrix [Bw]. The subroutine AXLOAD is provided to calculate stress components and the subroutine

DISPLMT computes in-plane displacements. Subroutine WRITE controls the arrangement of the large matrices in the write-outs.

Program PLATE 2 consists of a main program and subroutines AMATRX, WOPRT and WRITE, in addition to six other subroutines as follows:

The subroutine UVOPRT computes numerical values for the u and v operators in equations (2.36) and (2.38). The subroutine AUVMAT forms the coefficient matrices [Aul], [Au2], [Av1] and [Av2] which are assembled as in equation (2.43) by subroutine ASSMBL.

In subroutine WFUNCT, the derivatives of w are calculated and vectors [Buv1] and [Buv2], the right-hand side of equation (2.9), are formed. The subroutine KKVECT stores a nine node operator based on a 13-node operator and subroutine RSHW is designed to compute the vector {Bw}, the right-hand side of the equilibrium equation in the z-direction. The subroutine BWBUCKL forms the right-hand side of equation (2.24) for the eigensolution.

### C.2 VARIABLES USED IN THE PROGRAMS

The variable names used in the Programs are defined below in the order they appear in the Program:

# PROGRAM PLATE 1

NSOLN = Number of problems solved in one run;

TTYPE = Variable controlling solution type. If EQ. 1,

membrane solution only. If EQ. 2, solve also
the eigenvalue problem. If EQ. 3, postbuckling
solution (skip eigensolution). If EQ. 4,
solve all steps;

RATIO1 = R or RT values (stiffness or thickness ratios);

RINCR = R or RT increment for optimization;

L1 = Number of trials for optimization;

N = Number of real nodes;

NPR = Number of interior nodes;

NOUT = Number of imaginary exterior nodes;

NA = Number of intermediate nodes;

POS = Poisson's ratio;

H = Grid spacing;

E = Modulus of elasticity;

T = Reference thickness;

DF(I) = Degree of freedom. If EQ. 1, interior node.

If EQ. 0, boundary node. If EQ. -1, exterior node.

- NSYM(I) = Variable defining in-plane displacement symmetry.

  If EQ. 1, node of antisymmetry for u. If

  EQ. 2, pole of antisymmetry for v. If EQ.3,

  pole of antisymmetry for both u and v. If

  EQ. 4, node of diagon of symmetry (u south = v west).

  If EQ. 5, u-displacement zero (on boundary)

  If EQ. 6, v = 0. (on boundary);

  Kr
- DEL(I)=  $\frac{1}{\beta_i} = \frac{K_r}{K_i} = Membrane stiffness ratio;$
- DELA(I) = Membrane stiffness ratio for intermediate nodes;
- FEE(I) = The difference between stress function at exterior nodes, and first interior nodes (i.e. in Figure (C1),  $\phi_{18} = \phi_9 + (\text{FEE})_{18}$ ;

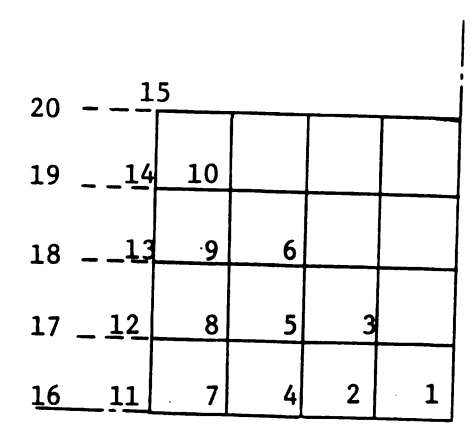


Figure C1. Node numbers.

K(I,J) = Vector defining the nodes participating in operators at each node, ordering from top node downward and rightward as shown on Figure C2;

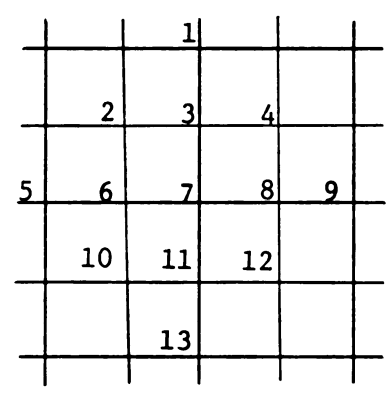


Figure C2. Arrangement of vector K.

TC = Central thickness (calculated);

RK = Reference membrane stiffness;

DR = Reference flexural stiffness;

FE(I) = Stress function  $\varphi$ ;

A(I,J) = Coefficient matrix for compatibility equation;

AW(I,J) = Coefficient matrix for left hand side of equilibrium equation;

PA(I,J) = Auxiliary matrix;

EIGVAL(I) = Eigenvalues (output);

NTRY = Number of loading steps required in iterative procedure;

NITR = Max. number of iterations allowed;

FORC = In-plane load N per unit width;

FORICR = Load increment,  $\Delta N$ ;

DIF =  $\varepsilon$  = Tolerance of convergence check;

Q(I) = Nodal lateral load vector;

 $QINCR(I) = \Delta Q = Lateral load increment;$ 

## SUBROUTINE FEOPRT

R(I) = Operator for compatibility equation;

D(I,J) = Matrix defining contribution of each node based

on the position of the node;

# SUBROUTINE AXLOAD

XN =  $N_x/N$  = Force ratio in x-direction;

YN =  $N_v/N$  = Force ratio in y-direction;

XYN =  $N_{xy}/N$  = In-plane shear force ratio;

XM =  $M_x$  = Bending moment in x-direction;

YM =  $M_v$  = Bending moment in y-direction;

XYM = M = Twisting moment;

SIGMAX = Bending stress at extreme fibers in x-direction;

SIGMAY = Bending stress at extreme fibers in y-direction;

SIGMANX = In-plane stress in x-direction;

SIGMANY = In-plane stress in y-direction;

RAD = Mohr's circle radius

PRSTRES = Maximum principal stress, ignoring transverse

shears;

### SUBROUTINE DISPLMT

U(I), V(I) = In-plane displacements;

# PROGRAM PLATE 2

AU1(I,J); AV1(I,J) = Sub-matrices representing contributions

of u and v in x-equilibrium equation;

AU2(I,J); AV2(I,J) = Sub-matrices representing contributions

of u and v in y-equilibrium equation;

AUV(I,J) = Coefficient matrix obtained by assembling
[AU1], [AV1], [AU2] and [AV2];

UINCR = Increment of edge-displacement u;

VINCR = Increment of edge-displacement v;

B1(I); B2(I) = Sub-matrices on the right-hand side of in-plane equilibrium equations;

## SUBROUTINE UVOPRT

RU1(I,J); RV1(I,J) = Operators representing u and v contributions in x-equilibrium equation;

RU2(I,J); RV2(I,J) = Operators representing u and v contributions in y-equilibrium equation;

# SUBROUTINE AUVMAT

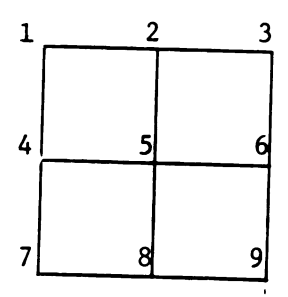


Figure C3. Arrangement of nodes in vector KK.

# SUBROUTINE WFUNCT

### C.3 COMPUTER PROGRAM

```
PROGRAM PLATE1(INPUT,OUTPUT,TAPE5=INPUT,TAPE6=OUTPUT)
C
        C
        THIS PROGRAM USES FINITE DIFFERENCE TO ANALYZE PRE-BUCKLING
C
        BUCKLING AND POSTBUCKLING OF VARIABLE STIFFNESS PLATES.
        SUITABLE FOR FORCE BOUNDARY CONDITIONS (NO RESTRICTION ON
C
C
        DISPLACEMENTS ALONG THE BOUNDARIES).
C
.
    DIMENSION WKAREA(50).ALFR(50).ALFI(50).BETA(50).ITER(50)
    DIMENSION EIGVAL(50),2(50,50), LP(65),Q(50),PB(50),PA(50,50)
                                        BW1(50)+Q1(50)+W3(50+50)
     DIMENSION PB1(50) + ABW(50+50) +
                              FE3(50,75),FEE(65),W1(65)
    DIMENSION FE1(65).
     COMMON/1/ POS.BB.CC.H.N.NPR.DR.T.RK
     COMMON/2/K(13,50),AM(4,50),DEL(60),DELA(50),NSYM(50)
     COMMON/3/DF(75) +D(13+13) +IBC(60) +R(13) +FE(75)
     COMMON/4/A(50.50).B(50)
    COMMON/5/AW(50,50),BW(50,50 ),RW(13),DELT(60),DELTA(50),W(65)
    INTEGER AMODE
C....READ INPUT DATA.
    READ (5.+) NSOLN
    DO 99 JJ=1.NSOLN
     READ (5.+) ITYP
     READ(5,+) RATIO1,RINCR,L1
     READ(5.1) N.NPR.NOUT.NA.POS.H.E.T
    NT=N+NOUT
    NP1=N+1
     NP2=NPR+1
    READ(5.+)(DF(I).I=1.NT)
     READ (5.+) (IBC(J).J=NP2.N)
     READ(5,*) (NSYM(I), I=1,N)
     READ(5.+)(DEL(J).J=1.N)
     READ(5++)(DELA(I)+I=1+NA)
     READ(5.+) (FEE(I).I=NP2.NT)
     READ(5++) (LP(I)+I=NP1+NT)
    DO 300 L=NP2+NT
    FE(L)=FEE(L)
 300 CONTINUE
    BB=1.+P0S
     CC=1.-POS
    DO 401 I=1.N
    DELT(I)=1./DEL(I)
 401 CONTINUE
    DO 402 J=1.NA
    DELTA(J)=1./DELA(J)
 402 CONTINUE
     WRITE(6.501)
    WRITE(6,502)
     WRITE(6.503) N.NPR.NOUT.NA.POS.H.DR.T
    WRITE(6,504)
     WRITE(6,505)(DF(I),I=1,NT)
    WRITE(6,511)
    DO 3 I=1.N
     READ(5.4) L. (K(J.I).J=1.13).(AM(J.I).J=1.4)
    WRITE(6+4) I_{+}(K(J_{+}I)_{+}J=1+13)_{+}(AH(J_{+}I)_{+}J=1+4)
   3 CONTINUE
     DO 999 LL=1.L1
     RK=F+T
     DR=E+T++3/(12.+B8+CC)
```

```
WRITE(6.506)
     WRITE(6.507) (DEL(J).J=1.N)
     WRITE(6.508)
     WRITE(6.507) (DELA(J).J=1.NA)
     WRITE(6,998) LL.RATIO,RK.DR.T
      FORMAT(////+*TRIAL NO *+13+* R=++F5.3+* ET CENTER=++F8.3+ D CENT
    $ER=++F8.3+* CENTRAL THICKNESS= ++F8.5)
     DO 65 I=1.NPR
     FE(I)=B(I)=Q1(I)=0.0
     00 66 J=1.NPR
     Z(I+J)=0.0
     A(I_{\bullet}J) = Au(I_{\bullet}J) = Bu(I_{\bullet}J) = 0.0
  66 CONTINUE
  65 CONTINUE
     DO 10 M=1.NPR
C.....CALCULATE OPERATOR FOR COMPATIBILITY EQUATION AT EACH NODE.
     CALL FEOPRT(M)
C.....FORM COEFFICIENT MATRIX A IN LEFT HAND SIDE OF COMPATIBILITY EQUATION.
     CALL AMATRX(M)
  10 CONTINUE
     WRITE(6.213)
     DO 53 J=1.NPR
     WRITE(6,214) B(J)
     PB(J)=B(J)
     DO 51 I=1.NPR
     PA(I,J)=A(I,J)
  51 CONTINUE
  53 CONTINUE
     DO 27 J=NP2.NT
     IF(FEE(J) .NE. 0.) GO TO 28
  27 CONTINUE
     GO TO 67
C.....SOLVE COMPATIBILITY EQUATION.FOR LARGE MATRICES APPROPRIATE BANDED
С
         MATRICES AND PROPER SOLUTION ROUTINES MUST BE USED.
  28 CALL LEGTIF( A.1.NPR.50.B.8.WKAREA.IER)
     DO 54 I=1.NPR
     FE(1)=B(1)
  54 CONTINUE
  67 WRITE(6,216)
     DO 56 J=NP1.NT
     FE(J)=FEE(J)+FE(LP(J))
  56 CONTINUE
     DO 55 J=1.NT
     WRITE(6+217) J.FE(J)
     FE1(J)=FE(J)
     W(J)=0.0
  55 CONTINUE
     FORC1=1.
C.....COMPUTE IN-PLANE FORCES-BENDING MOMENTS AND PRINCIPAL STRESSES.
     CALL AXLOAD(FE1, FORC1, FEE)
C.....COMPUTE IN-PLANE DISPLACEMENTS . U AND V.
```

```
CALL DISPLMT(FE1)
     IF(ITYP .EQ. 1) GO TO 99
     DO 19 I=1.NPR
     DO 2 J=1.NPR
     A(I.J)=0.0
   2 CONTINUE
  19 CONTINUE
    DO 403 M=1.NPR
C.....CALCULATE OPERATOR FOR LEFT HAND SIDE OF EQUILIBRIUM EQUATION.
CALL WOPRT(M)
C.....COMPUTE COEFFICIENT MATRIX.AW. FOR EQUILIBRIUM EQUATION.
     CALL AMATRX(M)
C.....FORM MATRIX, BW. IN RIGHT HAND SIDE OF EQUILIBRIUM EQUATION.
     CALL BWMAT(M)
 403 CONTINUE
     DO 404 I=1.NPR
     00 405 J=1.NPR
     (L.I)A=(L.I)WA
405 CONTINUE
 404 CONTINUE
     IF(ITYP .EQ. 3) GO TO 18
100
C.....COMPUTE EIGENVALUES AND EIGENVECTORS.
m
     CALL EQZQF(A ,50,BW,50,NPR,Z,50)
     CALL EQZTF(A ,50,8W,50,NPR,EPSA,EPSB,Z,50,IER)
     CALL EQZVF(A .50.BW.50.NPR.EPSA.EPSB.ALFR.ALFI.BETA.Z.50)
     WRITE(6.25)
     DO 41 I=1.NPR
     EIGVAL(I)=ALFR(I)/BETA(I)
     WRITE(6,26) ALFR(I), ALFI(I), BETA(I), EIGVAL(I)
  41 CONTINUE
 18 CONTINUE
C....READ INITIAL VALUES FOR POSTBUCKLING TRIALS.
m
     READ(5,11) NTRY, NITR, FORC, FORICR, DIF
     READ (5++) (Q(I)+I=1+NPR)
     READ(5.+) QINCR
     READ(5,+) (FE1(I),I=1,NPR)
     READ(5++) (W(I)+I=1+NPR)
     NN=0
     WRITE(6,224)
     WRITE(6,521)
     WRITE(6,522)NTRY,NITR,FORC,FORICR,DIF,H
     WRITE(6.523)
     WRITE(6,524) (Q(I),I=1,NPR)
     DO 5 M=1.NTRY
     FORC1=(FORC+NN*FORICR)*DR
     DO 6 I=1.NPR
     Q(I)=Q(I)+QINCR
     PB1(I)=PB(I)*FORC1
   6 CONTINUE
     DO 20 I=NP2 .N
     FE1(I)=FEE(I) +FORC1
```

```
FE(I)=FE1(I)
  20 CONTINUE
     NN=NN+1
     MM=0
     MMM=1
     WRITE (6,224)
     WRITE (6,221) NN.FORC1
     DO 7 L=1.NITR
     MM1=MM-1
     MM2=MM-2
     IF(MM-3+MMM) 226,225,226
225 MMM=MMM+1
C....APPLY CONVERGENCE-INDUCING TECHNIQUE.
     DO 60 I=1.NPR
     IF((FE3(MM+I)-FE3(MM1+I))+(FE3(MM1+I)-FE3(MM2+I))+GE+ 0+)GO TO 60
     FE(I)=(FE3(MM1.))++2-FE3(MM.I)+FE3(MM2.I))/(2.+FE3(MM1.I)-FE3(MM.
    +I)-FE3(MM2,I))
     W(I)=(W3(MM1,I)++2-W3(MM,I)+W3(MM2,I))/(2.+W3(MM1,I)-W3(MM,I)-W3(
    +MM2.1))
  60 CONTINUE
     GO TO 61
 226 DO 49 I=1.N
     FE(I)=FE1(I)
  49 CONTINUE
  61 MM=MM+1
     DO 58 I=1.NPR
     DO 59 J=1.NPR
     BW(I.J)=0.0
  59 CONTINUE
 58 CONTINUE
C.....CALCULATE RIGHT HAND SIDE OF EQUILIBRIUM EQUATION.
     D08 I=1.NPR
     CALL BWMAT(I)
     Q1(I)=0.0
   8 CONTINUE
     DO 50 I=1.NPR
     D09 J=1.NPR
     ABW(I,J)=AW(I,J)
     A(I.J)=PA(I.J)
     Q1(I)=Q1(I)+BW(I,J)+W(J)
   9 CONTINUE
     Q1(I) = (Q1(I) + Q(I) + H + + 4) / DR
     W1(I)=W(I)
 50 CONTINUE
C.....SOLVE EQUILIBRIUM EQUATION.GET NEW W.
     CALL LEGTIF (ABW, 1, NPR, 50, Q1, 8, WKAREA, IER)
     00 12 I=1.NPR
     W(I)=Q1(I)
  12 CONTINUE
    DO 14 J=1.NPR
C.....COMPUTE RIGHT HAND SIDE OF COMPATIBILITY EQUATION BASED ON NEW VALUES.
     G=0.0
     WFAC1=(W(K(12+J))+W(K(2+J))-W(K(10+J))-W(K(4+J)))/4.
     WFAC2=W(K(8+J))+W(K(6+J))-2.+W(K(7+J))
     WFAC3=W(K(3,J))+W(K(11,J))-2.+W(K(7,J))
```

```
G=G+WFAC1++2-WFAC2+WFAC3
    BW1(J)=G+RK+P81(J)
  14 CONTINUE
C....SOLVE COMPATIBILITY EQUATION.GET NEW FEE VALUES.
     CALL LEGTIF( A,1,NPR,50,BW1,8,WKAREA,IER)
    DO 15 I=1.NPR
    FE1(I)=BW1(I)
  15 CONTINUE
    DO 17 I=1.N
    FE3(MM.I)=FE1(I)
     W3(MM.I)=W(I)
  17 CONTINUE
C.....CHECK CONVERGENCE.
.
     00 16 J=1.NPR
     IF(ABS((W1(J)-W(J))/W(J)) .GT. DIF) GO TO 7
  16 CONTINUE
    GO TO 72
  7 CONTINUE
  72 WRITE(6,222) MM
    DO 71 I=1.N
    WRITE(6.13) FE1(I).W(I)
  71 CONTINUE
  64 DO 63 J=NP1.NT
    FE1(J)=FEE(J)*FORC1+FE1(LP(J))
  63 CONTINUE
C.....CALCULATE IN-PLANE FORCES AND DISPLACEMENTS.
     CALL AXLOAD(FE1.FORC1.FEE)
    CALL DISPLMT(FE1)
  5 CONTINUE
 999 CONTINUE
  99 CONTINUE
  1 FORMAT(415,F5.3,3F10.5)
   4 FORMAT(1814)
  11 FORMAT(215,4F10.5)
  13 FORMAT(10X.F15.8.5X.F15.8)
  25 FORMAT(///,10x,+ALFA REAL+,5x,+ALFA IMAG+,8x,+BETA+,10x,+EIG
   +ENVALUES+)
  26 FORMAT(/+10x+F10.5+5x+F10.5+5x+F10.5+5x+F12.4)
 211 FORMAT(1H1,20x,+ELEMENTS OF COEFFICIENT MATRIX-COLUMNS+,12,+ TO +
    +, I2)
 212 FORMAT(/,5X,10F10.5)
 213 FORMAT(//.8X.+B VECTOR+//)
 214 FORMAT(5X,F12.8)
 216 FORMAT(+0++10x++FE VALUES AT EACH NODE+)
 217 FORMAT(/+5X+12+8X+F12-8)
 218 FORMAT(///, 20x, +ELEMENTS OF MATRIX AU+)
 220 FORMAT(///, 20X, +EIGENVECTORS CORRESPONDING TO EACH EIGENVALUE-
   +VECTORS+, 12, +TO +, 12)
 221 FORMAT(///+50X++LOAD POINT NO ++13+5X++LOAD=++F8+2)
 222 FORMAT(//.*ITERATION NO *. 12.2X.* FE *.10X.***)
 501 FORMAT(//+20X++00000 GEOMETRICAL INPUT DATD 00000+)
 502 FORMAT(//o+NO OF NODES+o2xo+NO OF INTERNAL NODES+o2xo+NO OF EXTERI
   +OR NODES++2X++NO OF INTERMEDIAT NODES++2X++POISON S RATIO++2X+
    **GRID SPACING REF STUFNESS THICKNESS*)
```

```
503 FORMAT(/.3X.15.12X.15.15X.15.15X.15.20X.F5.3.10X.3F10.5)
  504 FORMAT(///,20x,+DEGREES OF FREEDOM FOR EACH NODE +1=INTERIOR, 0=BO
         +UNDARY POINT -- 1 = EXTERIOR NODE ++ +>
  505 FORMAT(/,5x,4013)
  506 FORMAT(///-20X-+1/BETA=DR/D+)
  507 FORMAT(5(5X,10F10.5/))
  508 FORMAT(///+20x++1/BETA FOR INTERMEDIATE POINTS+)
  511 FORMAT(///.20x..CORRESPONDING POINTS PARTICIPATING IN EACH NODE O
         +PERATOR+/)
  521 FORMAT(///.5x.+NO OF LOAD POINTS+.2x.+NO OF ITERATION+.2x.+FORCE+.
         +2X+*FORCE INCREMENT+,2X+*DIFFERENCE*,2X+*H=A/N*)
  522 FORMAT(/+12X+I5+12X+I5+5X+F9+3+8X+F6+3+10X+F6+3+5X+F6+3)
  523 FORMAT(//+20x+*EXTERNAL TRANSVERS LOAD+)
  524 FORMAT(5(5x,10F6.3/))
           END
.
SUBROUTINE FEOPRT(M)
C
                     THIS ROUTINE CALCULATES THE VALUES OF OPERATOR FOR COMPATIBILITY
C
                    EQUATION AND DETERMINES THE CONTRIBUTION OF EACH NODE BASED ON
C
C
                     NODE NUMBERS (MATRIX D )
C
           COMMON/1/ POS.BB.CC.H.N.NPR.DR.T
           COMMON/2/K(13,50),AM(4,50),DEL(60),DELA(50),NSYM(50)
           COMMON/3/DF(75),D(13,13),IBC(60),R(13),FE(75)
           COMMON/4/A(50,50),B(50)
           COMMON/5/AU(50,50),BU(50,50 ),RU(13),DELT(60),DELTA(50),U(65)
           INTEGER AM. DF
           R(1)=DEL(K(3.M))
           R(2) = - (DEL(K(3, M)) + DEL(K(6, M))) + POS+2. * BB + DELA(AM(3, M))
           R(3) = -2 \cdot *CC*(DEL(K(7 \cdot M)) + DEL(K(3 \cdot M))) - 2 \cdot *BB*(DELA(AM(3 \cdot M)) + DELA(AM(3 \cdot M)) + DELA(
         +(4,M)))
           R(4) = -POS*(DEL(K(3.M))+DEL(K(8.M)))+2.*BB*DELA(AM(4.M))
           R(5)=DEL(K(6,M))
           R(6)=-2.*CC*(DEL(K(7,M))+DEL(K(6,M)))-2.*BB*(DELA(AM(2,M))+DELA(AM
         +(3,M)))
           R(7)=DEL(K(3,M))+DEL(K(6,M))+DEL(K(8,M))+DEL(K(11,M))+8.*CC*DEL(K
         +(7.M))+2.*BB*(DELA(AM(1.M))+DELA(AM (2.M))+DELA(AM(3.M))+DELA(AM(
         +4.M)))
           R(8)=-2.+CC+(DEL(K(7.M))+DEL(K(8.M)))-2.+BB+(DELA(AM(1.M))+DELA(AM
         +(4,M)))
           R(9)=DEL(K(8,M))
           R(10) = -(DEL(K(6,M)) + DEL(K(11,M))) + POS + 2. + BB + DELA(AM(2,M))
           R(11) =-2.*CC*(DEL(K(7.M))+DEL(K(11.M)))-2.*BB*(DELA(AM(1.M))+DELA
         +(AM(2,H)))
           R(12)=-(DEL(K(8,M))+DEL(K(11,M)))+POS+2.+BB+DELA(AM(1,M))
           R(13)=DEL(K(11.M))
C.....CONSTRUCT D MATRIX AT EACH POINT.
           DO 72 J=1,13
           DO 71 I=1.13
           D(I,J)=0.0
    71 CONTINUE
    72 CONTINUE
```

```
D(7.7)=1.0
     IF(DF(K(1.H)) .NE. -1 .AND. DF(K(5.H)) .NE. -1) D(2.2)=1.0
     IF(DF(K(1,M)) .NE. -1 .AND. DF(K(9,M)) .NE. -1) D(4,4)=1.0
     IF(DF(K(5, M)) .NE. -1 .AND. DF(K(13, M)) .NE.-1) D(10,10)=1.0
     IF(DF(K(9,M)) \cdot NE \cdot -1 \cdot AND \cdot DF(K(13,M)) \cdot NE \cdot -1) D(12,12) = 1 \cdot 0
     IF(DF(K(1,M))) 100,101,102
 100 D(7.1)=1.0
     B(M)=B(M)-R(2)+FE(K(2,M))-R(3)+FE(K(3,M))-R(4)+FE(K(4,M))-R(1)+FE
    +(K(1.M))
     GO TO 40
 102 D(1.1)=1.0
 101 D(3.3)=1.0
     IF(DF(K(1,M)) \rightarrow EQ \rightarrow 0) B(M)=B(M)-R(1)+FE(K(1,M))
  40 IF(DF(K(5,M))) 110,111,112
 110 D(7.5)=1.0
     B(M)=B(M)-R(6)+FE(K(6,M))-R(10)+FE(K(10,M))-R(5)+FE(K(5,M))
     IF(DF(K(1+M)) +NE+-1) B(M)=B(M)-R(2)+FE(K(2+M))
     GO TO 41
 112 0(5,5)=1.0
 111 D(6.6)=1.0
     IF(DF(K(5.M)) .EQ. 0) B(M)=B(M)-R(5)+FE(K(5.M))
  41 IF(DF(K(9,M)) ) 120,121,122
 120 D(7.9)=1.0
     B(M)=B(M)-R(8)+FE(K(8,M))-R(9)+FE(K(9,M))-R(12)+FE(K(12,M))
     IF(DF(K(1,M)) \cdot NE \cdot -1) B(M)=B(M)-R(4)+FE(K(4,M))
     GO TO 42
 122 D(9.9)=1.0
 121 D(8.8)=1.0
  IF(DF(K(9,M)) .EQ. 0) B(M)=B(M)-R(9)*FE(K(9,M)) 42 IF(DF(K(13,M)) ) 130+131+132
 130 D(7,13)=1.0
     B(M)=B(M)-R(11)*FE(K(11,M))-R(13)*FE(K(13,M))
     IF(DF(K(5,M)) \cdot NE \cdot -1) \cdot B(M) = B(M) - R(10) + FE(K(10,M))
     IF(DF(K(9,M)) .NE. -1) B(M)=B(M)-R(12)+FE(K(12,M))
     GO TO 43
 132 D(13.13)=1.0
 131 0(11,11)=1.0
     IF(DF(K(13,M)) .EQ. 0) B(M)=B(M)-R(13)*FE(K(13,M))
  43 RETURN
     END
m
m
m
8
     SUBROUTINE AMATRX(M)
C
C....CALCULATE COEFFICIENT MATRIX FOR COMPATIBILITY EQUATION.
C
         COMMON/1/ POS.BB.CC.H.N.NPR.DR.T
     COMMON/2/K(13,50),AM(4,50),DEL(60),DELA(50),NSYM(50)
     COMMON/3/DF(75),D(13,13),IBC(60),R(13),FE(75)
     COMMON/4/A(50+50)+B(50)
     DO 51 J=1.13
     DO 52 L=1.13
     IF(K(L,M) .GT. NPR) GO TO 52
     A(M_{\bullet}K(L_{\bullet}M))=A(M_{\bullet}K(L_{\bullet}M))+D(L_{\bullet}J)+R(J)
  52 CONTINUE
  51 CONTINUE
```

```
RETURN
     END
.
æ
     SUBROUTINE WOPRT(M)
         THIS ROUTINE CALCULATES OPERATOR FOR EQUILIBRIUM EQUATION AND
C
         CONTRIBUTION OF EACH NODE BASED ON NODE NUMBERS.
C
         COMMON/1/ POS.BB.CC.H.N.NPR.DR.T
     COMMON/2/K(13.50),AM(4.50),DEL(60),DELA(50)
     COMMON/3/DF(75).D(13.13).IBC(60).R(13).FE(75)
     COMMON/5/AW(50+50)+BW(50+50 )+RW(13)+DELT(60)+DELTA(50)
     INTEGER AMODE
C.....CALCULATE OPERATOR AT EACH NODE USING FIGURE A1.
     RW(1)=DELT(K(3.M))
     RW(2)=2.*CC*DELTA(AM(3.M))+POS*(DELT(K(6.M))+DELT(K(3.M)))
     RW(3)=-2.+(88+(DELT(K(7.M))+DELT(K(3.M)))+CC+(DELTA(AM(3.M))+
    +DELTA(AM(4.M))))
     RW(4)=2.*CC*DELTA(AM(4.M))+POS*(DELT(K(3.M))+DELT(K(8.M)))
     RW(5)=DELT(K(6.M))
    RW(6)=-2.*(BB*(DELT(K(7.M))+DELT(K(6.M)))+CC*(DELTA(AM(2.M))+
    +DELTA(AM(3,M))))
    RW(7)=8.*BB*DELT(K(7,M))+DELT(K(8,M))+DELT(K(6,M))+DELT(K(3,M))+
    +DELT(K(11,M))+2.+CC+(DELTA(AM(1,M))+DELTA(AM(2,M))+DELTA(AM(3,M))
    ++DELTA(AM(4.M)))
    RW(8)=-2.*(BB*(DELT(K(7.M))+DELT(K(8.M)))+CC*(DELTA(AM(1.M))+
    +DELTA(AM(4,4))))
    RW(9) = DELT(K(8.M))
     RW(10)=2.+CC+DELTA(AM(2,M))+POS+(DELT(K(11,M))+DELT(K(6,M)))
    RW(11)=-2.*(BB*(DELT(K(7,M))+DELT(K(11,M)))+CC*(DELTA(AM(1,M))+
    +DELTA(AM(2.M))))
     RW(12)=2.+CC+DELTA(AM(1,M))+POS+(DELT(K(8,M))+DELT(K(11,M)))
     RW(13) = DELT(K(11.M))
        CONSTRUCT D MATRIX AT EACH POINT
C
     DO 72 J=1.13
    DO 71 I=1.13
    D(I.J)=0.0
 71 CONTINUE
     R(J) = RY(J)
 72 CONTINUE
    D(7,7)=1.0
     IF(DF(K(1,M)) .NE. -1 .AND. DF(K(5,M)) .NE. -1) D(2,2)=1.0
     IF(DF(K(1,M)) .NE. -1 .AND. DF(K(9,M)) .NE. -1) D(4,4)=1.0
     IF(DF(K(5,M)) .NE. -1 .AND. DF(K(13,M)) .NE.-1) D(10,10)=1.0
     IF(DF(K(9,M)) .NE. -1 .AND. DF(K(13,M)) .NE.-1) D(12,12)=1.0
     IF(DF(K(1.M))) 100.101.102
100 IF(IBC(K(3,M))-2) 1001,1002,1002
1001 D(7.1)=1.0
     GO TO 40
1002 D(7.1)=-1.0
    GO TO 40
```

```
102 D(1,1)=1.0
 101 D(3.3)=1.0
 40 IF(DF(K(5,M))) 110,111,112
 110 IF(IBC(K(6,4))-2) 1101,1102,1102
1101 D(7.5)=1.0
     GO TO 41
1102 D(7.5)=-1.0
     GO TO 41
112 D(5.5)=1.0
111 D(6.6)=1.0
  41 IF(DF(K(9,M)) ) 120,121,122
120 IF(IBC(K(8+M))-2) 1201+1202+1202
1201 D(7.9)=1.0
    GO TO 42
1202 D(7,9)=-1.0
    GO TO 42
 122 D(9.9)=1.0
 121 D(8.8)=1.0
  42 IF(DF(K(13,4)) )130,131,132
 130 IF(IBC(K(11.4))-2) 1301,1302,1302
1301 D(7.13)=1.0
     60 TO 43
1302 D(7.13)=-1.0
    GO TO 43
 132 D(13.13)=1.0
 131 D(11.11)=1.0
  43 RETURN
    FND
.
m
    SUBROUTINE BWMAT(J)
C
         ******************
C
         THIS ROUTINE IS UTILIIZED TO CALCULATE RIGHT HAND SIDE OF
C
        EQUILIBRIUM EQUATION.
C
     COMMON/1/ POS.BB.CC.H.N.NPR.DR.T
     COMMON/2/K(13,50),AM(4,50),DEL(60),DELA(50),NSYM(50)
     COMMON/3/DF(75).D(13.13).IBC(60).R(13).FE(75)
     COMMON/5/AW(50,50).BW(50,50 ).RW(13).DELT(60).DELTA(50)
    FEFAC1=FE(K(11,J))-2.*FE(K(7,J))+FE(K(3,J))
     FEFAC2=FE(K(8,J))-2.*FE(K(7,J))+FE(K(6,J))
    FEFAC3=-(FE(K(12.J))+FE(K(2.J))-FE(K(10.J))-FE(K(4.J)))/8.
     IF(K(2.J) .GT. NPR) GO TO 1
    BW(J,K(2,J))=BW(J,K(2,J))+FEFAC3
   1 IF(K(3.J) .GT. NPR) GO TO 2
     BW(J.K(3.J))=BW(J.K(3.J))+FEFAC2
   2 IF(K(4.J) .GT. NPR) GO TO 3
     BW(J.K(4.J))=BW(J.K(4.J))-FEFAC3
   3 IF(K(6.J) .GT. NPR) GO TO 4
     BW(J+K(6+J))=BW(J+K(6+J))+FEFAC1
   4 IF(K(7.J) .GT. NPR) GO TO 5
     BW(J,K(7,J))=BW(J,K(7,J))-2.*FEFAC1-2.*FEFAC2
   5 IF(K(8.J) .GT. NPR) GO TO 6
    BW(J,K(8,J))=BW(J,K(8,J))+FEFAC1
   6 IF(K(10.J).GT. NPR) GO TO 7
     BW(J,K(10,J))=BW(J,K(10,J))-FEFAC3
```

```
7 IF(K(11.J).GT. NPR) GO TO 8
     BW(J+K(11+J))=BW(J+K(11+J))+FEFAC2
   8 IF(K(12.J).GT. NPR) GO TO 9
     BW(J+K(12+J))=BW(J+K(12+J))+FEFAC3
   9 RETURN
     END
m
m
m
R
     SUBROUTINE AXLOAD(FE1.FORC1.FEE)
С
         THIS ROUTINE COMPUTES IN-PLANE FORCES. BENDING MOMENTS AND
C
        PRINCIPAL STRESSES AT EACH NODE.
С
    DIMENSION FE1(75) FEE(65)
     COPMON/1/ POS.BB.CC.H.N.NPR.DR.T
     COMMON/2/K(13,50),AM(4,50),DEL(60),DELA(50),NSYM(50)
     COMMON/3/DF(75),D(13,13),IBC(60),R(13),FE(75)
     COMMON/5/AW(50,50),BW(50,50 ),RW(13),DELT(60),DELTA(50),W(65)
     NP2=NPR+1
     MM=N-1
     WRITE (6,21)
  21 FORMAT(////+10x+*STRESS RESULTANT RATIO AT EACH NODE +)
     00 1 M=NP2.N
     WF=1.
     IF(IBC(M) .EQ. 2) WF=-1.
     IF(NSYM(M)-6) 35.36.37
  35 W(K(6.M))=WF+W(K(8.M))
     W(K(10,M))=WF+W(K(12,M))
     GO TO 1
  37 W(K(6,M))=WF+W(K(8,M))
     W(K(2,M))=WF+W(K(12,M))
  36 W(K(3,M))=WF+W(K(11,M))
     W(K(4.M))=WF+W(K(12.M))
  1 CONTINUE
     WRITE(6.22)
  22 FORMAT(///,2X,+NODE+,5X,+NX/N+,6X,+NY/N+,5X,+NXY/N+, 9X,+MX+,
    +8x9+MY+07x0+MXY+011X0+MXT/2I+05X0+NX/T+010X0+MYT/2I+05X0+NY/T PRI
    +NCIPAL STRESS+)
    DO 10 I=1.N
     IF(NSYM(I) .EQ. 7)FE1(K(2,I))=FE1(K(12,I))+2.*FEE(K(6,I))*FORC1
       XN = -(FE1(K(11,I)) + FE1(K(3,I)) - 2.* + FE1(K(7,I)))/(H**2*FORC1)
     YN=-(FE1(K(6,I))+FE1(K(8,I))-2.*FE1(K(7,I)))/(H**2*FORC1)
    XYN=+(FE1(K(2,I))+FE1(K(12,I))-FE1(K(4,I))-FE1(K(10,I)))/(4.*H**2
    ++FORC1)
     WXX=(W(K(6,I))+W(K(8,I))-2.+W(K(7,I)))/H++2
     WYY=(W(K(11,I))+W(K(3,I))-2.+W(K(7,I)))/H++2
     WXY=(W(K(4,I))+W(K(10,I))-W(K(12,I))-W(K(2,I)))/(4.+H*+2)
     DP=DR+DELT(I)
     XM=-DP+(WXX+POS+WYY)
     YM=-DP+(WYY+POS+WXX)
     XYM=DP+CC+WXY
     SIGMAX=XM+6./T++2
     SIGMAY=YM+6./T++2
     SIGMANX=XN+FORC1/T
     SIGMANY=YN+FORC1/T
     XSIGMAX=ABS(SIGMAX)+ABS(SIGMANX)
```

```
YSIGMAX=ABS(SIGMAY)+ABS(SIGMANY)
    RAD=SQRT(((XSIGMAX-YSIGMAX)/2.)++2+(XYN+FORC1/(2.+T))++2)
    PRSTRES = (XSIGMAX+YSIGMAX)/2.+RAD
    WRITE(6+23) I+XN+YN+XYN+XM+YM+XYM+SIGMAX+SIGMAX+SIGMAY+SIGMAY+
   $.PRSTRES
  23 FORMAT(//+2X+I2+2X+3F10.5+4X+3F10.3+2(2X+F10.3+F12.3)+F12.3)
 10 CONTINUE
    RETURN
    END
m
m
m
m
    SUBROUTINE DISPLMT(FE1)
        THIS ROUTINE COMPUTES IN-PLANE DISPLACEMENTS.U AND V AS
C
C
        DESCRIBED IN SECTION 3.1.3.2.
        C
    DIMENSION AU(50+50)+AV(50+50)+BU(50)+BV(50)+FE1(75)+WKAREA(50)
    DIMENSION NU(50),NY(50),AUU(50,50),AVV(50,50),BBU(50),BBV(50)
    COMMON/1/ POS.BB.CC.H.N.NPR.DR.T.RK
    COMMON/2/K(13.50).A4(4.50).DEL(60).DELA(50).NSYM(50)
    COMMON/3/DF(75).D(13.13).IBC(60).R(13).FE(75)
    COMMON/5/AW(50,50),BW(50,50 ),RW(13),DELT(60),DELTA(50),W(65)
    INTEGER DF
    DO 1 I=1.N
    DO 2 J=1.N
    0.0=(L.I)VA=(L.I)UA
   2 CONTINUE
    BBU(I)=BBV(I)=0.0
   1 CONTINUE
C.....IMPLY OUT-OF-PLANE BOUNDARY CONDITION.
    NP2=NPR+1
    DO 22 M=NP2.N
    WF=1.
    IF(IBC(M) .EQ. 2) WF=-1.
    IF(NSYM(M)-6) 35.36.37
  35 W(K(6,M))=WF+W(K(8,M))
    W(K(3,M))=WF+W(K(11,M))
    GO TO 22
  37 W(K(6,M))=WF+W(K(8,M))
    W(K(2.M))=WF+W(K(12.M))
  36 W(K(3,M))=WF+W(K(11,M))
  22 CONTINUE
    N1=N2=0
    DO 3 M=1.N
    WX=(W(K(8,M))-W(K(6,M)))/(2.+H)
    WY = (W(K(3,M)) - W(K(11,M)))/(2.*H)
    XN=(FE1(K(11,M))+FE1(K(3,M))-2.*FE1(K(7,M)))/(H**2)
    YN=(FE1(K(6,M))+FE1(K(8,M))-2.*FE1(K(7,M)))/(H**2)
    C1=.5+WX++2
    C2=.5+WY++2
C.....CONSIDERING SYMMETRY AND BOUNDARY NODES .FORM COEFFICIENT MATRICES.
    IF(NSYM(M) .NE. 0) GO TO 6
  25 N1=N1+1
    N2=N2+1
    NU(N1)=M
    NV(N2)=M
```

```
IF(NSYM(K(8,M)) .EQ. 1 .OR. NSYM(K(8,M)) .EQ. 4) GO TO 18
     AU(N1.K(7.M))=AU(N1.K(7.M))-1./H
     AU(N1.K(8.M))=AU(N1.K(8.M))+1./H
     GO TO 19
  18 AU(N1+K(7+M))=AU(N1+K(7+M))-1-/H
  19 AV(N2.K(7.M))=AV(N2.K(7.M))+1./H
     AV(N2.K(11.M))=AV(N2.K(11.M))-1./H
     BU(N1)=DEL (M)+(XN-POS+YN)/RK-C1
     BV(N2)=DEL (M )+(YN-POS+XN)/RK-C2
     GO TO 3
  6 GO TO(7,8,3,15,25,25,25) NSYM(M)
   7 N2=N2+1
     NV(N2)=M
     IF(DF(K(3.M)) .EQ.-1) GO TO 20
     AV(N2,K(3,M))=AV(N2,K(3,M))+.5/H
     AV(N2+K(11+M))=AV(N2+K(11+M))-.5/H
     GO TO 21
  20 AV(N2,K(7,M))=AV(N2,K(7,M))+1./H
     AV(N2.K(11.M))=AV(N2.K(11.M))-1./H
  21 BV(N2) = DEL (M ) + (YN-POS+XN)/RK-C2
     GO TO 3
   8 N1=N1+1
     NU(N1)=M
     AU(N1.K(8.M))=AU(N1.K(8.M))+1./H
     AU(N1,K(7,M)) = AU(N1,K(7,M)) - 1./H
     BU(N1)=DEL (M)+(XN-POS+YN)/RK-C1
     GO TO 3
  15 N2=N2+1
     NV (N2)=M
     AV(N2,K(7,M))=AV(N2,K(7,M))+1./H
     AV(N2.K(11.M))=AV(N2.K(11.M))-1./H
     BV(N2)=DEL (M )*(YN-POS*XN)/RK-C2
   3 CONTINUE
     DO 5 I=1.N1
     DO 4 J=1.N1
     AUU(I.J)=AU(I.NU(J))
   4 CONTINUE
   5 CONTINUE
     DO 17 I=1.N2
     DO 14 J=1.N2
     ((L)VM.I)VA=(L.I)VVA
  14 CONTINUE
 17 CONTINUE
C.....SOLVE FOR V-DISPLSCEMENT.
     CALL LEGT1F(AVV.1.N2.50.BV.8.WKAREA.IER)
     DO 10 J=1.N2
     BBV(NV(J))=BV(J)
  10 CONTINUE
     NN = 0
     DO 23 M=1.N
     IF(NSYM(M) .EQ. 1 .OR. NSYM(M) .EQ.3) GO TO 23
     IF(NSYM(M) .EQ. 4) GO TO 24
     NN=NN+1
     IF(NSYM(K(8+M)) .NE. 4) GO TO 23
     BU(NN)=BU(NN)+BBV(K(8,M))/H
     GO TO 23
 24 BBU(M) = - BBV(M)
  23 CONTINUE
C.....SOLVE FOR U-DISPLSCEMENT.
     CALL LEGTIF(AUU,1,N1,50,BU,8,WKAREA,IER)
     DO 9 I=1.N1
```

```
BBU(NU(I))=BU(I)
  9 CONTINUE
    BBU(N) =-BBV(N)
    WRITE (6.11)
 11 FORMAT(////.10x.+NODE U-DISPLACEMENT V-DISPLACEMENT+.//)
    DO 16 I=1.N
    WRITE(6.12) I.BBU(I).BBV(I)
 12 FORMAT(11X.12.3X.F12.6.8X.F12.6)
 16 CONTINUE
    RETURN
    END
m
m
m
    SUBROUTINE WRITE(NPR.A)
C
       ***********************************
C.....THIS ROUTINE ARRANGES THE WRITE-OUT OF LARGE MATRICES.
C
       DIMENSION A(50,50)
    NMAT=NPR/10+1
    DO 57 I1=1.NMAT
    I11=10+(I1-1)+1
    I12=10 * I1
    IF(I12 .GT. NPR) I12=NPR
    IF(I11 .GT. NPR) GO TO 57
    WRITE(6,3) I11,I12
  3 FORMAT(////.30x...----- COLUMNS *.12.* TO *.12.* -----
   $----+,//)
    DO 52 I=1.NPR
    WRITE(6,4) (A(I,J),J=I11,I12)
  4 FORMAT(/,5X,10F12.5)
 52 CONTINUE
 57 CONTINUE
    RETURN
    END
```

```
PROGRAM PLATE2(INPUT,OUTPUT,TAPE5=INPUT,TAPE6=OUTPUT)
C
         THIS PROGRAM IS UTILIZED TO SOLVE PRE-BUCKLING BUCKLING AND
С
         POSTBUCKLING OF VARIABLE STIFFNESS PLATES SUITABLE FOR
         DISPLACEMENT BOUNDARY CONDITIONS.
С
         THIS PROGRAM USES THE GIVEN SUBROUTINES IN ADDITION TO THREE
С
         ROUTINES (AMATRX.WOPRT AND WRITE) AS GIVEN IN PROGRAM PLATE1.
С
     DIMENSION Q(81), BW(81), A(128, 128), B(128), UINCR(81), VINCR(81)
     DIMENSION AWW(64,64), WW(64,25), WKAREA(128)
     DIMENSION EIGVAL(64), ALFR(64), ALFI(64), BETA(64), Z(64,64)
     COMMON/1/POS.88.CC.K(13.81).DEL(81).DF(101).H.NSYM(81).DR.RK
     COMMON/2/DU(9,9),DV(9,9),KK(9,64),RU1(9),RU2(9),RV1(9),RV2(9)
     COMMON/3/B1(65).B2(65).U(81).V(81).BW1(64).BW2(64).W(100)
     COMMON/4/ AU1(64,64),AU2(64,64),AV1(64,64),AV2(64,64),AUV(128,128)
     COMMON/5/ BUV1(64),BUV2(64),BUV(128)
     COMMON/6/DELT(81), DELTA(8 ), AM(4,81), DELA(8 ), IBC(81)
     COMMON/7/RW(13), DW(13,13), AW(64,64), BWB(64,64)
     COMMON/8/XNX.YNY.XNY
     INTEGER AMODF
C....READ INPUT DATA.
     READ (5.+) NSOLN
     DO 99 NO=1.NSOLN
     READ(5.+) ITYP
     READ(5.+) RATIO1.RINCR.L1
     READ (5.1) N.NPR.NOUT.NA.POS.ALFA.H.E.T
     NP2=NPR+1
     NT=N+NOUT
     READ (5,+) (IBC(I),I=NP2,N)
     READ (5,*) (DF(I).I=1.NT)
     READ(5++) (NSYM(I)+I=1+N)
     READ (5.*) (U(I).I=NP2.N)
     READ (5++) (V(I)+I=NP2+N)
     DO 100 I=1.N
     READ(5,4) L. (K(J.I).J=1.13) .(AM(J.I).J=1.4)
     WRITE(6,4) I, (K(J_0I)_0J=1,13), (AM(J_0I)_0J=1,4)
100 CONTINUE
     BB=1.+P0S
     CC=1.-POS
     WRITE(6,501)
     READ(5++) (W(J)+J=1+N)
     READ (5.+) (Q(I).I=1.N)
     WRITE(6,511)
     WRITE(6,502)
     WRITE(6,503) N. NPR. NOUT. NA. POS. H. DR. T
     WRITE(6.504)
     WRITE(6,505)(DF(I),I=1,NT)
     N2=2*NPR
     CALL KKVECT(NPR)
     DO 999 LL=1.L1
     CALL DESIGN(RATIO1+RINCR+N+LL+TC+RATIO+NA)
     T=TC
     DR=E+T++3/(12.+BB+CC)
     RK=E+T
     WRITE(6,506)
     WRITE(6,507) (DEL(J),J=1,N)
     WRITE(6.508)
```

```
WRITE(6.507) (DELA(J).J=1.NA)
    WRITE(6,998) LL,RATIO,RK,DR,T
 998
      FORMAT(////+TRIAL NO ++13++ R=++F5.3++ ET CENTER=++F8.3+ D CENT
    $ER=+.F8.3.* CENTRAL THICKNESS= +.F8.5)
    DO 103 I=1.NPR
    B1(I)=B2(I)=0.0
     DO 104 J=1.NPR
     AU1(I,J)=AU2(I,J)=AV1(I,J)=AV2(I,J)=AW(I,J)=BWB(I,J)=0.0
 104 CONTINUE
103 CONTINUE
C.....CALCULATE OPERATORS AND FORM THE MATRICES FOR IN-PLANE
C
        EQUILIBRIUM EQUTIONS.
    DO 110 M=1.NPR
    CALL UVOPRT(M)
    CALL AUVMAT(M.NPR)
C.....COMPUTE W-OPERATOR FOR OUT-OF-PLANE EQUILIBRIUM EQUATION.
    CALL WOPRT(M)
.
C.....CALCULATE CONTRIBUTION OF W IN RIGHT HAND SIDE OF IN-PLANE
        EQUILIBRIUM EQUATIONS.
C
13
    CALL WFUNCT(ALFA,M)
C.....FORM COEFFICIENT MATRIX FOR OUT-OF-PLANE EQUILIBRIUM EQUATION.
    CALL AMATRX(M.NPR)
110 CONTINUE
C....ASSEMBLE U AND V COEFFICIENT MATRICES.
    CALL ASSMBL(NPR)
    WRITE(6,265)
     WRITE(6.240)
    DO 115 I=1.N2
    B(I)=BUV(I)
115 CONTINUE
    DO 117 I=1.N2
     DO 116 J=1.N2
    A(I.J)=AUV(I.J)
 116 CONTINUE
117 CONTINUE
C.....SOLVE IN-PLANE EQUILIBRIUM EQUATIONS.
С
                FOR LARGE MATRICES PROPER BANDED MATRICES MUST BE
         NOTE.
C
                 FORMED AND APPROPRIATE SOLUTION ROUTINES USED.
13
     CALL LEGTIF(A,1,N2,128,B,8,WKAREA,IER)
     DO 150 I=1.NPR
    U(I)=B(I)
    NPV=I+NPR
     V(I)=B(NPV)
 150 CONTINUE
     WRITE(6.201)
     DO 156 M=1.NPR
     ITREND=1
C....CALCULATE RIGHT HAND SIDE OF OUT-OF-PLANE EQUILIBRIUM EQUATION.
```

```
CALL RHSW(M.Q.ALFA.BW.NPR.N.ITREND)
C.....FORM COEFFICIENT MATRIX IN RIGHT HAND SIDE OF OUT-OF-PLANE
C
         EQUILIBRIUM EQUATION.
-
     CALL BUBUCKL (MaNPR)
     DO 154 I=1.NPR
     AUU(M.I) = AU(M.I)
 154 CONTINUE
 156 CONTINUE
     IF(ITYP .EQ. 1) GO TO 99
IF(ITYP .EQ. 3) GO TO 119
     DO 131 I=1.NPR
     DO 132 J=1.NPR
     AW(I+J)=AW(I+J)+DR/H++4
 132 CONTINUE
 131 CONTINUE
     WRITE(6.261)
C.....SOLVE EIGENVALUE PROBLEM.
     CALL EQZQF(AW+64+BWB+64+NPR+Z+64)
     CALL EQZTF (AW+64+BWB+64+NPR+EPSA+EPSB+Z+64+IER)
     CALL EQZVF(AW,64.BW8,64.NPR.EPSA.EPSB.ALFR.ALFI.BETA,2,64)
     WRITE(6,25)
     DO 41 I=1.NPR
     EIGVAL(I)=ALFR(I)/BETA(I)
     WRITE(6,26) ALFR(I), ALFI(I), BETA(I), EIGVAL(I)
  41 CONTINUE
 999 CONTINUE
119 IF(ITYP .EQ. 2) GO TO 99
C....READ INITIAL VALUES FOR POSTBUCKLING TRIALS.
.
     READ(5++) (W(I), I=1, NPR)
     READ (5.*) (UINCR(I).I=NP2.N) .DIF.NTRY.NITR
     READ (5.+) (VINCR(I).I=NP2.N)
     READ(5,+) GINCR
     WRITE(6,224)
     WRITE(6.521)
     WRITE(6,522)NTRY.NITR.FORC.FORICR.DIF.H
     WRITE(6,523)
     WRITE(6.524) (Q(I).I=1.NPR)
     WRITE(6.525) QINCR
     DO 111 II=1.NTRY
     IF(II .EQ. 1) GO TO 118
     DO 121 I=1.NPR
     Q(I)=Q(I)+QINCR
 121 CONTINUE
C....INCREASE EDGE DISPLACEMENTS.
     DO 112 L=NP2.N
     U(L)=U(L)+(1.+(II-1)+UINCR(L))/(1.+(II-2)+UINCR(L))
     V(L)=V(L)+(1.+(II-1)+VINCR(L))/(1.+(II-2)+VINCR(L))
 112 CONTINUE
 118 WRITE(6.262) II.Q(1)
     JJJ=1
     DO 120 JJ=1.NITR
     ITREND=0
```

```
DO 114 I=1.NPR
     81(I)=B2(I)=0.0
     DO 2 J=1.NPR
     AU1(I_{\bullet}J)=AU2(I_{\bullet}J)=AV1(I_{\bullet}J)=AV2(I_{\bullet}J)=0.0
   2 CONTINUE
C.....FORM COEFFICIENT MATRICES IN RIGHT HAND SIDE OF IN-PLANE
С
         EQUILIBRIUM EQUATIONS.
m
     CALL UVOPRT(I)
     CALL AUVMAT(I.NPR)
C.....CALCULATE RIGHT HAND SIDE OF IN-PLANE EQUILIBRIUM EQUATIONS.
     CALL WFUNCT(ALFA,I)
 114 CONTINUE
C....ASSEMBLE U AND V COEFFICIENT MATRICES.
8
     CALL ASSMBL(NPR)
     DO 42 I=1.N2
     DO 43 J=1.N2
     A(I,J)=AUV(I,J)
  43 CONTINUE
  42 CONTINUE
C.....SOLVE IN-PLANE EQUILIBRIUM EQUATIONS.
     CALL LEGTIF(A,1,N2,128,BUV,8,WKAREA,IER)
     DO 44 I=1.NPR
     L=I+NPR
     U(I)=BUV(I)
     V(I)=BUV(L)
  44 CONTINUE
     DO 68 J=1.NPR
C.....CALCULATE RIGHT HAND SIDE OF IN-PLANE EQUILIBRIUM EQUATIONS.
      CALL RHSW(J.Q.ALFA.BW.NPR.N.ITREND)
  68 CONTINUE
     DO 45 J=1.NPR
     DO 46 L=1.NPR
     AW(JoL)=AWW(JoL)
  46 CONTINUE
  45 CONTINUE
C.....SOLVE OUT-OF-PLANN EQUILIBRIUM EQUATION.
m
     CALL LEGT1F(AW +1+NPR+64+BW+8+WKAREA+IER)
     DO 151 I=1.NPR
      W(I)=WW(I,JJ)=BW(I)
 151 CONTINUE
     JJ1=JJ-1
     JJ2=JJ-2
     IF(JJ .EQ. 1) GO TO 120
C.....CHECK CONVERGENCE.
     DO 152 J=1.NPR
     IF(WW(J+(JJ-1)) .EQ. 0.) GO TO 152
     IF(ABS((WW(J,JJ)-WW(J,(JJ-1)))/WW(J,(JJ-1))) .GT. DIF) GO TO 160
```

```
152 CONTINUE
    GO TO 1111
160 IF(JJ-3+JJJ)120,158,120
158 JJJ=JJJ+1
    DO 159 I=1.NPR
C....APPLY CONVERGENCE -INDUCING TECHNIQUE.
    IF((WW(I.JJ)-WW(I.JJ1))+(WW(I.JJ1)-WW(I.JJ2)) .GT. 0.) GO TO 159
    $I.JJ2))
159 CONTINUE
120 CONTINUE
1111 ITREND=1
    WRITE(6+263) JJ
    WRITE(6.251)
    DO 153 L=1.N
    WRITE(6,252)U(L),V(L),W(L)
153 CONTINUE
    WRITE(6.201)
    DO 688 J=1.V
C....CALCULATE IN-PLANE FORCES, BENDING MOMENTS AND PRINCIPAL STRESSES.
    CALL RHSW(J,Q,ALFA,BW,NPR,N,ITREND)
688 CONTINUE
111 CONTINUE
 99 CONTINUE
  1 FORMAT(415,2F5.3,F15.12,2F10.3)
  4 FORMAT(1814)
  5 FORMAT(//.15,9F7.4,5X,9F7.4)
  6 FORMAT (/,5X,9F3.0,10X,9F3.0)
 25 FORMAT(////+10x++ALFA REAL++5X++ALFA IMAG++8X++BETA++10x++EIG
   +ENVALUES+)
 26 FORMAT(/,10x,F10.5,5x,F10.5,5x,F10.5,5x,F10.5)
201 FORMAT(////-4X-+NODE+-7X-+NX+-8X-+NY+-7X-+NXY+-16X-+MX+-8X-+MY+
   $.7X.*MXY*.7X.*MAX STRESS IN X*.2X.*MAX STRESS IN Y PRINCIPL STRES
   $5+1
220 FORMAT(////,20X,+EIGENVECTORS CORRESPONDING TO EACH EIGENVALUE+)
240 FORMAT(////.5X.*ELEMENTS OF BUV-VECTOR*)
250 FORMAT(/,10x,F10.5)
251 FORMAT(////8X++U-DISPLACEMEMENT++9X++V-DISPLACEMENT++12X++W-DISPL
   +ACEMENT+)
252 FORMAT(/+8X+F10.5+15X+F10.5+15X+F10.5)
261 FORMAT(////+20X+40(1H$)++ MATRIX 8W ++40(1H$)//)
262 FORMAT(///+20x+40(1H$)++ LOADING STEP NO ++13++ Q=++F10.2+40(1H$))
265 FORMAT(///,20x,40(1HS),* MATRIX AUV *,40(1HS)//)
501 FORMAT(//+20X++00000 GEOMETRICAL INPUT DATD 00000+)
502 FORMAT(//,+NO OF NODES+,2X,+NO OF INTERNAL NODES+,2X,+NO OF EXTERI
   +OR NODES+,2X,+NO OF INTERMEDIAT NODES+,2X,+POISON S RATIO+,2X,
   **GRID SPACING REF STUFNESS THICKNESS*)
503 FORMAT(/+3x+15+12x+15+15x+15+15x+15+20x+F5-3+10x+3F10-5)
 504 FORMAT(///,20x,+DEGREES OF FREEDOM FOR EACH NODE +1=INTERIOR, 0=BO
   +UNDARY POINT,-1=EXTERIOR NODE+++)
 505 FORMAT(/.5X.4013)
 506 FORMAT(///+20X++1/BETA=DR/D+)
507 FORMAT(5(5x-10F10-5/))
 508 FORMAT(///+20X++1/BETA FOR INTERMEDIATE POINTS+)
511 FORMAT(///•20x•+CORRESPONDING POINTS PARTICIPATING IN EACH NODE O
```

```
+PERATOR+/)
 521 FORMAT(///.5x.+NO OF LOAD POINTS+.2X.+NO OF ITERATION+.2X.+FORCE+.
   +2x+*FORCE INCREMENT*+2x+*DIFFERENCE*+2X+*H=A/N*)
 522 FORMAT(/,12x,15,12x,15,5x,F9.3,8x,F6.3,10x,F6.3,5x,F6.3)
523 FORMAT(//+20x++EXTERNAL TRANSVERS LOAD+)
524 FORMAT(5(5X+10F12-2/))
525 FORMAT(//, 20x, +-----LATERAL LOAD IHCREMENT=+, F8.2, +-----+)
    STOP
    END
m
SUBROUTINE UVOPRT(M)
C
        THIS ROUTINE CALCULATES OPERATORS FOR U AND V FOR IN-PLANE
        EQUILIBRIUM EQUATION AND THE CONTRIBUTION OF EACH NODE.
C
С
    COMMON/1/POS.BB.CC.K(13.81).DEL(81).DF(101).H.NSYM(81).DR.RK
    COMMON/2/DU(9,9).DV(9,9).KK(9,64).RU1(9).RU2(9).RV1(9).RV2(9)
    COMMON/3/B1(65) + B2(65) + U(81) + V(81) + BW1(64) + BW2(64) + W(100)
    INTEGER DF
    DO 1 I=1.9
    RU1(I)=RU2(I)=RV1(I)=RV2(I)=0.0
    DO 2 J=1.9
    0.0=(L.I)VO=(L.I)UO
  2 CONTINUE
   1 CONTINUE
    X1=1./DEL(KK(5.M))
    X2=1./DEL(KK(6.M))-1./DEL(KK(4.M))
    X3=1./DEL(KK(8.M))-1./DEL(KK(2.M))
C.....CALCULATE OPERATOR FOR U1 IN X- EQUILIBRIUM
m,
    RU1(2)=.5*CC*(X1-.25*X3)
    RU1(4)=X1-X2/4.
    RU1(5)=(POS-3.) +X1
    RU1(6)=X1+X2/4.
    RU1(8) = .5 * CC * (X1 * X3/4.)
C....CALCULATE OPERATOR FOR U2 IN Y-EQUILIBRIUM
8
    RU2(1)=RU2(9)=0.5*BB*X1
    RU2(2)=-.5*CC*X2
    RU2(3) = RU2(7) = -RU2(1)
    RU2(4)=-P0S+X3
    RU2(6) = -RU2(4)
    RU2(8) = -RU2(2)
C.....CALCULATE OPERATOR FOR V1 IN X-EQUILIBRIUM
    RV1(1)=RV1(9)=RU2(1)
    RV1(2)=-POS+X2
    RV1(3) = RV1(7) = -RV1(1)
    RV1(4)=-.5+CC+X3
    RV1(6)=-RV1(4)
    RV1(8) = -RV1(2)
```

```
C.....CALCULATE OPERATOR FOR V2 IN Y-EQUILIBRIUM
     RV2(2) = X1 - .25 \pm X3
     RV2(4) = CC * (.5 * X1 - .125 * X2)
     RV2(5) = (POS-3.) * X1
     RV2(6)=CC*(.5*X1+.125*X2)
     RV2(8) = X1 + X3/4
     DO 3 J=1.9
  20 IF(NSYM(M) .NE. 0) GO TO 21
     DU(J.J)=DV(J.J)=1.0
     GO TO 3
  21 IF(NSYM(M)-2) 22,23,24
  22 DU(1.3)=DU(4.6)=DU(7.9)=-1.0
     DU(1.1)=DU(2.2)=DU(4.4)=DU(5.5)=DU(7.7)=DU(8.8)=1.0
     DV(J_{\bullet}J) = 1.0
     GO TO 3
  23 DV(1,7)=DV(2,8)=DV(3,9)=-1.0
     DV(1,1)=DV(2,2)=DV(3,3)=DV(4,4)=DV(5,5)=DV(6,6)=1.0
     DU(J.J)=1.0
     GO TO 3
  24 DU(1.3)=DU(4.6)=DU(7.9)=-1.0
     DV(1,7) = DV(2,8) = DV(3,9) = -1.0
     DU(1,1)=DU(2,2)=DU(4,4)=DU(5,5)=DU(7,7)=DU(8,8)=1.0
     DV(1,1)=DV(2,2)=DV(3,3)=DV(4,4)=DV(5,5)=DV(6,6)=1.0
   3 CONTINUE
     RETURN
     ENC
m
m
m
     SUBROUTINE AUVMAT(M.NPR)
m
С
          CALCULATES SUB-MATRICES FOR IN-PLANE EQUILIBRIUM EQUATIONS.
M
     COMMON/2/DU(9,9),DV(9,9),KK(9,64),RU1(9),RU2(9),RV1(9),RV2(9)
     COMMON/3/B1(65),B2(65),U(81),V(81),BW1(64),BW2(64),W(100)
     COMMON/4/ AU1(64,64),AU2(64,64),AV1(64,64),AV2(64,64),AUV(128,128)
С
          CALCULATE A-MATRIX FOR U IN X EQUILIBRIUM
     DO 2 L=1.9
     IF(KK(L.M) .GT. NPR) GO TO 3
     DO 1 I=1.9
     AU1(M_{\bullet}KK(L_{\bullet}M))=AU1(M_{\bullet}KK(L_{\bullet}M))+DU(L_{\bullet}I)+RU1(I)
     AU2(M,KK(L,M))=AU2(M,KK(L,M))+DU(L,I)+RU2(I)/4.
     AV1(M+KK(L+M))=AV1(M+KK(L+M))+DV(L+I)+RV1(I)/4.
     AV2(M_{\bullet}KK(L_{\bullet}M))=AV2(M_{\bullet}KK(L_{\bullet}M))+DV(L_{\bullet}I)+RV2(I)
   1 CONTINUE
     GO TO 2
   3 DO 4 J=1,9
     B1(M)=B1(M)-DU(L,J)+RU1(J)+U(KK(L,M))-DV(L,J)+RV1(J)+V(KK(L,M))/4.
     B2(M)=B2(M)-DU(L_{9}J)+RU2(J)+U(KK(L_{9}M))/4.-DV(L_{9}J)+RV2(J)+V(KK(L_{9}M))
   4 CONTINUE
   2 CONTINUE
     RETURN
     END
```

```
.
m
    SUPROUTINE ASSMBL(NPR)
C
        C
        ASSEMBLE MATRICES FOR IN-PLANE EQUILIBRIUM EQUATIONS.
C
        COMMON/4/ AU1(64,64),AU2(64,64),AV1(64,64),AV2(64,64),AUV(128,128)
    COMMON/5/ BUV1(64).BUV2(64).BUV(128)
    DO 1 I=1.NPR
    NPI=I+NPR
    BUV(I)=BUV1(I)
    BUV(NPI)=BUV2(I)
    DO 2 J=1.NPR
    NPR2=NPR+J
    AUV(I.J)=AU1(I.J)
    AUV(I.NPR2)=AV1(I.J)
    AUV(NPI,J)=AU2(I,J)
    AUV(NPI+NPR2)=AV2(I+J)
  2 CONTINUE
  1 CONTINUE
    RETURN
    END
•
m
1
    SUBROUTINE WFUNCT(ALFA.M)
C
C
        CALCULATE RIGHT HAND SIDE OF IN-PLANE EQUILIBRIUM EQUATIONS.
C
    COMMON/1/POS,98,CC,K(13,81),DEL(81),DF(101),H,NSYM(81),DR,RK
    COMMON/3/B1(65),B2(65),U(81),V(81),BW1(64),BW2(64),W(100)
    COMMON/5/ BUV1(64),BUV2(64),BUV(128)
    WX=.5+(W(K(8,M))-W(K(6,M)))/H
    WY=.5+ALFA+(W(K(11,M))-W(K(3,M)))/H
    WXX=(W(K(8,M))+W(K(6,M))-2.+W(K(7,M)))/H++2
    WYY=ALFA++2+(W(K(3,M))+W(K(11,M))-2.+W(K(7,M)))/H++2
    WXY=.25+ALFA+(W(K(2,M))-W(K(4,M))-W(K(10,M))+W(K(12,M)))/H++2
    X1=1./DEL(K(7.M))
    X2=.5*(1./DEL(K(8,M))-1./DEL(K(6,M)))/H
    X3=.5+ALFA+(1./DEL(K(11.M))-1./DEL(K(3.M)))/H
    BW1(M)=X1+WXX+WX+.5+X1+(BB+WXY+WY+CC+WYY+WX)+.5+X2+(WX++2+POS+
   $WY**2)+CC*X3*WX*WY*.5
    BU2(M)=-5*X1*BB*UXY*UX+-5*X1*CC*UXX*UY+-5*CC*X2*UX*UY+-5*X3*(UY**2
   $+P0S+WX++2)+X1+WYY+WY
    BUV1(M)=B1(M)-BW1(M)+H++2
    BUV2(M)=B2(M)-BW2(M)*H**2
    RETURN
    END
m
```

```
SUBROUTINE KKVECT(NPR)
C
     ....STORES A 3 BY 3 STENCIL PATTERN FROM USUAL 13 NODE STENCIL.
C ...
С
m
    COMMON/1/POS.88.CC.K(13.81).DEL(81).DF(101).H.NSYM(81).DR.RK
    COMMON/2/DU(9,9),DV(9,9),KK(9,64),RU1(9),RU2(9),RV1(9),RV2(9)
    00 1 J=1 .NPR
     KK(1.J)=K(2.J)
     KK(2.J)=K(3.J)
     KK(3.J)=K(4.J)
     KK(4.J)=K(6.J)
     KK(5.J)=K(7.J)
     KK(6.J)=K(8.J)
     KK(7.J)=K(10.J)
    KK(8,J) = K(11,J)
     KK(9.J)=K(12.J)
  1 CONTINUE
    RETURN
    END
m
m
    SUBROUTINE RHSW(M.Q.ALFA.BW.NPR.N.ITREND)
        THIS ROUTINE CALCULATES RIGHT HAND SIDE OF OUT-OF-PLANE
C
C
        EQUILIBRIUM EQUATION AS WELL AS IN-PLANE FORCES, BENDING
C
        MOMENTS AND PRINCIPAL STRESSES.
C
     DIMENSION Q(81), BW(81)
    COMMON/1/POS.BB.CC.K(13.81).DEL(81).DF(101).H.NSYM(81).DR.RK
     COMMON/3/B1(65),B2(65),U(81),V(81),BW1(64),BW2(64),W(100)
    COMMON/6/DELT(81).DELTA(8 ).AM(4.81).DELA(8 ).IBC(81)
     COMMON/8/XNX.YNY.XNY
     IF(NSYM(M) .NE. 0) GO TO 104
    UX=.5+(U(K(8.M))-U(K(6.M)))/H
     VY=ALFA+.5+(V(K(11,M))-V(K(3,M)))/H
    GO TO 20
 104 GO TO (11+12+13+14+15+16+17) NSYM(M)
  11 UX=-U(K(6.M))/H
    VY=ALFA+.5+(V(K(11,M))-V(K(3,M)))/H
    GO TO 20
 12 UX=.5+(U(K(8.M))-U(K(6.M)))/H
    VY=-ALFA+V(K(3.M))/H
    GO TO 20
 13 UX=-U(K(6,M))/H
    VY=-ALFA+V(K(3,M))/H
 20 UY=ALFA+.5+(U(K(11.M))-U(K(3.M)))/H
    VX=.5*(V(K(8,M))-V(K(6,M)))/H
  14 GO TO 25
  15 UX=(U(K(8,M))-U(K(7,M)))/H
    VX=(V(K(8,M))-V(K(7,M)))/H
     UY=ALFA+.5+(U(K(11.H))-U(K(3.H)))/H
     VY=ALFA+.5+(V(K(11,M))-V(K(3,M)))/H
     NP2=NPR+1
     IF(M .EQ. NP2) VY=ALFA+(V(K(7,M))-V(K(3,M)))/H
```

```
IF(IBC(M) .EQ. 2) GO TO 22
    W(K(2,M))=W(K(4,M))
    W(K(6,M))=W(K(8,M))
    W(K(10+M))=W(K(12+M))
    GO TO 25
22 W(K(10,M))=-W(K(12,M))
    U(K(2,M)) = -U(K(4,M))
    W(K(6,M)) = -W(K(8,M))
    GO TO 25
16 UY=ALFA+(U(K(11.M))-U(K(7.M)))/H
    VY=ALFA+(V(K(11,M))-V(K(7,M)))/H
    UX=.5+(U(K(8,M))-U(K(6,M)))/H
    IF(M .EQ. N) UX=(U(K(7,M))-U(K(6,M)))/H
    VX=.5+(V(K(8.M))-V(K(6.M)))/H
    W(K(4,M))=W(K(12,M))
    IF(IBC(M) \bulletEQ\bullet' 2) W(K(4\bulletM))=-W(K(12\bulletM))
    GO TO 25
17 UX=(U(K(8.M))-U(K(7.M)))/H
    VX=(V(K(8,M))-V(K(7,M)))/H
    UY=ALFA+(U(K(11+M))-U(K(7+M)))/H
    VY=ALFA+(V(K(11+M))-V(K(7+M)))/H
    IF(IBC(M) .EQ. 2) GO TO 21
     W(K(6,M))=W(K(8,M))
    W(K(3.M))=W(K(11.M))
    W(K(2,M))=W(K(4,M))=W(K(12,M))
    GO TO 25
21 W(K(6.M))=-W(K(8.M))
    W(K(3,M)) = -W(K(11,M))
    W(K(2,M))=W(K(4,M))=-W(K(12,M))
 25 WX=.5+(W(K(8,M))-W(K(6,M)))/H
    WY=.5+ALFA+(W(K(11.M))-W(K(3.M)))/H
    WXX=(W(K(8,M))+W(K(6,M))-2.+W(K(7,M)))/H++2
    WYY=ALFA++2+(W(K(3,M))+W(K(11,M))-2.+W(K(7,M)))/H++2
    UXY=.25+ALFA+(U(K(2,M))-U(K(4,M))-U(K(10,M))+U(K(12,M)))/H++2
    X1=1./DEL(K(7.M))
 1 XNX=X1+RK+(UX+.5+WX++2+POS+VY+.5+POS+WY++2)/(BB+CC)
    YNY=X1*RK*(VY+.5*WY**2*POS*UX+POS*.5*WX**2)/(BB*CC)
    XNY=.5+X1+RK+(UY+VX+WX+WY)/BB
    IF(ITREND .EQ. 0) GO TO 2
    DP=DR+DELT(M)
    XM=-DP+(WXX+POS+WYY)
    YM=-DP+(WYY+POS+WXX)
    XYM=DP+CC+WXY
    T2=12. + BB + CC + DP/(X1+RK)
    T=SQRT(T2)
    SIGMAX=6.*XM/T2
    SIGMAY=6.+YM/T2
    SIGMANX=XNX/T
        SIGMANY=YNY/T
    XSIGMAX=ABS(SIGMAX)+ABS(SIGMANX)
    YSIGMAX=ABS(SIGMAY)+ABS(SIGMANY)
    RAD=SQRT(((XSIGMAX-YSIGMAX)/2.)++2+(XNY/(2.+T))++2)
    PRSTRES=(XSIGMAX+YSIGMAX)/2.+RAD
    WRITE(6,202) M,XNX,YNY,XNY,XM,YM,XYM,XSIGMAX,YSIGMAX,PRSTRES
202 FORMAT(//+5X+12+3X+3F10+4+5X+3F10+4+10X+2F12+4+5X+F12+4)
  2 BW(M)=Q(M)+XNX+WXX+YNY+WYY+2.+XNY+WXY
    BU(M)=BU(M)+H++4/DR
    RETURN
    END
```

```
m
.
    SUBROUTINE BWBUCKL(M.NPR)
C.....FORM COEFFICIENT MATRIX IN RIGHT HAND SIDE OF Z-EQUILIBRIUM EQUATION.
C
     COMMON/1/POS.BB.CC.K(13.81).DEL(81).DF(101).H.NSYM(81).DR.RK
    COMMON/7/RW(13), DW(13,13), AW(64,64), BWB(64,64)
    COMMON/8/XNX.YNY.XNY
    IF(K(2.M) .GT. NPR) GO TO 2
    BWB(M,K(2,M))=BWB(M,K(2,M))+XNY/(2.+H++2)
  2 IF(K(3.M) .GT. NPR) GO TO 3
    BWB(M+K(3+M))=BWB(M+K(3+M))+YNY/H++2
  3 IF(K(4,M) .GT. NPR) GO TO 4
    BWB(M.K(4.M))=BWB(M.K(4.M))-XNY/(2.*H**2)
  4 IF(K(6.M) .GT. NPR) GO TO 5
    BWB(M,K(6,M))=BWB(M,K(6,M))+XNX/H++2
  5 IF(K(7,M) .GT. NPR) GO TO 6
    BWB(M+K(7+M))=BWB(M+K(7+M))-2++(XNX+YNY)/H++2
  6 IF(K(8,M) .GT. NPR) GO TO 7
    BWB(M+K(8+M))=BWB(M+K(8+M))+XNX/H++2
  7 IF(K(10.M) .GT. NPR) GO TO 8
    BWB(M,K(10,M))=BWB(M,K(10,M))-XNY/(2.+H++2)
  8 IF(K(11.M) .GT. NPR) GO TO 9
    BWB(M,K(11,M))=BWB(M,K(11,M))+YNY/H++2
  9 IF(K(12.M) .GT. NPR) GO TO 10
    BWB(M+K(12+M))=BWB(M+K(12+M))+XNY/(2++++2)
  10 RETURN
    END
```

